Supplementary Information

Synthesis, Conformational Properties and Molecular Recognition Abilities of Novel Prism[5]arenes with Branched and Bulky Alkyl Groups

[a.] *Dipartimento di Chimica e Biologia "A. Zambelli". Università di Salerno, Via Giovanni Paolo II, I-84084, Fisciano (SALERNO). E-mail: cgaeta@unisa.it*
[b.] *Centro di Eccellenza in Biocristallografia, Dipartimento di Scienze Chimiche e Farmaceutiche, Università di Trieste, Via L. Giorgieri 1, I-34127, Trieste, Italy.*
E mail: sgeremia@units.it.

Table of Contents	**Pages**

General Experimental Details

HR MALDI mass spectra were recorded using a Bruker Solaris XR Fourier transform ion cyclotron resonance mass spectrometer equipped with a 7T refrigerated actively shielded superconducting magnet. All samples were recorded in MALDI (4 laser shots were used for each scan) and they were prepared by mixing 10 µL of analyte in dichloromethane (1 mg/mL) with 10 µL of solution of 2,5-dihydroxybenzoic acid (10 mg/mL in Methanol). The mass spectra were calibrated externally, and a linear calibration was applied. All chemical reagents grade was used without further purification and were used as purchased by Merck, TCI and Fluorochem. Reaction temperatures were measured externally. Reactions were monitored by Merck TLC silica gel plates (0.25 mm) and visualized by UV light 254 nm, or by spraying with H_2SO_4-$Ce(SO_4)_2$. NMR spectra were recorded on a Bruker Avance-600 [600 (^{1}H) and 150 MHz (^{13}C)], Avance-400 [400 (^{1}H) and 100 MHz (^{13}C)] or Avance-300 MHz [300 (^{1}H) and 75 MHz (^{13}C)]. Chemical shifts are reported relative to the residual solvent peak[1]. Standard pulse programs, provided by the manufacturer, were used for 2D COSY (cosygpqf), 2D HSQC (hsqcedetgpsisp2.2) and 2D NOESY (noesygpphpp) experiments. Structural assignments were made with additional information from gCOSY, gHSQC, and geNOESY experiments.

General procedure for the synthesis of Prism[5]arenes PrS[5]^R.

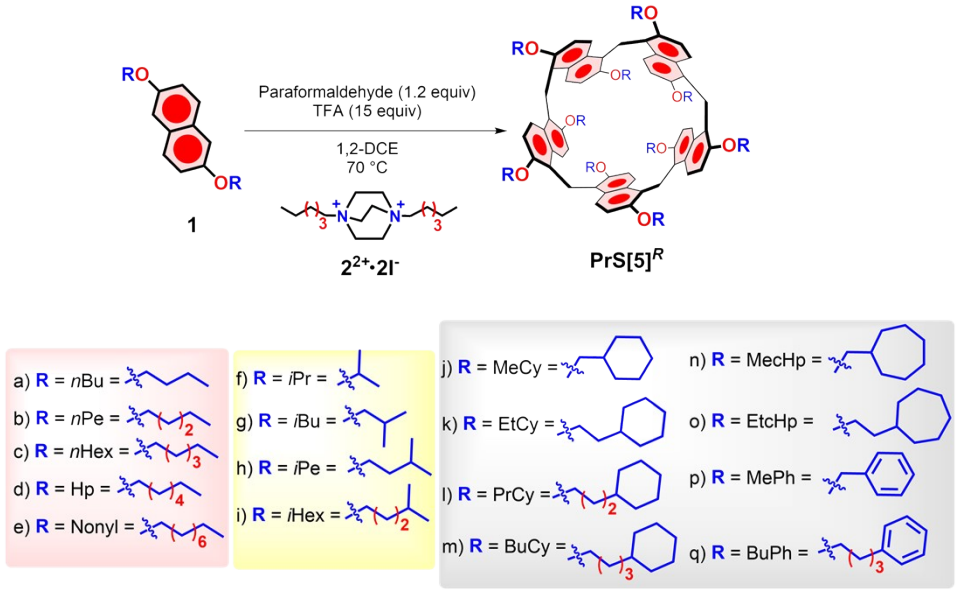

Templated synthesis in presence of $2^{2+}\cdot 2I^-$ salt:

In a solution of 2,6-dialkoxynaphthalene **1a-q** (1.0 equiv) in 1,2-dichloroethane (Table S1, 5 mM) was added paraformaldehyde (1.2 equiv) and templating agent (1.0 equiv). The mixture was heated at 70 °C and then trifluoroacetic acid (15 equiv) was added. The solution was stirred at 70 °C for the time indicated in Table S1. Then, an aqueous saturated solution of $NaHCO_3$ (50 mL) was added in the reaction mixture. The organic layer was extracted and then, washed with a 10 % aqueous solution of sodium thiosulfate (50 mL). Finally, the organic layer was dried on Na_2SO_4 and evaporated in vacuum to give a light-yellow solid.

- Starting by derivative **1a** (0.10 g, 0.37 mmol): The crude product was purified through chromatographic column on silica gel (*n*-hexane/dichloromethane = 6/4) to give the pure product **PrS[5]^{nBu}** (48 mg, 46 %) as white solid.

- Starting by derivative **1b** (0.10 g, 0.33 mmol): The crude product was purified through chromatographic column on silica gel (*n*-hexane/dichloromethane = 1/1) to give the pure product **PrS[5]^{nPe}** (44 mg, 45 %) as white solid.

- Starting by derivative **1c** (0.10 g, 0.30 mmol): The crude product was purified through chromatographic column on silica gel (*n*-hexane/dichloromethane = 6.5/3.5) to give the pure product **PrS[5]^{nHex}** (50 mg, 48 %) as white solid.

- Starting by derivative **1d** (0.10 g, 0.28 mmol): The crude product was purified through chromatographic column on silica gel (*n*-hexane/dichloromethane = 7/3) to give the pure product **PrS[5]^{Hp}** (36 mg, 35 %) as white solid.

- Starting by derivative **1e** (0.10 g, 0.24 mmol): The crude product was purified through chromatographic column on silica gel (*n*-hexane/dichloromethane = 7.5/2.5) to give the pure product **PrS[5]^{Nonyl}** (47 mg, 46 %) as white solid.

- Starting by derivative **1f** (0.10 g, 0.41 mmol): The crude product was purified through chromatographic column on silica gel (*n*-hexane/toluene/dichloromethane = 1/1/8) to give the pure product **PrS[5]^{iPr}** (50 mg, 48 %) as white solid.

- Starting by derivative **1g** (0.10 g, 0.37 mmol): The crude product was purified through chromatographic column on silica gel (*n*-hexane/dichloromethane = 7.5/2.5) to give the pure product **PrS[5]^{iBu}** (31 mg, 30 %) as white solid.

- Starting by derivative **1h** (0.10 g, 0.33 mmol): The crude product was purified through chromatographic column on silica gel (*n*-hexane/dichloromethane = 8/2) to give the pure product **PrS[5]^{iPe}** (38 mg, 37 %) as white solid.

- Starting by derivative **1i** (0.10 g, 0.30 mmol): The crude product was purified through chromatographic column on silica gel (*n*-hexane/dichloromethane = 8/2) to give the pure product **PrS[5]^{iHex}** (45 mg, 43 %) as white solid.

- Starting by derivative **1j** (0.10 g, 0.28 mmol): The crude product was purified through chromatographic column on silica gel (*n*-hexane/dichloromethane = 7.5/2.5) to give the pure product **PrS[5]^{MeCy}** (25 mg, 25 %) as white solid.

- Starting by derivative **1k** (0.10 g, 0.26 mmol): The crude product was purified through chromatographic column on silica gel (*n*-hexane/dichloromethane = 7.5/2.5) to give the pure product **PrS[5]^{EtCy}** (45 mg, 44 %) as white solid.

- Starting by derivative **1l** (0.10 g, 0.24 mmol): The crude product was purified through chromatographic column on silica gel (*n*-hexane/dichloromethane = 7.5/2.5) to give the pure product **PrS[5]^{PrCy}** (44 mg, 43 %) as white solid.

- Starting by derivative **1m** (0.10 g, 0.23 mmol): The crude product was purified through chromatographic column on silica gel (*n*-hexane/dichloromethane = 8/2) to give the pure product **PrS[5]^{BuCy}** (13 mg, 12 %) as white solid.

- Starting by derivative **1n** (0.10 g, 0.26 mmol): The crude product was purified through chromatographic column on silica gel (*n*-hexane/dichloromethane = 7/3) to give the pure product **PrS[5]^{MecHp}** (31 mg, 30 %) as white solid.

- Starting by derivative **1o** (0.10 g, 0.24 mmol): The crude product was purified through chromatographic column on silica gel (*n*-hexane/dichloromethane = 7.5/2.5) to give the pure product **PrS[5]^{EtcHp}** (46 mg, 45 %) as white solid.

- Starting by derivative **1p** (0.10 g, 0.29 mmol): The crude product was purified through chromatographic column on silica gel (*n*-hexane/dichloromethane = 1/1) to give the pure product **PrS[5]^{MePh}** (18 mg, 20 %) as white solid.

- Starting by derivative **1q** (0.10 g, 0.23 mmol): The crude product was purified through chromatographic column on silica gel (*n*-hexane/dichloromethane = 5.8/4.2) to give the pure product **PrS[5]^{BuPh}** (28 mg, 27 %) as white solid.

Table S1.

Monomer	Time	PrS[5]^{R} (%)
1a	120 h	46
1b	120 h	45
1c	120 h	48
1d	120 h	35
1e	120 h	46
1f	24 h	48
1g	120 h	30
1h	120 h	37
1i	120 h	43
1j	120 h	25
1k	120 h	44
1l	120 h	43
1m	120 h	12
1n	120 h	30
1o	120 h	45
1p	120 h	20
1q	120 h	27

Derivative PrS[5]^{nBu}:

M.p.: > 295 °C dec. ^{1}H NMR (CD_2Cl_2, 600 MHz, 298 K): *δ* 8.19 (*d*, 10H, Ar-*H,* *J* = 9.6 Hz), 6.92 (*d*, 10H, Ar-*H,* *J* = 9.0 Hz), 4.70 (*s*, 10H, ArC*H*$_2$Ar), 3.97 (*m*, 10H, O*CH*$_2$), 3.90 (*m*, 10H, O*CH*$_2$), 1.75 (*m*, 20H, $OCH_2CH_2CH_2CH_3$), 1.53 (*m*, 20H, $OCH_2CH_2CH_2CH_3$), 0.97 (*t*, 30H, $OCH_2CH_2CH_2CH_3$, *J* = 7.5 Hz). ^{13}C{^{1}H} NMR (CD_2Cl_2, 150 MHz, 298 K): *δ* 152.0,

130.2, 125.4, 123.8, 114.6, 69.7, 32.4, 21.5, 19.9, 14.2. HRMS (FT-ICR MALDI) m/z $[M]^+$ calcd for $C_{95}H_{120}O_{10}$: 1420.8882; found: 1420.8862.

Derivative PrS[5]^{nPe}:

M.p.: 248.5-249.3. ^{1}H NMR (CD_2Cl_2, 400 MHz, 298 K): *δ* 8.31 (*d*, 10H, Ar-*H, J* = 9.6 Hz), 6.95 (*d*, 10H, Ar-*H, J* = 9.2 Hz), 4.68 (*s*, 10H, ArC*H*$_2$Ar), 3.98 (*m*, 20H, O*CH*$_2$), 1.85 (*m*, 20H, $OCH_2CH_2(CH_2)_2CH_3$), 1.55 (*m*, 20H, $OCH_2CH_2CH_2CH_2CH_3$), 1.43 (*m*, 20H, $OCH_2(CH_2)_2CH_2CH_3$), 0.96 (*t*, 30H, $OCH_2(CH_2)_3CH_3$, *J* = 7.2 Hz). $^{13}C\{^1H\}$ NMR (CD_2Cl_2, 100 MHz, 298 K): *δ* 151.7, 130.2, 125.4, 123.7, 114.6, 70.1, 30.0, 29.0, 23.0, 21.3, 14.3. HRMS (FT-ICR MALDI) m/z $[M]^+$ calcd for $C_{105}H_{140}O_{10}$: 1561.0447; found: 1561.0444.

Derivative PrS[5]^{nHex}:

M.p.:196.7-198.1. ^{1}H NMR (CD_2Cl_2, 600 MHz, 298 K): *δ* 8.31 (*d*, 10H, Ar-*H, J* = 9.6 Hz), 6.95 (*d*, 10H, Ar-*H, J* = 9.6 Hz), 4.68 (*s*, 10H, ArC*H*$_2$Ar), 3.97 (*m*, 20H, O*CH*$_2$), 1.84 (*m*, 20H, $OCH_2CH_2(CH_2)_3CH_3$), 1.58 (*m*, 20H, $OCH_2CH_2CH_2(CH_2)_2CH_3$), 1.39 (*overlapped*, 40H, $OCH_2CH_2CH_2(CH_2)_2CH_3$), 0.93 (*t*, 30H, $OCH_2(CH_2)_4CH_3$, *J* = 7.2 Hz). $^{13}C\{^1H\}$ NMR (CD_2Cl_2, 75 MHz, 298 K): *δ* 150.7, 129.2, 124.4, 122.7, 113.6, 69.1, 31.1, 29.2, 25.4, 22.0, 20.2, 13.2. HRMS (FT-ICR MALDI) m/z $[M]^+$ calcd for $C_{115}H_{160}O_{10}$: 1701.2012; found: 1701.2021.

Derivative PrS[5]^{Hp}:

M.p.: 152.1-153.0. ^{1}H NMR (CD_2Cl_2, 600 MHz, 298 K): *δ* 8.33 (*d*, 10H, Ar-*H, J* = 9.6 Hz), 6.96 (*d*, 10H, Ar-*H, J* = 9.0 Hz), 4.69 (*s*, 10H, ArC*H*$_2$Ar), 3.98 (*m*, 20H, O*CH*$_2$), 1.84 (*m*, 20H, $OCH_2CH_2(CH_2)_4CH_3$), 1.58 (*m*, 20H, $OCH_2CH_2CH_2(CH_2)_3CH_3$), 1.43 (*m*, 20H, $OCH_2(CH_2)_2CH_2(CH_2)_2CH_3$), 1.35 (*overlapped*, 40H, $OCH_2(CH_2)_2(CH_2)_2CH_3$), 0.91 (*t*, 30H, $OCH_2(CH_2)_5CH_3$, *J* = 6.9 Hz). $^{13}C\{^1H\}$ NMR (CD_2Cl_2, 150 MHz, 298 K): *δ* 151.9, 130.4, 125.6, 124.0, 114.8, 70.3, 32.4, 30.4, 29.7, 26.9, 23.1, 21.4, 14.3. HRMS (FT-ICR MALDI) m/z $[M]^+$ calcd for $C_{125}H1_{80}O_{10}$: 1841.3577; found: 1841.3527.

Derivative PrS[5]^{Nonyl}:

M.p.: 78.6-79.2. ^{1}H NMR (CD_2Cl_2, 400 MHz, 298 K): *δ* 8.30 (*d*, 10H, Ar-*H, J* = 8.8 Hz), 6.94 (*d*, 10H, Ar-*H, J* = 9.2 Hz), 4.69 (*s*, 10H, ArC*H*$_2$Ar), 3.96 (*broad*, 20H, O*CH*$_2$), 1.83 (*m*, 20H, $OCH_2CH_2(CH_2)_6CH_3$), 1.57 (*m*, 20H, $OCH_2CH_2CH_2(CH_2)_5CH_3$), 1.42-1.27 (*overlapped*, 100 H, C*H*$_2$ of alkyl chains), 0.88 (*t*, 30H, $OCH_2(CH_2)_5CH_3$, *J* = 6.6 Hz). $^{13}C\{^1H\}$ NMR (CD_2Cl_2, 100 MHz, 298 K): *δ* 151.9, 130.3, 125.5, 123.9, 114.8, 70.2, 32.4, 30.4, 30.2, 30.1, 29.8, 26.9, 23.1, 21.4, 14.3. HRMS (FT-ICR MALDI**)** m/z $[M]^+$ calcd for $C_{145}H_{220}O_{10}$: 2121.6707; found: 2121.6711.

Derivative PrS[5]^{iPr}:

M.p.: > 325 °C dec. ^{1}H NMR (CD_2Cl_2, 600 MHz, 298 K): *δ* 7.81 (*d*, 10H, Ar-*H, J* = 9.6 Hz), 6.80 (*d*, 10H, Ar-*H, J* = 9.0 Hz), 4.67 (*s*, 10H, ArC*H*$_2$Ar), 4.34 (*m*, 10H, O*CH*$(CH_3)_2$), 1.16 (*d*, 30H, OCH$(CH_3)_2$, *J* = 6.0 Hz), 0.77 (*d*, 30H, OCH$(CH_3)_2$, *J* = 6.0 Hz). $^{13}C\{^1H\}$ NMR (CD_2Cl_2, 150 MHz, 298 K): *δ* 151.0, 130.1, 125.3, 125.1, 115.7, 71.7, 22.7, 22.5, 22.3. HRMS (FT-ICR MALDI) m/z $[M]^+$ calcd for $C_{85}H_{100}O_{10}$: 1280.7316; found: 1280.7334.

Derivative PrS[5]^{iBu}:

M.p.: > 309 °C dec. ^{1}H NMR (CD_2Cl_2, 600 MHz, 298 K): *δ* 8.42 (*d*, 10H, Ar-*H, J* = 9.6 Hz), 6.98 (*d*, 10H, Ar-*H, J* = 9.6 Hz), 4.72 (*s*, 10H, ArC*H*$_2$Ar), 3.88 (*m*, 10H, O*CH*$_2$), 3.78 (*m*, 10H, O*CH*$_2$), 2.22 (*m*, 10H, OCH$_2$*CH*(CH$_3$)$_2$), 1.14 (*d*, 30H, OCH$_2$CH(CH$_3$)$_2$, *J* = 6.6 Hz), 1.11 (*d*, 30H, OCH$_2$CH(*CH*$_3$)$_2$, *J* = 6.6 Hz). ^{13}C{^{1}H} NMR (CD_2Cl_2, 150 MHz, 298 K): *δ* 151.7, 130.4, 125.6, 123.8, 114.8, 76.6, 29.3, 21.2, 19.8, 19.8. HRMS (FT-ICR MALDI) m/z [M]$^+$ calcd for $C_{95}H_{120}O_{10}$: 1420.8482; found: 1420.8894.

Derivative PrS[5]^{iPe}:

M.p: 277.2-278.2 °C.^{1}H NMR (CD_2Cl_2, 600 MHz, 298 K): *δ* 8.33 (*d*, 10H, Ar-*H, J* = 9.0 Hz), 6.98 (*d*, 10H, Ar-*H, J* = 9.0 Hz), 4.70 (*s*, 10H, ArC*H*$_2$Ar), 4.05 (*broad*, 20H, O*CH*$_2$), 1.98 (*m*, 10H, CH$_2$*CH*(CH$_3$)$_2$), 1.80 (*m*, 20H, *CH*$_2$CH(CH$_3$)$_2$), 1.06 (*d*, 30H, CH$_2$CH(C*H*$_3$)$_2$, *J* = 6.6 Hz), 1.02 (*d*, 30H, CH$_2$CH(C*H*$_3$)$_2$, *J* = 6.6 Hz). ^{13}C{^{1}H} NMR (CD_2Cl_2, 150 MHz, 298 K): *δ* 151.8, 130.3, 125.5, 123.8, 114.7, 68.4, 39.1, 25.7, 23.0, 22.9, 21.3. HRMS (FT-ICR MALDI) m/z [M]$^+$ calcd for $C_{105}H_{140}O_{10}$: 1561.0447; found: 1561.0423.

Derivative PrS[5]^{iHex}:

M.p.: 205.6-206.2. ^{1}H NMR (CD_2Cl_2, 600 MHz, 298 K): *δ* 8.43 (*d*, 10H, Ar-*H, J* = 9.0 Hz), 7.00 (*d*, 10H, Ar-*H, J* = 9.6 Hz), 4.70 (*s*, 10H, ArC*H*$_2$Ar), 4.03 (*broad*, 20H, O*CH*$_2$), 1.92 (*m*, 20H, *CH*$_2$CH$_2$CH(CH$_3$)$_2$), 1.69 (*m*, 10H, CH$_2$CH$_2$*CH*(CH$_3$)$_2$), 1.50 (*m*, 20H, CH$_2$*CH*$_2$CH(CH$_3$)$_2$), 0.99-0.97 (*overlapped*, 60H, CH$_2$CH$_2$CH(C*H*$_3$)$_2$). ^{13}C{^{1}H} NMR (CD_2Cl_2, 150 MHz, 298 K): *δ* 151.7, 130.4, 125.6, 123.9, 114.8, 70.5, 36.0, 28.4, 28.3, 22.9, 22.8, 21.2. HRMS (FT-ICR MALDI) m/z [M]$^+$ calcd for $C_{115}H_{160}O_{10}$: 1701.2012; found: 1701.2007.

Derivative PrS[5]^{MeCy}:

M.p.: 201.4-202.2. ^{1}H NMR (CD_2Cl_2, 400 MHz, 298 K): *δ* 8.24 (*d*, 10H, Ar-*H, J* = 9.6 Hz), 6.92 (*d*, 10H, Ar-*H, J* = 9.3 Hz), 4.68 (*s*, 10H, ArC*H*$_2$Ar), 3.74 (*m*, 20H, O*CH*$_2$), 2.01-1.70 (*overlapped*, 50H, *CH* and *CH*$_2$ of cyclohexyl groups), 1.53-1.32 (*overlapped*, 60H, *CH*$_2$ of cyclohexyl groups). ^{13}C{^{1}H} NMR (CD_2Cl_2, 100 MHz, 298 K): *δ* 152.0, 130.1, 125.5, 123.6, 114.7, 75.6, 38.7, 30.6, 30.1, 27.0, 26.4, 26.3, 21.3 HRMS (FT-ICR MALDI) m/z [M]$^+$ calcd for $C_{125}H_{160}O_{10}$: 1821.2012; found: 1821.2027.

Derivative PrS[5]^{EtCy}:

M.p.: 170.8-171.6. ^{1}H NMR (CD_2Cl_2, 400 MHz, 298 K): *δ* 8.29 (*d*, 10H, Ar-*H, J* = 9.4 Hz), 6.96 (*d*, 10H, Ar-*H, J* = 9.4 Hz), 4.69 (*s*, 10H, ArC*H*$_2$Ar), 4.02 (*m*, 20H, O*CH*$_2$), 1.90-1.67 (*overlapped*, 80H, *CH* and *CH*$_2$ of cyclohexyl groups), 1.37-1.16 (*overlapped*, 30H, *CH*$_2$ of cyclohexyl groups), 1.11-0.99 (*m*, 20H, *CH*$_2$ of cyclohexyl groups).^{13}C{^{1}H} NMR (CD_2Cl_2, 100 MHz, 298 K): *δ* 151.8, 130.2, 125.5, 123.7, 114.6, 68.0, 37.8, 35.2, 34.0, 33.9, 27.0, 26.9, 26.8, 21.4. HRMS (FT-ICR MALDI) m/z [M]$^+$ calcd for $C_{135}H_{180}O_{10}$: 1961.3577; found: 1961.3554.

Derivative PrS[5]^{PrCy}:

M.p.: 159.5-160.4. ^{1}H NMR (CD_2Cl_2, 400 MHz, 298 K): *δ* 8.39 (*d*, 10H, Ar-*H, J* = 8.6 Hz), 6.98 (*d*, 10H, Ar-*H, J* = 8.6 Hz), 4.69 (*s*, 10H, ArC*H*$_2$Ar), 4.00 (*broad*, 20H, O*CH*$_2$), 1.90-0.87 (*overlapped*, 150H, *CH* and *CH*$_2$ of cyclohexyl groups). ^{13}C{^{1}H} NMR (CD_2Cl_2, 100 MHz, 298 K): *δ* 151.8, 130.4, 125.6, 123.9, 114.8, 70.6, 38.1, 34.6, 34.0, 33.9, 27.8, 27.2,

26.9, 26.9, 21.3. HRMS (FT-ICR MALDI) m/z $[M]^+$ calcd for $C_{145}H_{200}O_{10}$: 2101.5142; found: 2101.5132.

Derivative PrS[5]^{BuCy}:

M.p.: 64.8-65.2. ^{1}H NMR ($CDCl_3$, 400 MHz, 298 K): *δ* 8.55 (*d*, 10H, Ar-*H, J* = 9.6 Hz), 6.98 (*d*, 10H, Ar-*H, J* = 9.6 Hz), 4.70 (*s*, 10H, ArC*H*$_2$Ar), 4.10 (*m*, 10H, O*CH*$_2$), 4.02 (*m*, 10H, O*CH*$_2$), 1.89 (*m*, 20H, *CH*$_2$CH$_2$CH$_2$Cy), 0.87-0.94, 1.12-1.33, 1.56-1.76 (*overlapped*, 150H, cyclohexyl and methylene protons). ^{13}C{^{1}H} NMR ($CDCl_3$, 100 MHz, 298 K): *δ* 151.4, 130.5, 125.7, 123.9, 115.0, 70.2, 37.9, 37.7, 33.6, 33.5, 30.5, 26.9, 26.6, 26.6, 24.0, 20.9. HRMS (FT-ICR MALDI) m/z $[M]^+$ calcd for $C_{155}H_{220}O_{10}$: 2241.6707; found: 2241.6736.

Derivative PrS[5]^{MecHp}:

M.p.: 163.2-164.2. ^{1}H NMR (CD_2Cl_2, 600 MHz, 298 K): *δ* 8.34 (*d*, 10H, Ar-*H, J* = 9.4 Hz), 6.95 (*d*, 10H, Ar-*H, J* = 9.3 Hz), 4.69 (*s*, 10H, ArC*H*$_2$Ar), 3.79 (*m*, 20H, O*CH*$_2$), 2.11 (*m*, 10H, OCH$_2$*CH*), 2.02-1.96 (m, 20H, *CH*$_2$ of cyclohexyl groups), 1.79-1.76 (m, 20H, *CH*$_2$ of cyclohexyl groups), 1.65-1.47 (overlapped, 80H, *CH*$_2$ of cyclohexyl groups).^{13}C{^{1}H} NMR (CD_2Cl_2, 150 MHz, 298 K): *δ* 151.9, 130.3, 125.6, 123.8, 114.9, 75.7, 40.2, 31.8, 29.2, 27.0, 27.0, 21.4. HRMS (FT-ICR MALDI) m/z $[M]^+$ calcd for $C_{135}H_{180}O_{10}$: 1961.3577; found: 1961.3531.

Derivative PrS[5]^{EtcHp}:

M.p.: 145.8-146.4. ^{1}H NMR (CD_2Cl_2, 600 MHz, 298 K): *δ* 8.32 (*d*, 10H, Ar-*H, J* = 9.6 Hz), 6.97 (*d*, 10H, Ar-*H, J* = 9.0 Hz), 4.68 (*s*, 10H, ArC*H*$_2$Ar), 4.02 (*m*, 20H, O*CH*$_2$), 1.89 -1.30 (*overlapped*, 150H, cycloheptyl and methylene protons). ^{13}C{^{1}H} NMR (CD_2Cl_2, 150 MHz, 298 K): *δ* 151.8, 130.3, 125.5, 123.8, 114.7, 68.6, 38.4, 36.8, 35.2, 35.1, 29.0, 28.9, 26.9, 26.8, 21.3. HRMS (FT-ICR MALDI) m/z $[M]^+$ calcd for $C_{145}H_{200}O_{10}$: 2101.5142; found: 2101.5125.

Derivative PrS[5]^{MePh}:

M.p.: > 240 °C dec. ^{1}H NMR (CD_2Cl_2, 600 MHz, 298 K): *δ* 8.04 (*broad*, 10H, Ar-*H*), 7.29-7.36 (*overlapped*, 50H, OCH$_2$Ar-*H,*), 6.79 (*broad*, 10H, Ar-*H*), 4.80 (*overlapped*, 30H, ArC*H*$_2$Ar and O*CH*$_2$). ^{13}C{^{1}H} NMR (CD_2Cl_2, 75 MHz, 298 K): *δ* 152.3, 138.6, 129.9, 128.8, 128.0, 127.6, 125.3, 123.9, 115.0, 71.6, 22.2. HRMS (FT-ICR MALDI) m/z $[M]^+$ calcd for $C_{125}H_{100}O_{10}$: 1760.7316; found: 1760.7330.

Derivative PrS[5]^{BuPh}:

M.p.: 68.8-69.7. ^{1}H NMR (CD_2Cl_2, 600 MHz, 298 K): *δ* 8.37 (*broad*, 10H, Ar-*H*), 7.14-7.26 (*overlapped*, 50H, OCH$_2$Ar-*H,*), 6.90 (*d*, 10H, Ar-*H, J* = 8.4 Hz), 4.68 (*s*, 10H, ArC*H*$_2$Ar), 3.95 (*broad*, 20H, O*CH*$_2$), 2.74 (*t*, 20H, O(CH$_2$)$_3$*CH*$_2$Ar, *J* = 7.2 Hz), 1.91 (*overlapped*, 40H, OCH$_2$(*CH*$_2$)$_2$CH$_2$Ar). ^{13}C{^{1}H} NMR (CD_2Cl_2, 150 MHz, 298 K): *δ* 151.7, 142.9, 130.4, 128.8, 128.7, 126.1, 125.5, 124.0, 114.9, 70.0, 36.2, 30.0, 28.8, 21.3. HRMS (FT-ICR MALDI) m/z $[M]^+$ calcd for $C_{155}H_{160}O_{10}$: 2181.2012; found: 2181.2005.

Copies of 1D and 2D NMR and HR Mass Spectra of PrS[5]^{R}

Copies of 1D and 2D NMR and HR mass spectrum of derivative PrS[5]^{nBu}

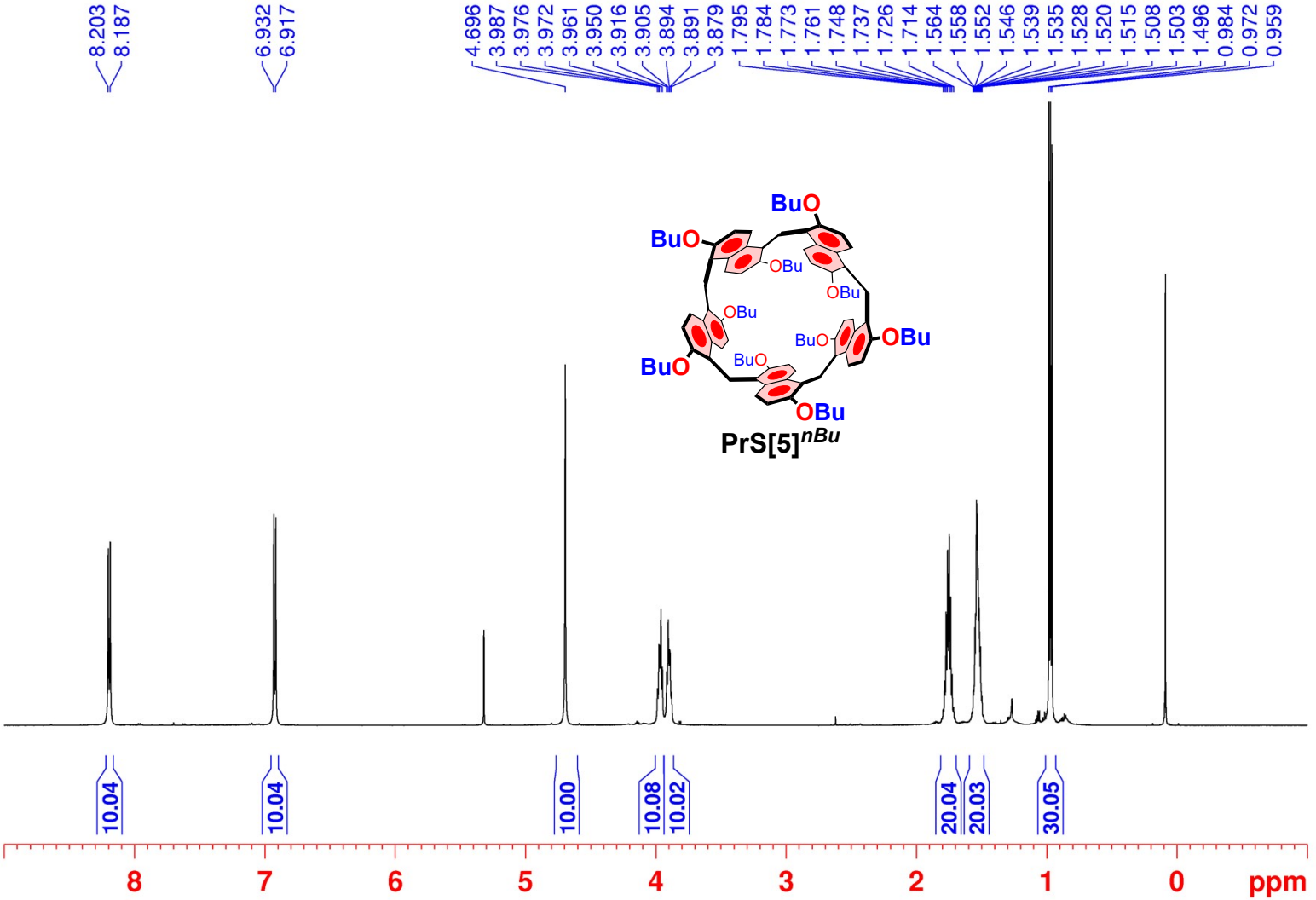

Figure S1: ^{1}H NMR spectrum of derivative **PrS[5]^{nBu}** (CD_2Cl_2, 600 MHz, 298 K).

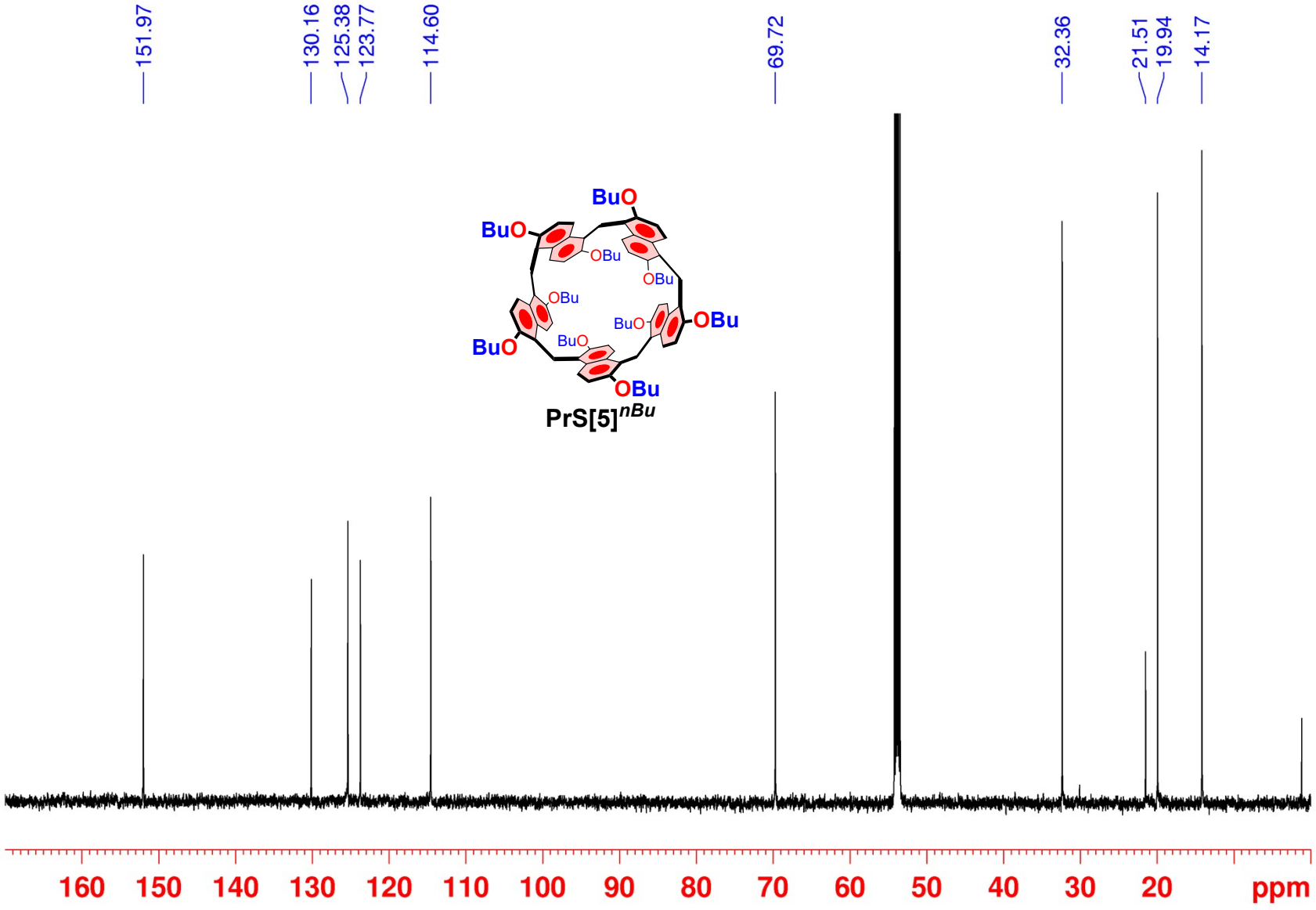

Figure S2: ^{13}C NMR spectrum of **PrS[5]^{nBu}** (CD_2Cl_2, 150 MHz, 298 K).

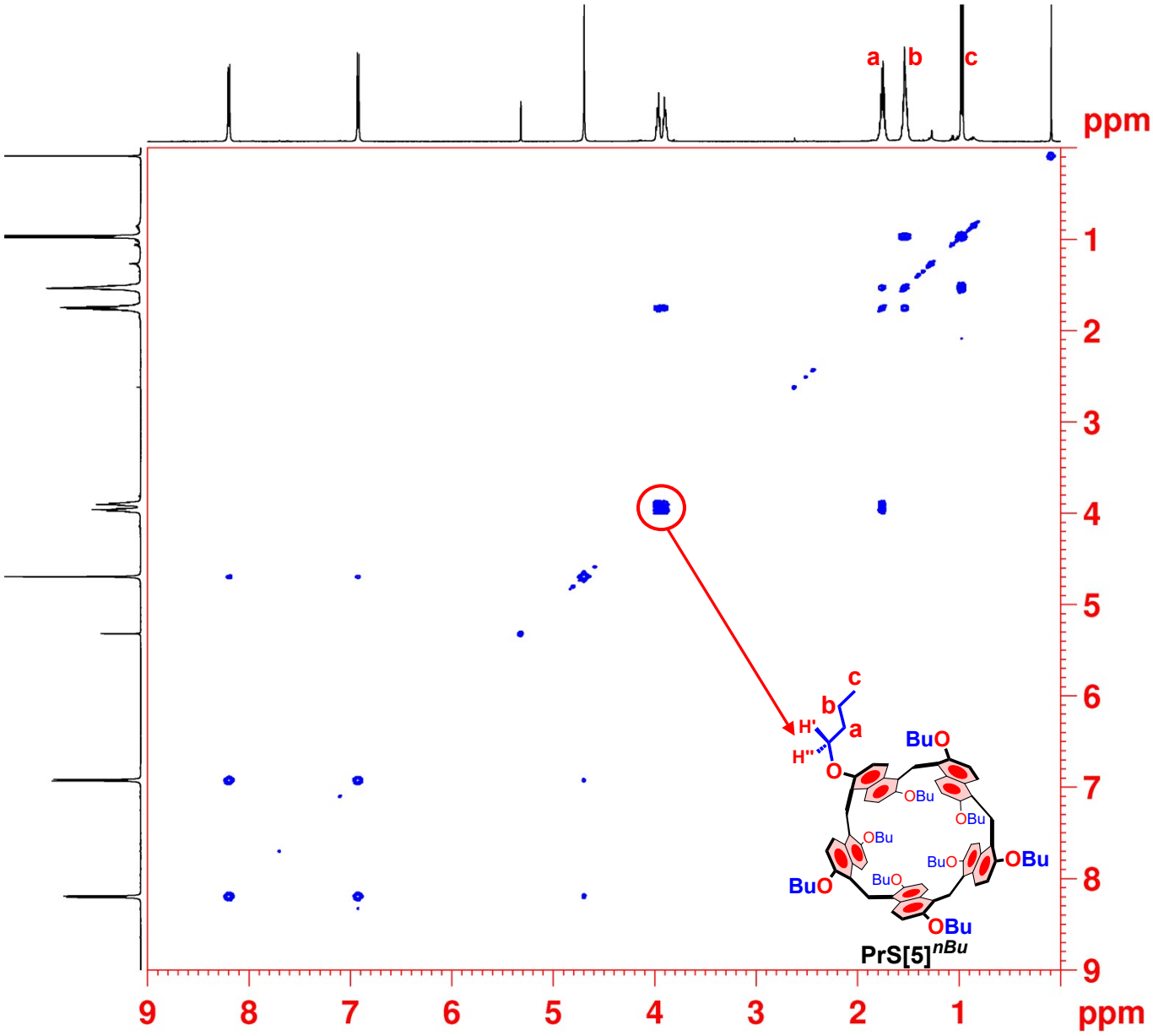

Figure S3: 2D-DQF COSY spectrum of **PrS[5]*nBu*** (CD_2Cl_2, 600 MHz, 298 K).

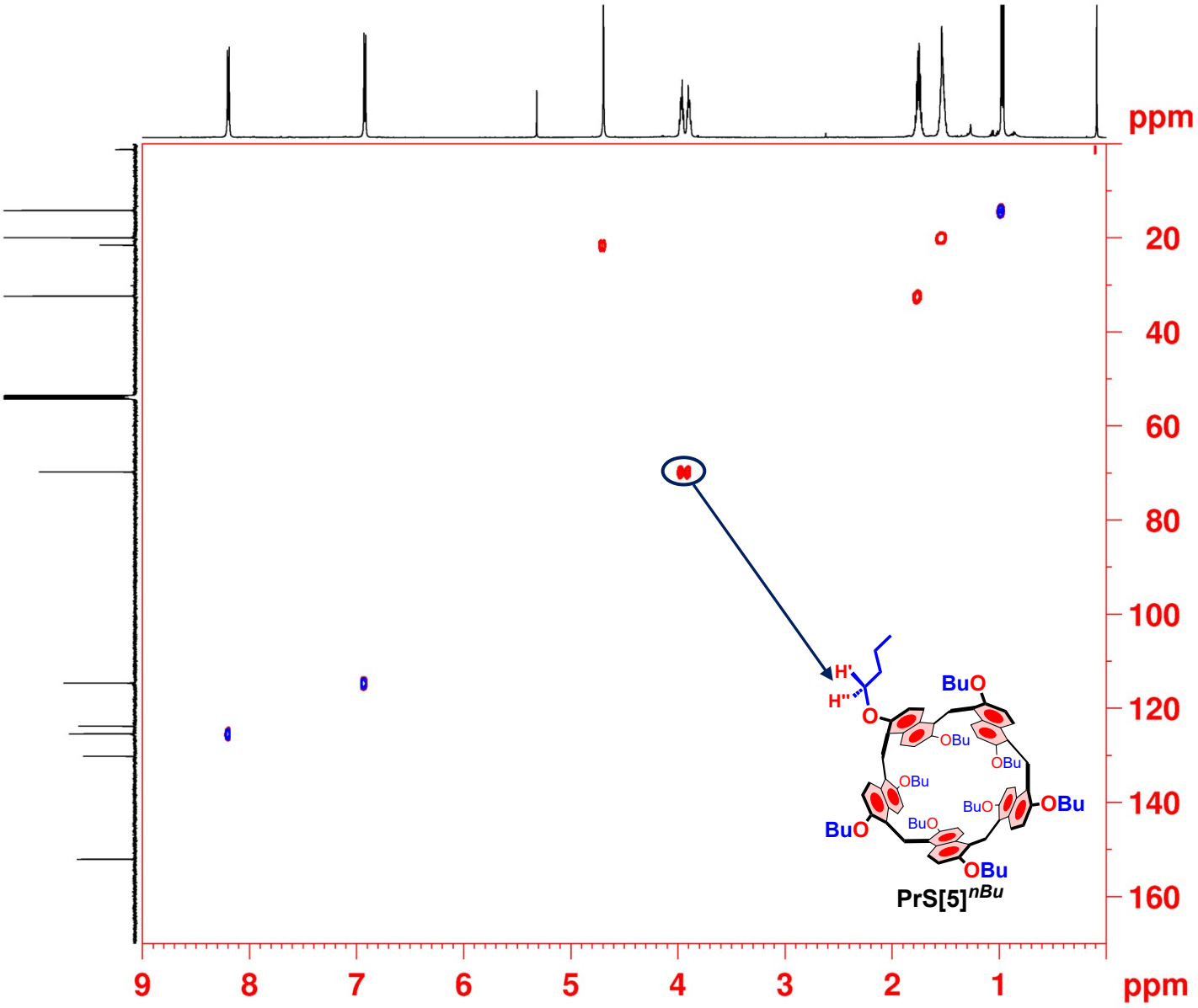

Figure S4: 2D-HSQC spectrum of **PrS[5]^{nBu}** (CD_2Cl_2, 600 MHz, 298 K).

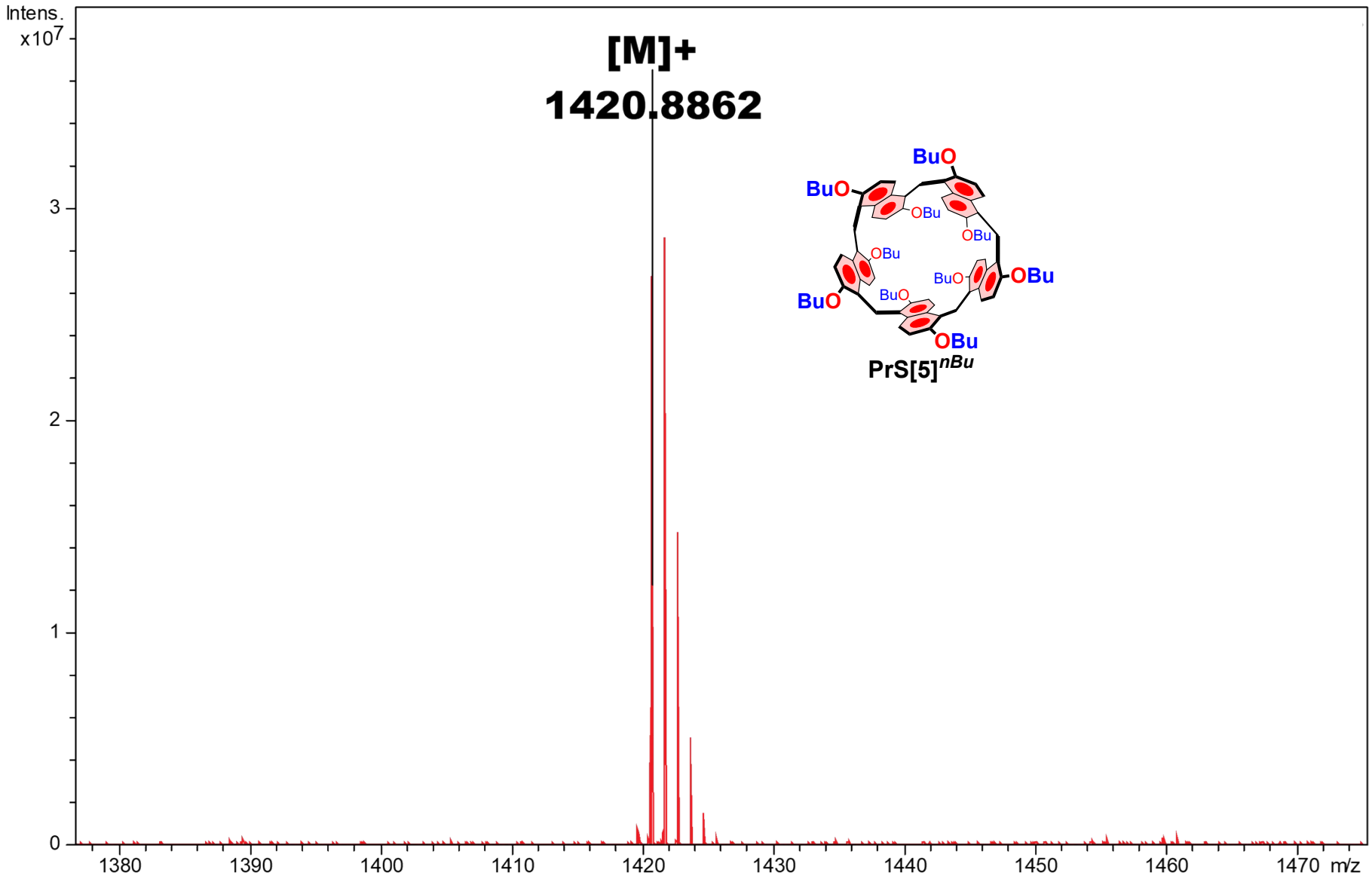

Figure S5: Significant portion of the HR MALDI FT-ICR mass spectrum of **PrS[5]**^{nBu} $[M]^+$.

Copies of 1D and 2D NMR and HR mass spectrum of derivative PrS[5]^{nPe}

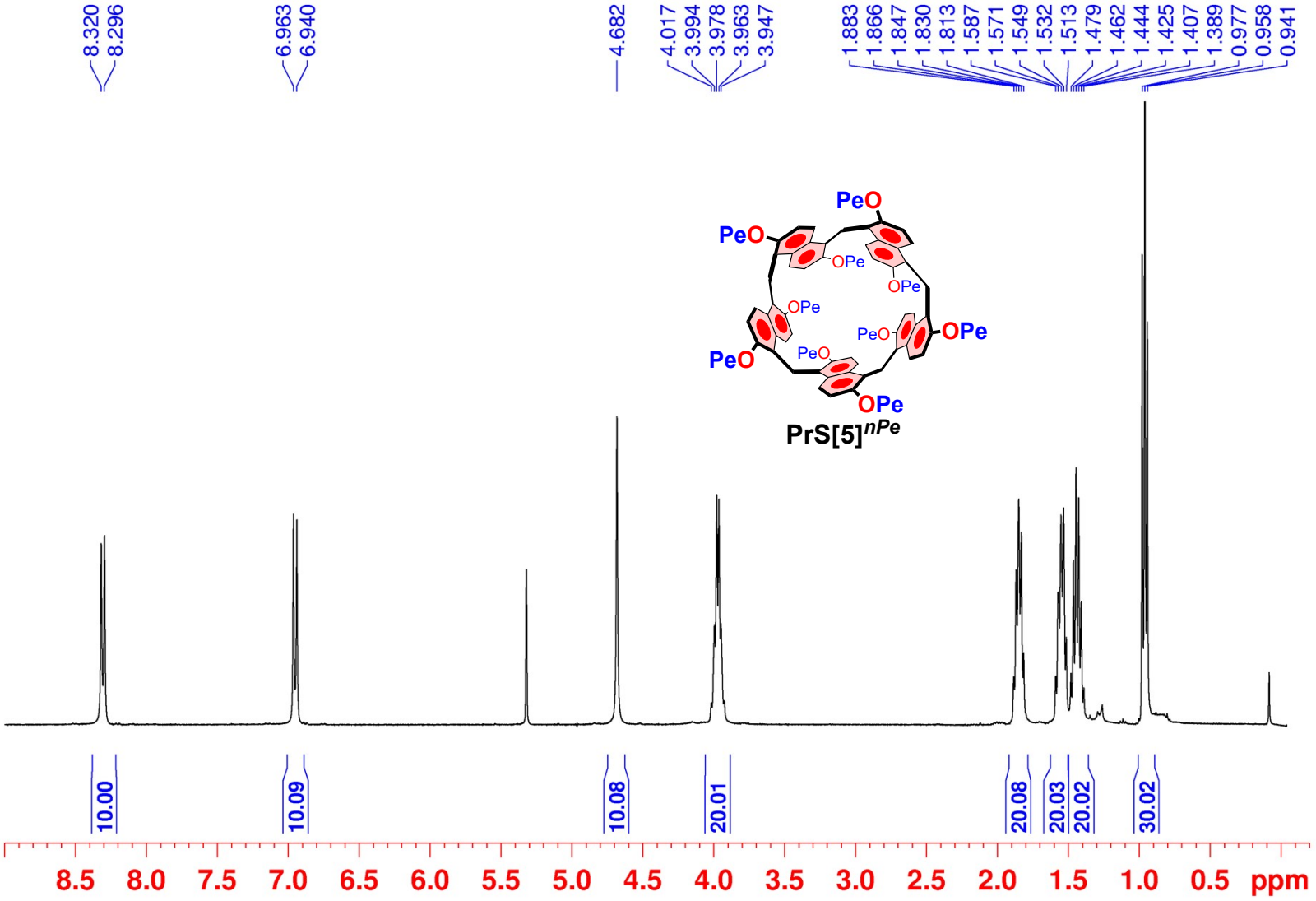

Figure S6: ^{1}H NMR spectrum of derivative **PrS[5]^{nPe}** (CD_2Cl_2, 400 MHz, 298 K).

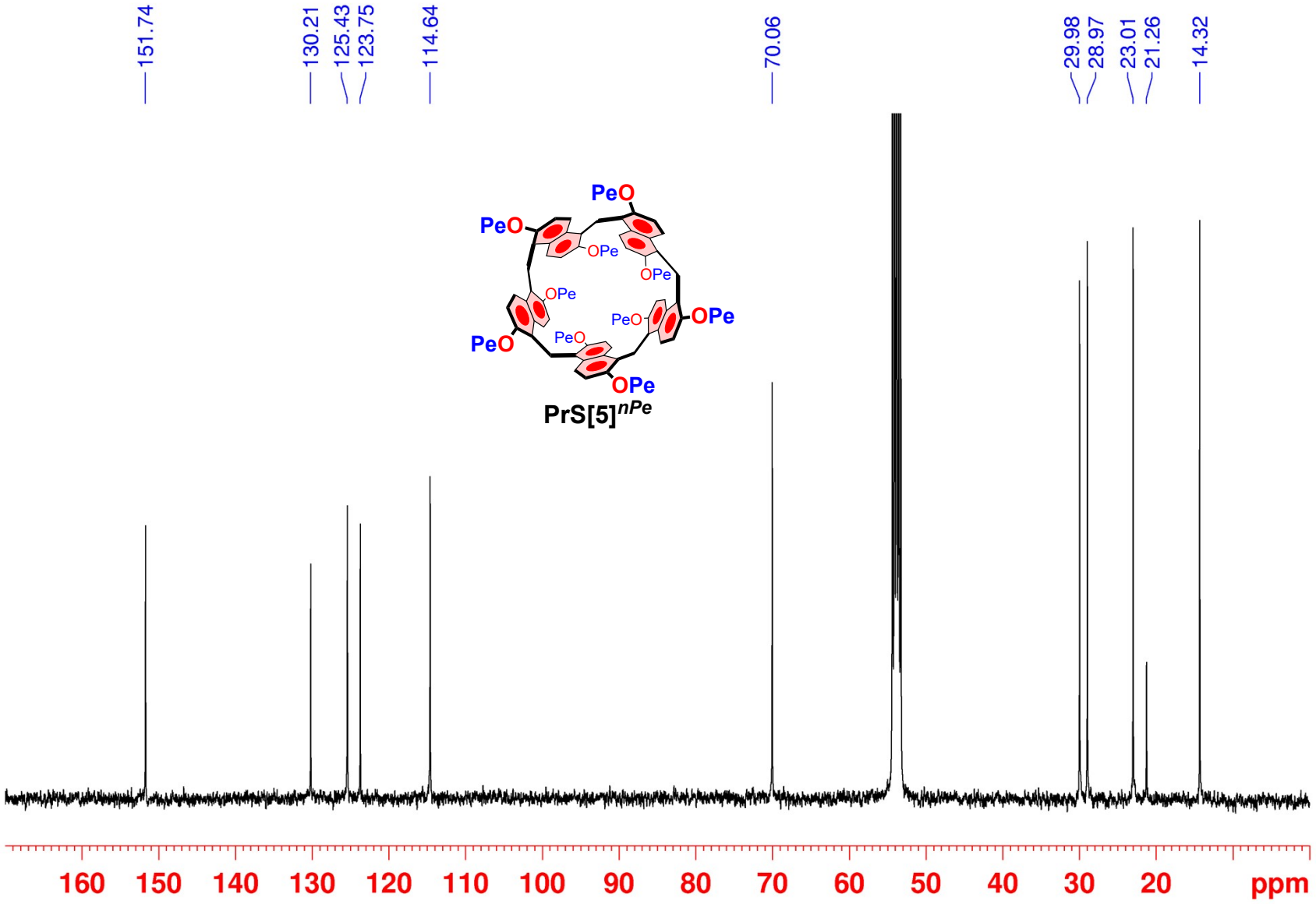

Figure S7: ^{13}C NMR spectrum of **PrS[5]^{nPe}** (CD_2Cl_2, 100 MHz, 298 K).

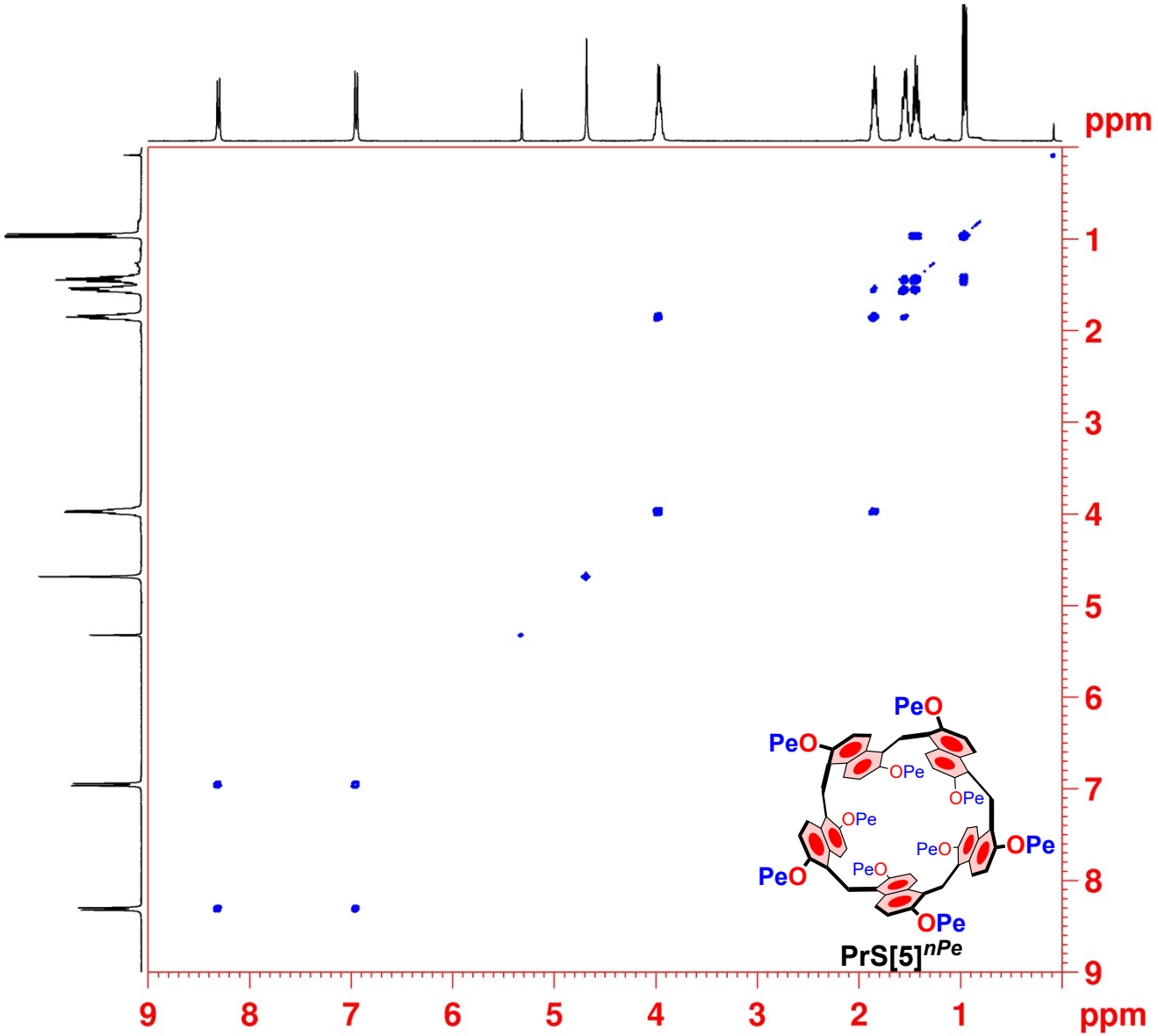

Figure S8: 2D-DQF COSY spectrum of **PrS[5]*nPe*** (CD_2Cl_2, 400 MHz, 298 K).

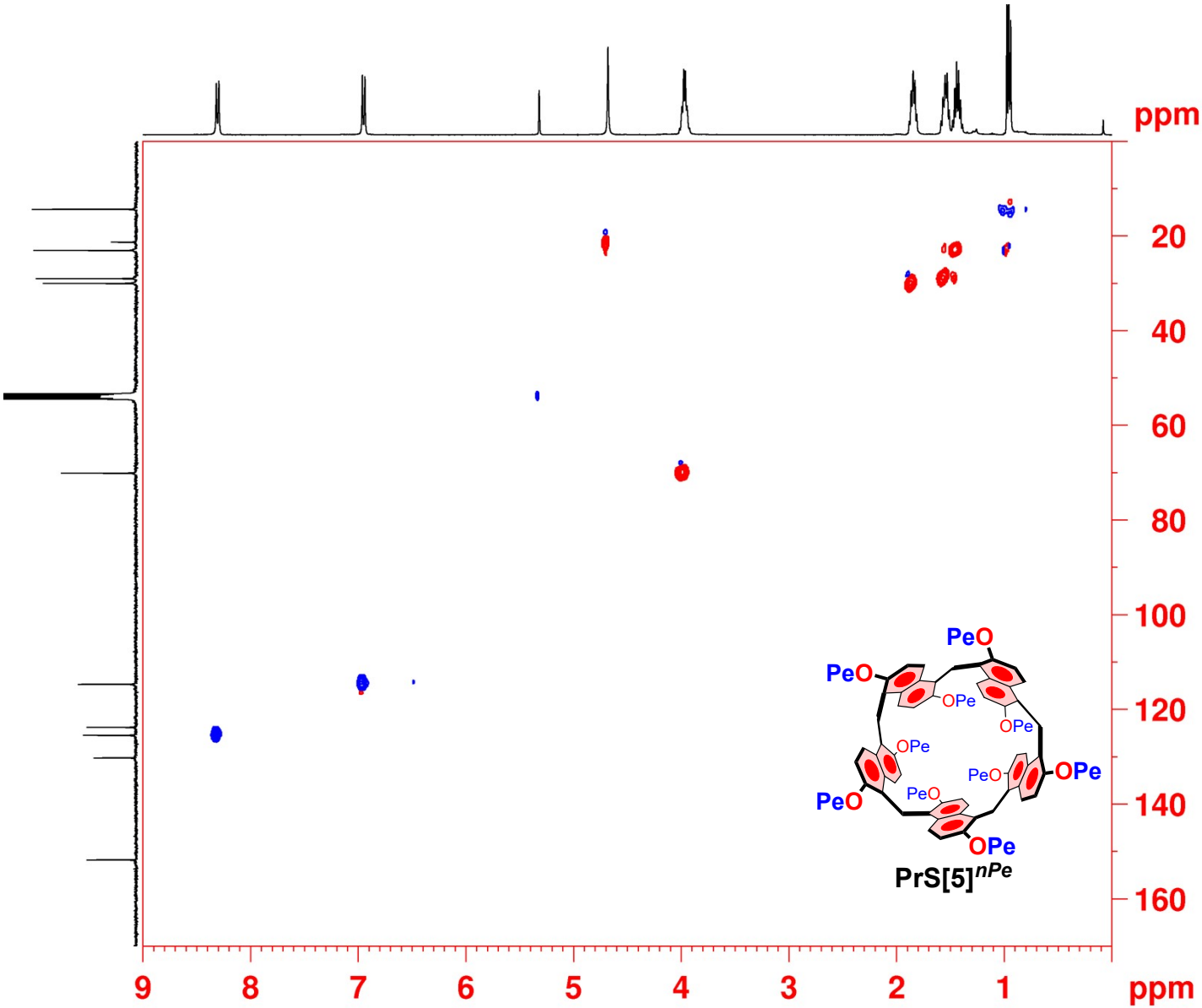

Figure S9: 2D-HSQC spectrum of **PrS[5]*nPe*** (CD_2Cl_2, 400 MHz, 298 K).

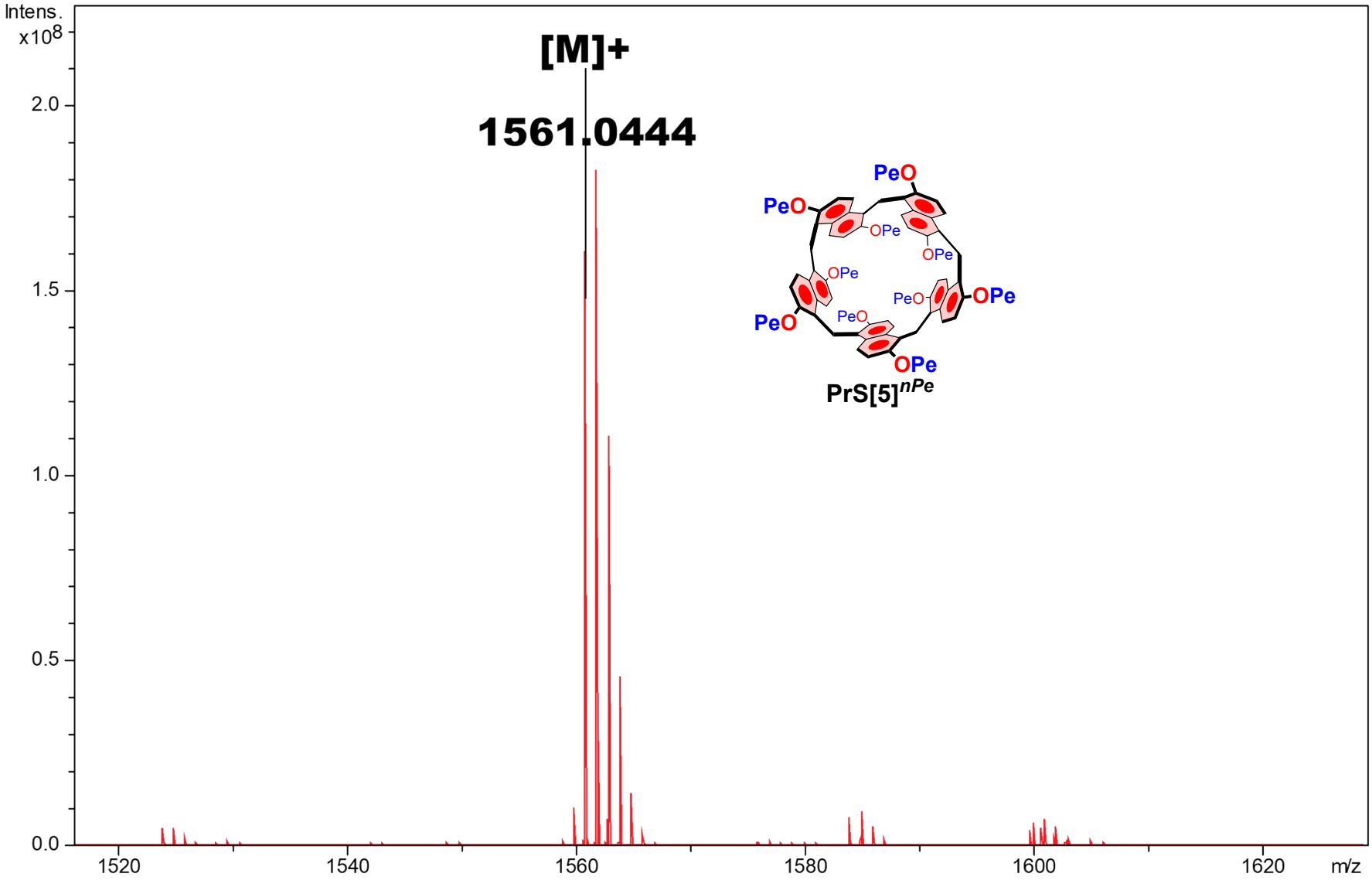

Figure S10: Significant portion of the HR MALDI FT-ICR mass spectrum of **PrS[5]*nPe*** $[M]^+$.

Copies of 1D and 2D NMR and HR mass spectrum of derivative PrS[5]^{nHex}

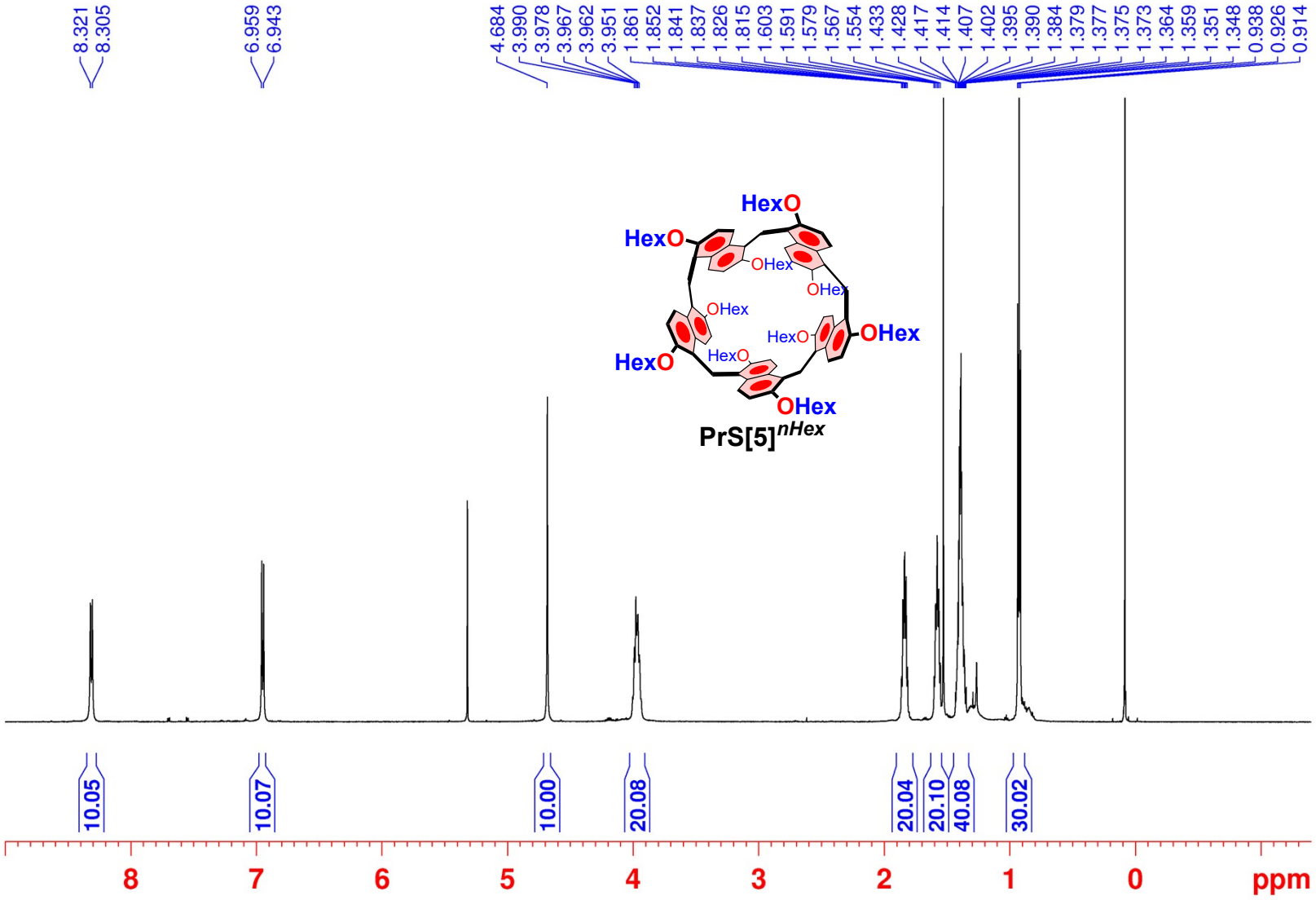

Figure S11: ^{1}H NMR spectrum of derivative **PrS[5]^{nHex}** (CD_2Cl_2, 600 MHz, 298 K).

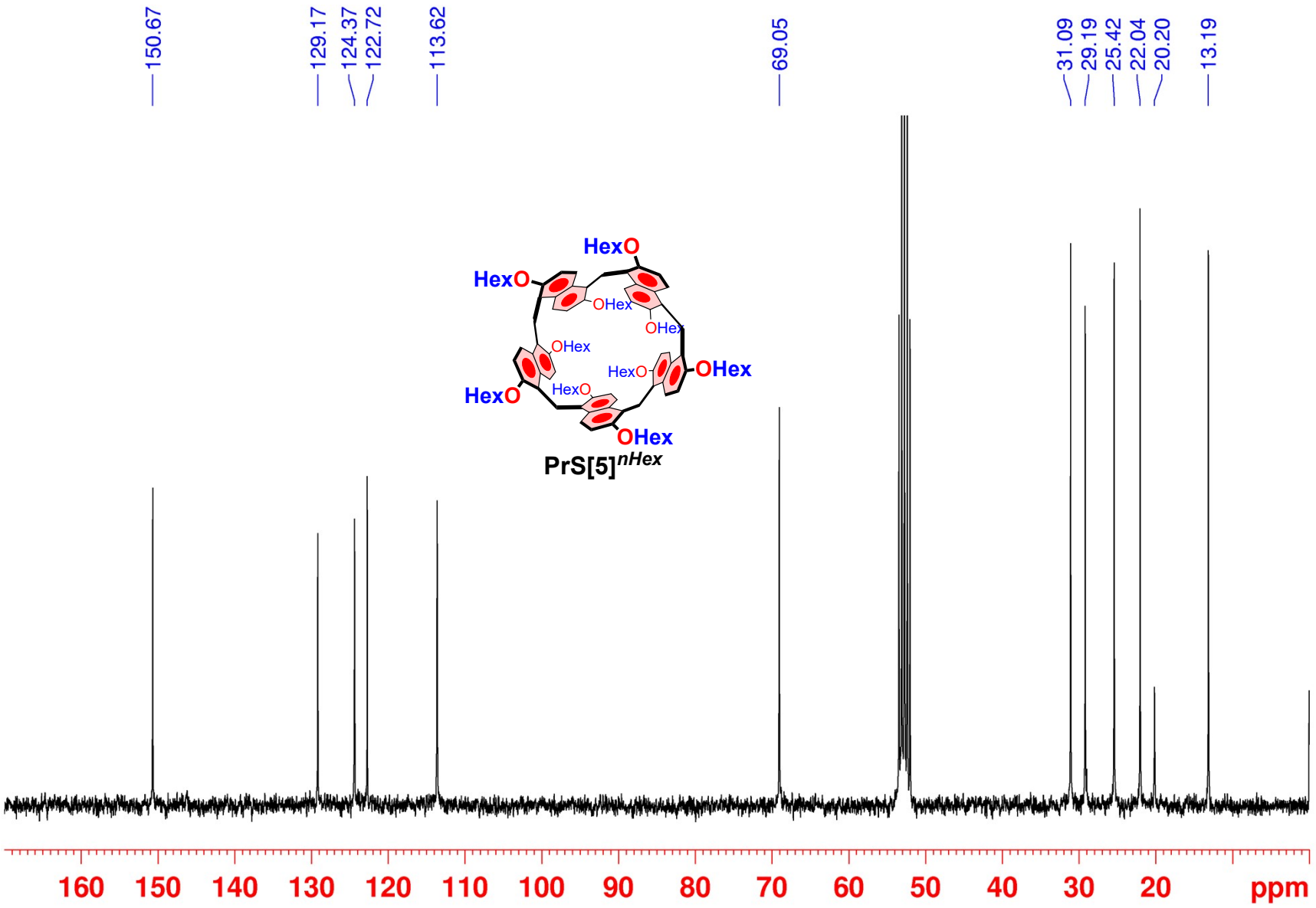

Figure S12: ^{13}C NMR spectrum of **PrS[5]*nHex*** (CD_2Cl_2, 75 MHz, 298 K).

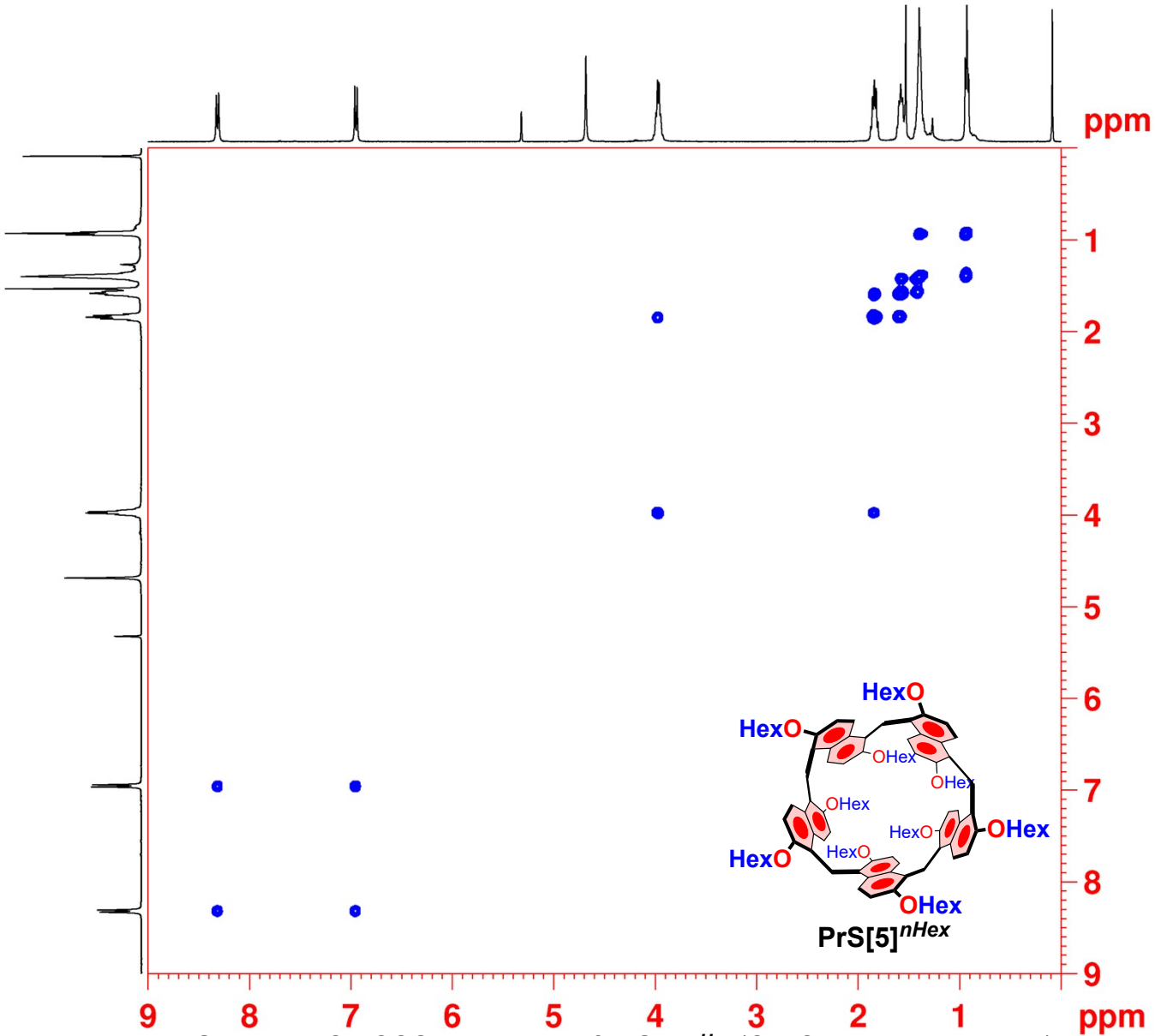

Figure S13: 2D-DQF COSY spectrum of **PrS[5]*nHex*** (CD_2Cl_2, 400 MHz, 298 K).

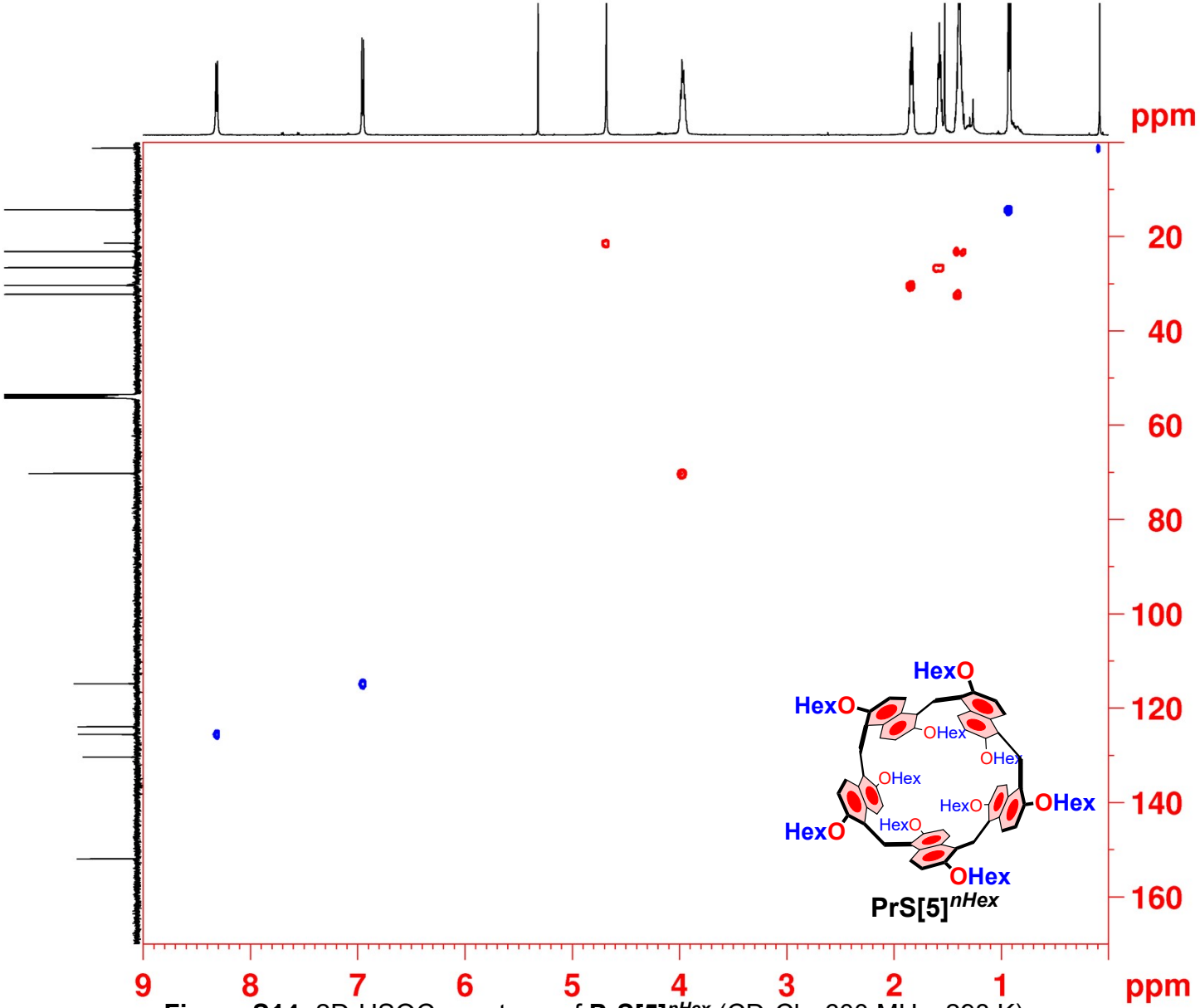

Figure S14: 2D-HSQC spectrum of **PrS[5]*nHex*** (CD_2Cl_2, 600 MHz, 298 K).

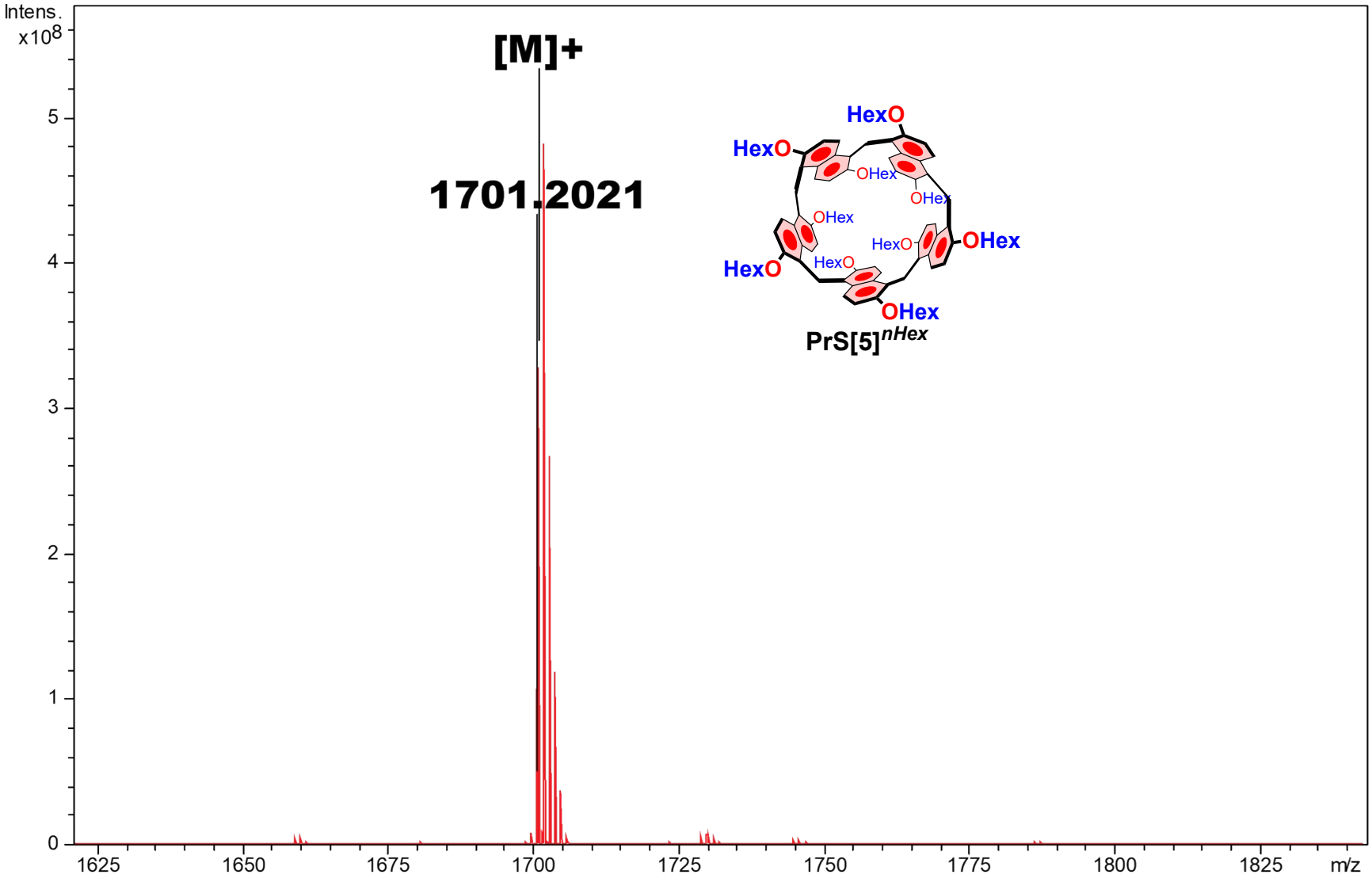

Figure S15: Significant portion of the HR MALDI FT-ICR mass spectrum of **PrS[5]*nHex*** $[M]^+$.

Copies of 1D and 2D NMR and HR mass spectrum of derivative PrS[5]^{Hp}

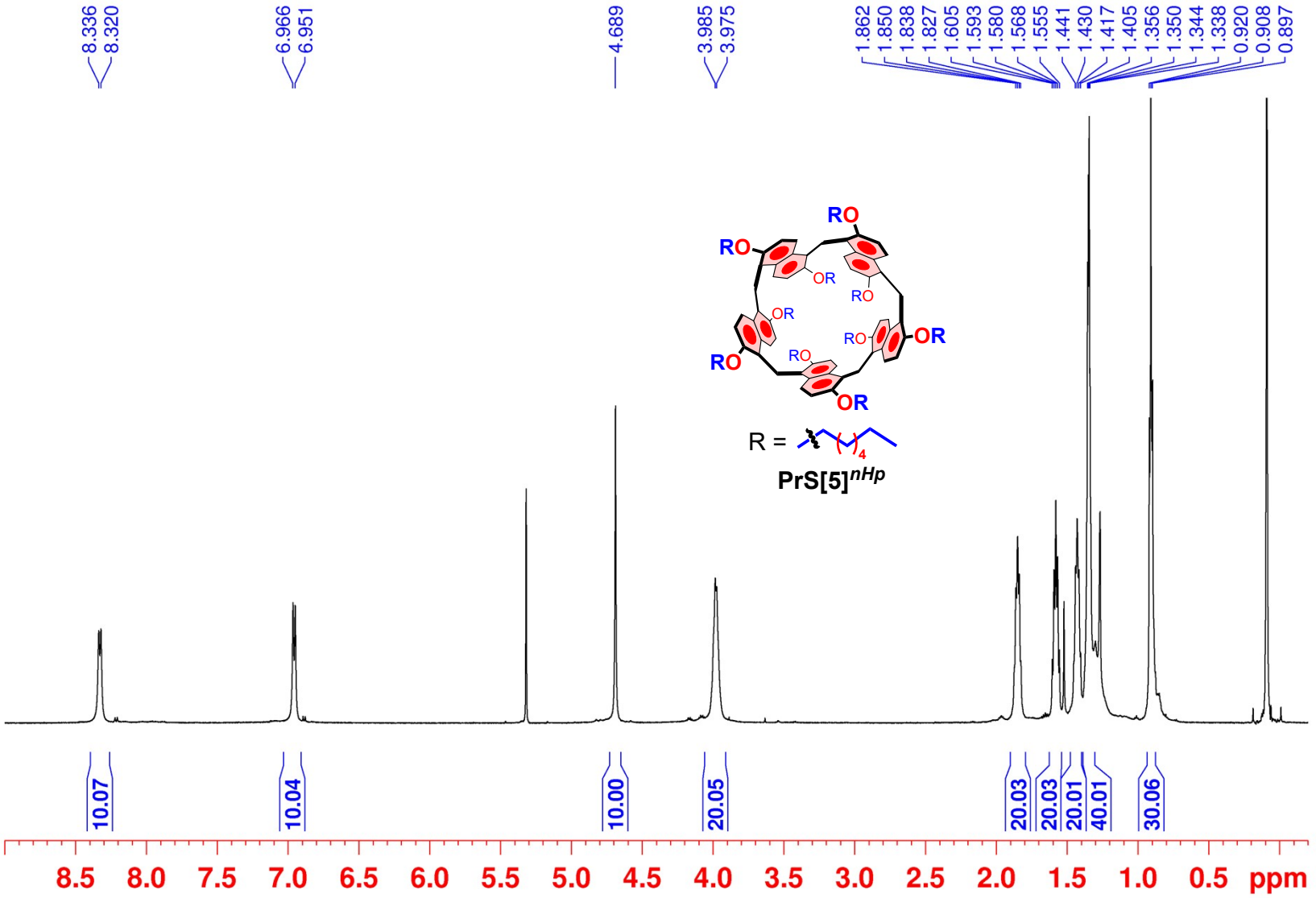

Figure S16: ^{1}H NMR spectrum of derivative **PrS[5]^{Hp}** (CD_2Cl_2, 600 MHz, 298 K).

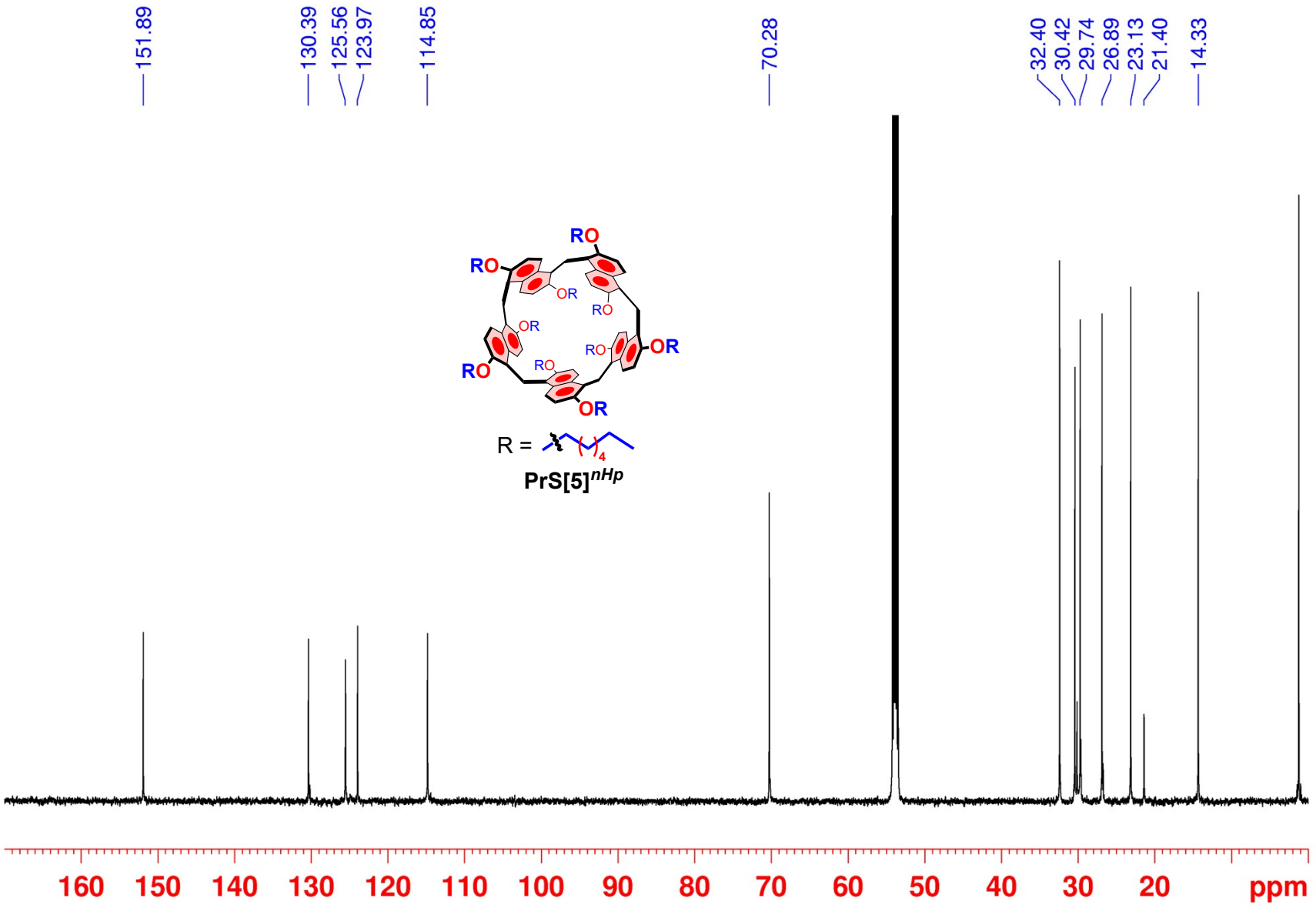

Figure S17: ^{13}C NMR spectrum of **PrS[5]^{Hp}** (CD_2Cl_2, 150 MHz, 298 K).

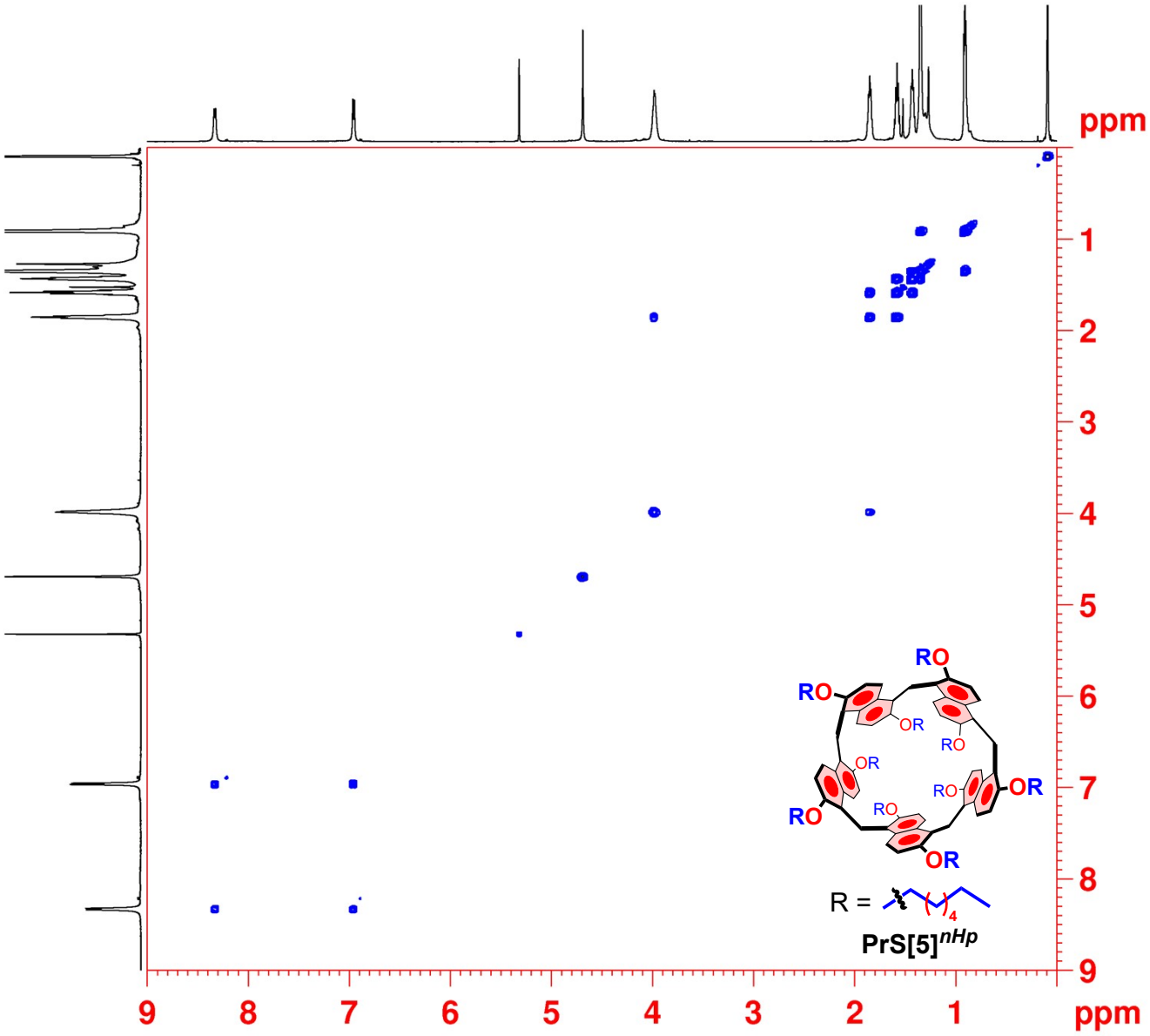

Figure S18: 2D-DQF COSY spectrum of **PrS[5]*Hp*** (CD_2Cl_2, 600 MHz, 298 K).

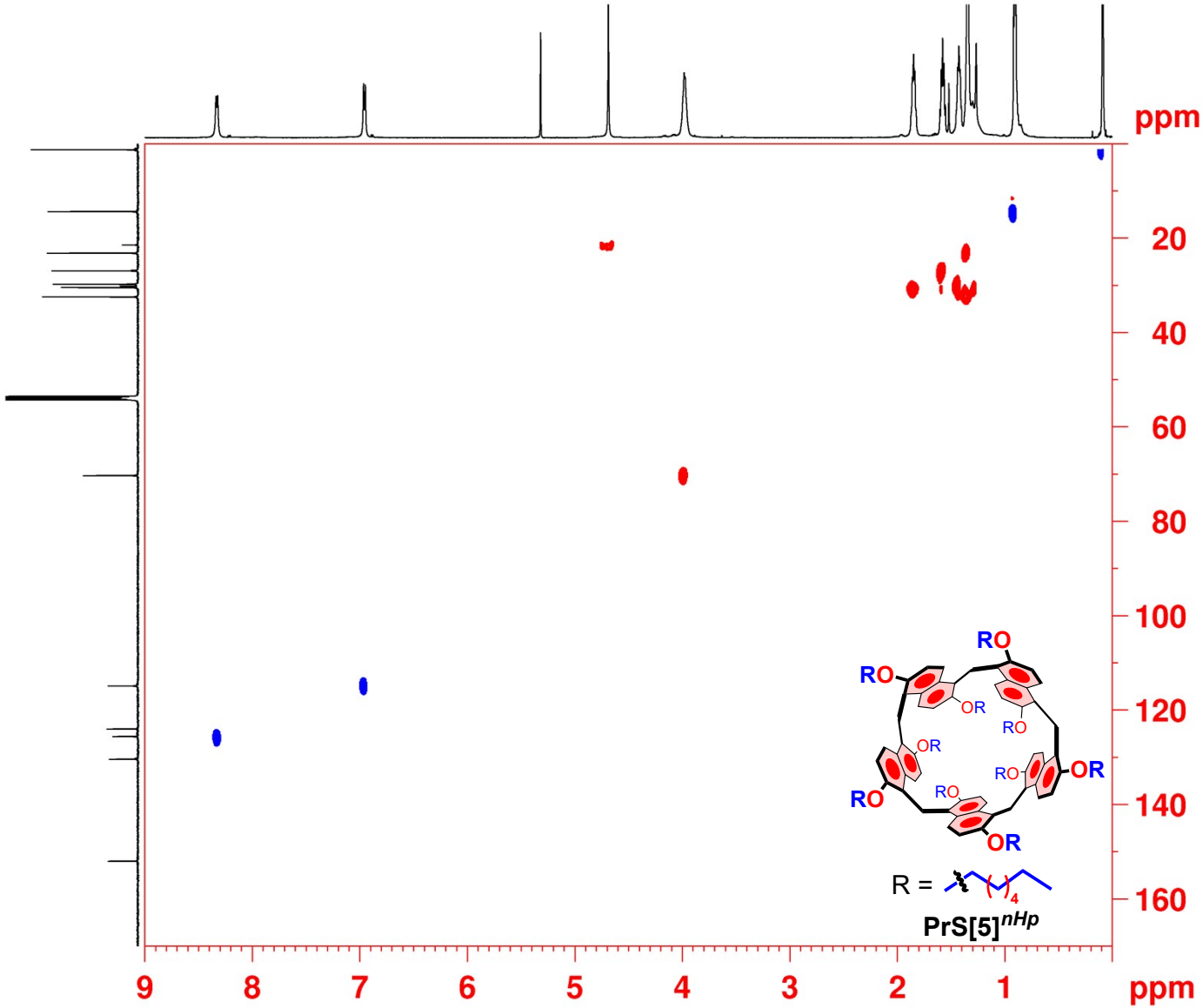

Figure S19: 2D-HSQC spectrum of **PrS[5]^{Hp}** (CD_2Cl_2, 600 MHz, 298 K).

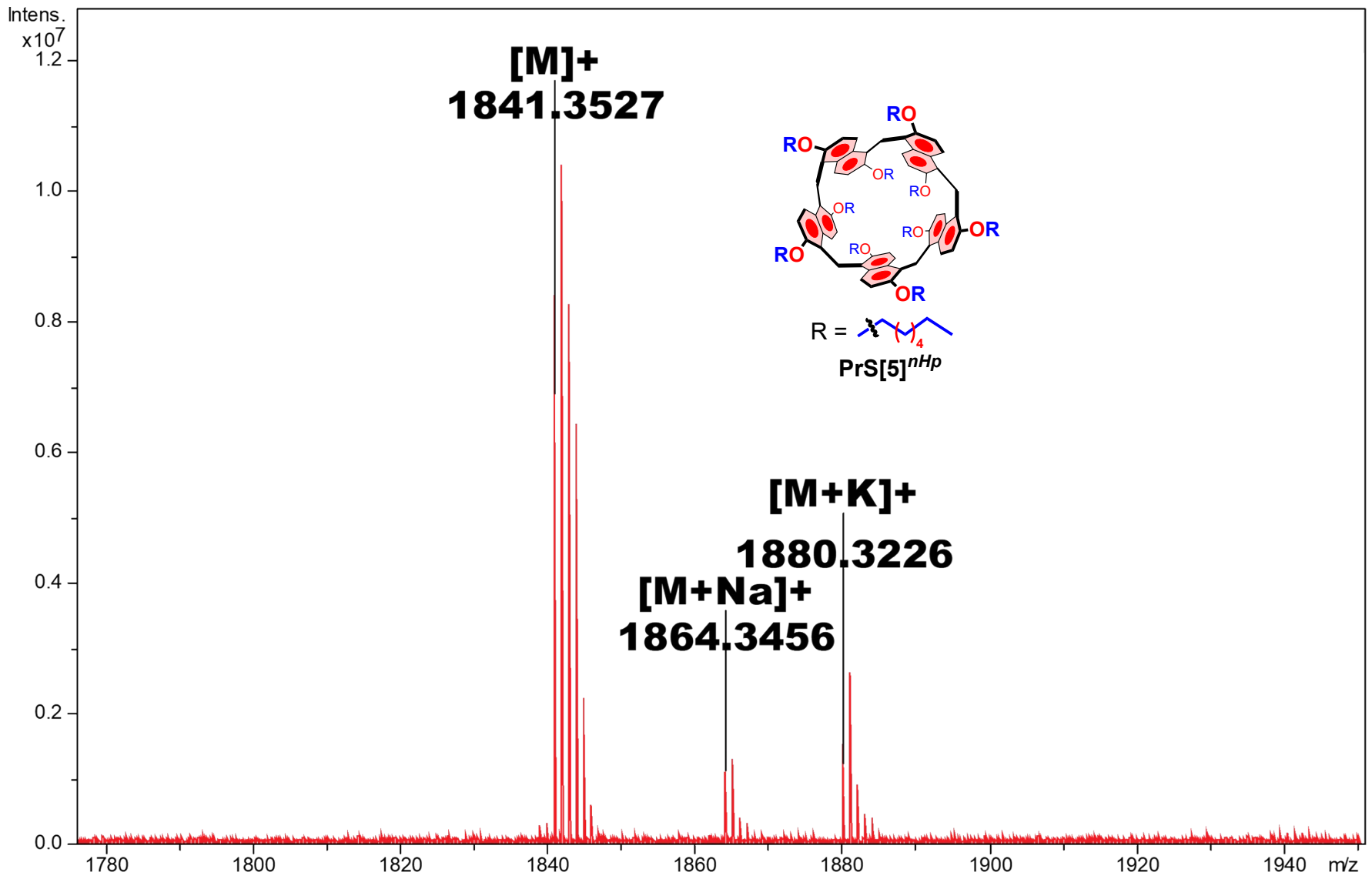

Figure S20: Significant portion of the HR MALDI FT-ICR mass spectrum of **PrS[5]^{Hp}** $[M]^+$, $[M+Na]^+$ and $[M+K]^+$.

Copies of 1D and 2D NMR and HR mass spectrum of derivative PrS[5]*Nonyl*

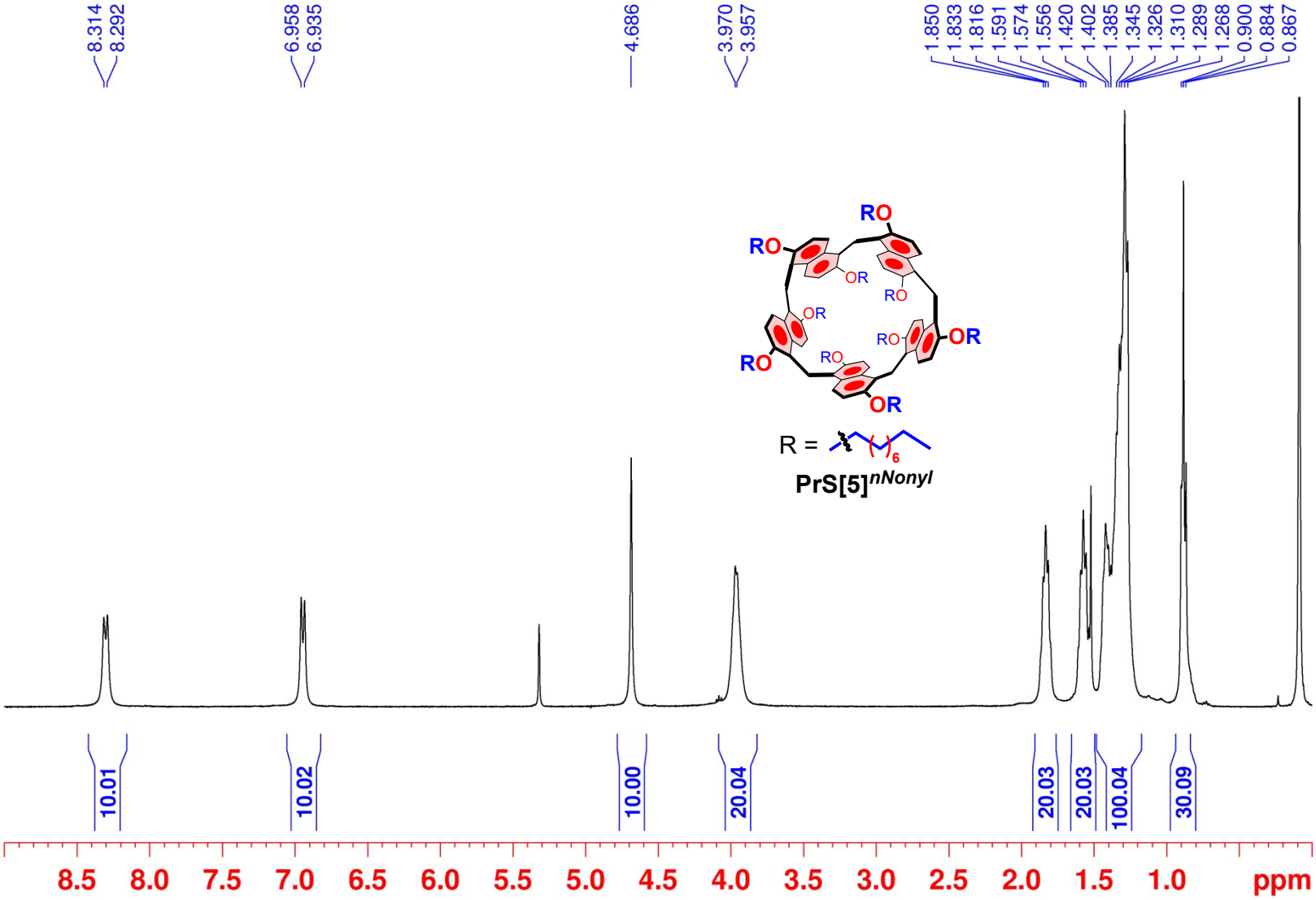

Figure S21: ^{1}H NMR spectrum of derivative **PrS[5]*Nonyl*** (CD_2Cl_2, 400 MHz, 298 K).

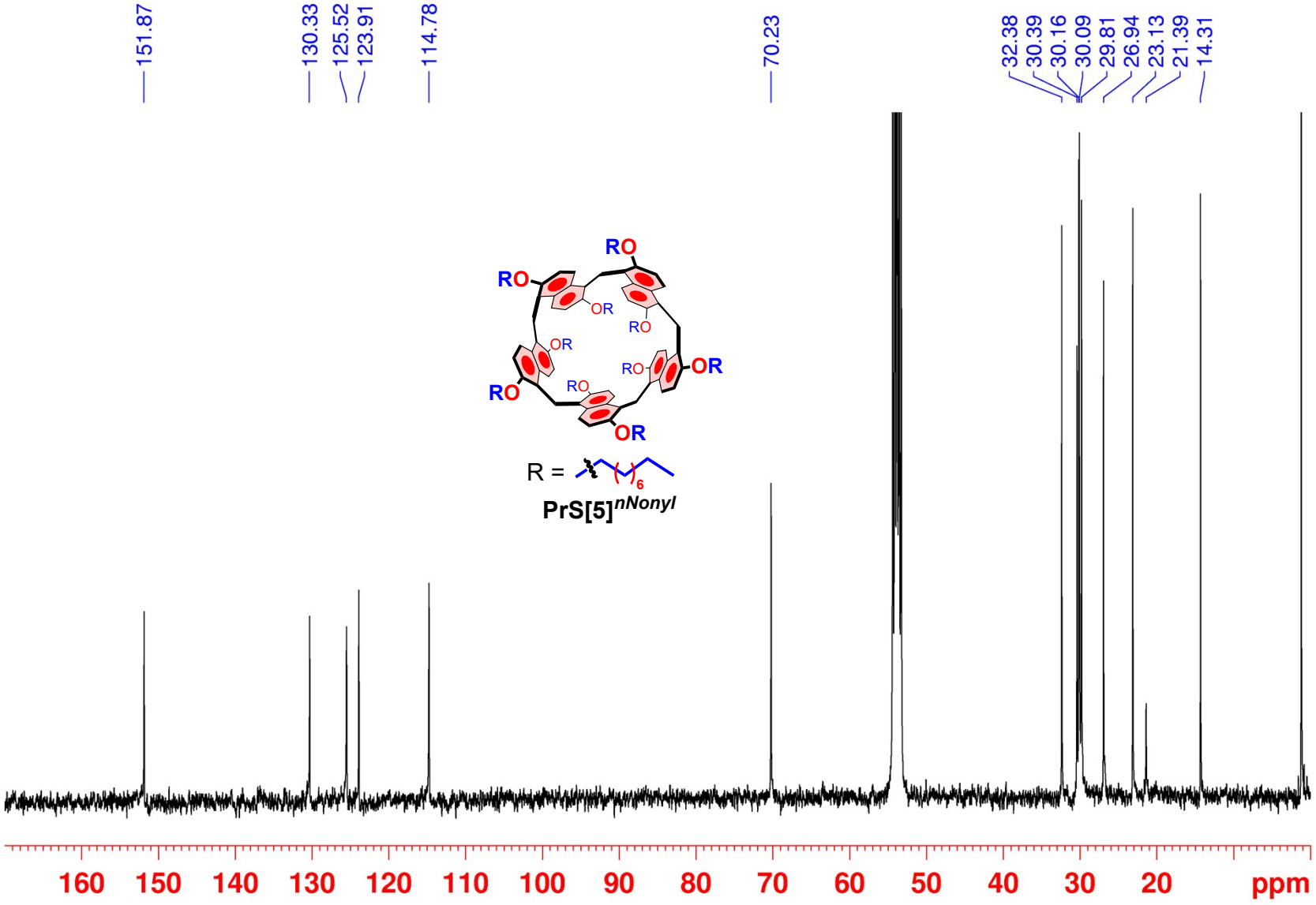

Figure S22: ^{13}C NMR spectrum of **PrS[5]*Nonyl*** (CD_2Cl_2, 100 MHz, 298 K).

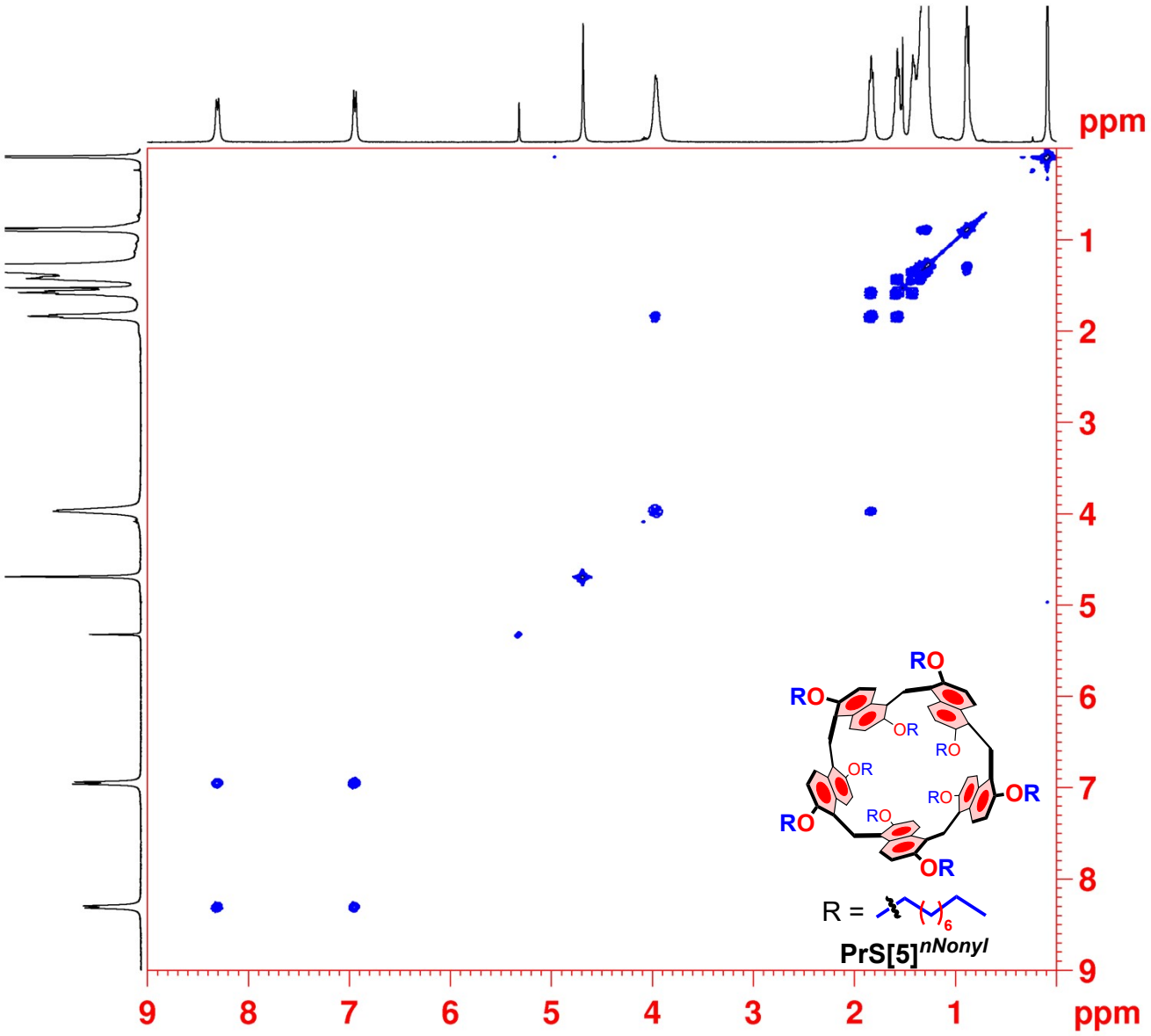

Figure S23: 2D-DQF COSY spectrum of **PrS[5]*Nonyl*** (CD_2Cl_2, 600 MHz, 298 K).

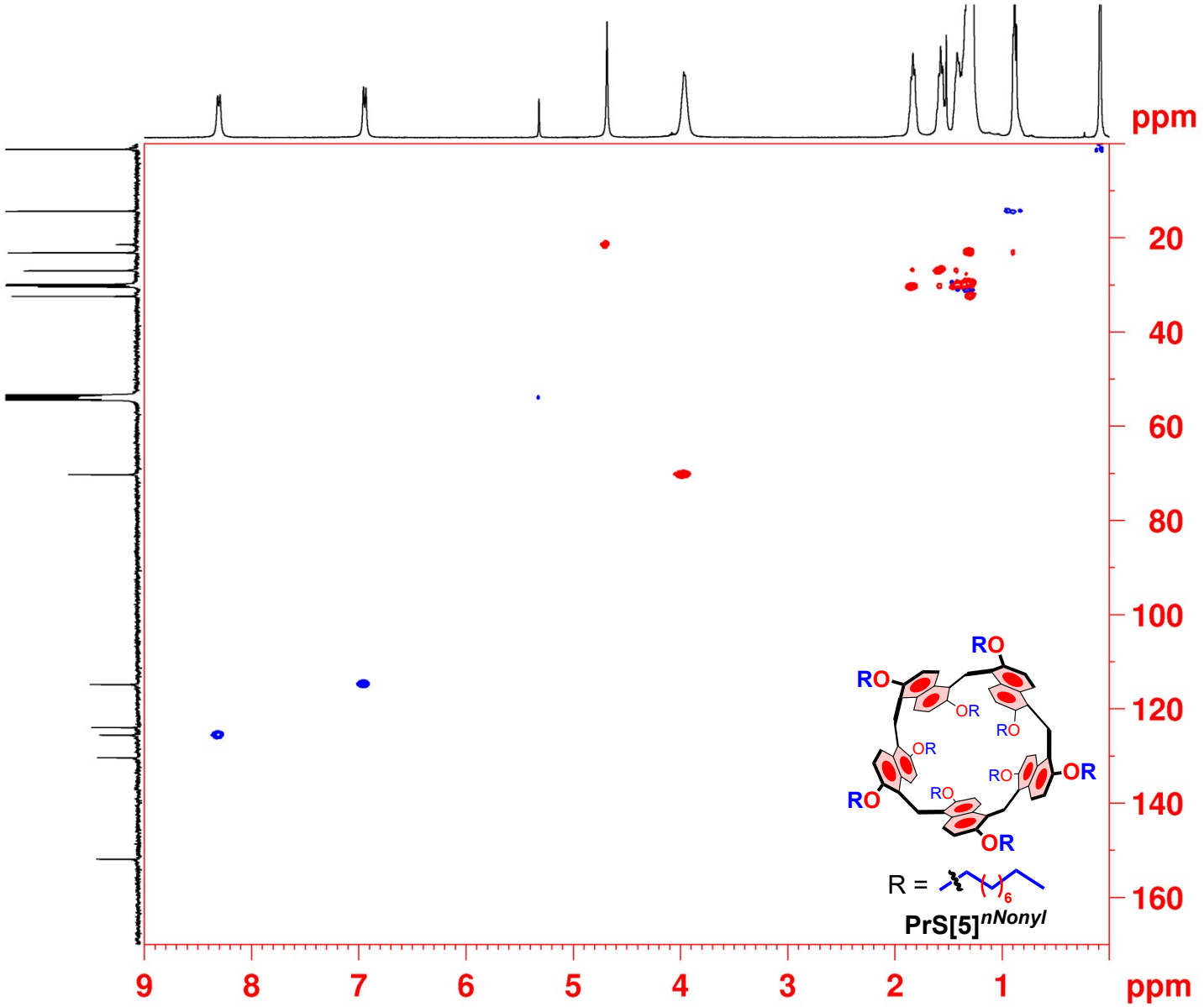

Figure S24: 2D-HSQC spectrum of **PrS[5]*Nonyl*** (CD_2Cl_2, 600 MHz, 298 K).

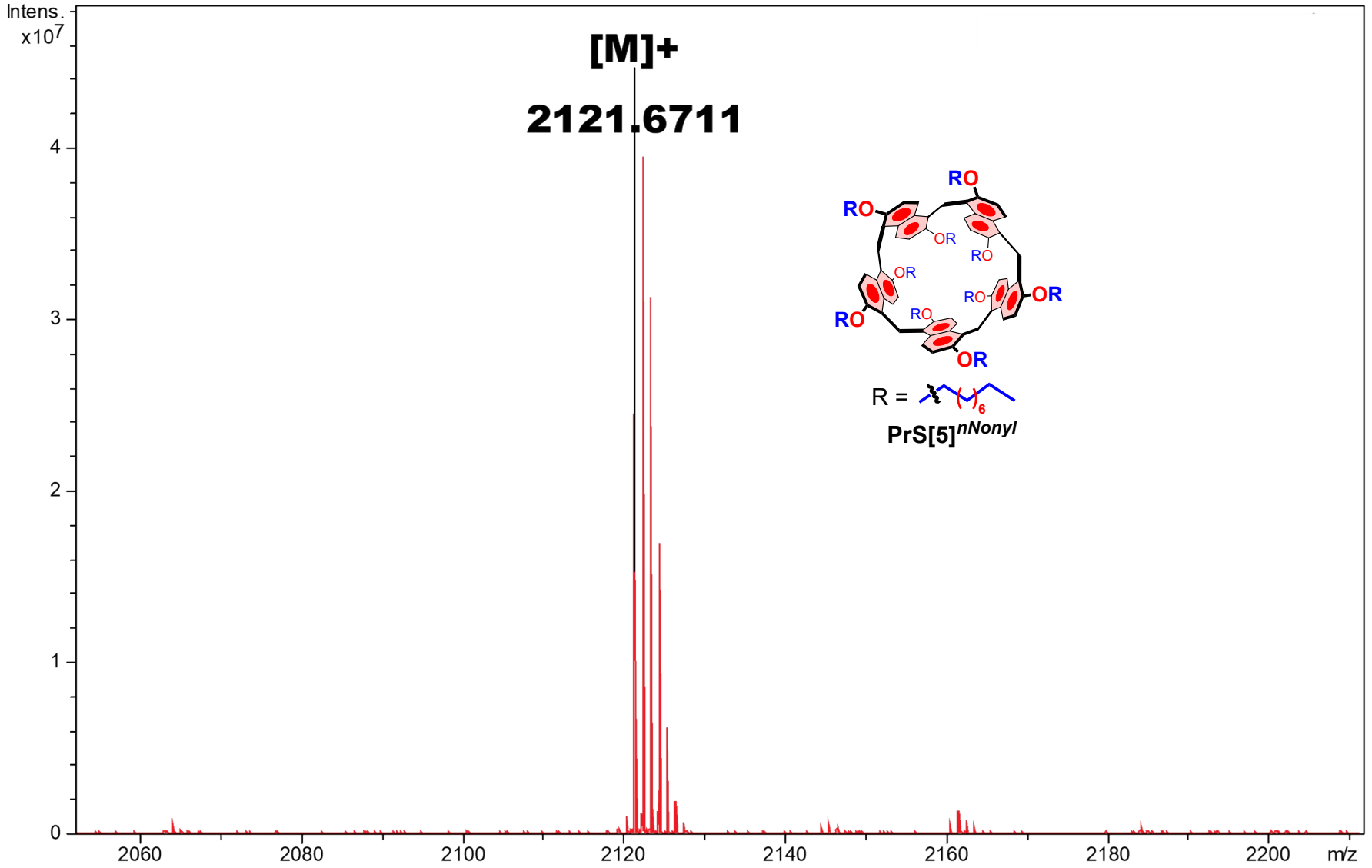

Figure S25: Significant portion of the HR MALDI FT-ICR mass spectrum of **PrS[5]*Nonyl*** $[M]^+$.

Copies of 1D and 2D NMR and HR mass spectrum of derivative PrS[5]^{iPr}

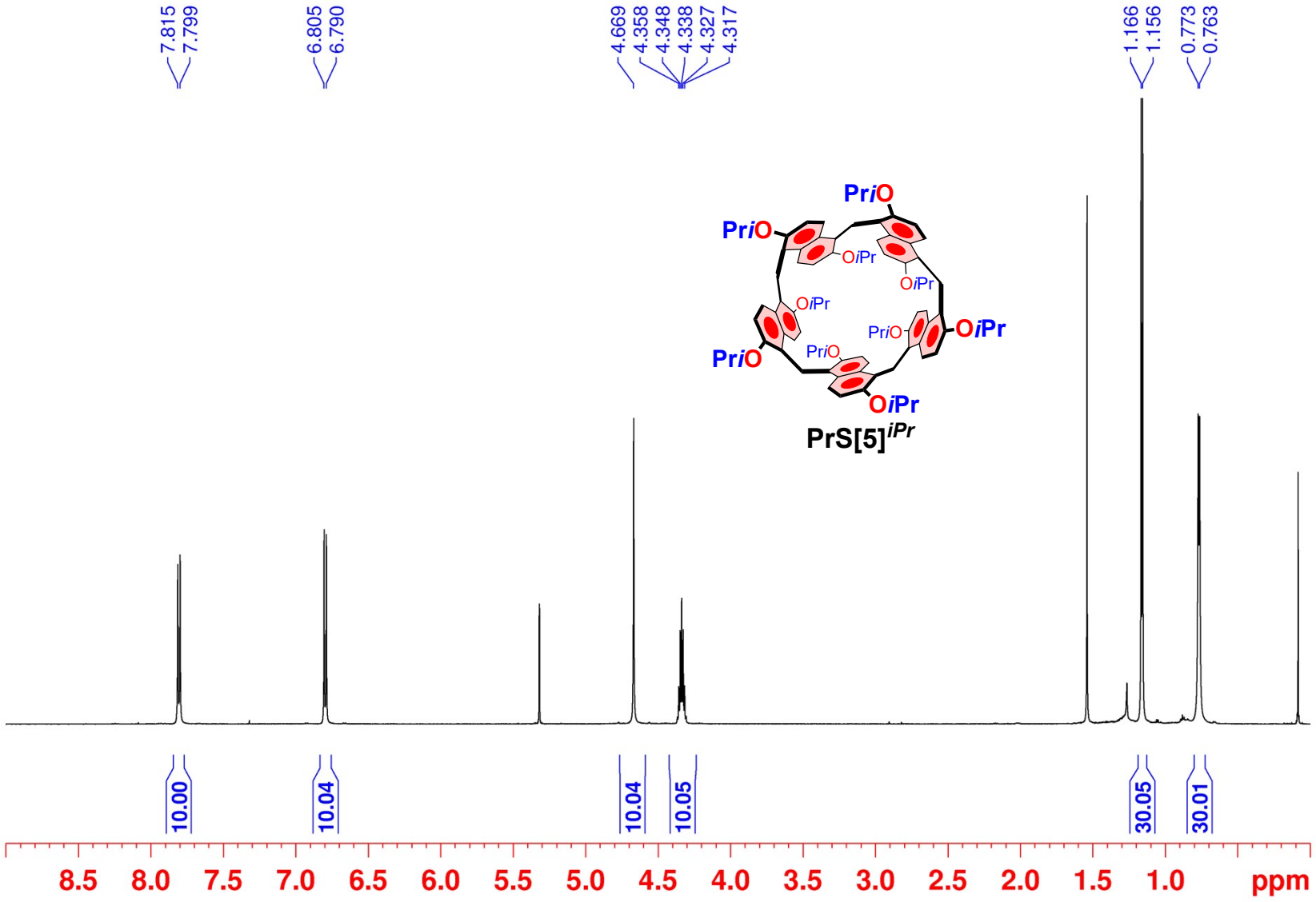

Figure S26: ^{1}H NMR spectrum of derivative **PrS[5]^{iPr}** (CD_2Cl_2, 600 MHz, 298 K).

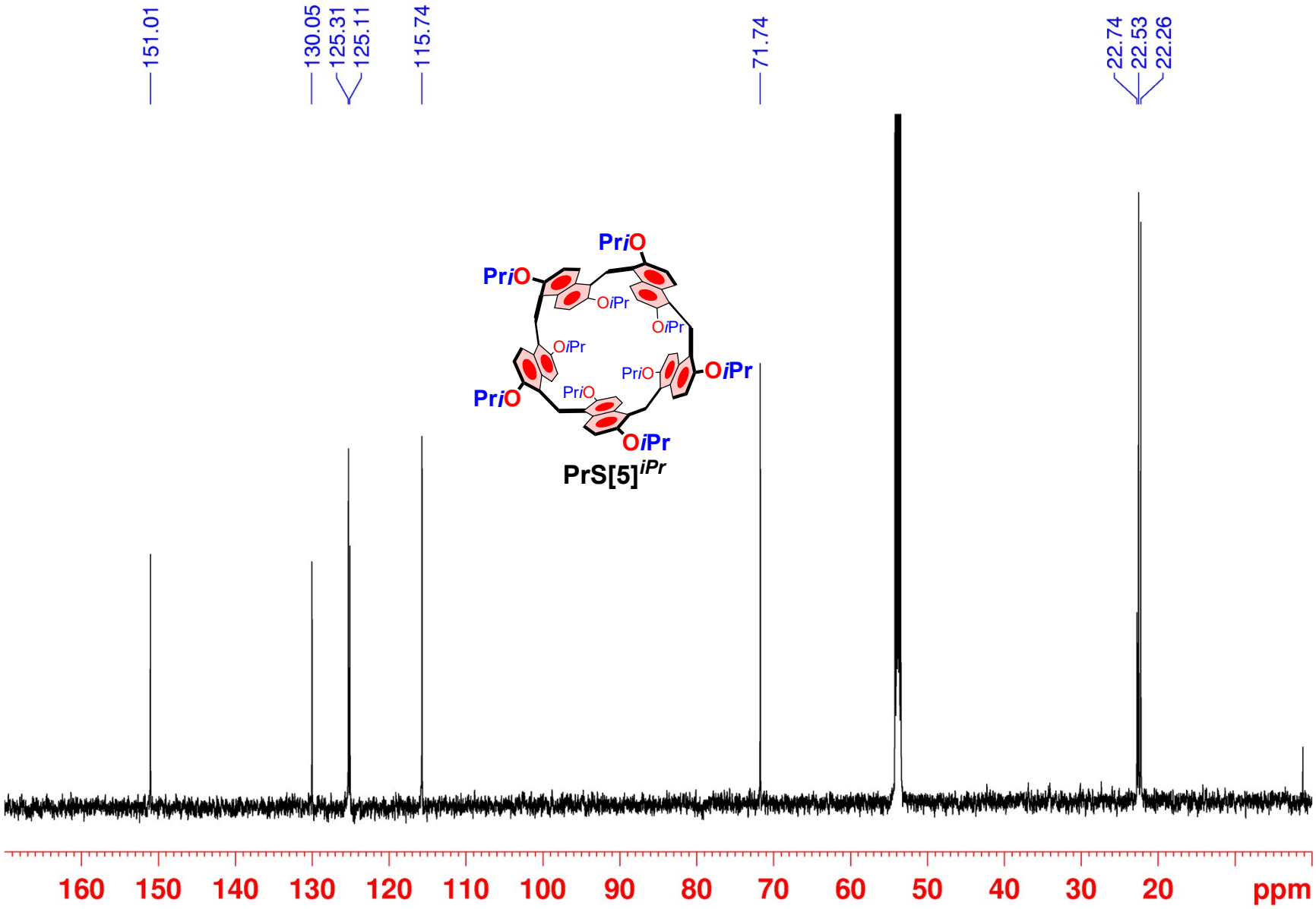

Figure S27: ^{13}C NMR spectrum of **PrS[5]^{iPr}** (CD_2Cl_2, 150 MHz, 298 K).

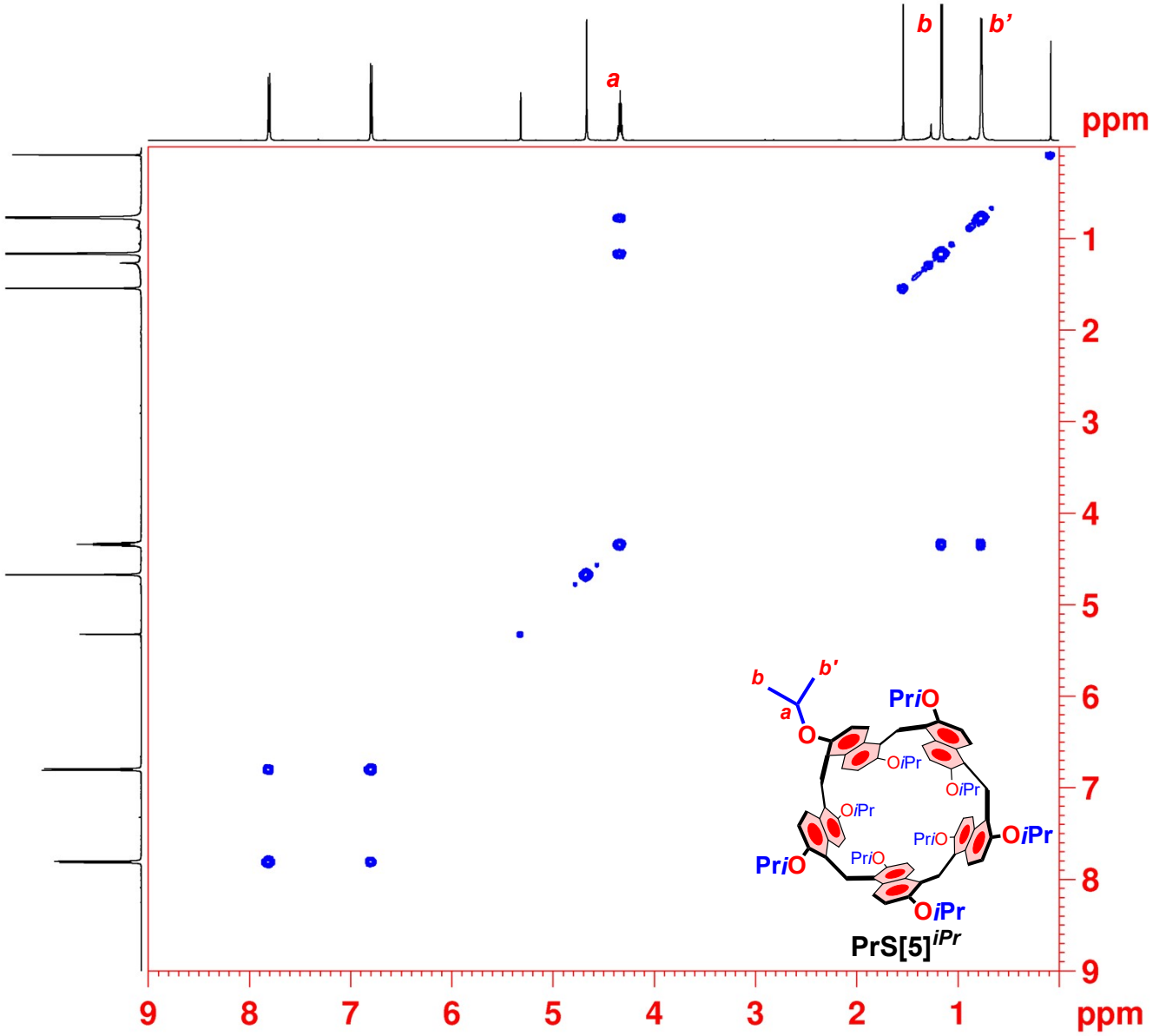

Figure S28: 2D-DQF COSY spectrum of **PrS[5]^{iPr}** (CD_2Cl_2, 600 MHz, 298 K).

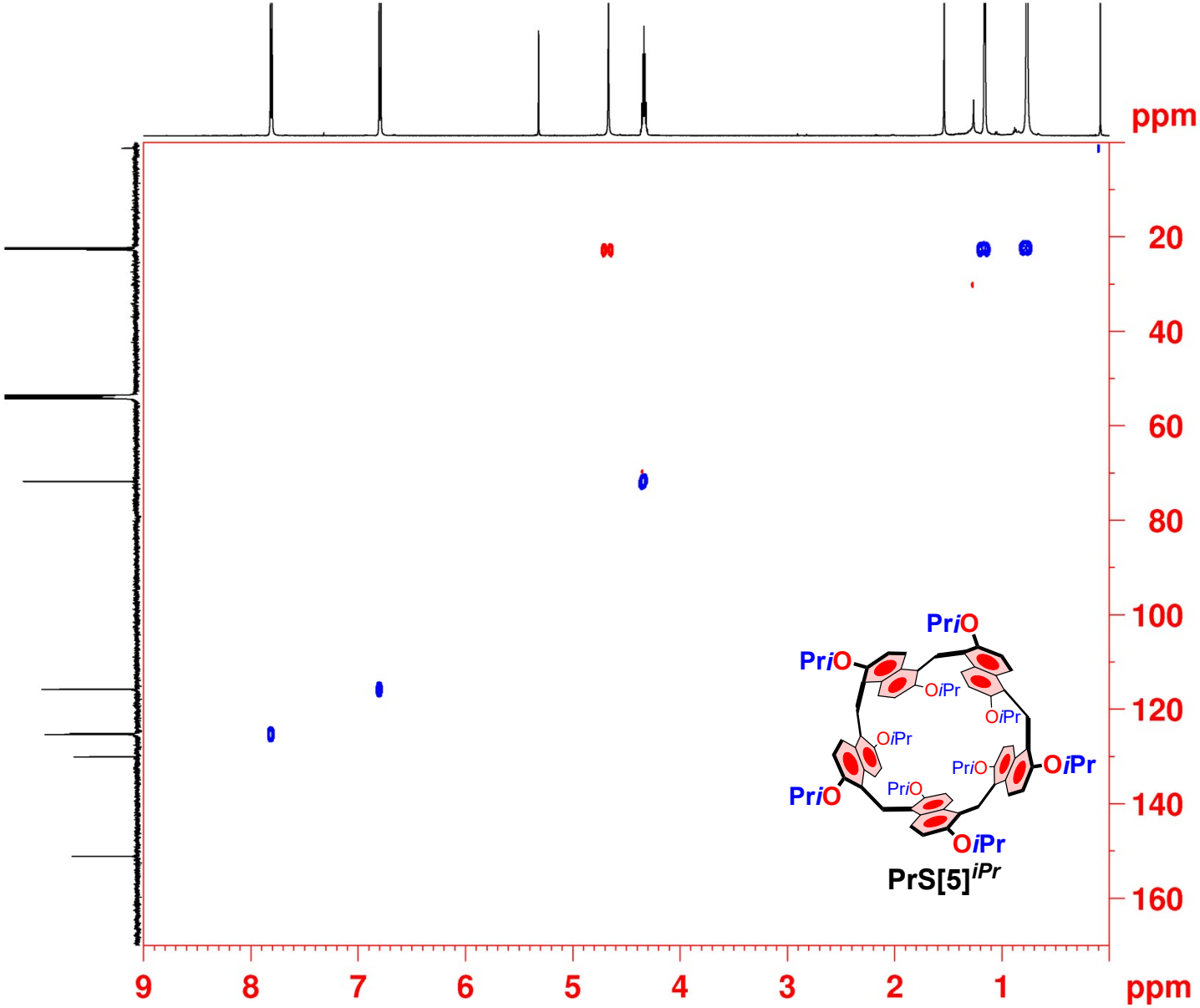

Figure S29: 2D-HSQC spectrum of **PrS[5]^{iPr}** (CD_2Cl_2, 600 MHz, 298 K).

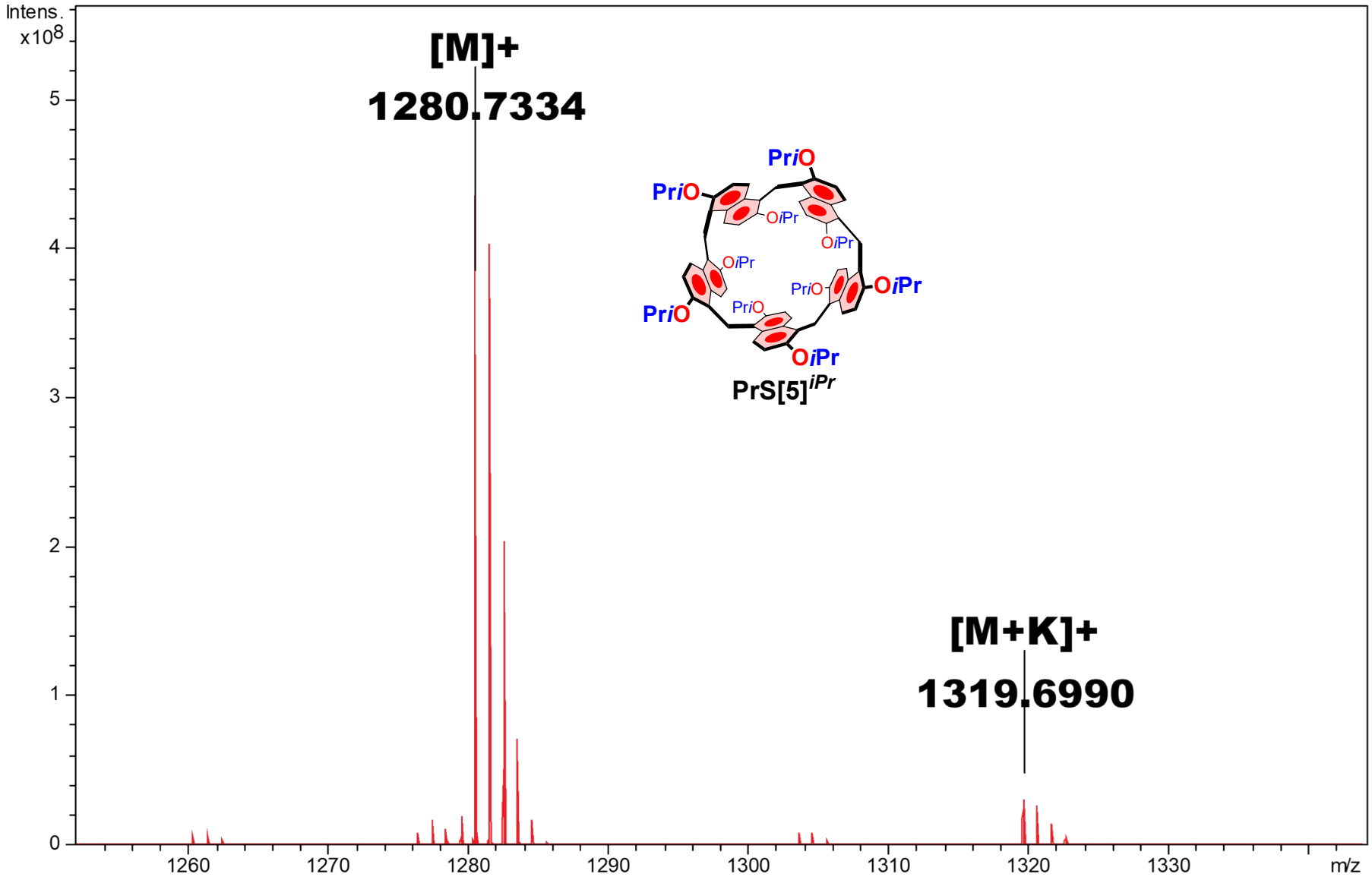

Figure S30: Significant portion of the HR MALDI FT-ICR mass spectrum of **PrS[5]*iPr*** $[M]^+$ and $[M+K]^+$.

Copies of 1D and 2D NMR and HR mass spectrum of derivative PrS[5]^{iBu}

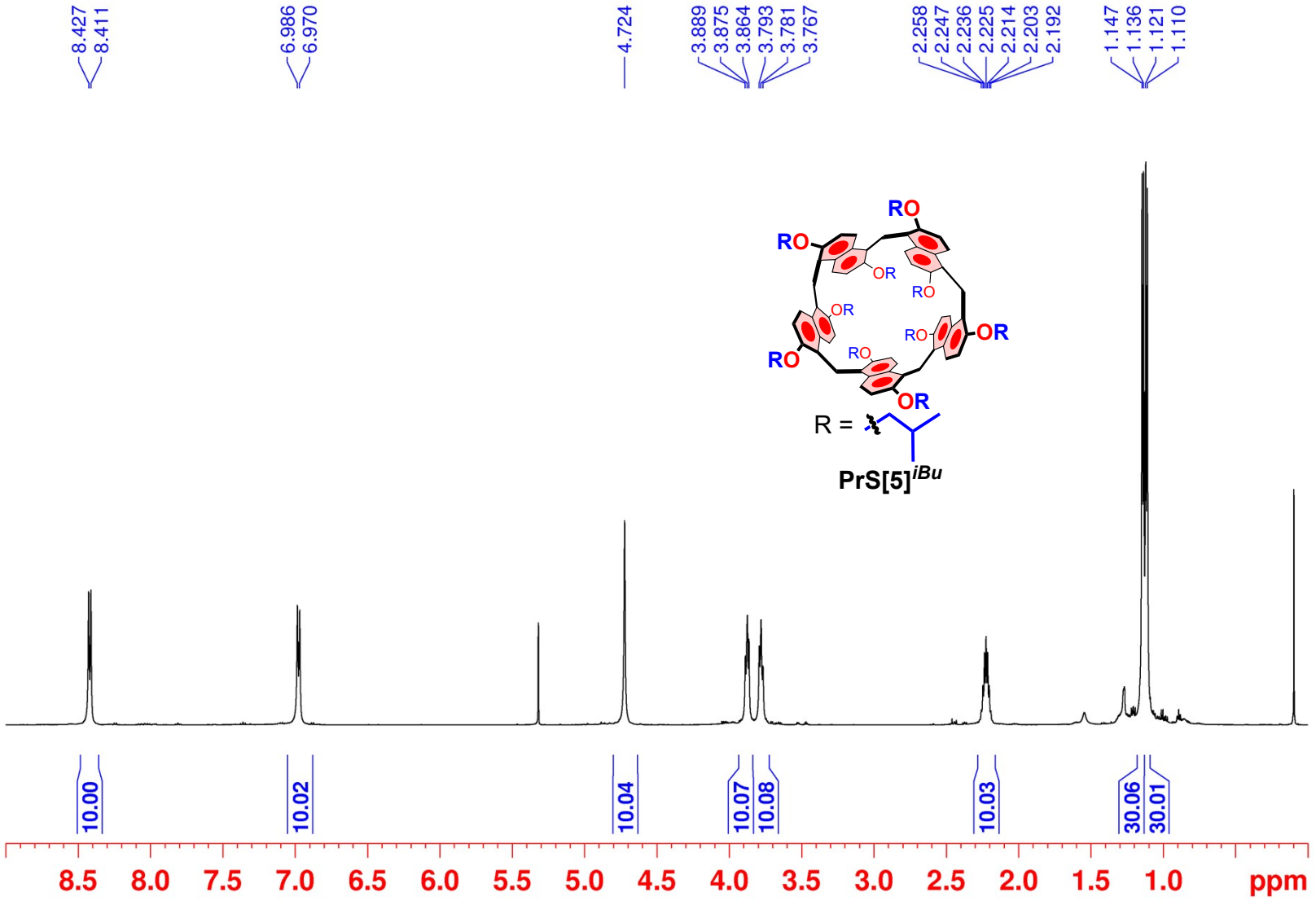

Figure S31: ^{1}H NMR spectrum of derivative **PrS[5]^{iBu}** (CD_2Cl_2, 600 MHz, 298 K).

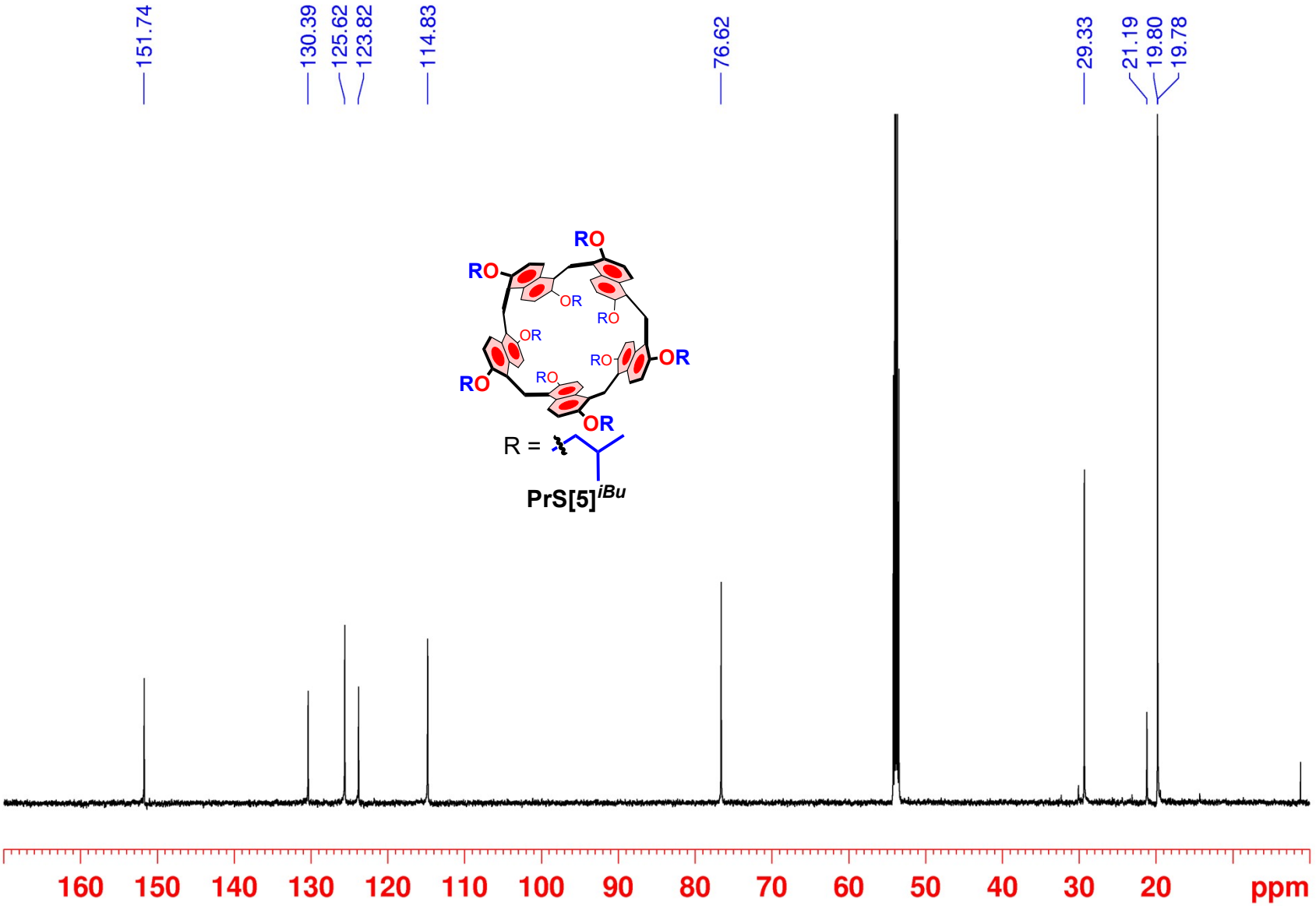

Figure S32: ^{13}C NMR spectrum of **PrS[5]^{iBu}** (CD_2Cl_2, 150 MHz, 298 K).

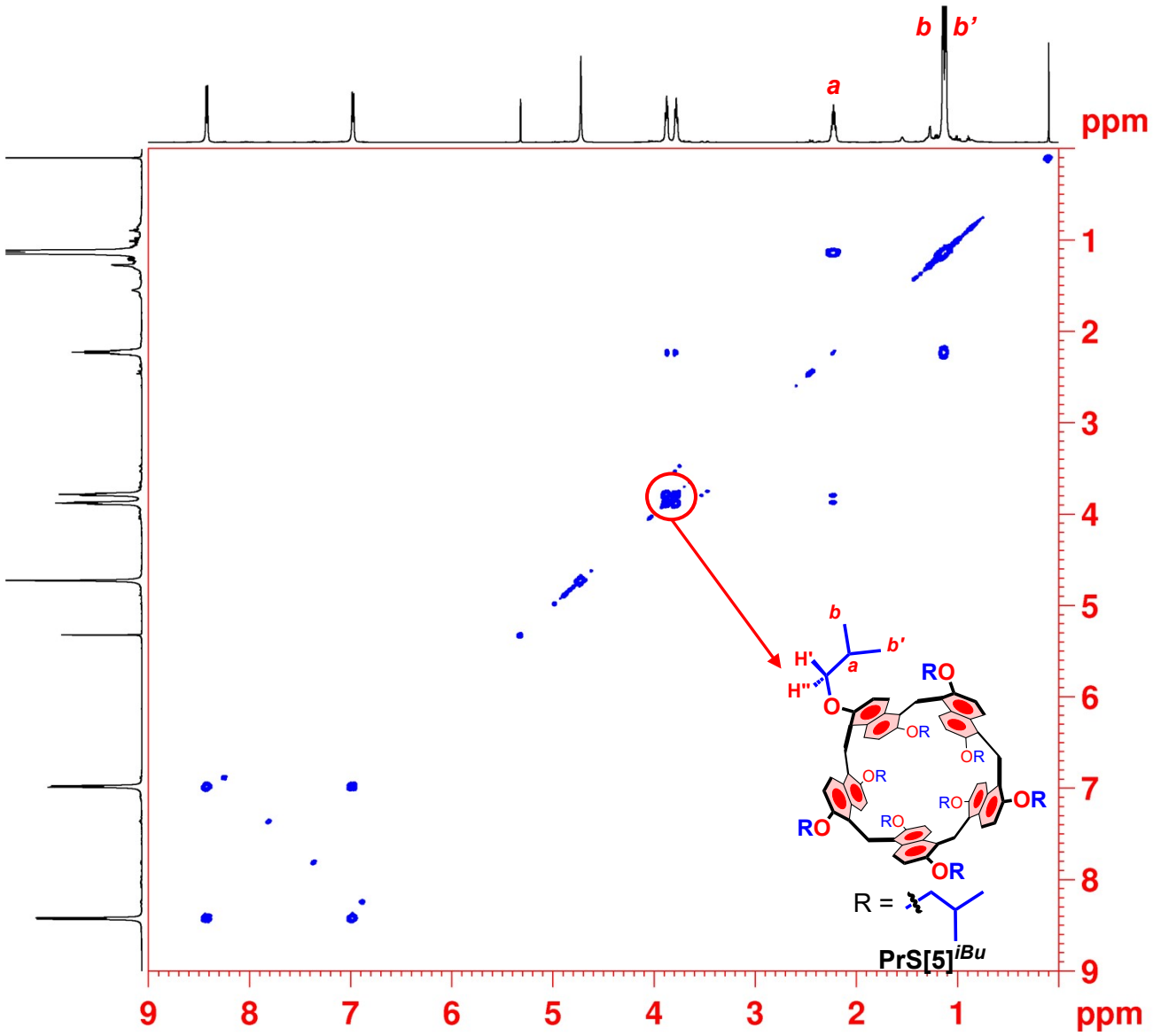

Figure S33: 2D-DQF COSY spectrum of **PrS[5]^{iBu}** (CD_2Cl_2, 600 MHz, 298 K).

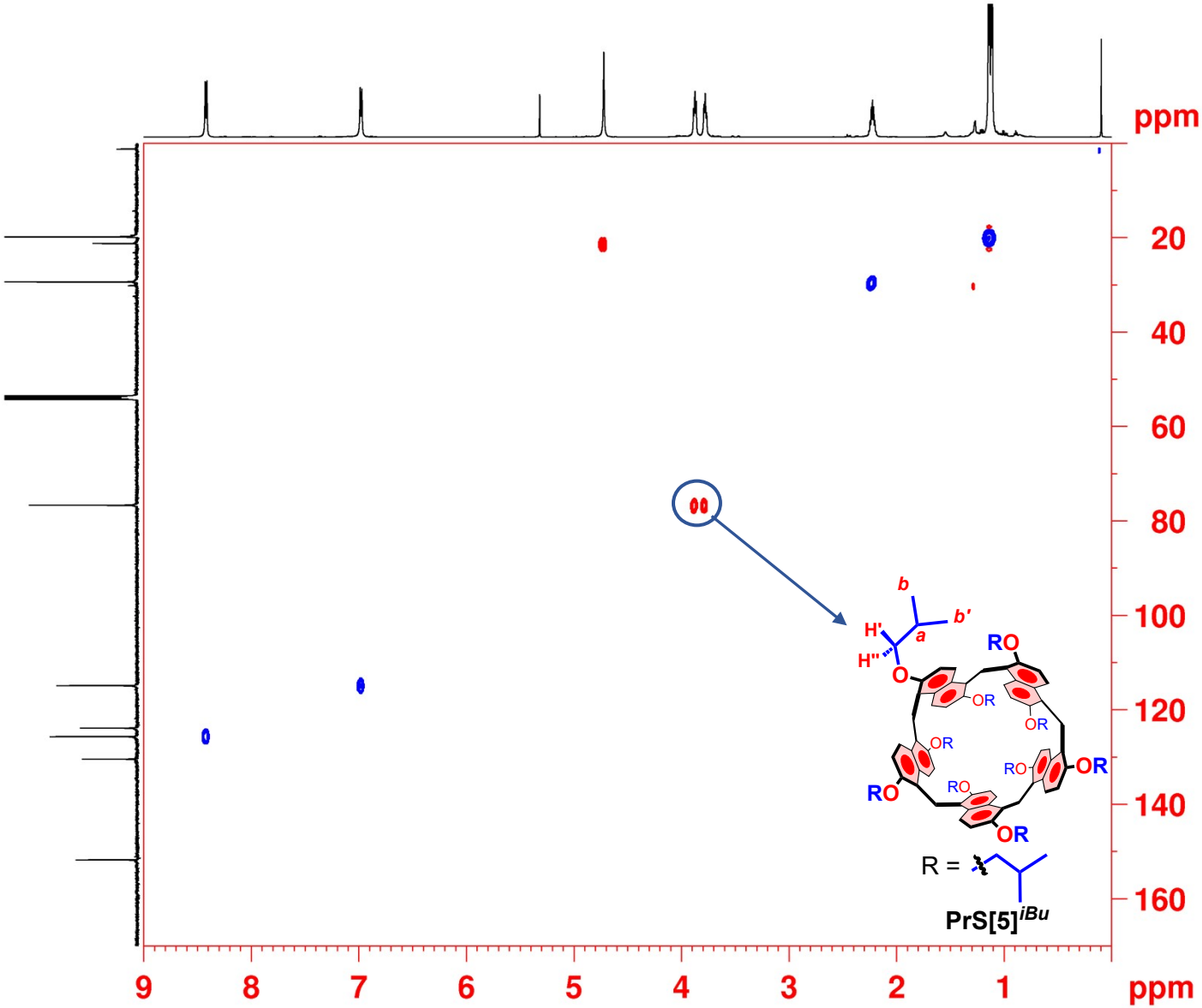

Figure S34: 2D-HSQC spectrum of **PrS[5]*iBu*** (CD_2Cl_2, 600 MHz, 298 K).

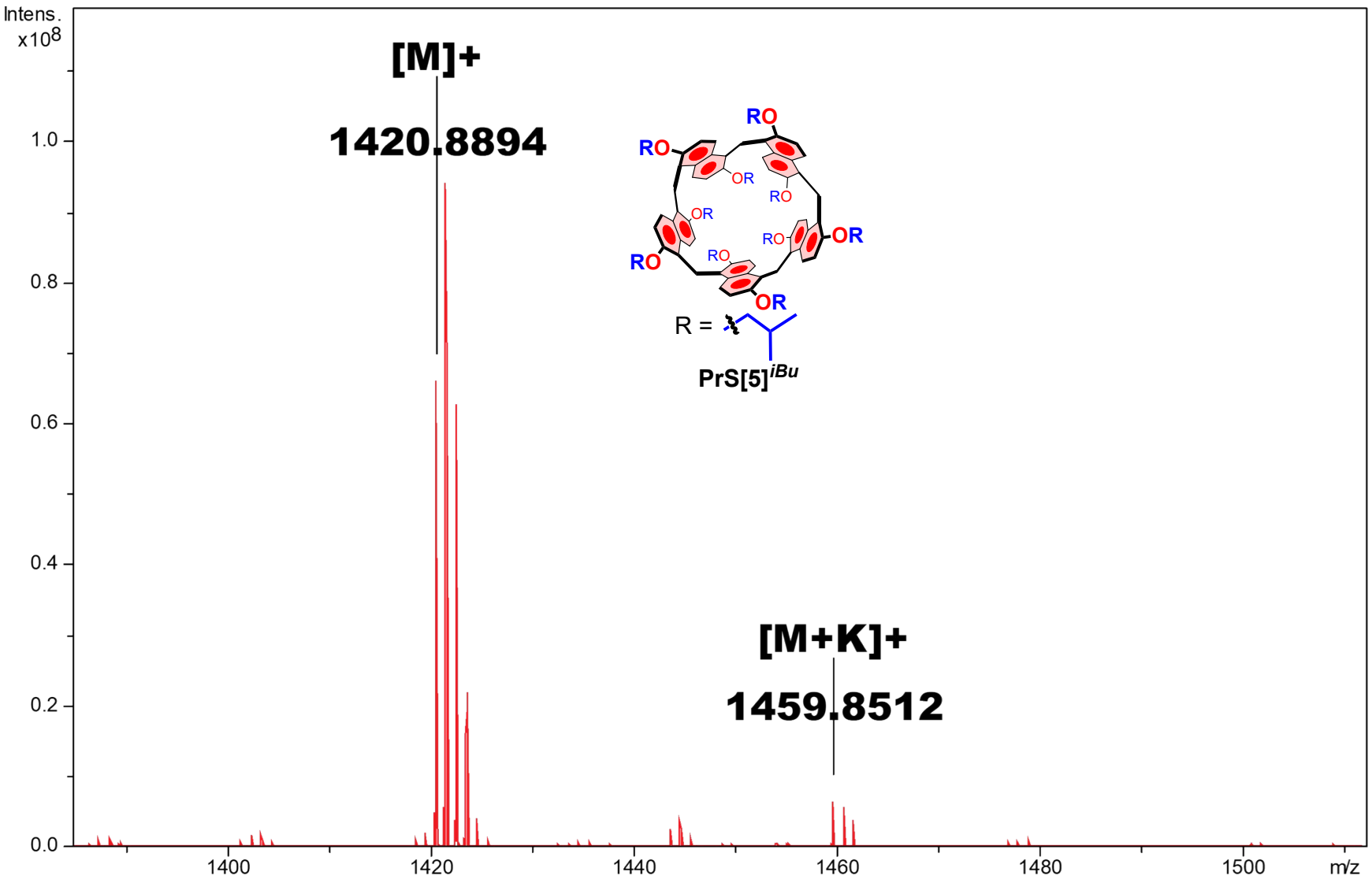

Figure S35: Significant portion of the HR MALDI FT-ICR mass spectrum of **PrS[5]*iBu*** $[M]^+$ and [M+K]+.

Copies of 1D and 2D NMR and HR mass spectrum of derivative PrS[5]^{iPe}

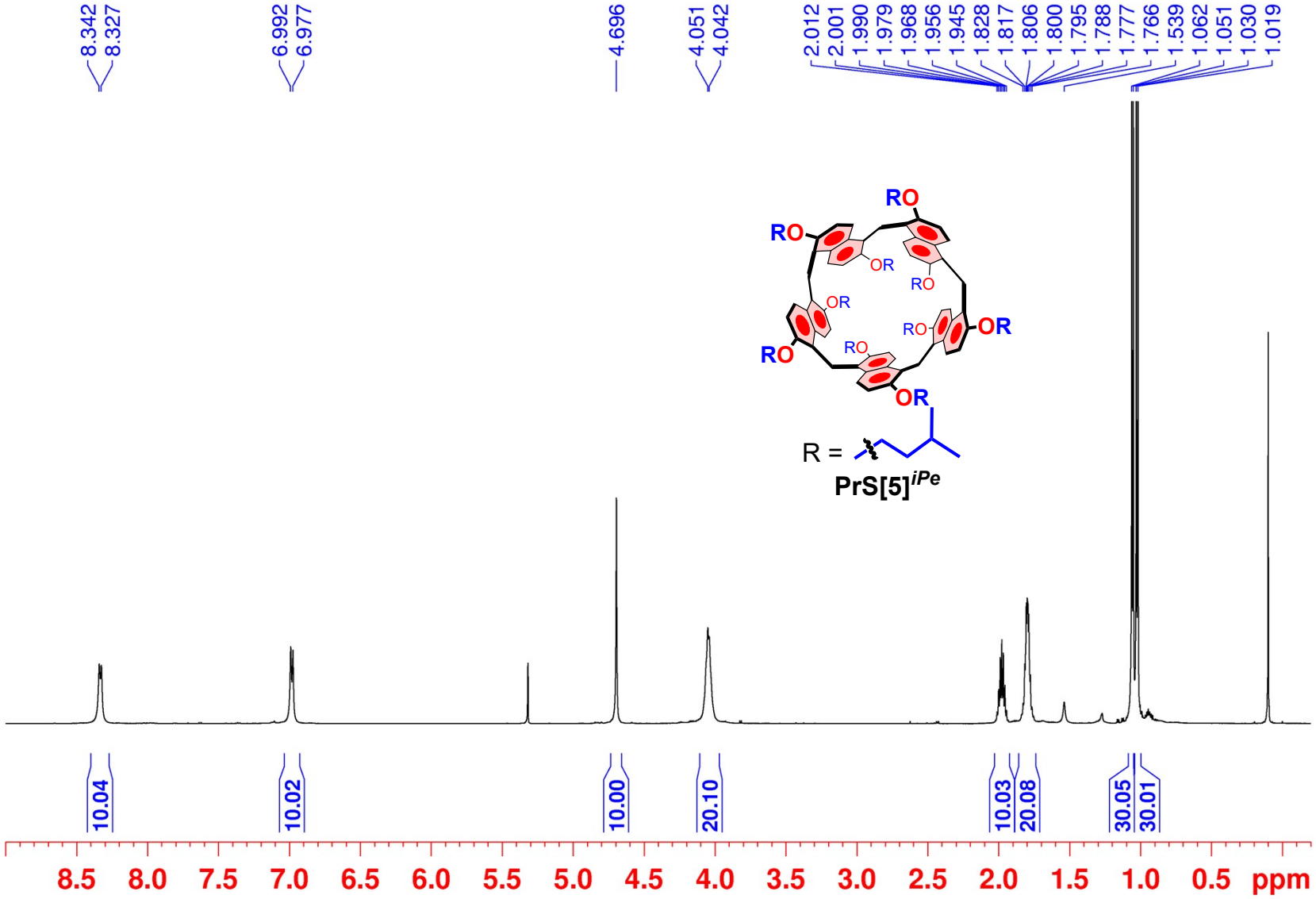

Figure S36: ^{1}H NMR spectrum of derivative **PrS[5]^{iPe}** (CD_2Cl_2, 600 MHz, 298 K).

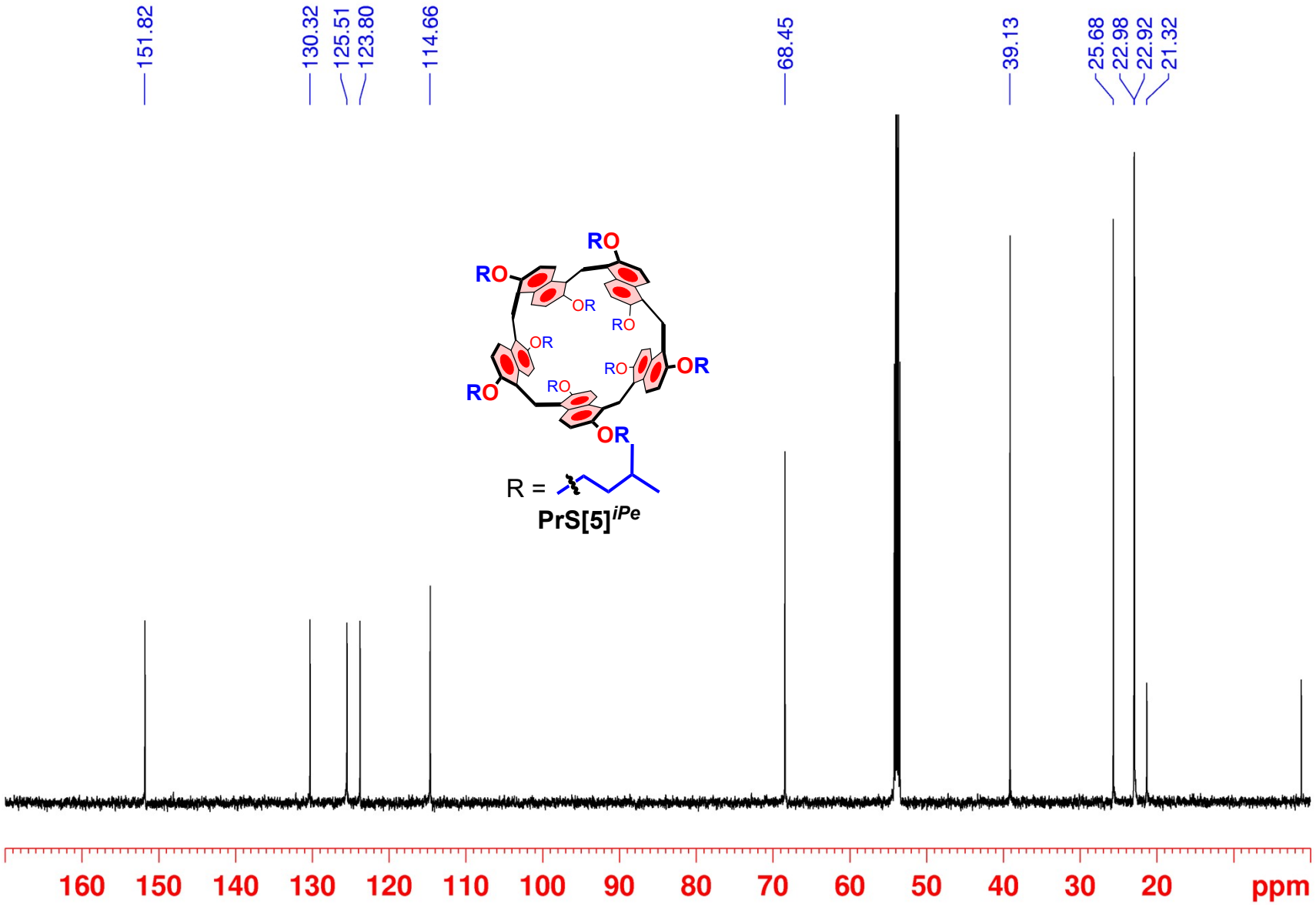

Figure S37: ^{13}C NMR spectrum of **PrS[5]*iPe*** (CD_2Cl_2, 150 MHz, 298 K).

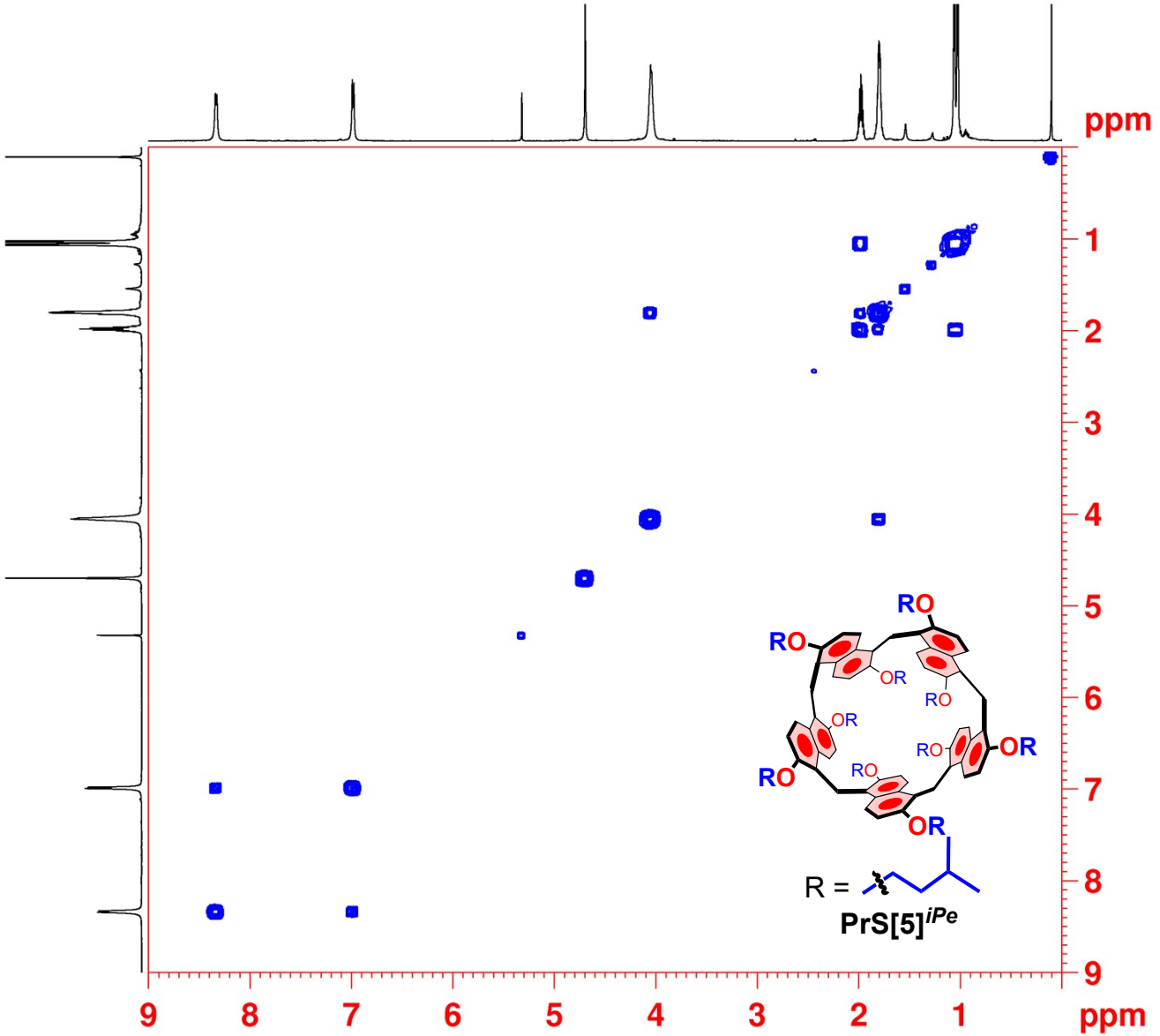

Figure S38: 2D-DQF COSY spectrum of **PrS[5]^{iPe}** (CD_2Cl_2, 600 MHz, 298 K).

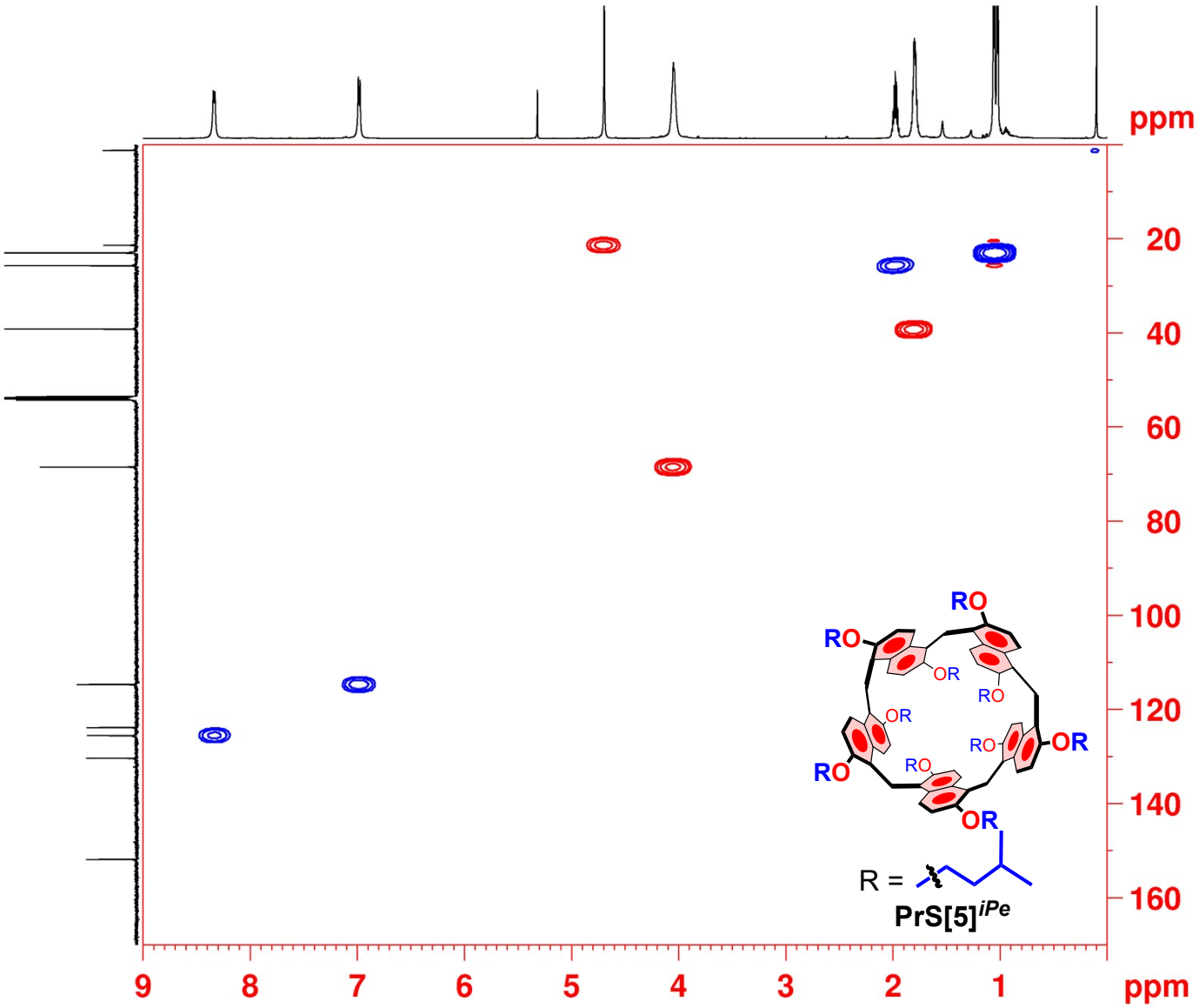

Figure S39: 2D-HSQC spectrum of **PrS[5]^{iPe}** (CD_2Cl_2, 600 MHz, 298 K).

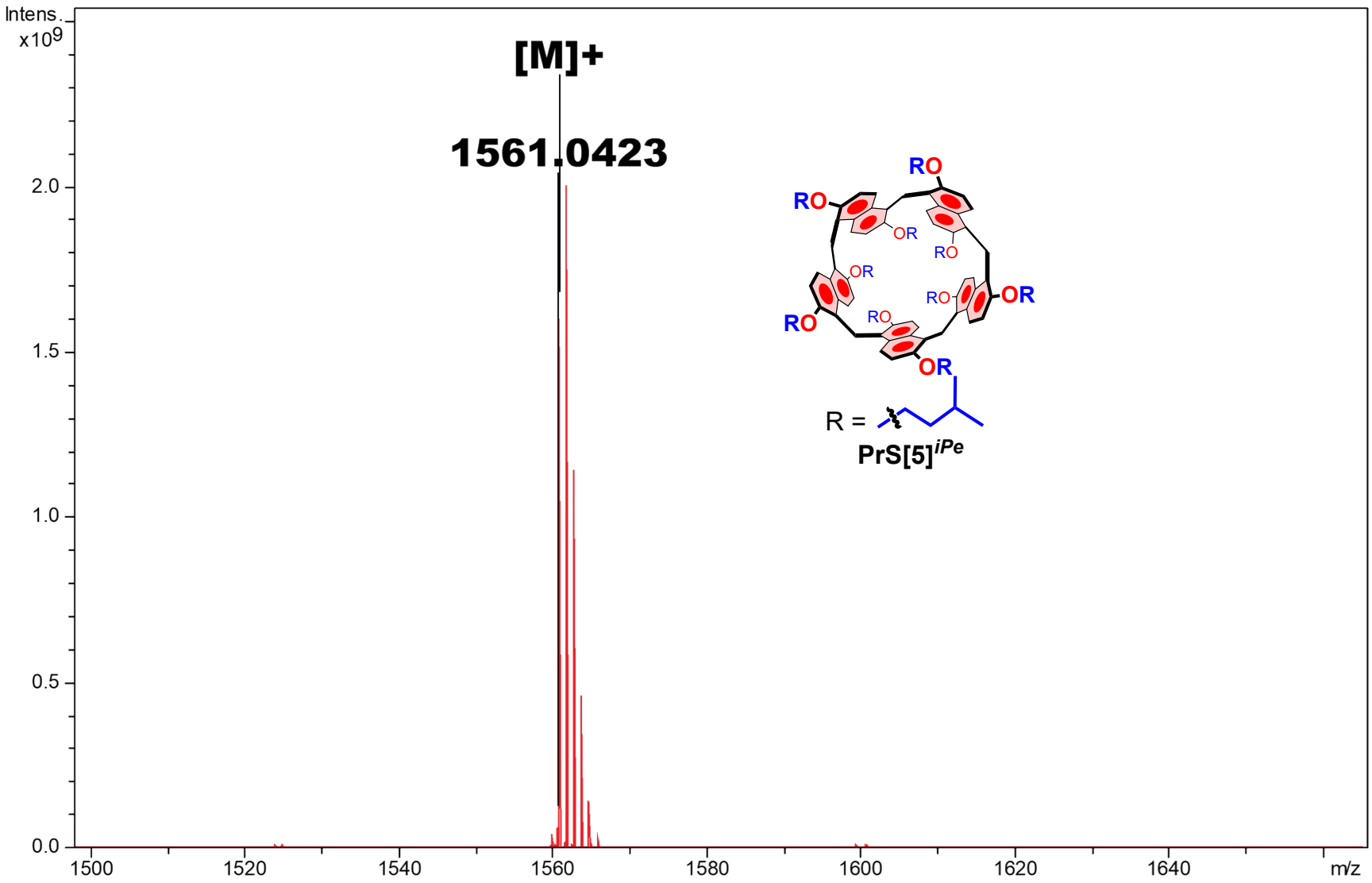

Figure S40: Significant portion of the HR MALDI FT-ICR mass spectrum of **PrS[5]*iPe*** $[M]^+$.

Copies of 1D and 2D NMR and HR mass spectrum of derivative PrS[5]*iHex*

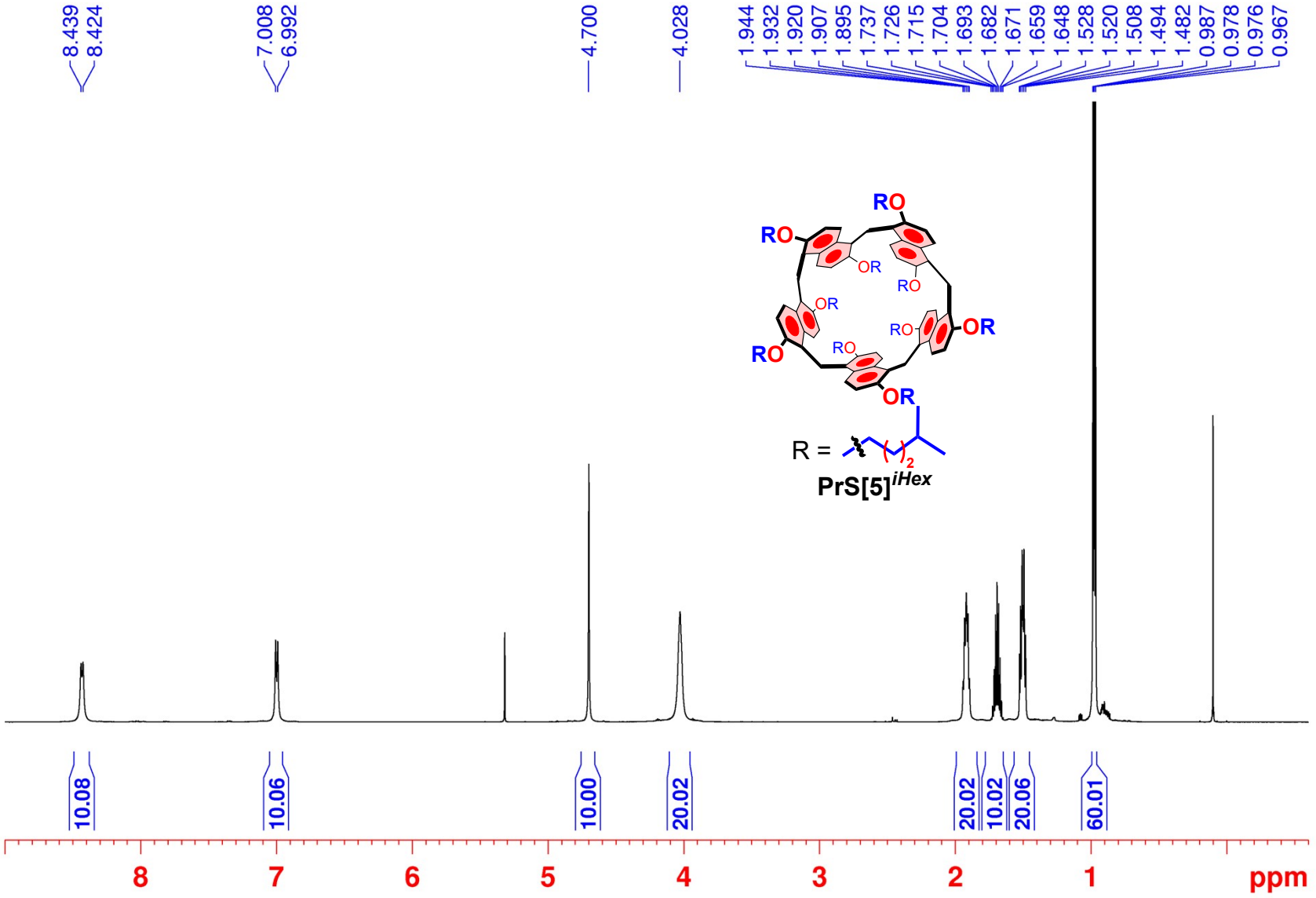

Figure S41: ^{1}H NMR spectrum of derivative **PrS[5]*iHex*** (CD_2Cl_2, 600 MHz, 298 K).

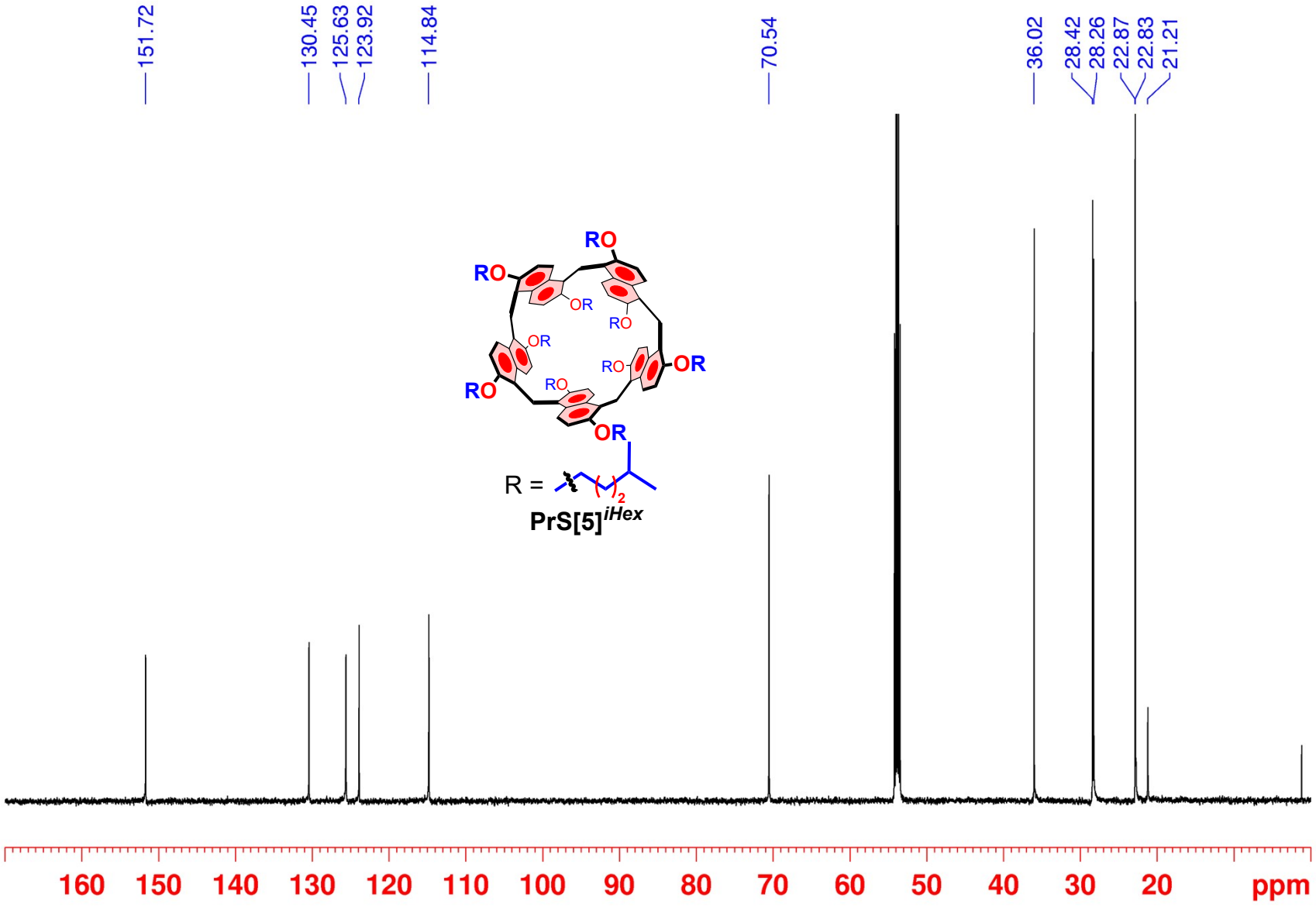

Figure S42: ^{13}C NMR spectrum of **PrS[5]^{iHex}** (CD_2Cl_2, 150 MHz, 298 K).

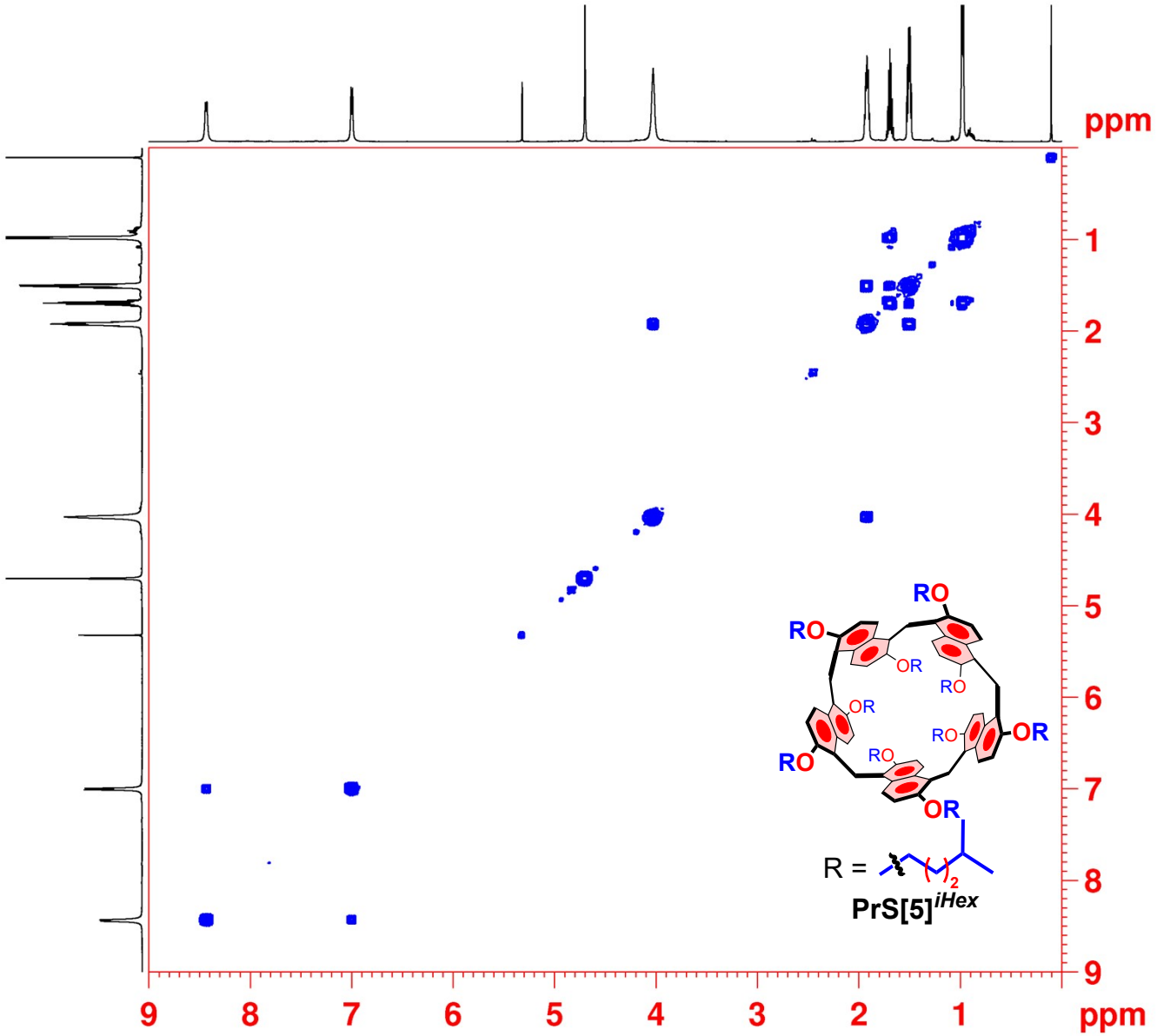

Figure S43: 2D-DQF COSY spectrum of **PrS[5]^{iHex}** (CD_2Cl_2, 600 MHz, 298 K).

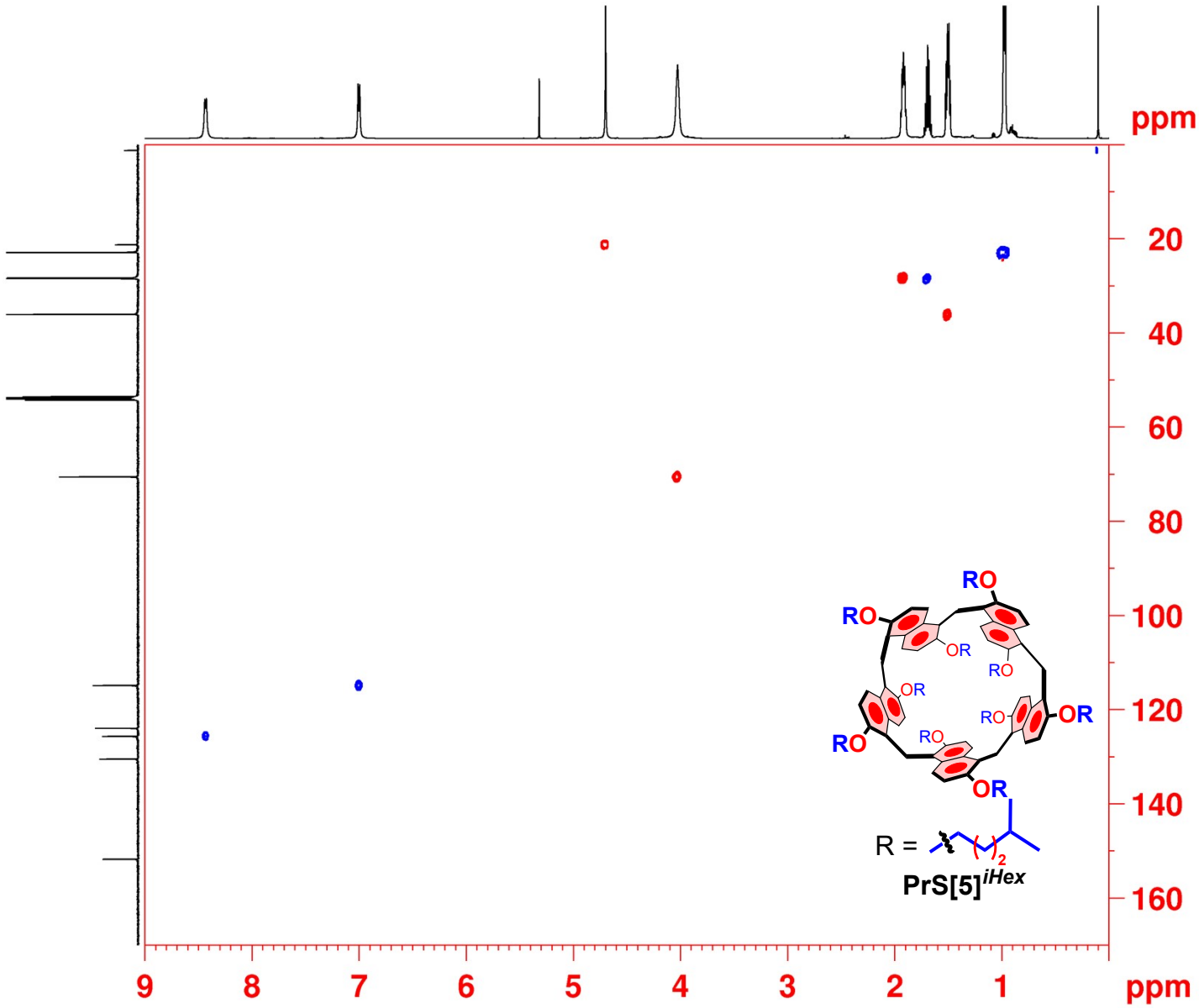

Figure S44: 2D-HSQC spectrum of **PrS[5]**^{iHex} (CD_2Cl_2, 600 MHz, 298 K).

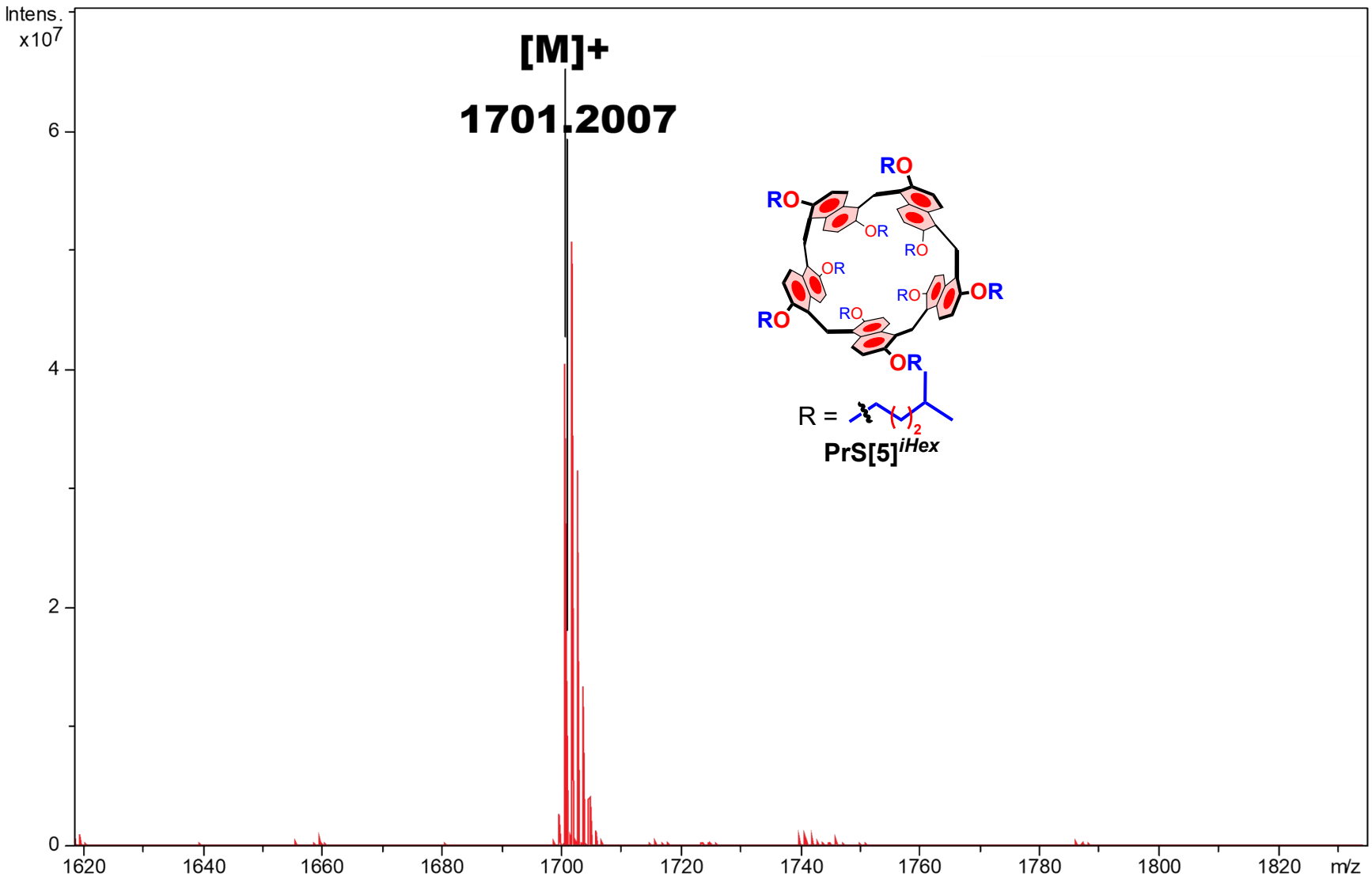

Figure S45: Significant portion of the HR MALDI FT-ICR mass spectrum of **PrS[5]*iHex*** $[M]^+$.

Copies of 1D and 2D NMR and HR mass spectrum of derivative PrS[5]*MeCy*

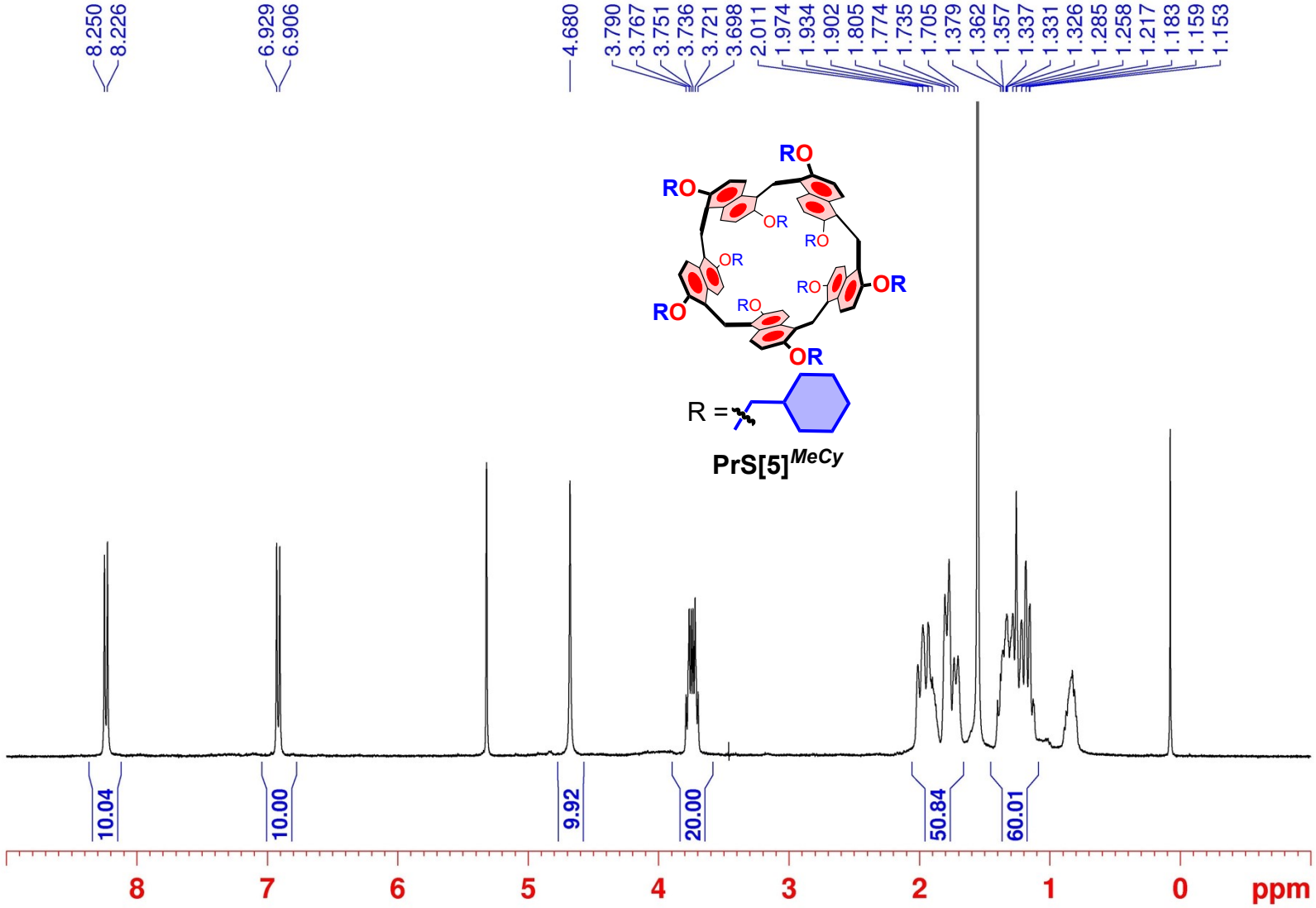

Figure S46: ^{1}H NMR spectrum of derivative **PrS[5]*MeCy*** (CD_2Cl_2, 400 MHz, 298 K).

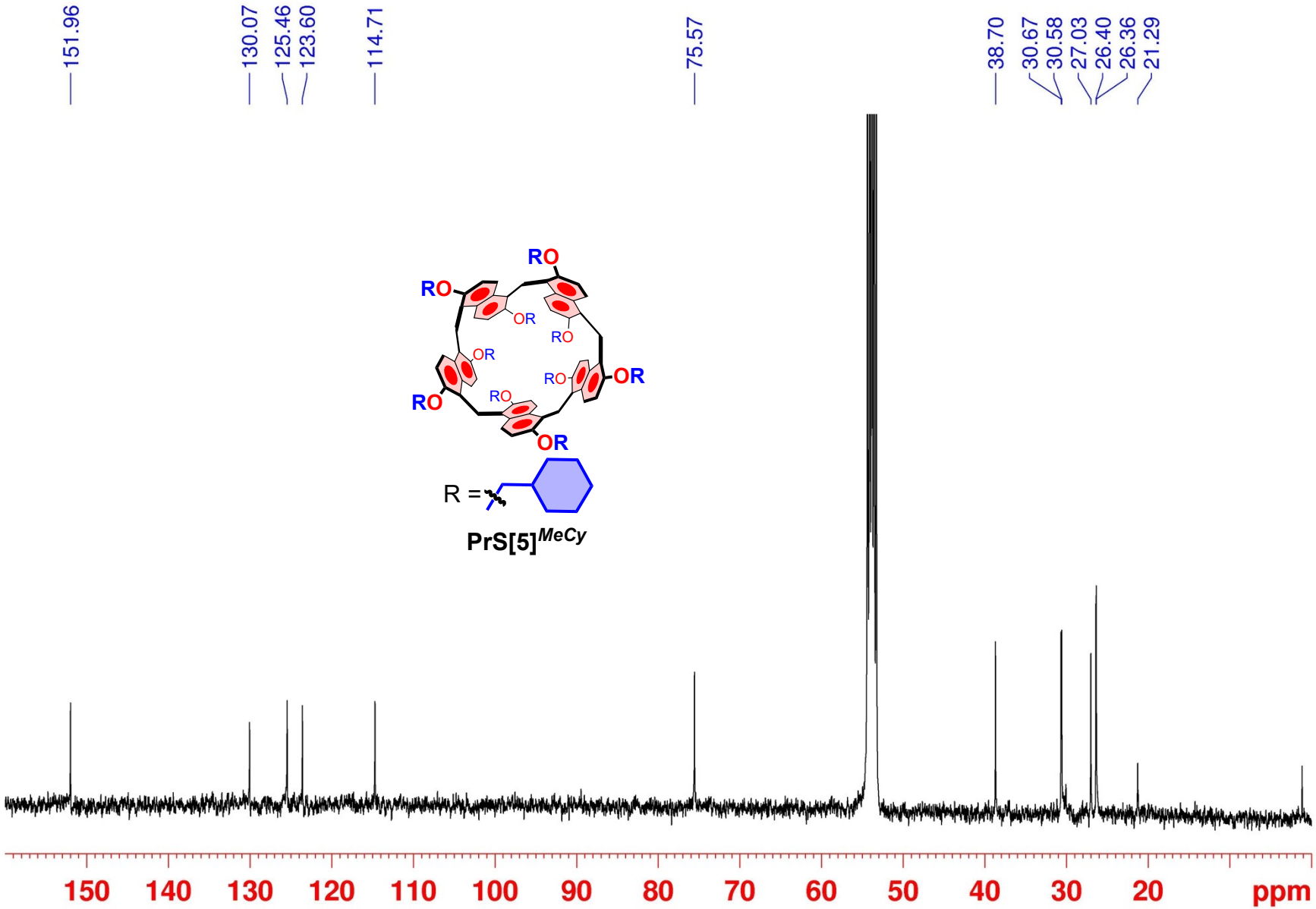

Figure S47: ^{13}C NMR spectrum of **PrS[5]*MeCy*** (CD_2Cl_2, 100 MHz, 298 K).

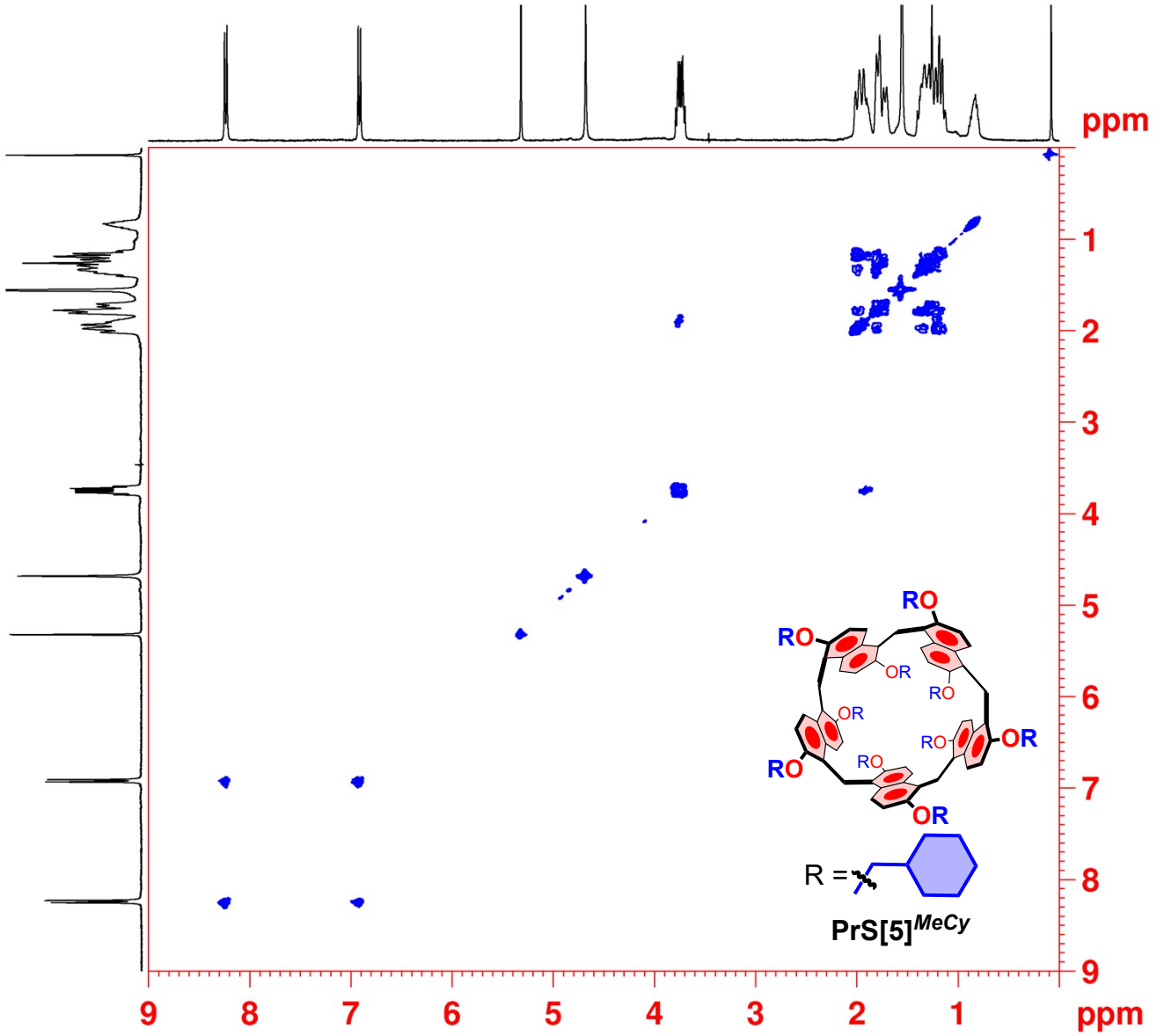

Figure S48: 2D-DQF COSY spectrum of **PrS[5]*MeCy*** (CD_2Cl_2, 400 MHz, 298 K).

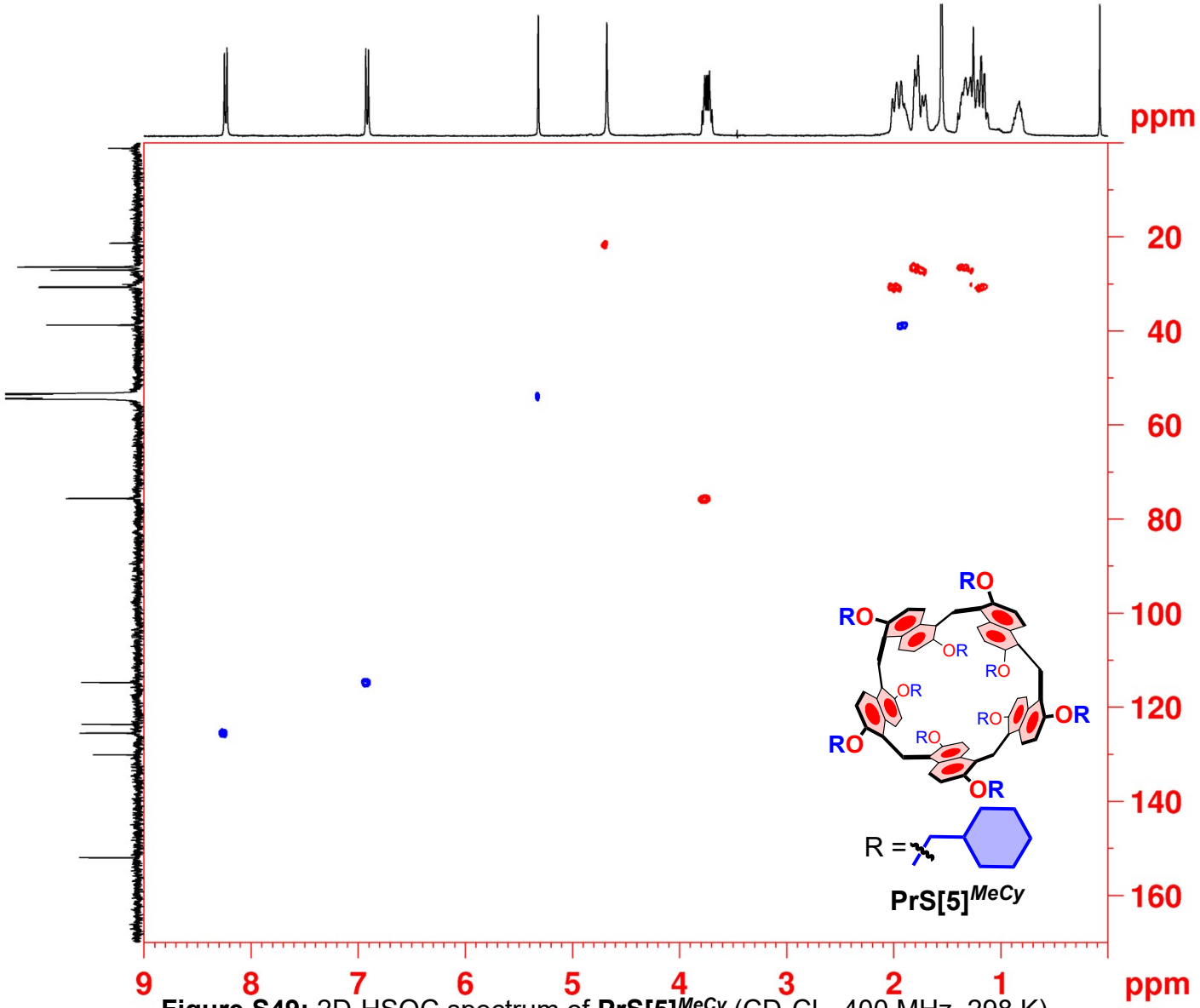

Figure S49: 2D-HSQC spectrum of **PrS[5]**^{MeCy} (CD_2Cl_2, 400 MHz, 298 K).

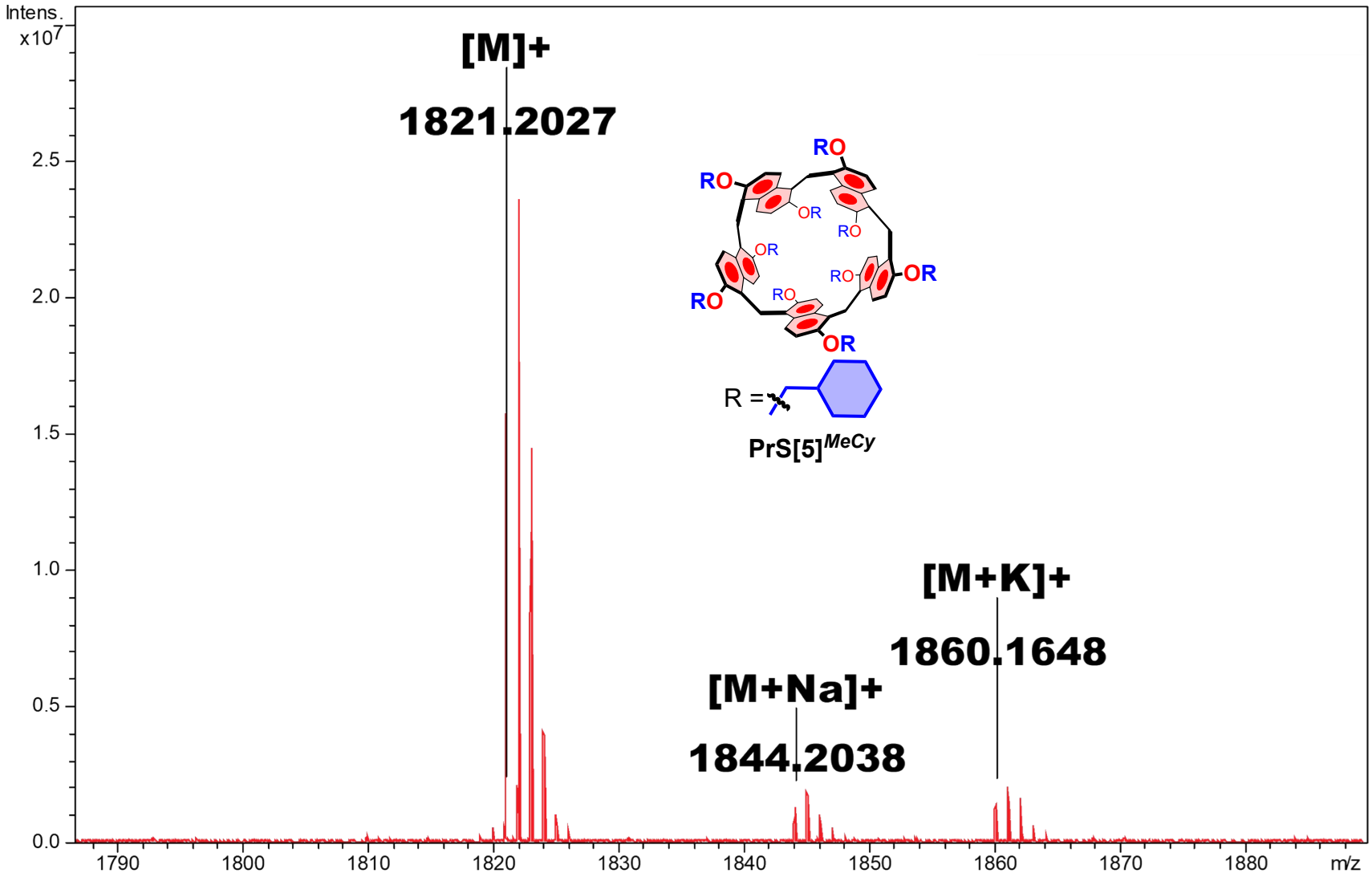

Figure S50: Significant portion of the HR MALDI FT-ICR mass spectrum of **PrS[5]*MeCy*** $[M]^+$, $[M+Na]^+$ and $[M+K]^+$.

Copies of 1D and 2D NMR and HR mass spectrum of derivative PrS[5]*EtCy*

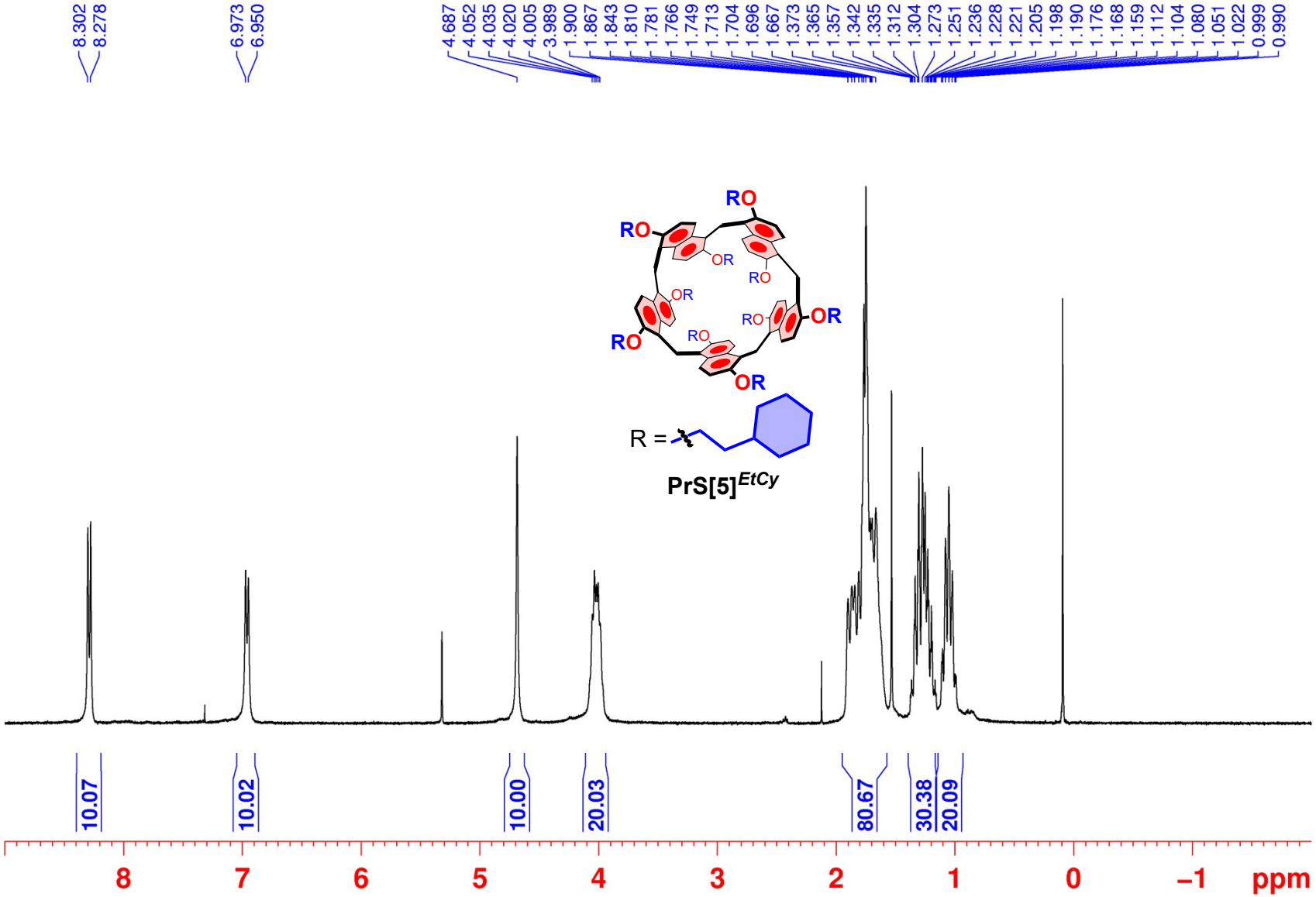

Figure S51: ^{1}H NMR spectrum of derivative **PrS[5]*EtCy*** (CD_2Cl_2, 400 MHz, 298 K).

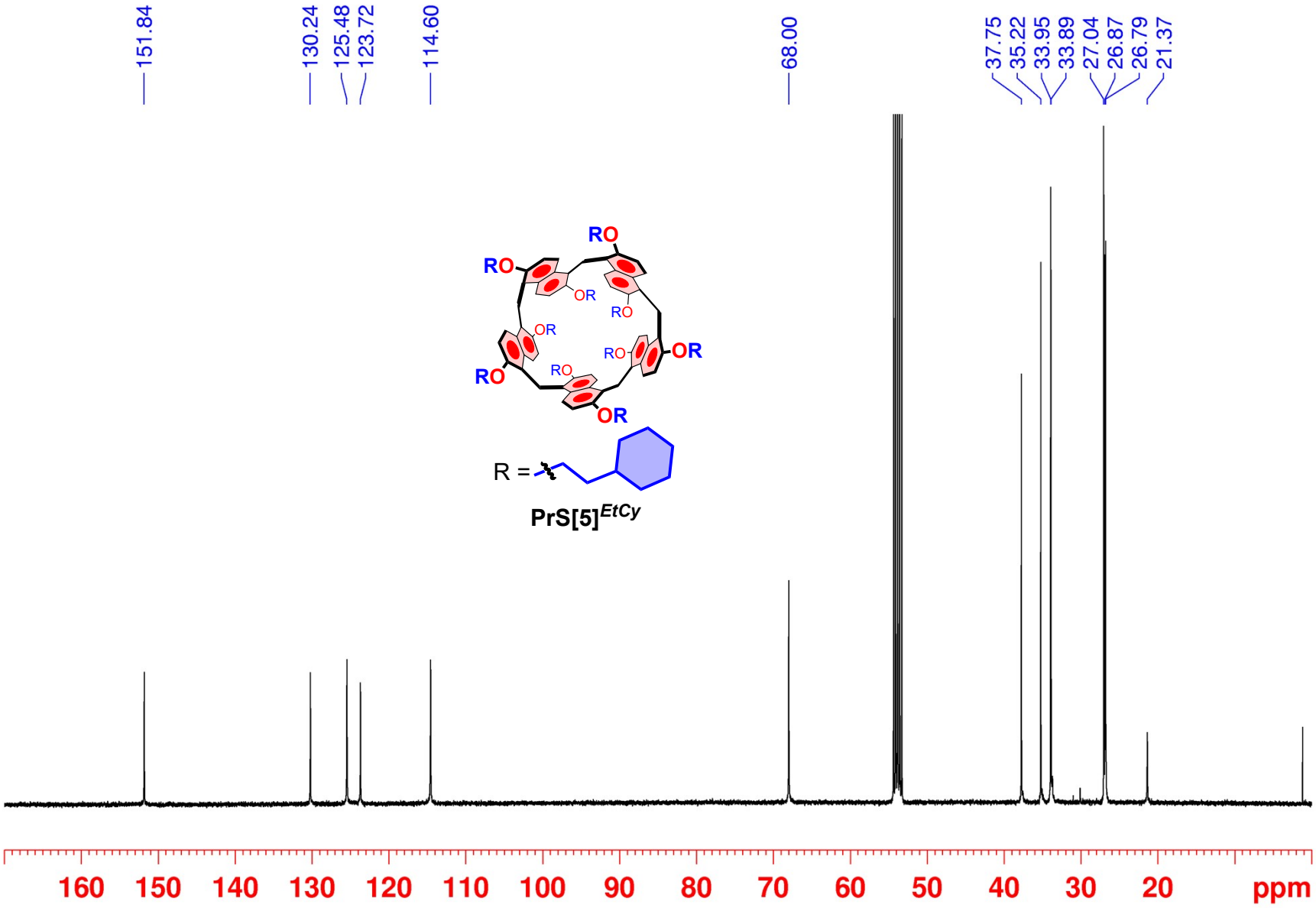

Figure S52: ^{13}C NMR spectrum of **PrS[5]*EtCy*** (CD_2Cl_2, 100 MHz, 298 K).

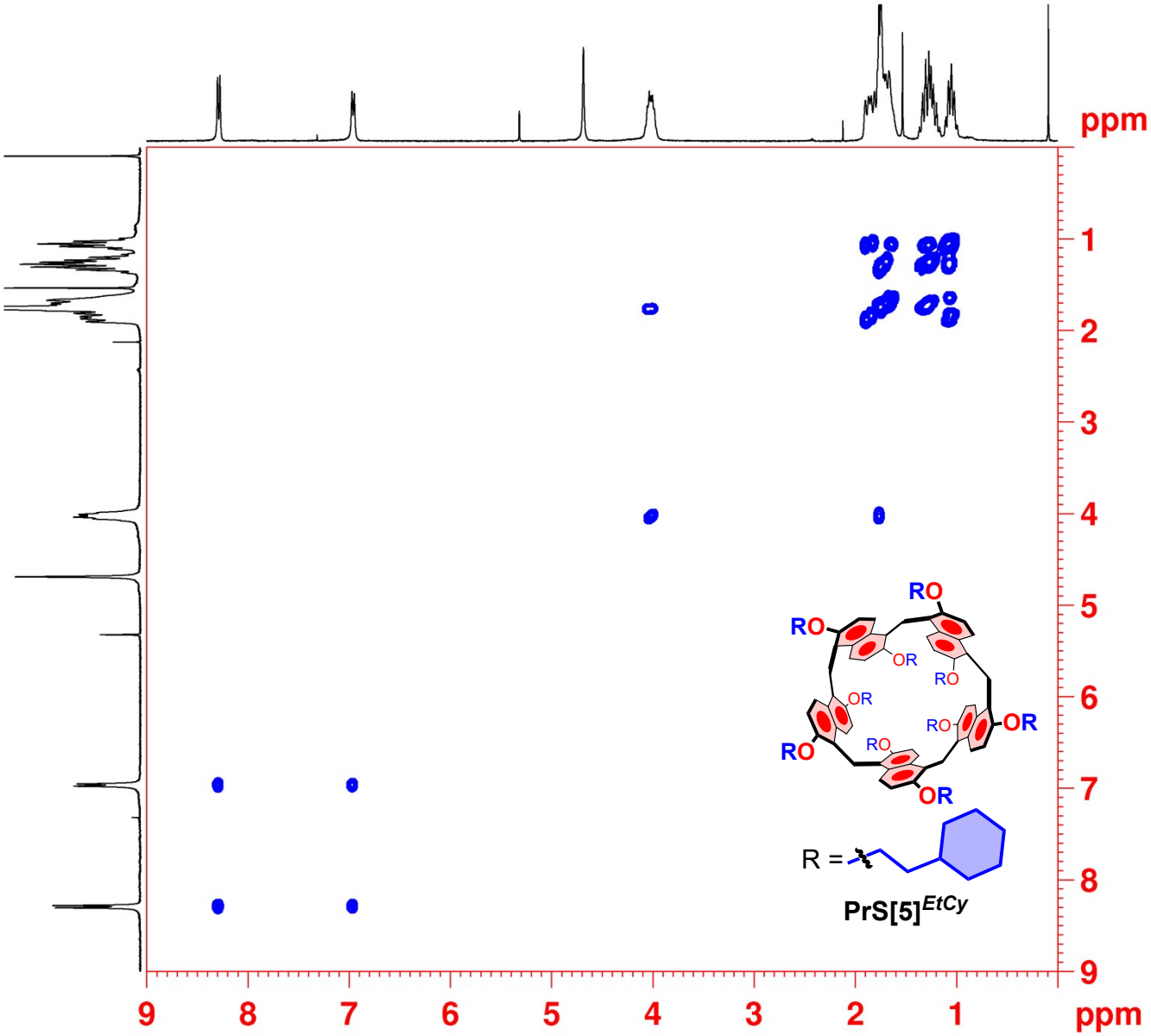

Figure S53: 2D-DQF COSY spectrum of **PrS[5]**^{EtCy} (CD_2Cl_2, 400 MHz, 298 K).

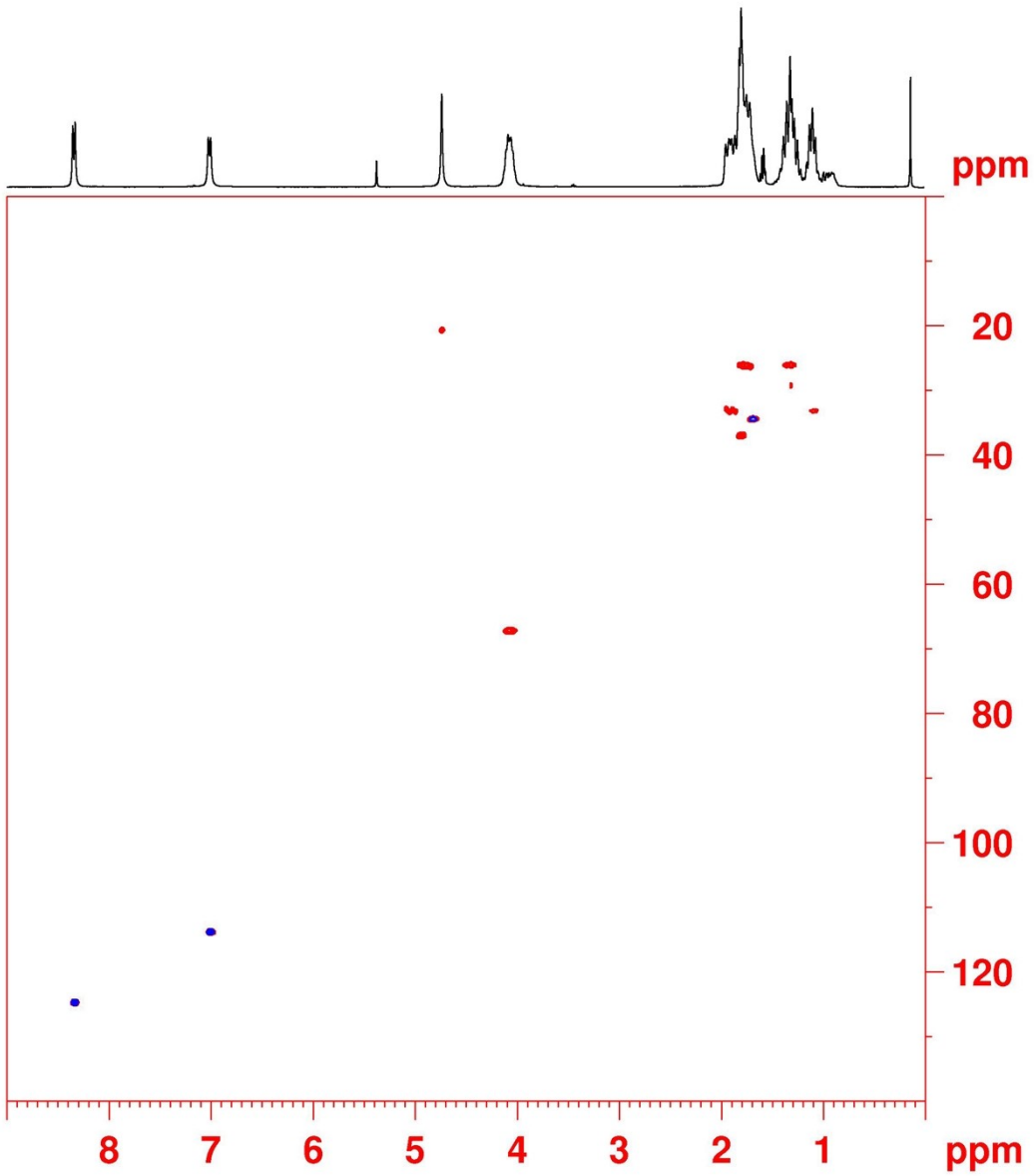

Figure S54: 2D-HSQC spectrum of **PrS[5]**^{EtCy} (CD_2Cl_2, 400 MHz, 298 K).

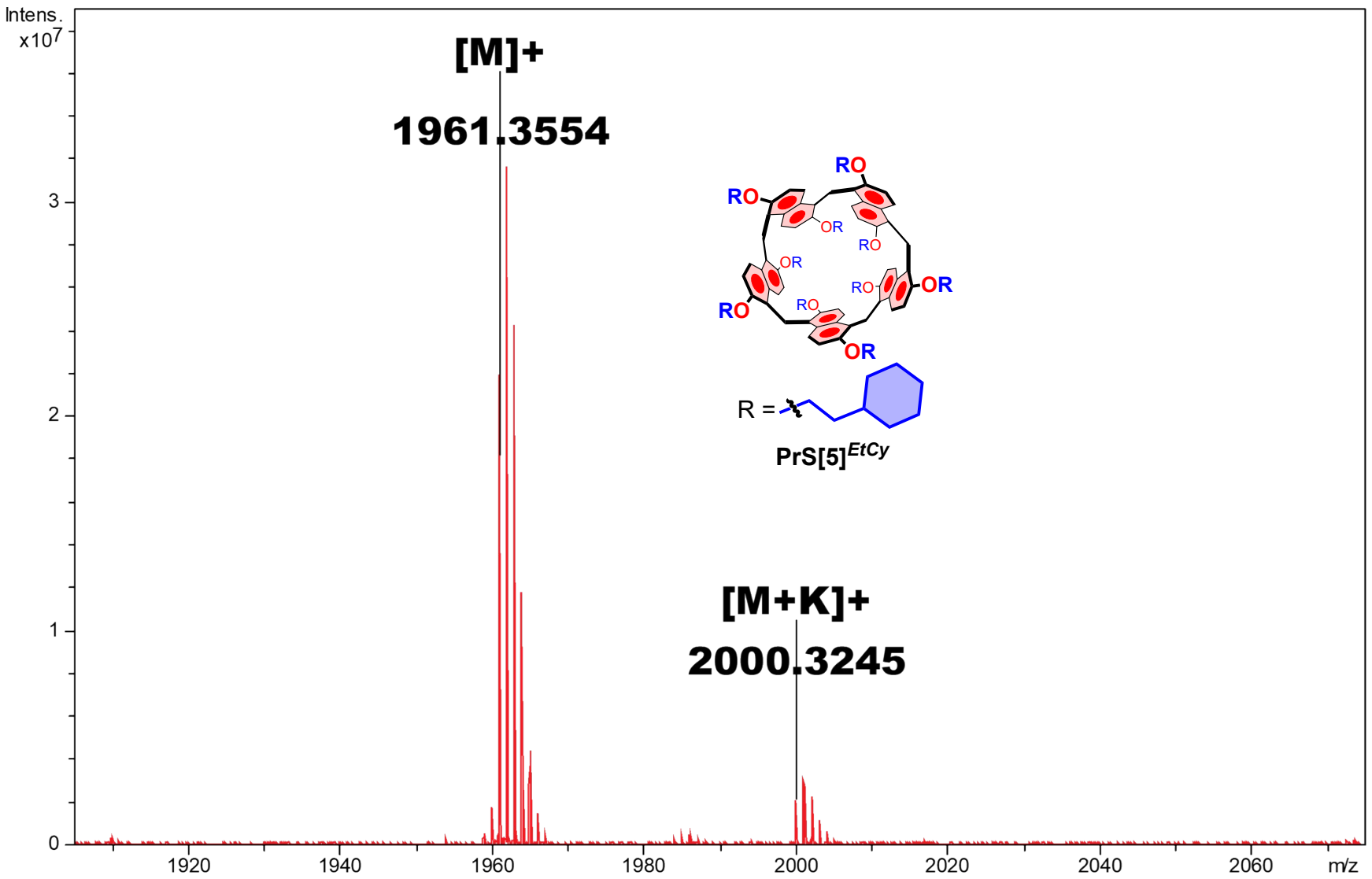

Figure S55: Significant portion of the HR MALDI FT-ICR mass spectrum of **PrS[5]**^{EtCy} $[M]^+$ and $[M+K]^+$.

Copies of 1D and 2D NMR and HR mass spectrum of derivative PrS[5]*PrCy*

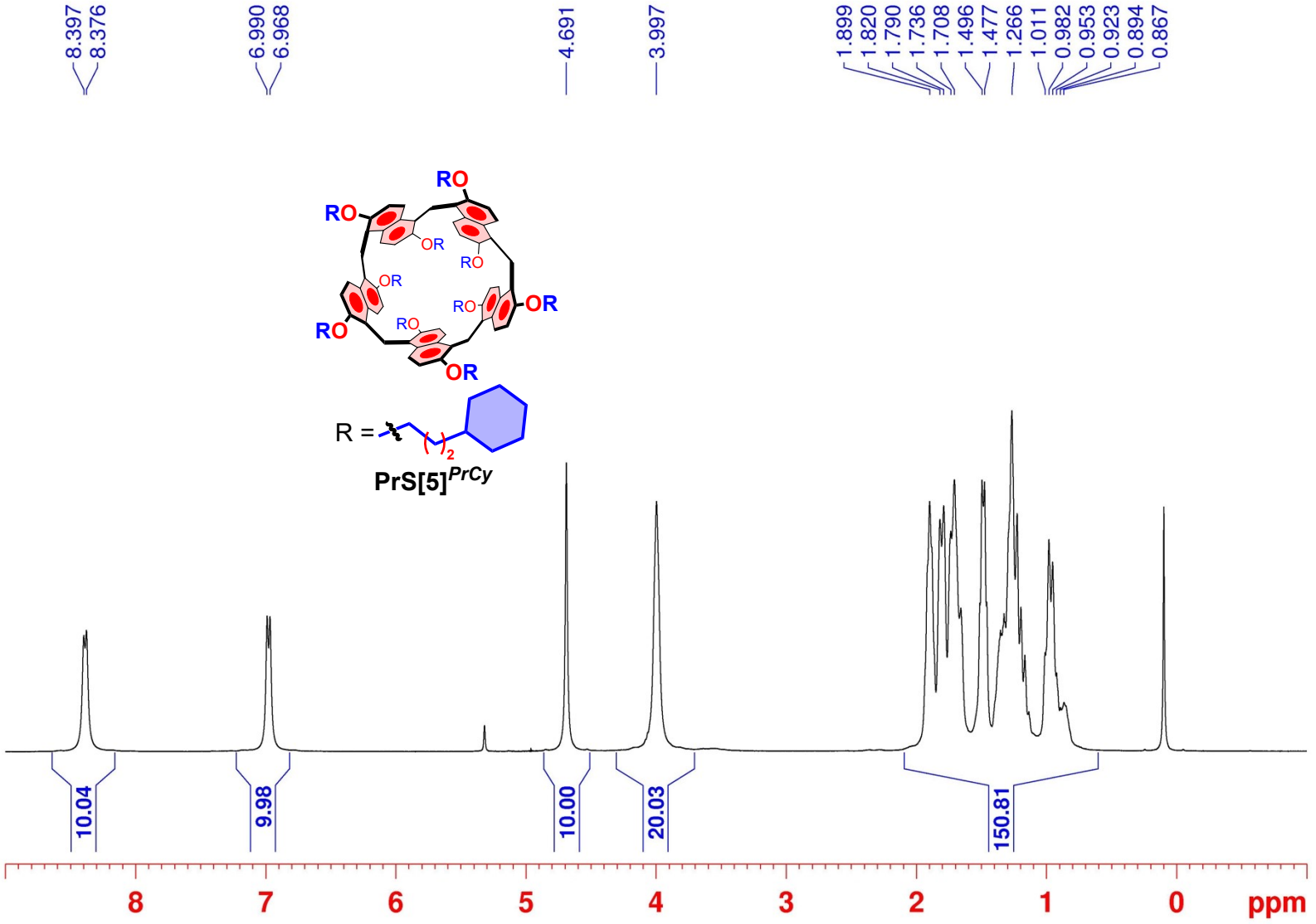

Figure S56: ^{1}H NMR spectrum of derivative **PrS[5]*PrCy*** (CD_2Cl_2, 400 MHz, 298 K).

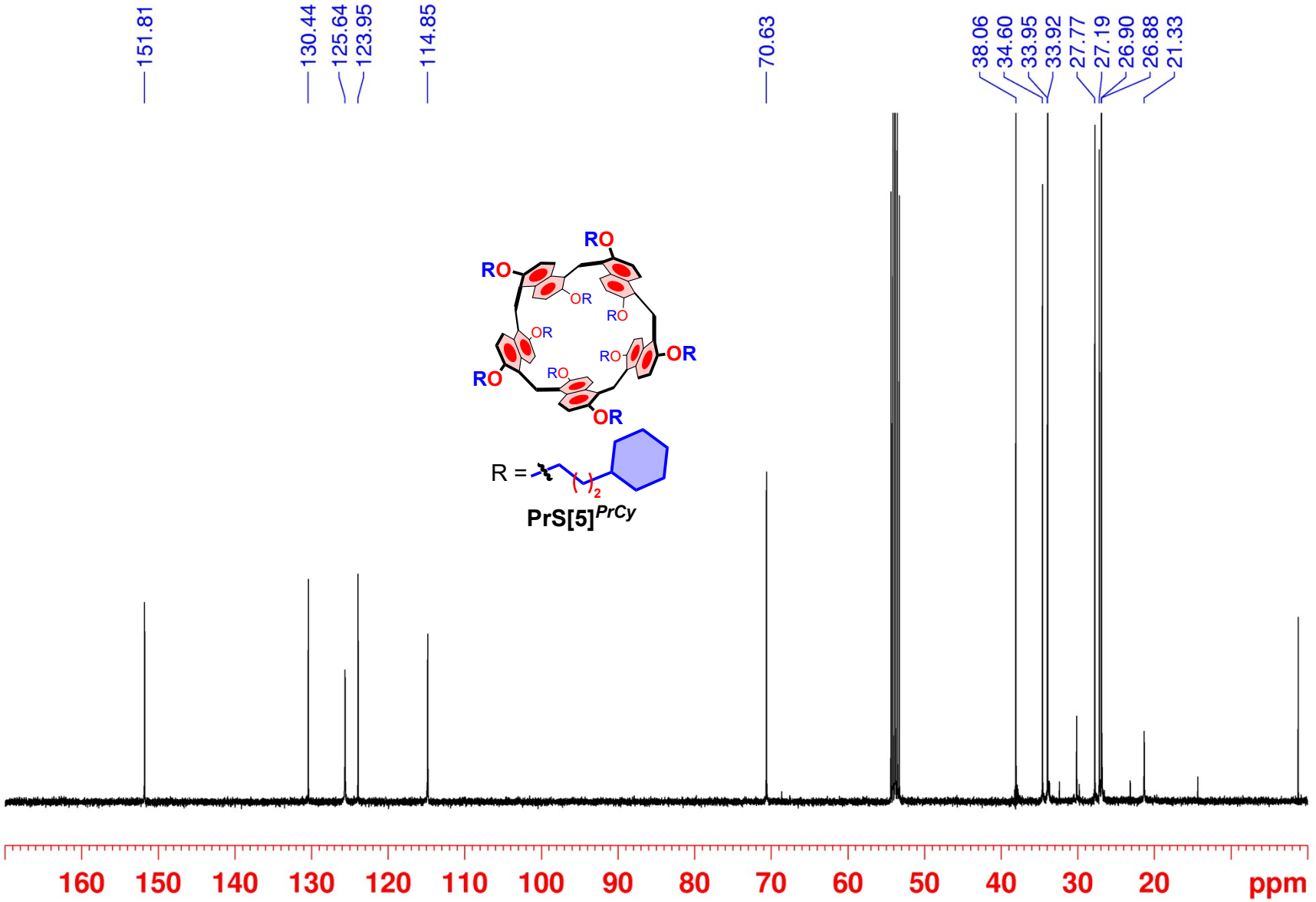

Figure S57: ^{13}C NMR spectrum of **PrS[5]*PrCy*** (CD_2Cl_2, 100 MHz, 298 K).

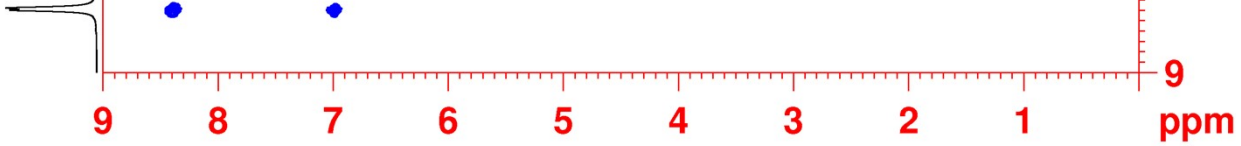

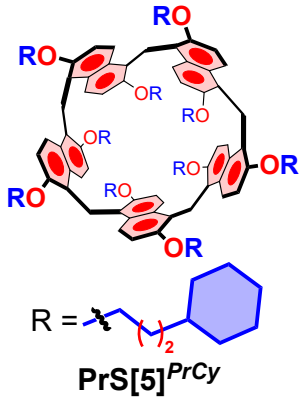

Figure S58: 2D-DQF COSY spectrum of **PrS[5]**^{PrCy} (CD_2Cl_2, 600 MHz, 298 K).

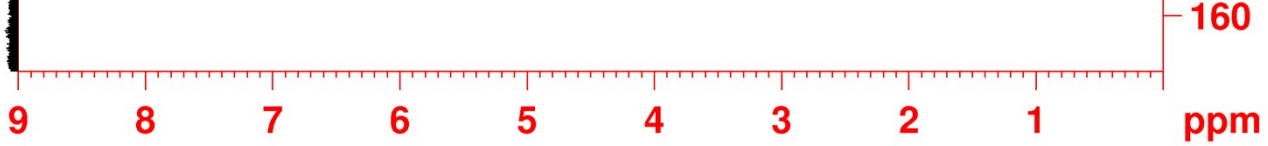

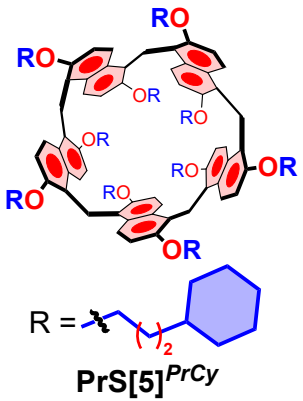

Figure S59: 2D-HSQC spectrum of **PrS[5]**^{PrCy} (CD_2Cl_2, 600 MHz, 298 K).

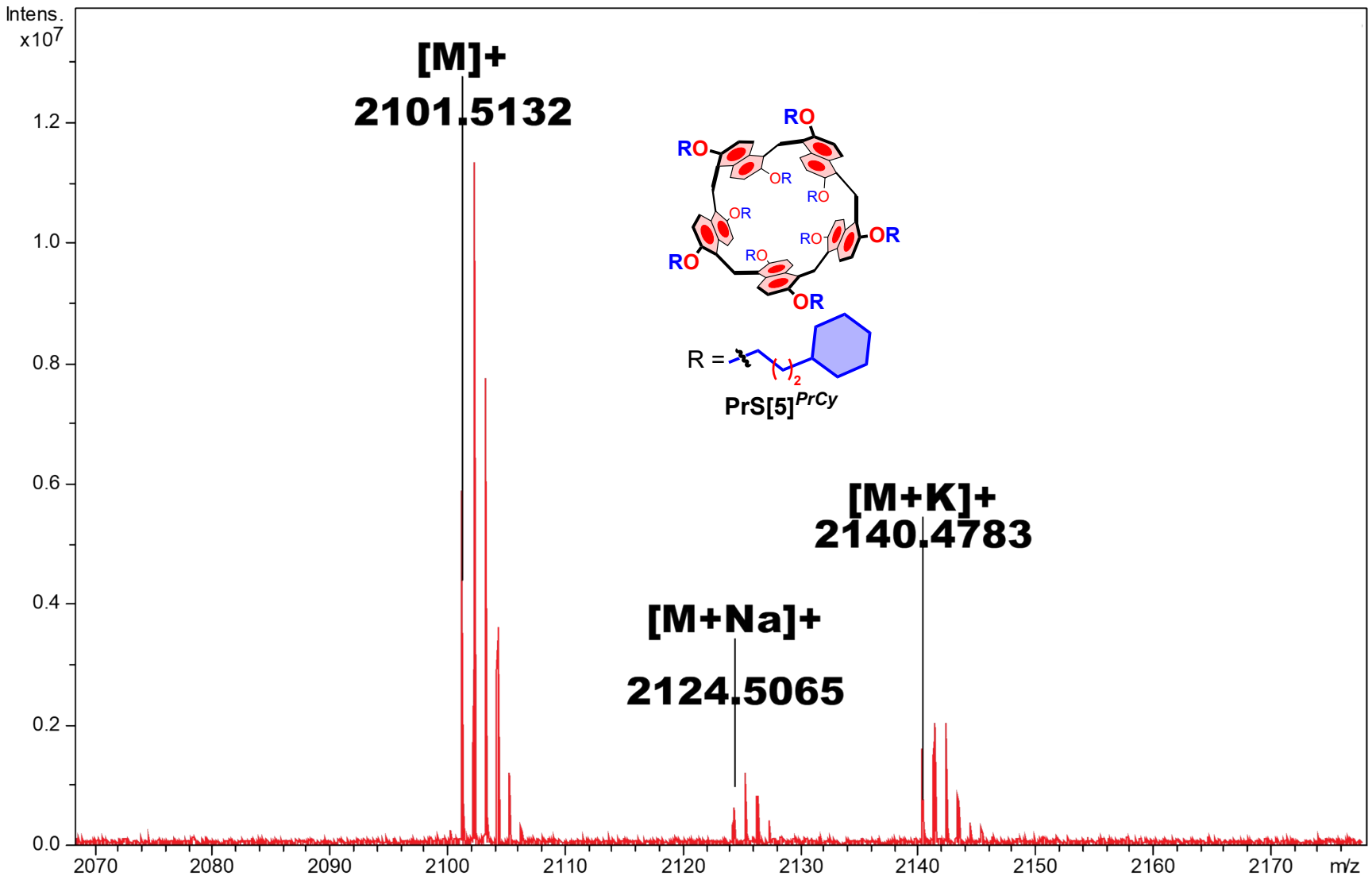

Figure S60: Significant portion of the HR MALDI FT-ICR mass spectrum of **PrS[5]*PrCy*** $[M]^+$, $[M+Na]^+$ and $[M+K]^+$.

Copies of 1D and 2D NMR and HR mass spectrum of derivative PrS[5]^{BuCy}

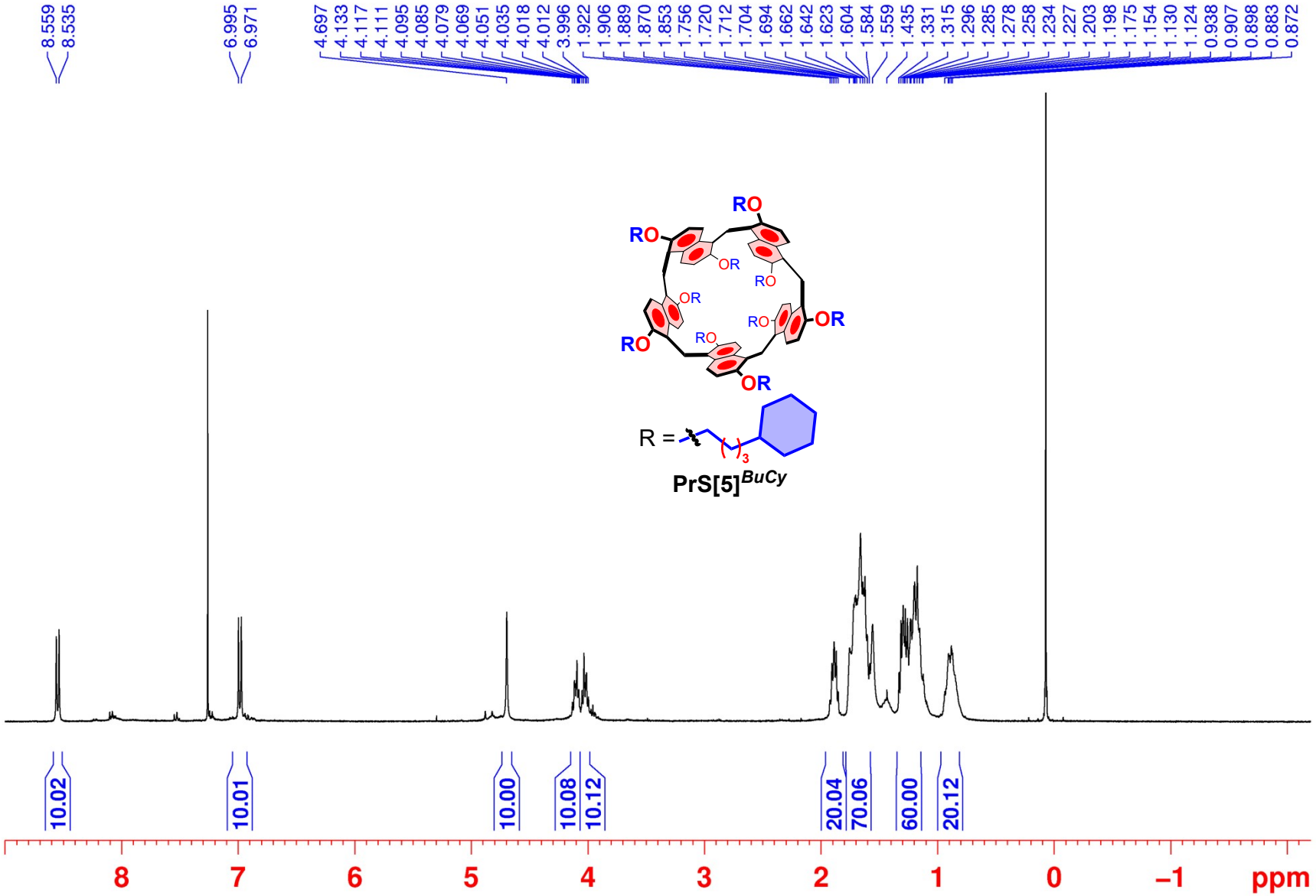

Figure S61: ^{1}H NMR spectrum of derivative **PrS[5]^{BuCy}** ($CDCl_3$, 400 MHz, 298 K).

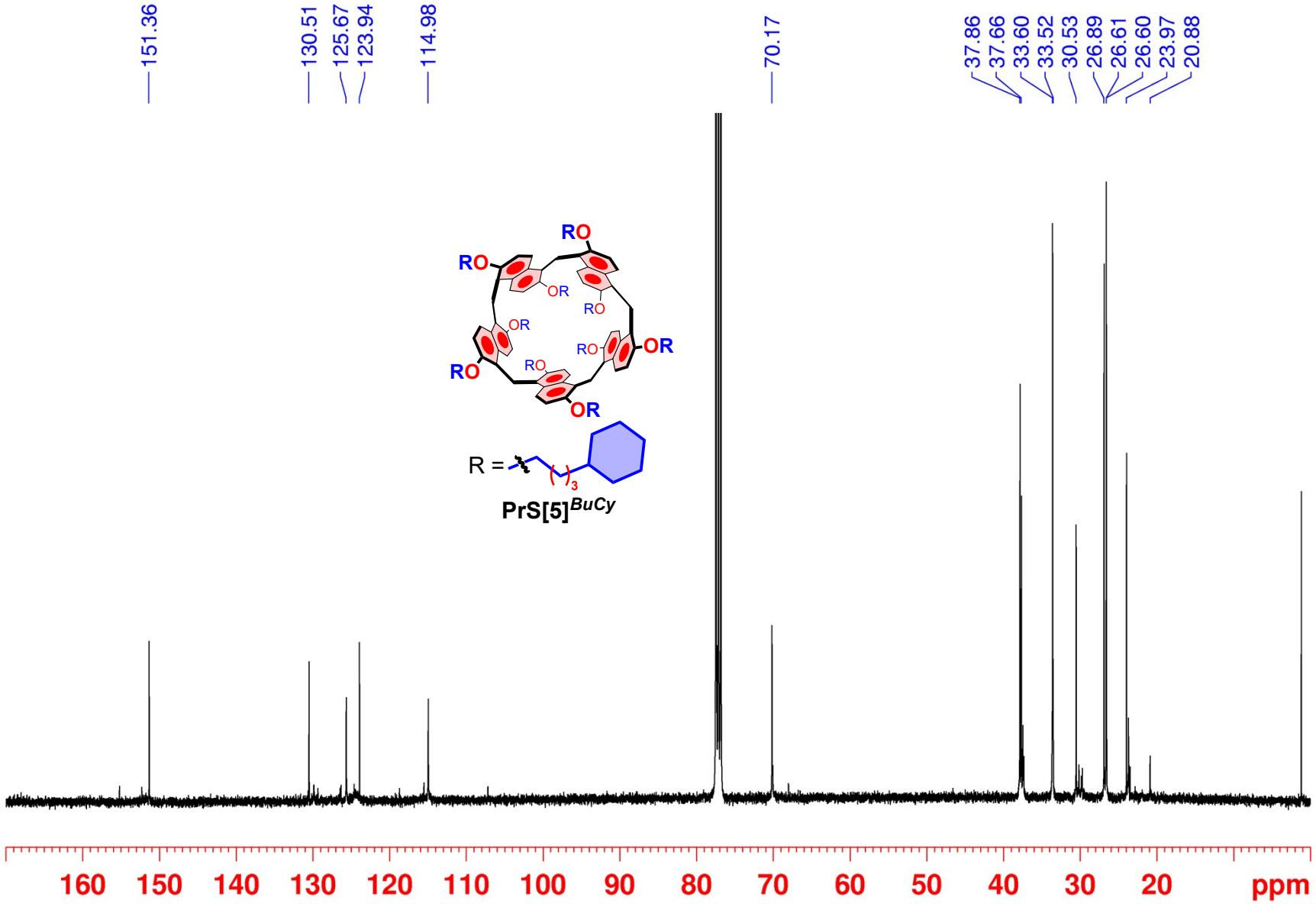

Figure S62: ^{13}C NMR spectrum of **PrS[5]^{BuCy}** ($CDCl_3$, 100 MHz, 298 K).

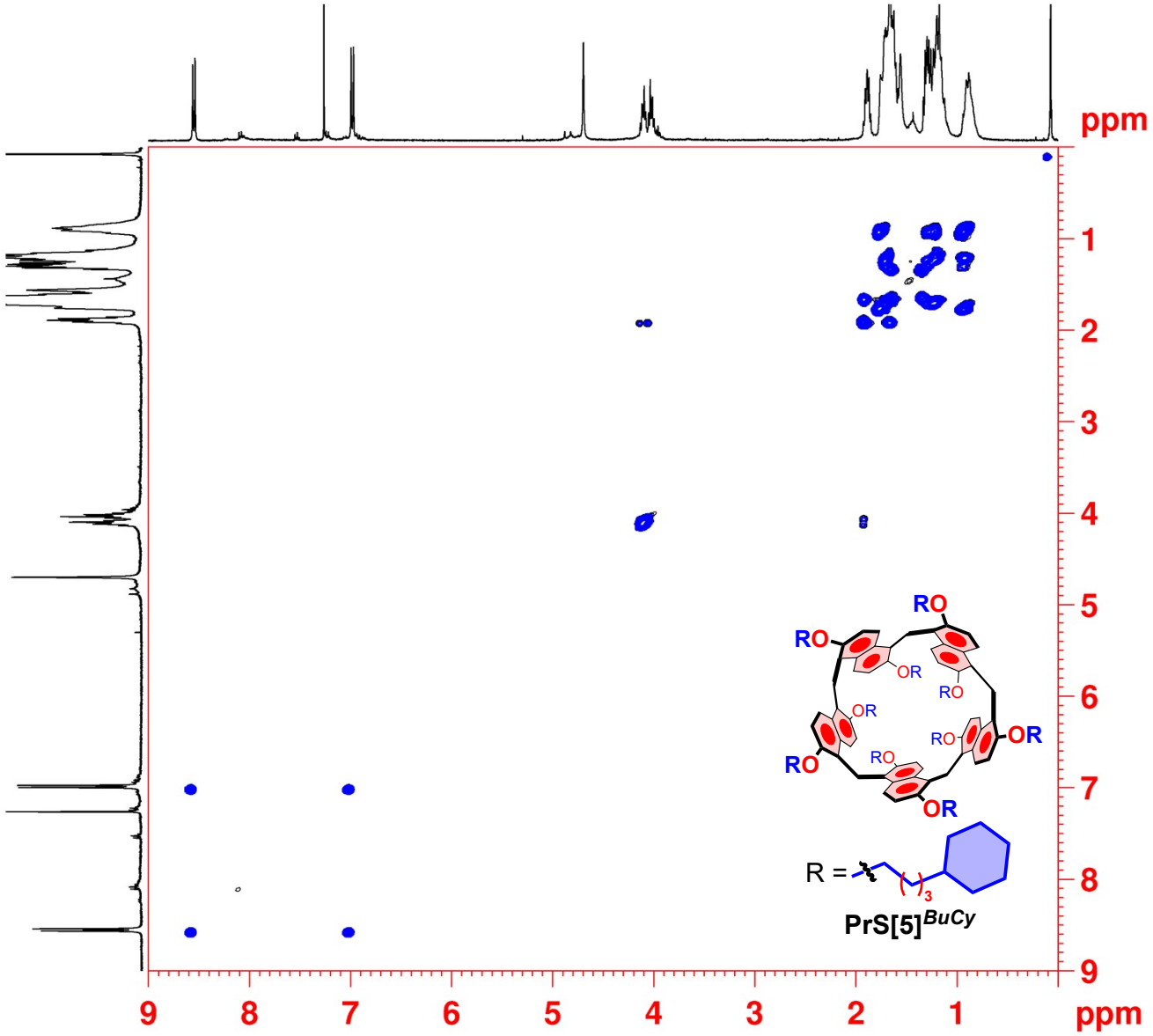

Figure S63: 2D-DQF COSY spectrum of **PrS[5]^{BuCy}** ($CDCl_3$, 400 MHz, 298 K).

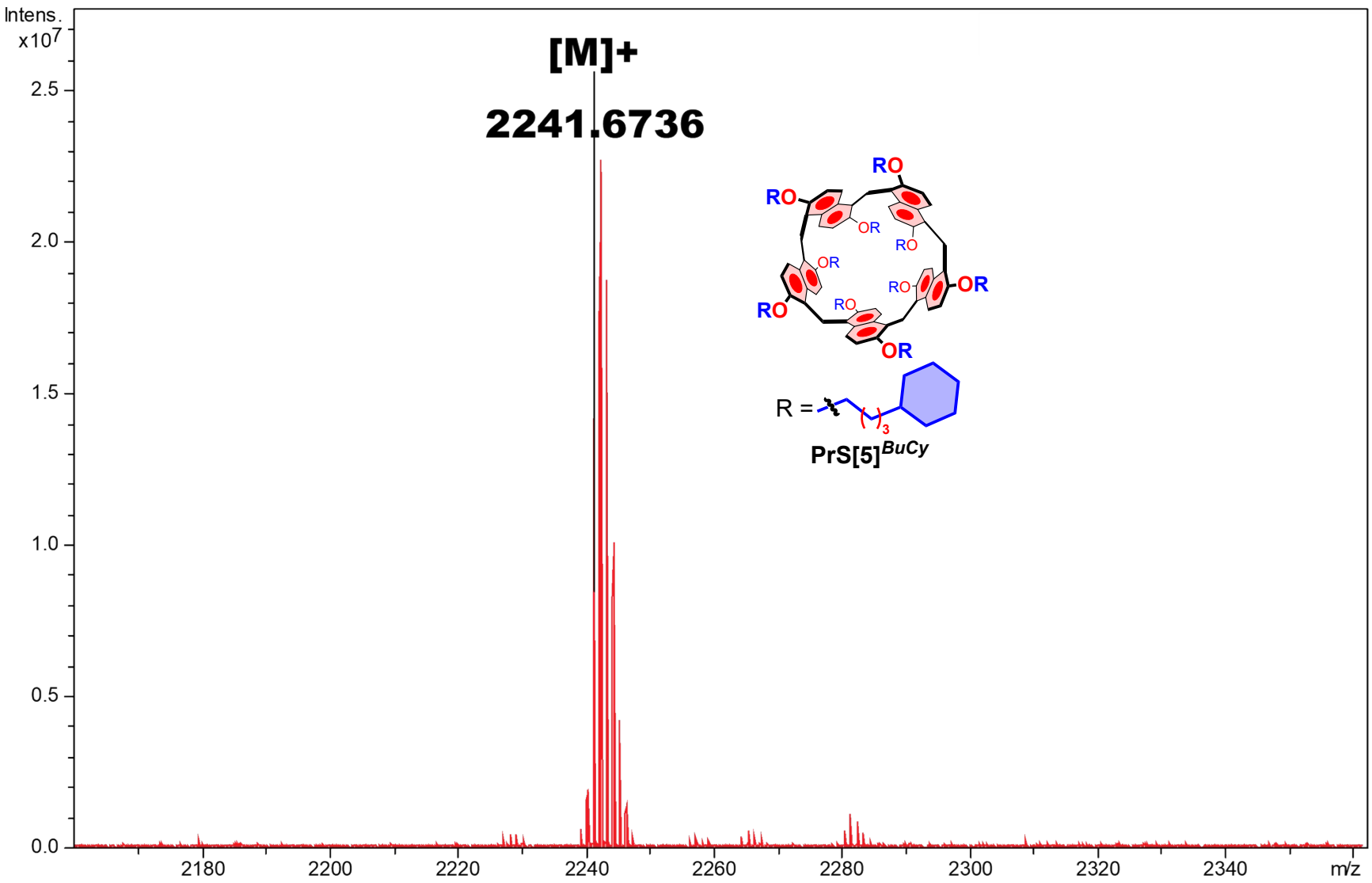

Figure S64: Significant portion of the HR MALDI FT-ICR mass spectrum of **PrS[5]*BuCy*** $[M]^+$.

Copies of 1D and 2D NMR and HR mass spectrum of derivative PrS[5]*MecHp*

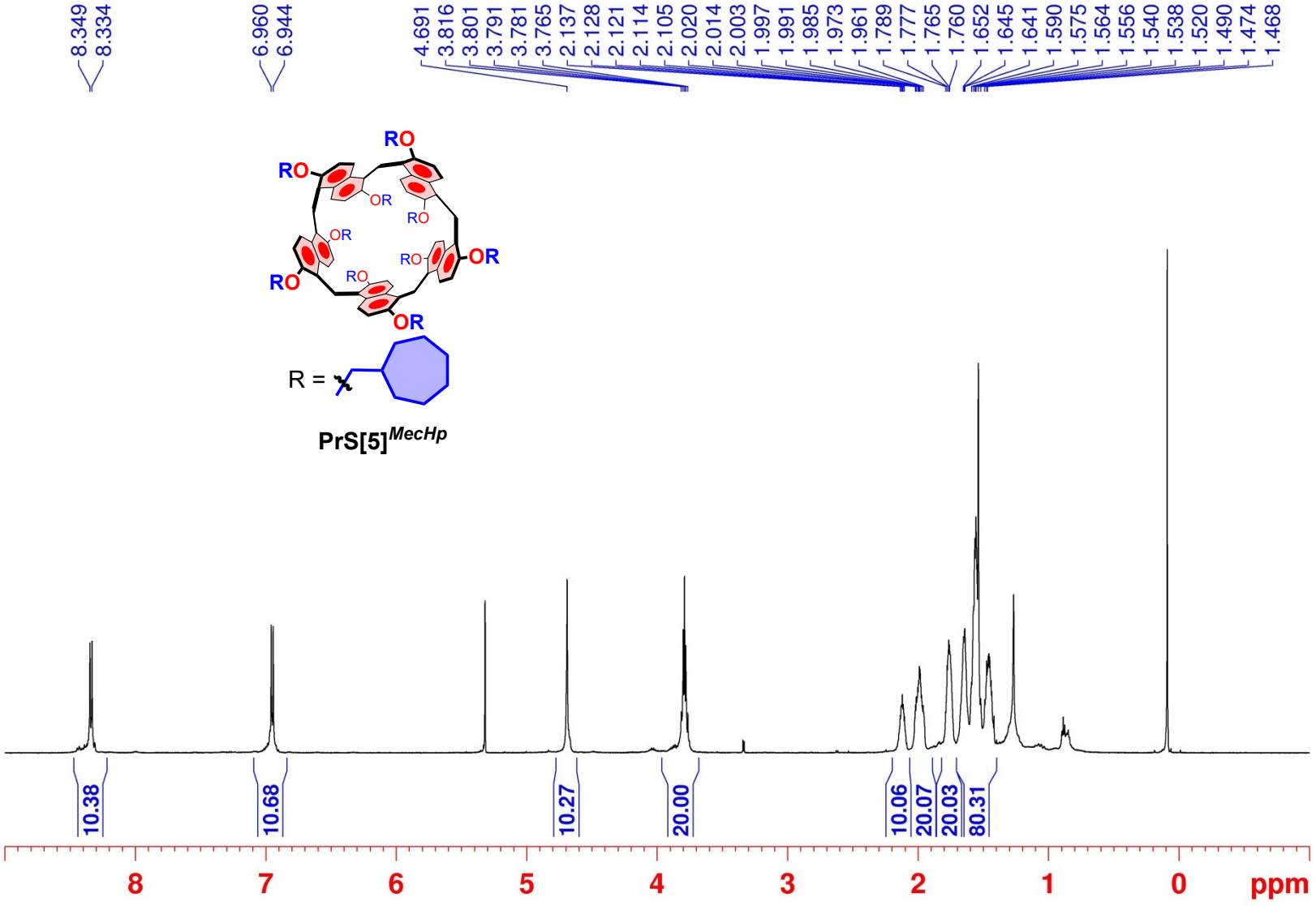

Figure S65: ^{1}H NMR spectrum of derivative **PrS[5]*MecHp*** (CD_2Cl_2, 600 MHz, 298 K).

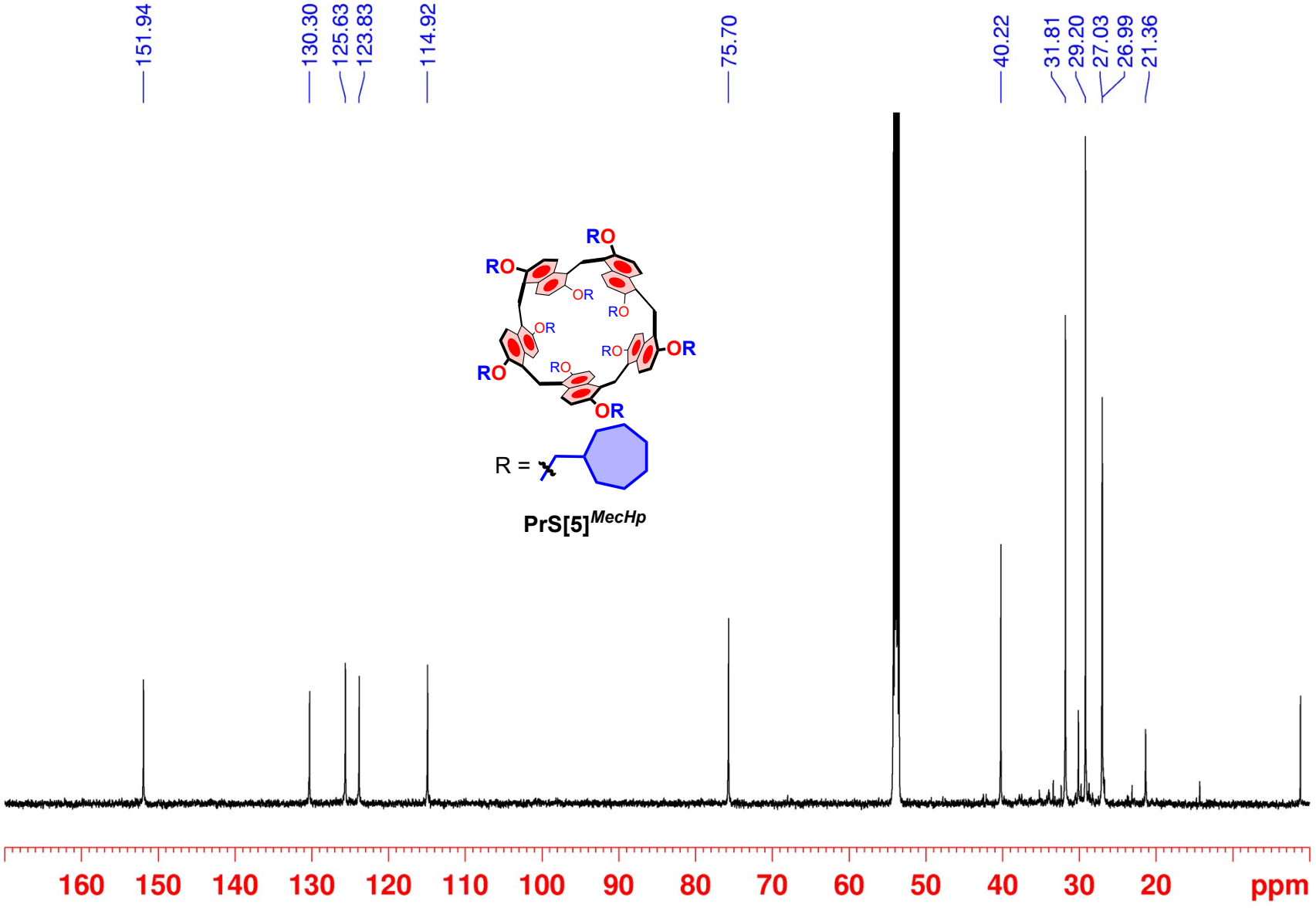

Figure S66: ^{13}C NMR spectrum of **PrS[5]*MecHp*** (CD_2Cl_2, 150 MHz, 298 K).

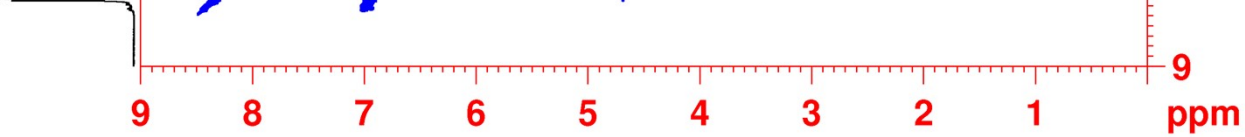

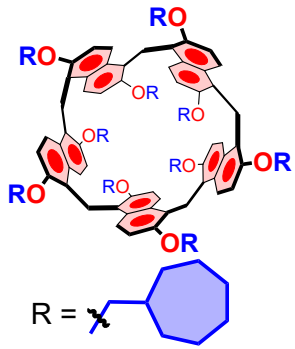

PrS[5]*MecHp*

Figure S67: 2D-DQF COSY spectrum of **PrS[5]*MecHp*** (CD_2Cl_2, 600 MHz, 298 K).

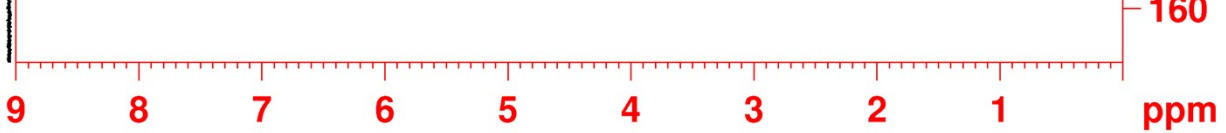

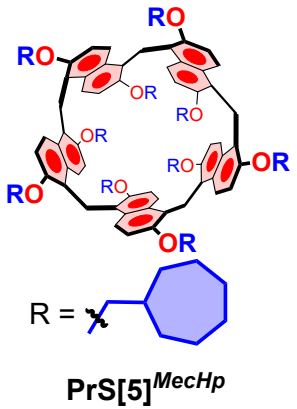

Figure S68: 2D-HSQC spectrum of **PrS[5]*MecHp*** (CD_2Cl_2, 600 MHz, 298 K).

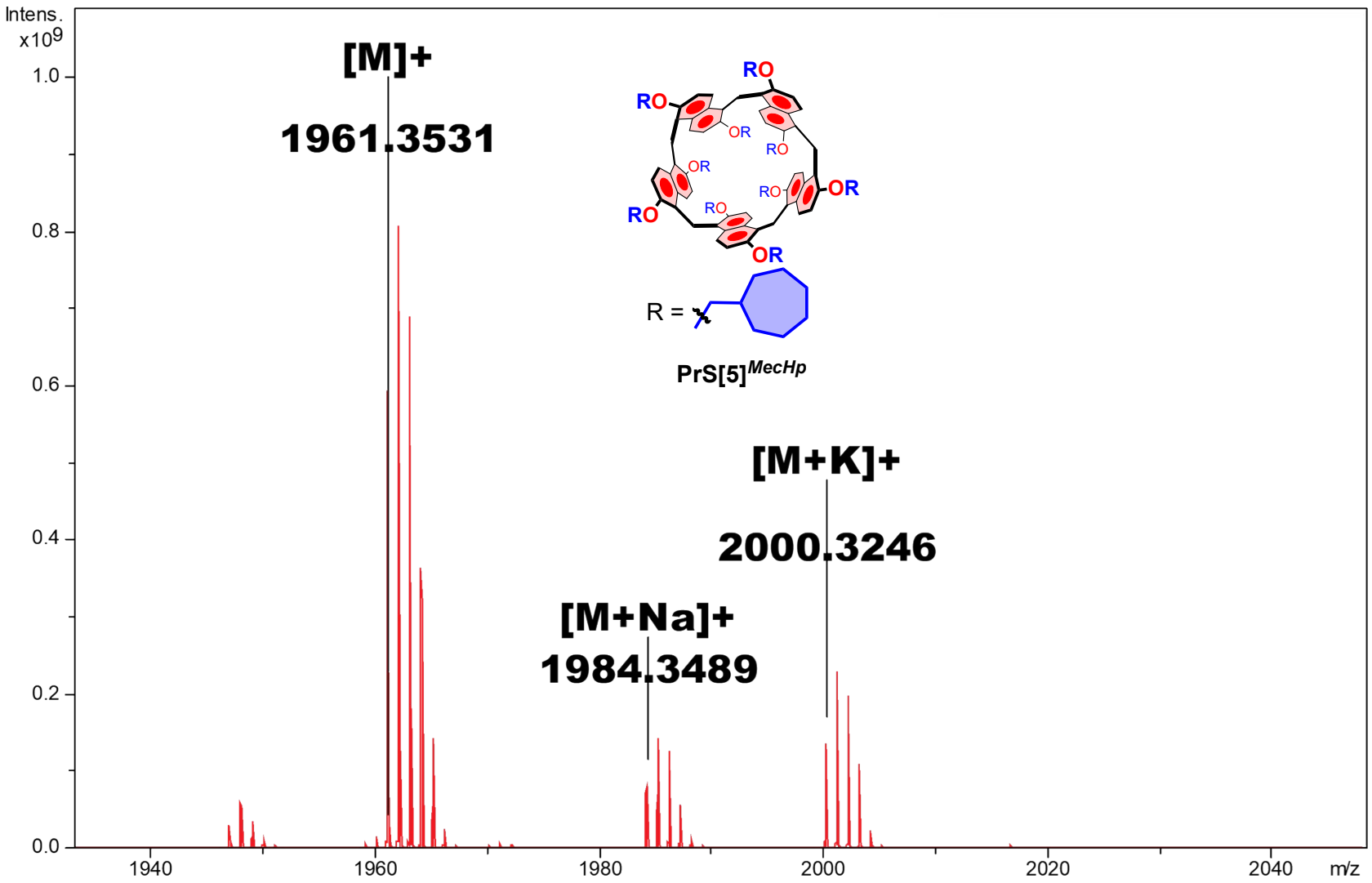

Figure S69: Significant portion of the HR MALDI FT-ICR mass spectrum of **PrS[5]*MecHp*** $[M]^+$, $[M+Na]^+$ and $[M+K]^+$.

Copies of 1D and 2D NMR and HR mass spectrum of derivative PrS[5]*EtcHp*

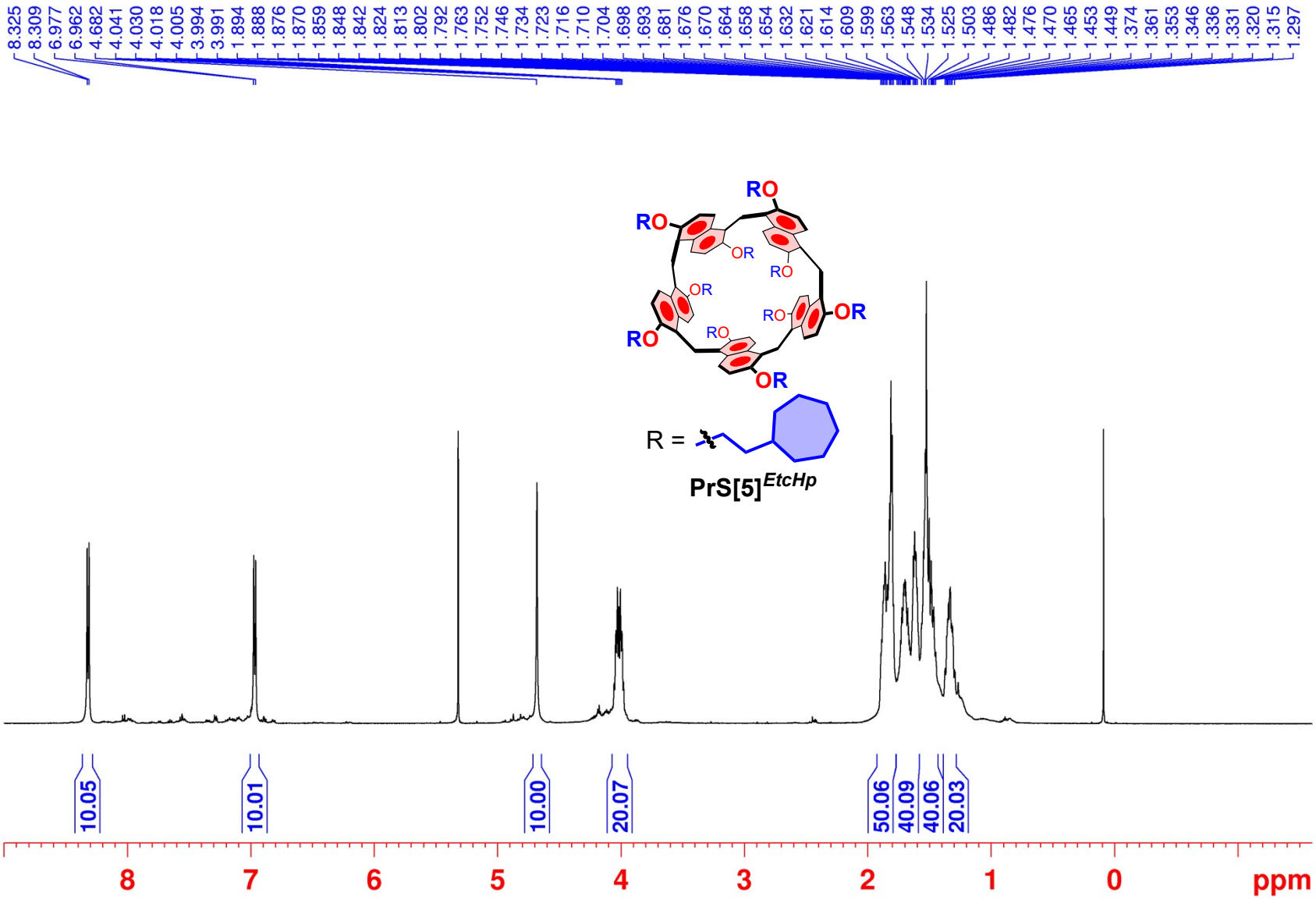

Figure S70: ^{1}H NMR spectrum of derivative **PrS[5]*EtcHp*** (CD_2Cl_2, 600 MHz, 298 K). RIFARE PROTONICO

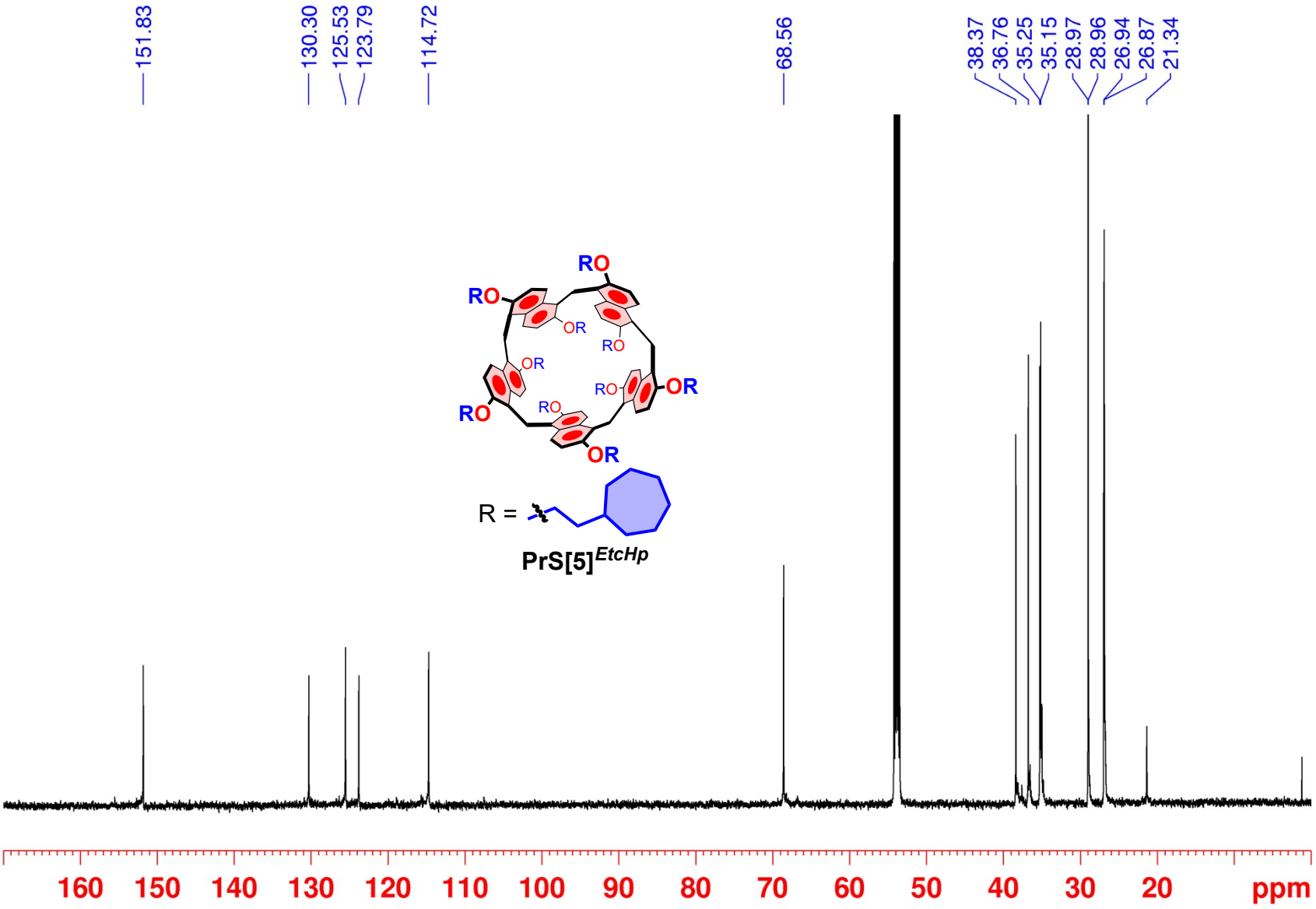

Figure S71: ^{13}C NMR spectrum of **PrS[5]*EtcHp*** (CD_2Cl_2, 150 MHz, 298 K).

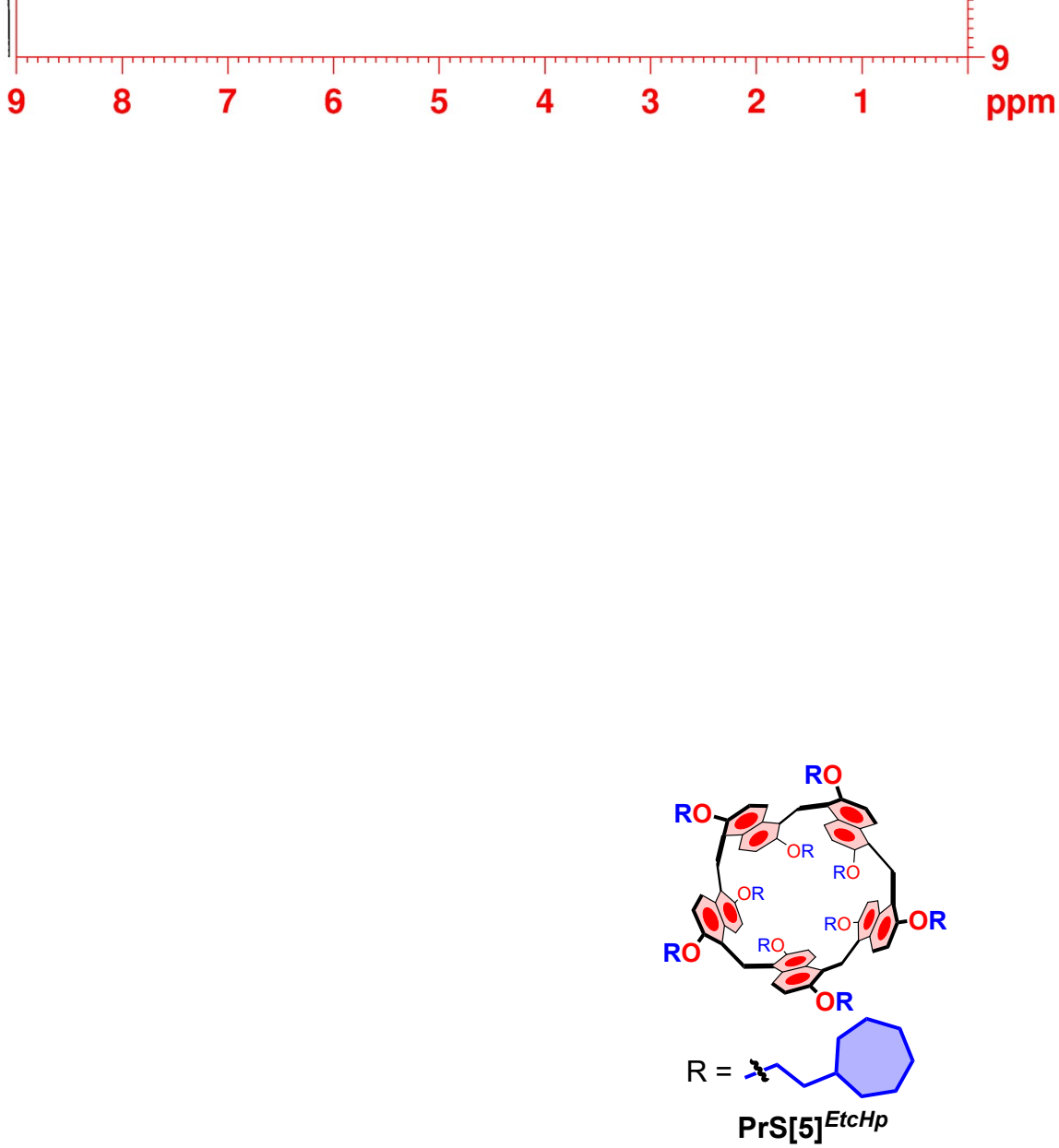

Figure S72: 2D-DQF COSY spectrum of **PrS[5]*EtcHp*** (CD_2Cl_2, 600 MHz, 298 K).

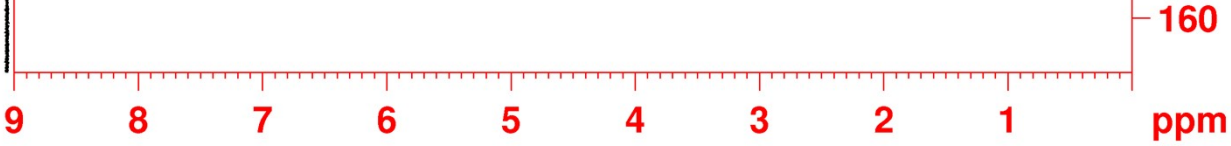

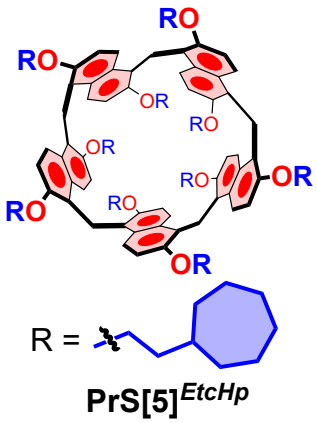

Figure S73: 2D-HSQC spectrum of **PrS[5]*EtcHp*** (CD_2Cl_2, 600 MHz, 298 K).

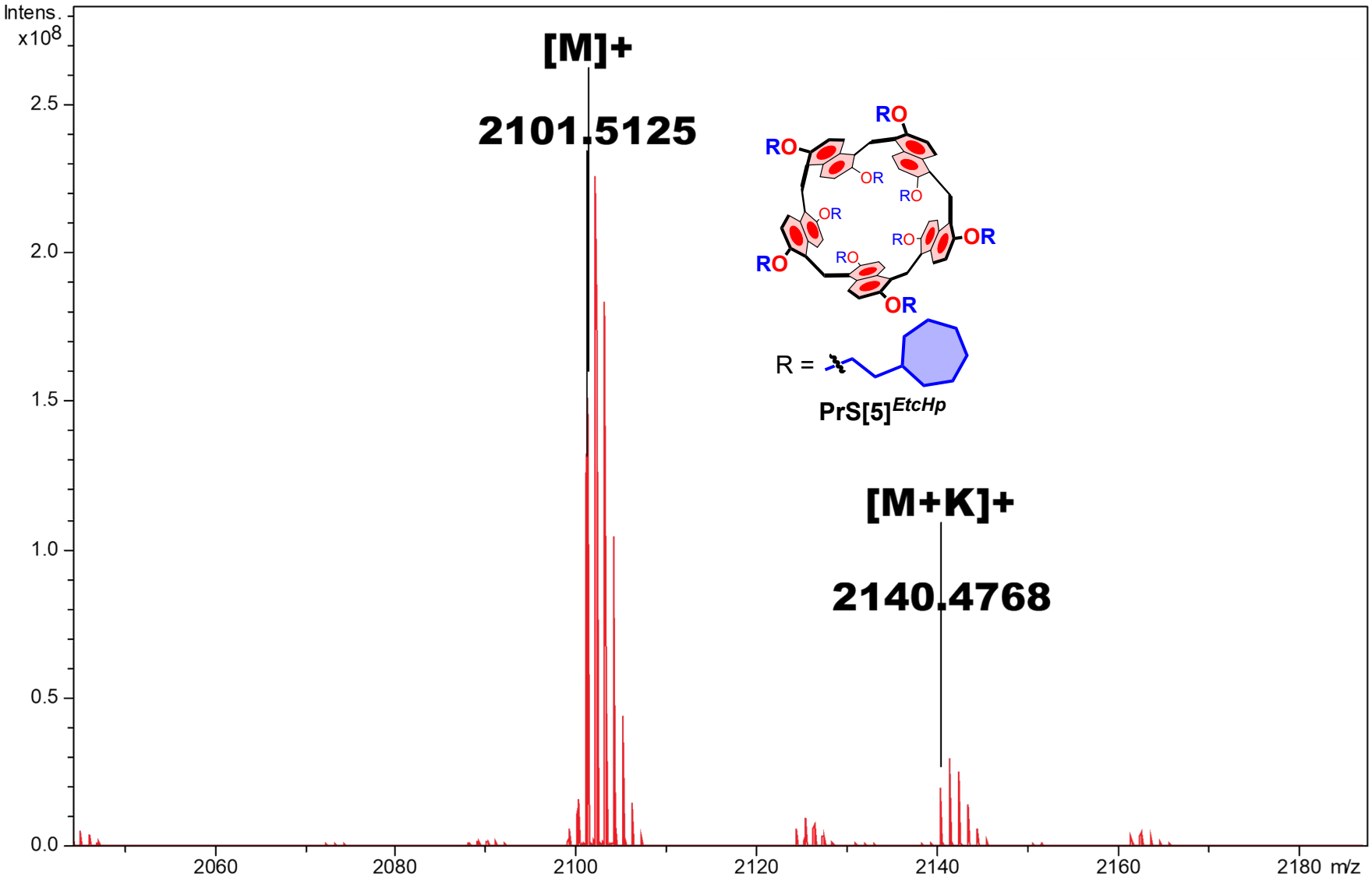

Figure S74: Significant portion of the HR MALDI FT-ICR mass spectrum of **PrS[5]*EtcHp*** $[M]^+$ and $[M+K]^+$.

Copies of 1D and 2D NMR and HR mass spectrum of derivative PrS[5]*MePh*

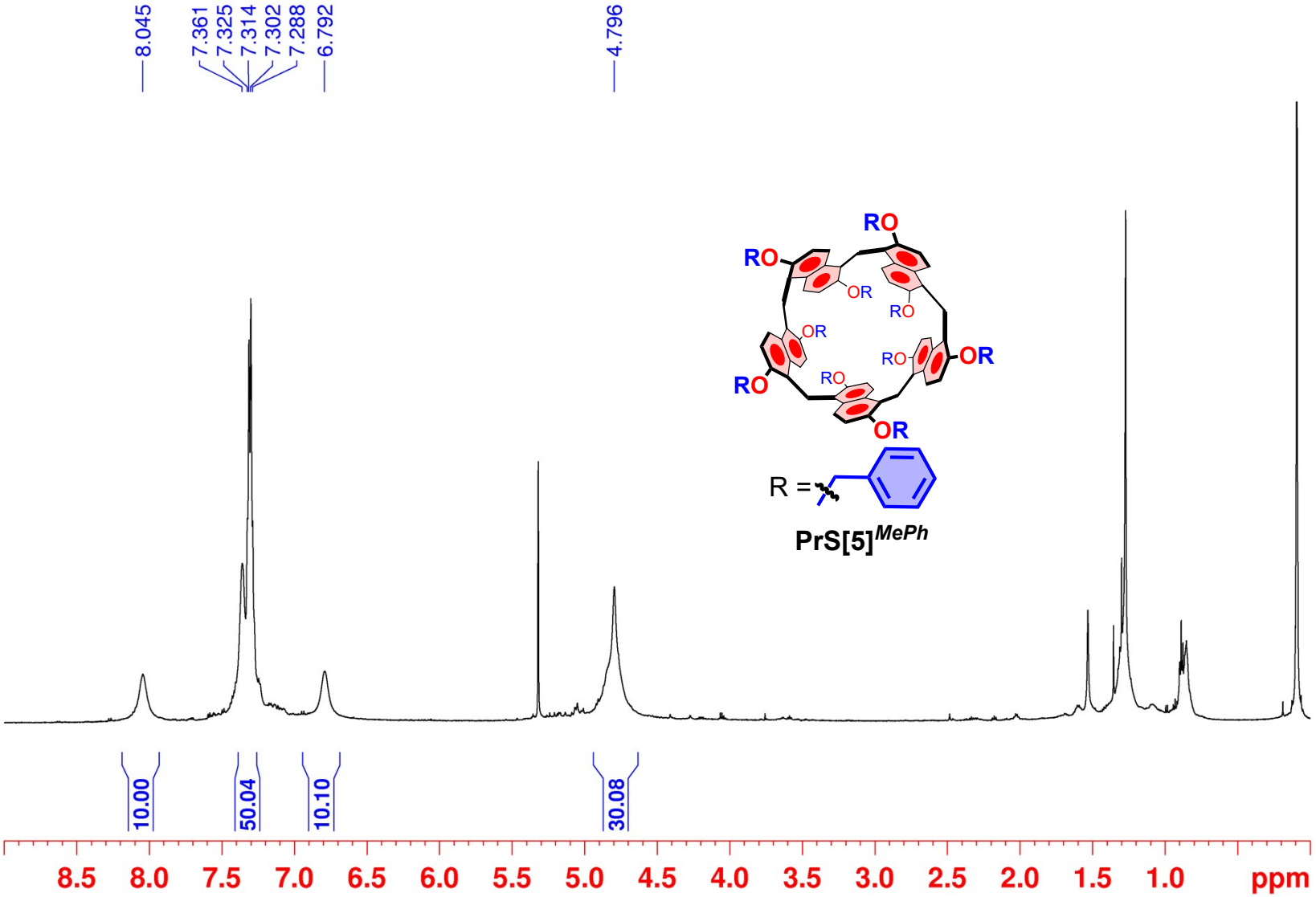

Figure S75: ^{1}H NMR spectrum of derivative **PrS[5]*MePh*** (CD_2Cl_2, 600 MHz, 298 K).

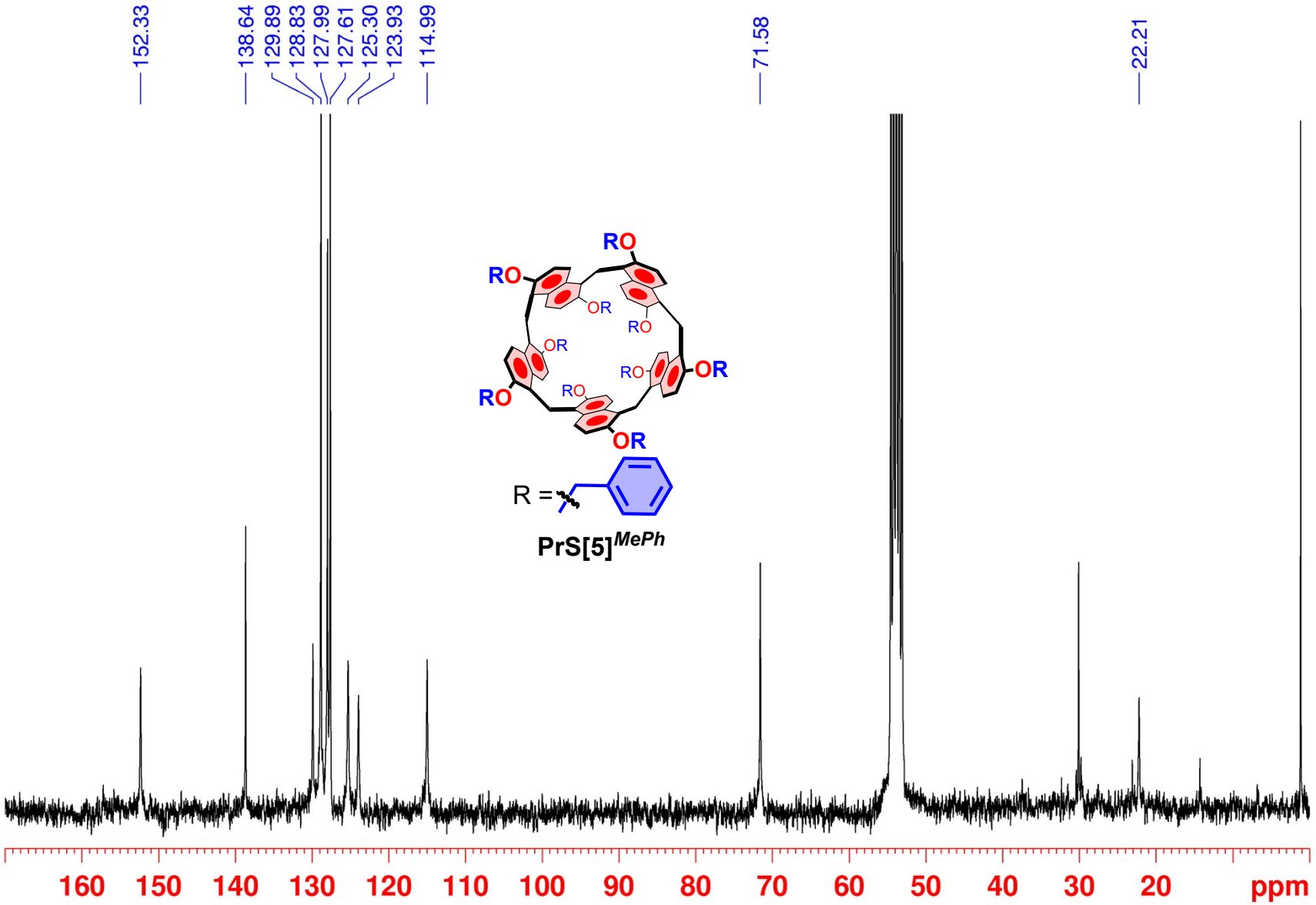

Figure S76: ^{13}C NMR spectrum of **PrS[5]*MePh*** (CD_2Cl_2, 75 MHz, 298 K).

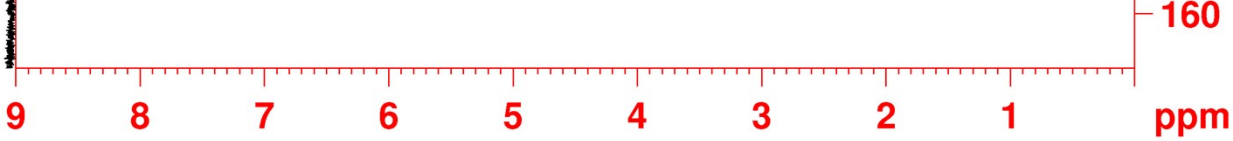

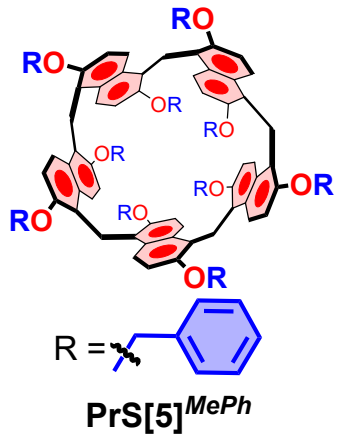

Figure S77: 2D-HSQC spectrum of **PrS[5]*MePh*** (CD_2Cl_2, 600 MHz, 298 K).

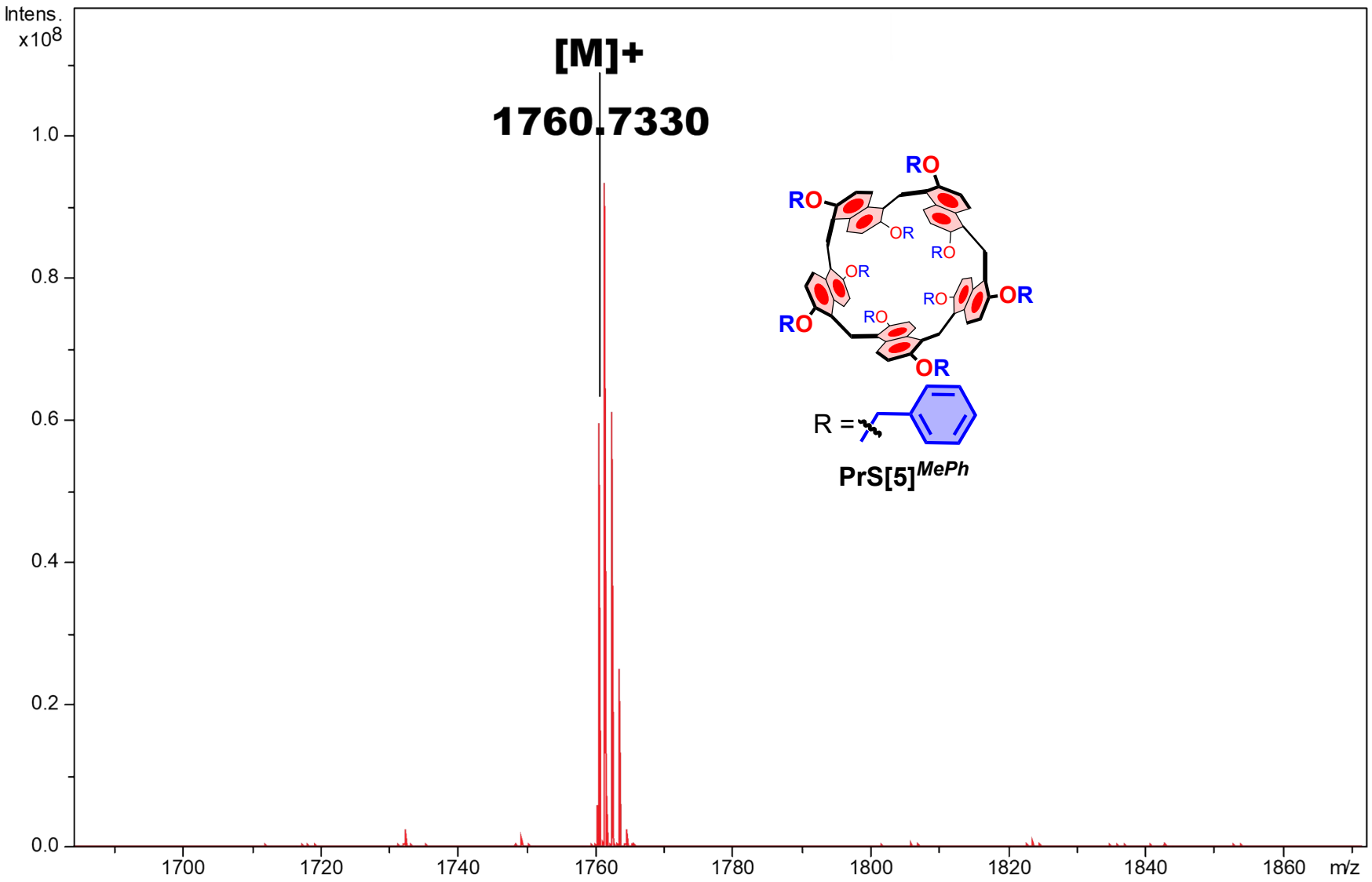

Figure S78: Significant portion of the HR MALDI FT-ICR mass spectrum of **PrS[5]*MePh*** $[M]^+$.

Copies of 1D and 2D NMR and HR mass spectrum of derivative PrS[5]^{BuPh}

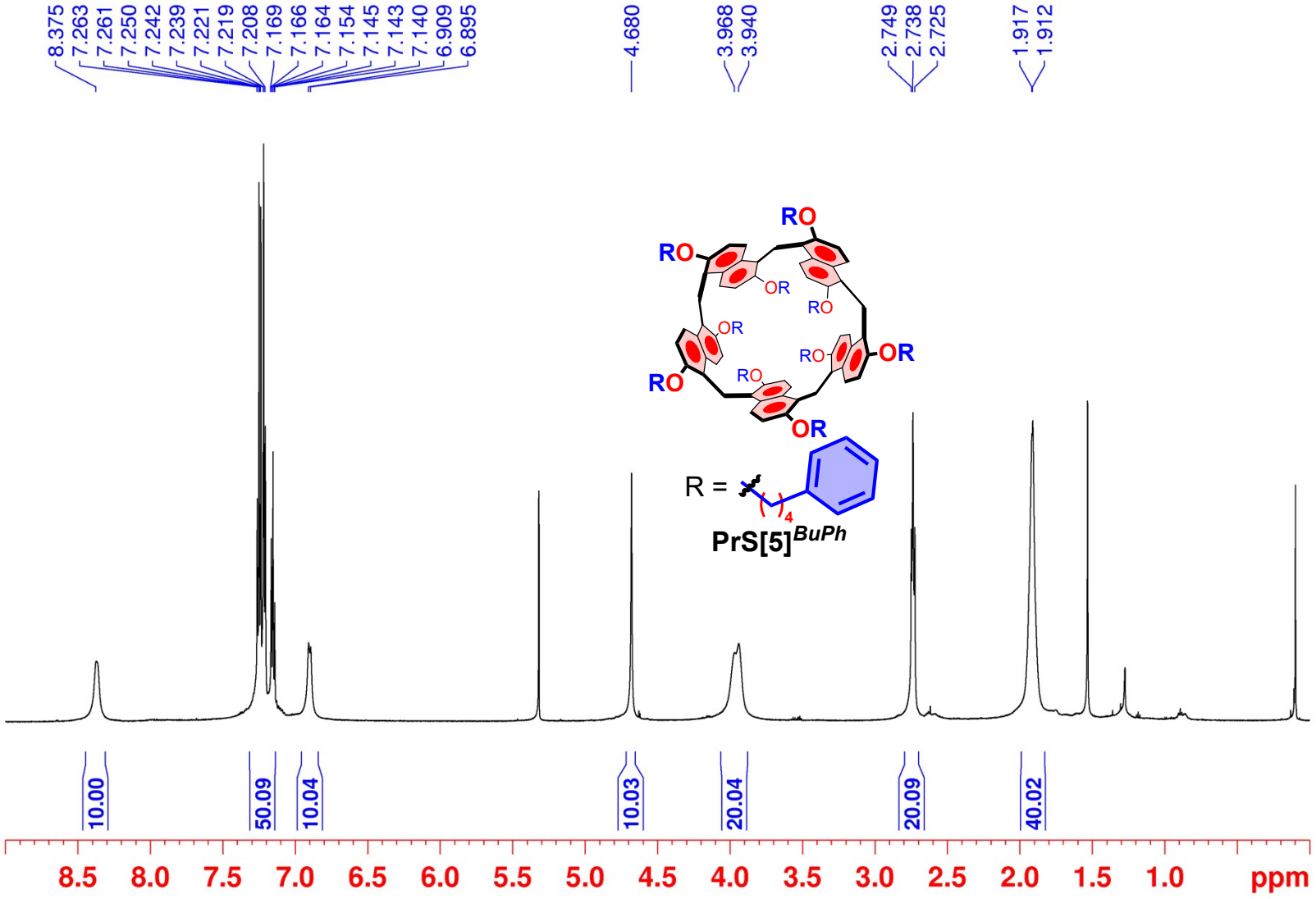

Figure S79: ^{1}H NMR spectrum of derivative **PrS[5]^{BuPh}** (CD_2Cl_2, 600 MHz, 298 K).

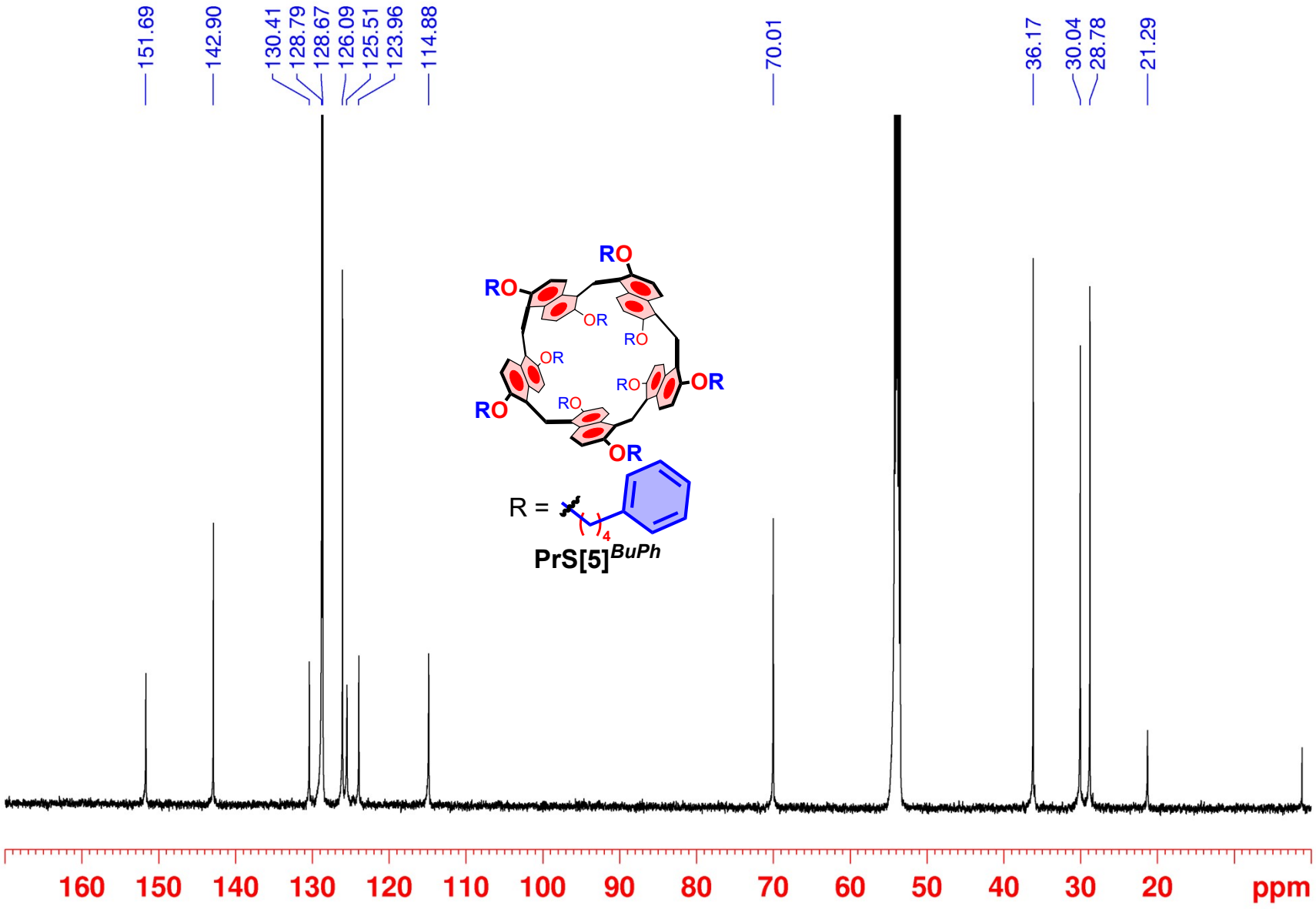

Figure S80: ^{13}C NMR spectrum of **PrS[5]^{BuPh}** (CD_2Cl_2, 150 MHz, 298 K).

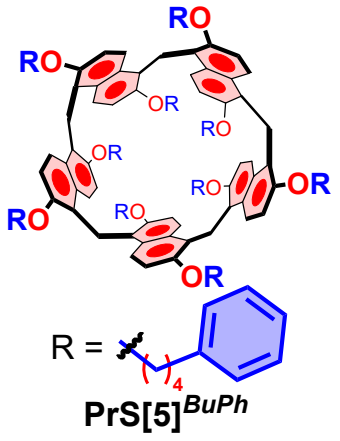

Figure S81: 2D-DQF COSY spectrum of **PrS[5]**^{BuPh} (CD_2Cl_2, 600 MHz, 298 K).

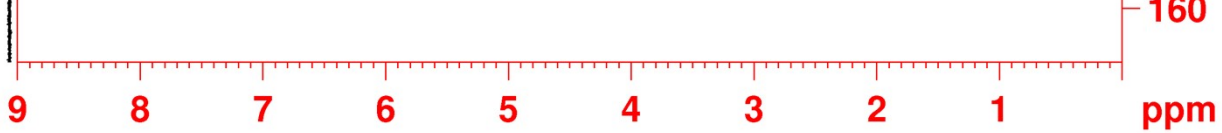

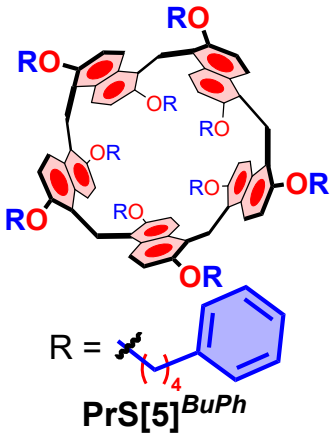

Figure S82: 2D-HSQC spectrum of **PrS[5]**^{BuPh} (CD_2Cl_2, 600 MHz, 298 K).

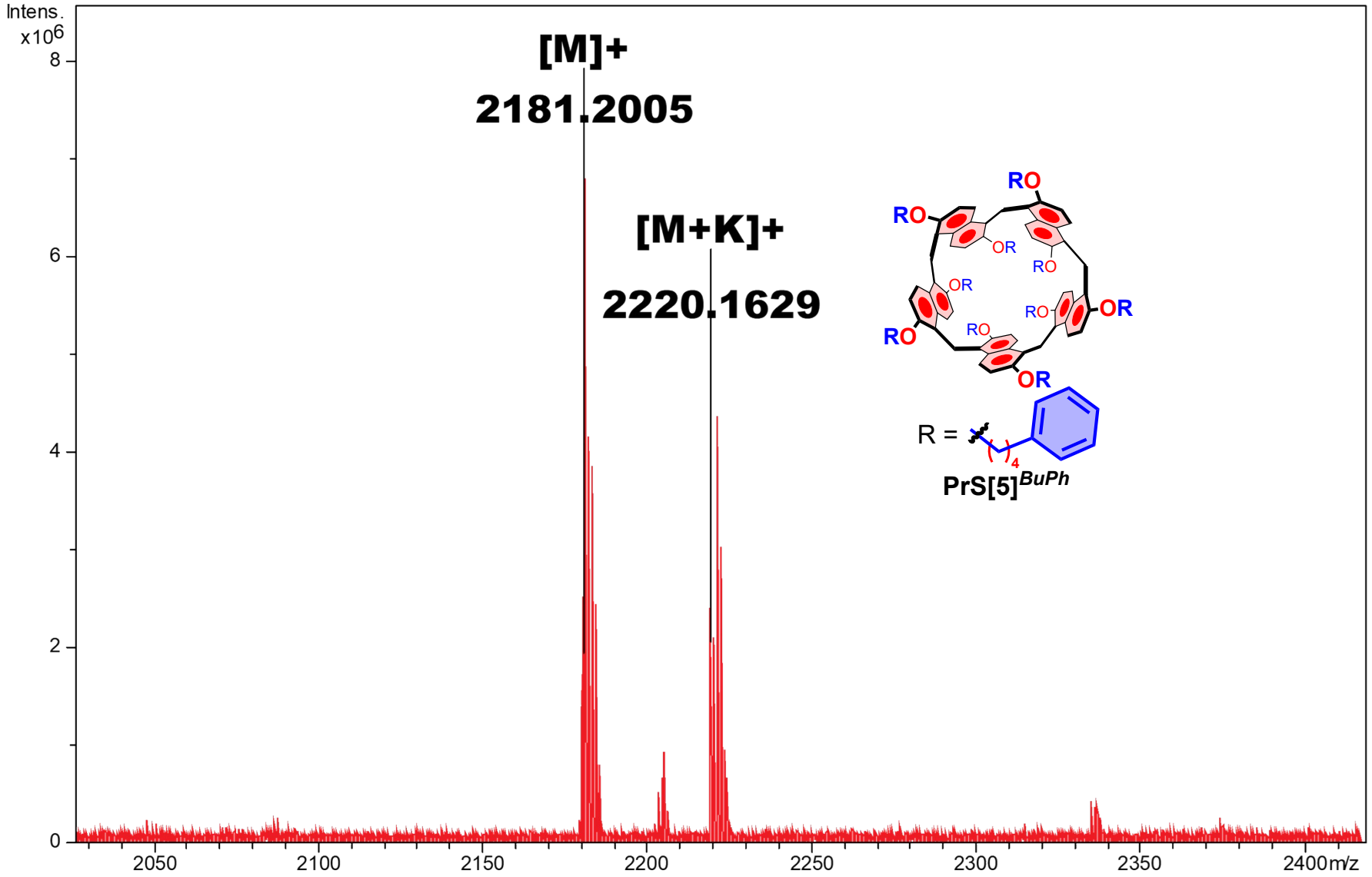

Figure S83: Significant portion of the HR MALDI FT-ICR mass spectrum of **PrS[5]*BuPh*** $[M]^+$ and $[M+K]^+$.

Copies of VT NMR Spectra

Table S2: Coalescence temperatures T_C (K) and $\Delta G^{\ddagger}$ (kcal/mol) values for the oxygen-through-the-annulus rotation of the peralkylated prism[5]arenes **PrS[5]^{R}**

Entry	**PrS[5]^{R}**	**R**	T_C (K)	$\Delta G^{\ddagger}$ (Kcal/mol)
1	**PrS[5]^{Et}**	Ethyl	338	16.8
2	**PrS[5]^{nPr}**	*n*-propyl	348	17.4
3	**PrS[5]^{nBu}**	*n*-butyl	353	17.8
4	**PrS[5]^{nPe}**	*n*-pentyl	358	18.0
5	**PrS[5]^{nHex}**	*n*-hexyl	363	18.5
6	**PrS[5]^{Hp}**	*n*-heptyl	373	18.6
7	**PrS[5]^{Nonyl}**	*n*-nonyl	*	> 19,2
8	**PrS[5]^{iPr}**	isopropyl	**	-----
9	**PrS[5]^{iBu}**	isobutyl	373	18.9
10	**PrS[5]^{iPe}**	isopentyl	373	18.3
11	**PrS[5]^{iHex}**	isohexyl	383	19.2
12	**PrS[5]^{MeCy}**	cyclohexylmethyl	***	---
13	**PrS[5]^{EtCy}**	cyclohexylethyl	**	-----
14	**PrS[5]^{PrCy}**	cyclohexylpropyl	**	-----
15	**PrS[5]^{BuCy}**	cyclohexylbutyl	**	-----
16	**PrS[5]^{EtcHp}**	cycloheptylethyl	**	-----
17	**PrS[5]^{BuPh}**	phenylbutyl	**	-----

*A broadening of the OCH_2 diastereotopic signals was observed at 383 K. **No hint of coalescence was observed in the temperature range investigated (298−383 K) in Toluene-d_8. *** Deuterated chlorobenzene was used as solvent due to the accidental isochronous appearance of OCH_2 signals in deuterated toluene. No hint of coalescence was observed in the temperature range investigated (298−383 K) in C_6D_5Cl.

HT NMR studies of PrS[5]^{Et}

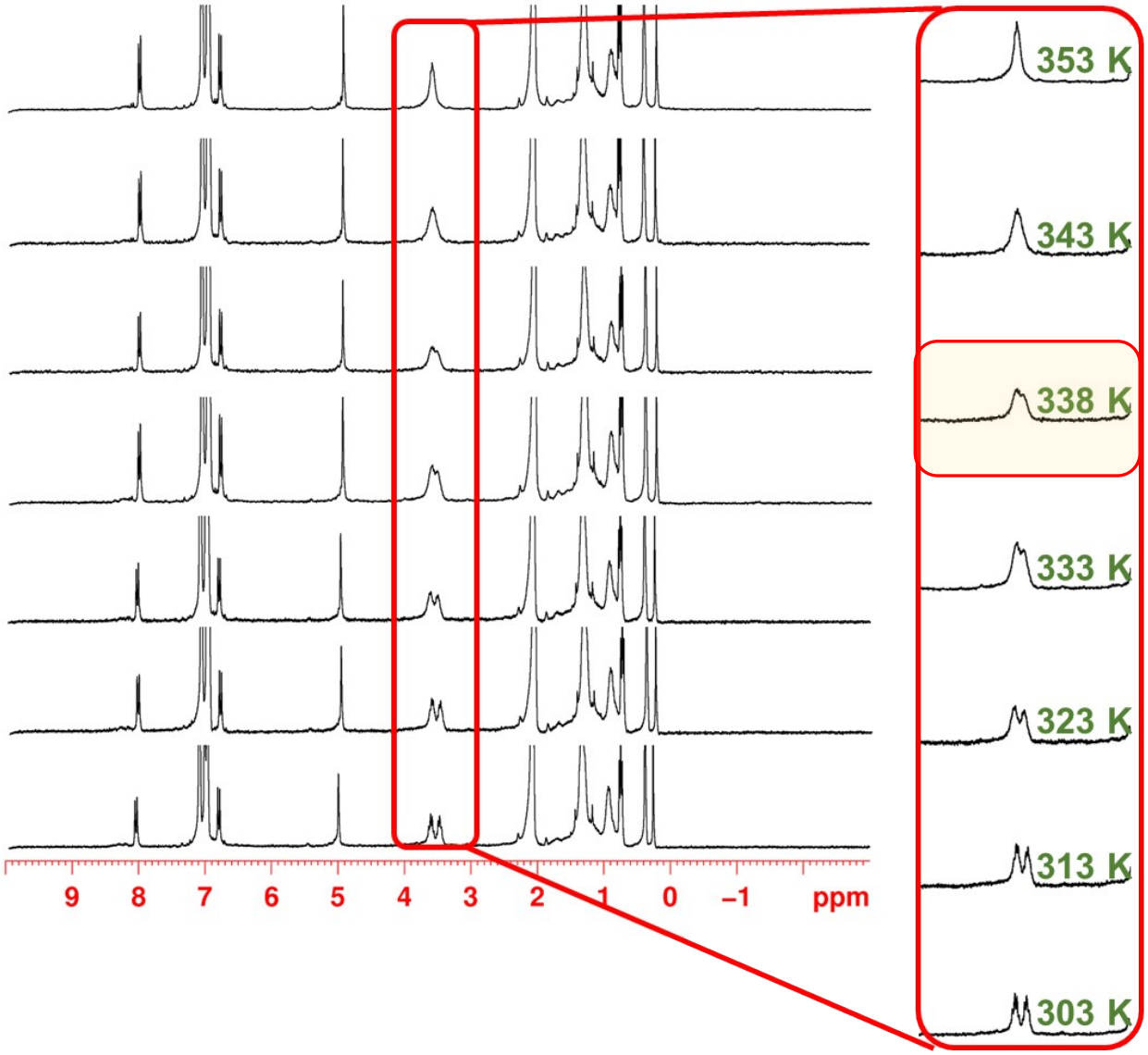

Figure S84: ^{1}H NMR spectra of **PrS[5]^{Et}** (300 MHz, Toluene-d_8) at (from bottom to top): 303, 313, 323, 333, 338, 343 and 353 K. Highlighted in the red box the OCH_2 signals and their shape at the coalescence temperature of 338 K.

Energy barrier calculation[2] by ^{1}H VT NMR studies

$$\Delta G_c^{\neq} = aT_c\left[9.972 + \log\left(\frac{T_c}{\Delta\nu}\right)\right]$$

Tc = 338 K; Δv = 42 Hz calculated for OCH_2 signals at 3.60 and 3.46 ppm at 303 K;

a = $4.575 \cdot 10^{-3}$ ($\Delta G^{\neq}_c$ in Kcal/mol)

$\Delta G^{\neq}_c$ = 16.8 Kcal/mol

HT NMR studies of PrS[5]^{nPr}

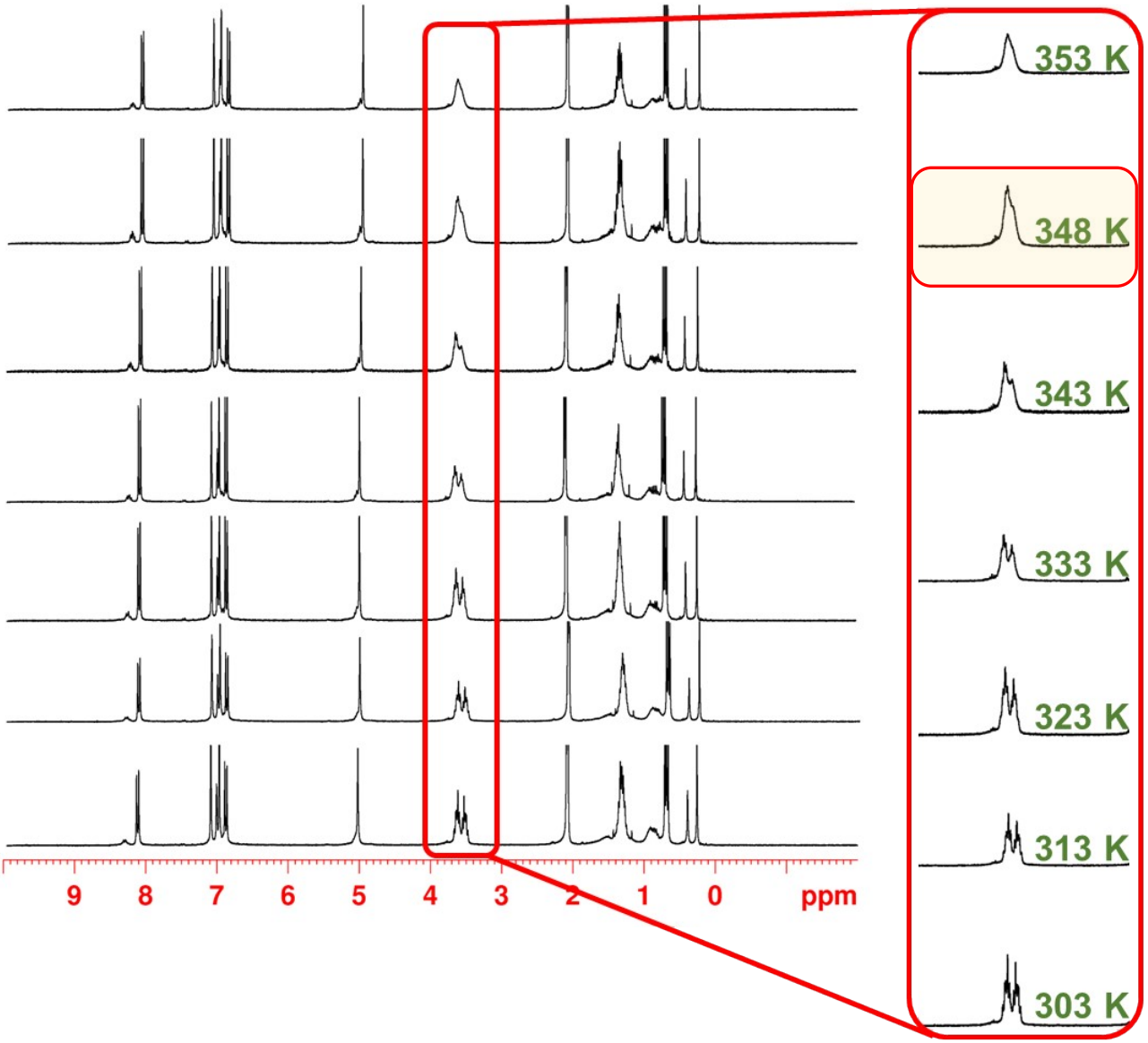

Figure S85: ^{1}H NMR spectra of **PrS[5]^{Pr}** (300 MHz, Toluene-d_8) at (from bottom to top): 303, 313, 323, 333, 343, 348 and 353 K. Highlighted in the red box the OCH_2 signals and their shape at the coalescence temperature of 348 K.

Energy barrier calculation[2] by ^{1}H VT NMR studies

$$\Delta G_{\mathrm{c}}^{\neq} = aT_c\left[9.972 + \log\left(\frac{T_c}{\Delta\nu}\right)\right]$$

Tc = 348 K; Δv = 36 Hz calculated for OCH_2 signals at 3.63 and 3.51 ppm at 303 K;

a = $4.575 \cdot 10^{-3}$ ($\Delta G^{\neq}_c$ in Kcal/mol)

$\Delta G^{\neq}_c$ = 17.4 Kcal/mol

HT NMR studies of PrS[5]^{nBu}

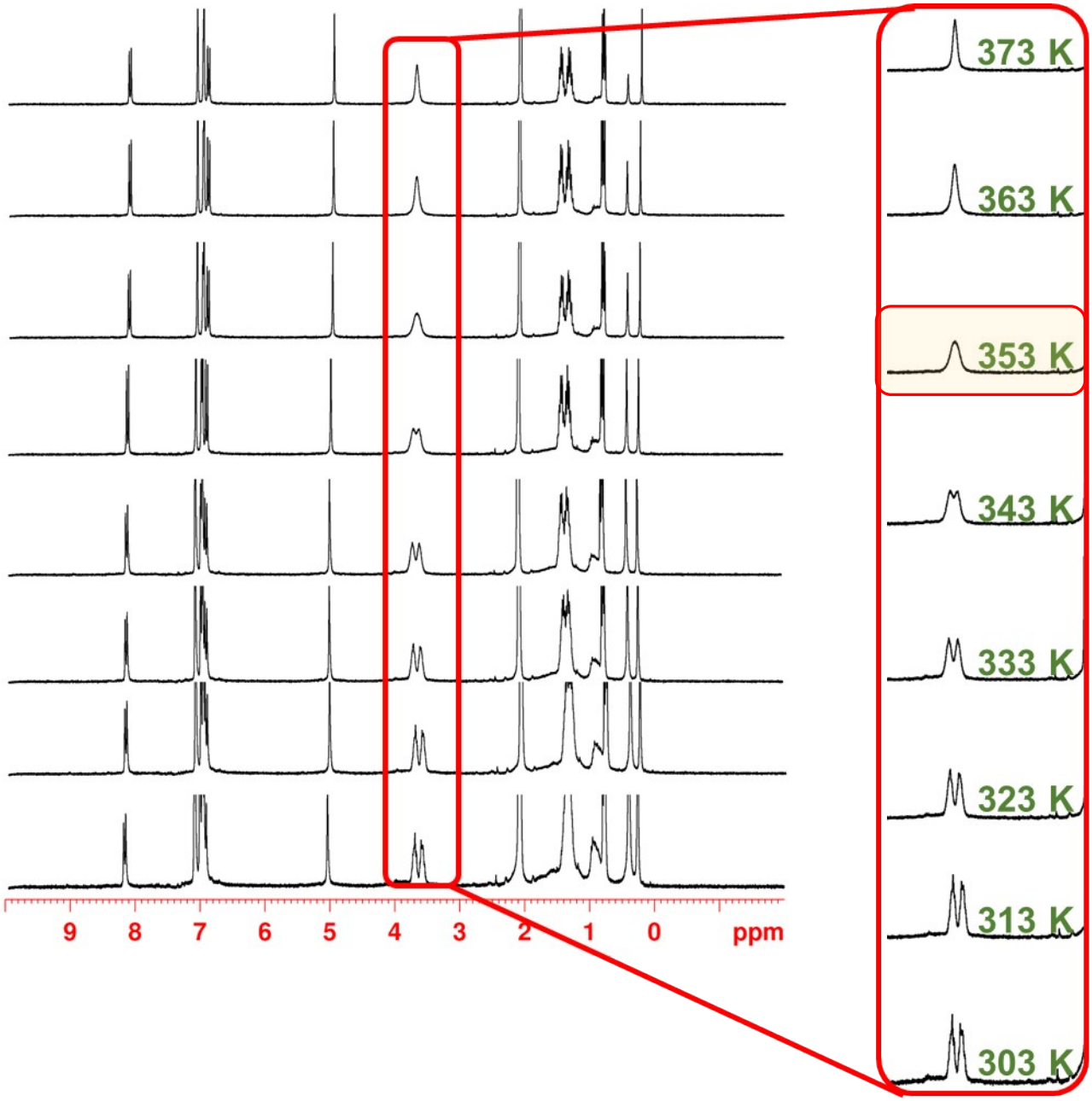

Figure S86: ^{1}H NMR spectra of **PrS[5]^{nBu}** (300 MHz, Toluene-d_8) at (from bottom to top): 303, 313, 323, 333, 343, 353, 363 and 373 K. Highlighted in the red box the OCH_2 signals and their shape at the coalescence temperature of 353 K.

Energy barrier calculation[2] by ^{1}H VT NMR studies

$$\Delta G_c^{\neq} = aT_c\left[9.972 + \log\left(\frac{T_c}{\Delta\nu}\right)\right]$$

Tc = 353 K; Δv = 30 Hz calculated for OCH_2 signals at 3.68 and 3.58 ppm at 303 K;

a = $4.575 \cdot 10^{-3}$ ($\Delta G^{\neq}_c$ in Kcal/mol)

$\Delta G^{\neq}_c$ = 17.8 Kcal/mol

HT NMR studies of PrS[5]^{nPe}

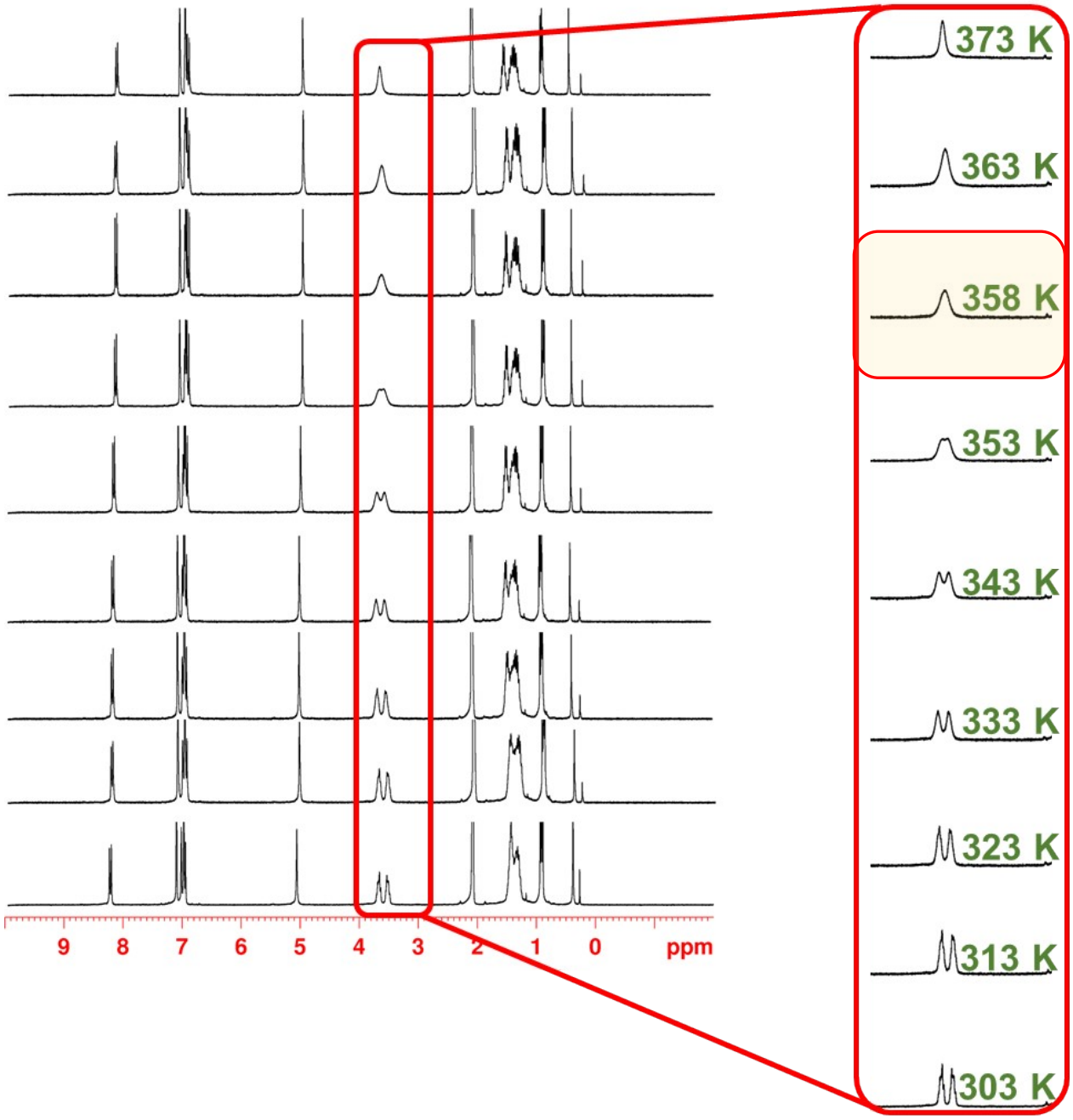

Figure S87: ^{1}H NMR spectra of **PrS[5]^{nPe}** (300 MHz, Toluene-d_8) at (from bottom to top): 303, 313, 323, 333, 343, 353, 358, 363 and 373 K. Highlighted in the red box the OCH_2 signals and their shape at the coalescence temperature of 358 K.

.

Energy barrier calculation[2] by ^{1}H VT NMR studies

$$\Delta G_{c}^{\neq} = aT_{c}\left[9.972 + \log\left(\frac{T_{c}}{\Delta\nu}\right)\right]$$

Tc = 358 K; Δv = 36 Hz calculated for OCH_2 signals at 3.65 and 3.53 ppm at 303 K;

a = $4.575 \cdot 10^{-3}$ ($\Delta G^{\neq}_{c}$ in Kcal/mol)

$\Delta G^{\neq}_{c}$ = 18.0 Kcal/mol

HT NMR studies of PrS[5]^{nHex}

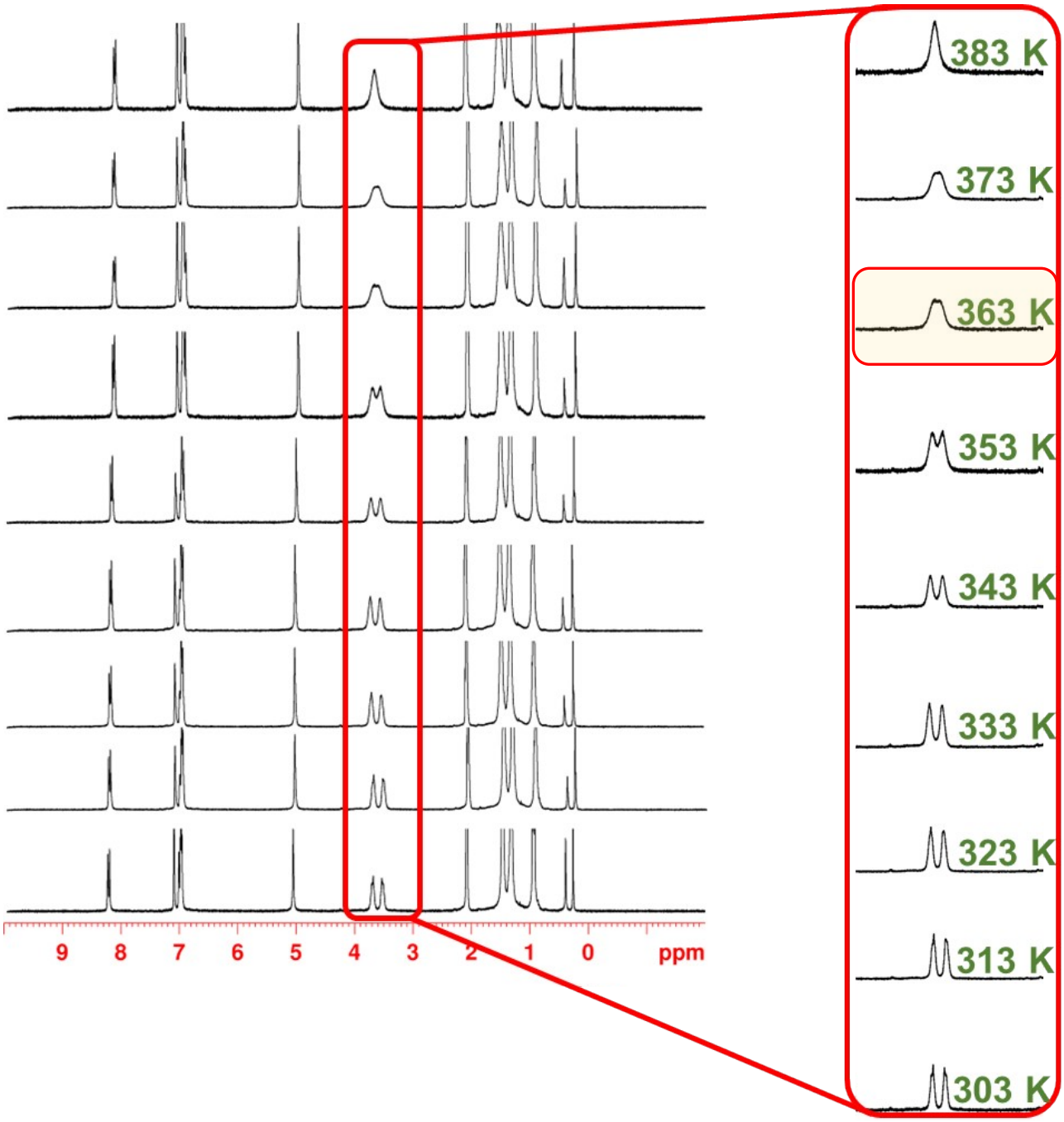

Figure S88: ^{1}H NMR spectra of **PrS[5]^{nHex}** (300 MHz, Toluene-d_8) at (from bottom to top): 303, 313, 323, 333, 343, 353, 363, 373 and 383 K. Highlighted in the red box the OCH_2 signals and their shape at the coalescence temperature of 373 K.

.

Energy barrier calculation[2] by ^{1}H VT NMR studies

$$\Delta G_{c}^{\neq} = aT_{c}\left[9.972 + \log\left(\frac{T_{c}}{\Delta\nu}\right)\right]$$

Tc = 373 K; Δv = 51 Hz calculated for OCH_2 signals at 3.69 and 3.52 ppm at 303 K;

a = $4.575 \cdot 10^{-3}$ ($\Delta G^{\neq}_{c}$ in Kcal/mol)

$\Delta G^{\neq}_{c}$ = 18.5 Kcal/mol

HT NMR studies of PrS[5]^{Hp}

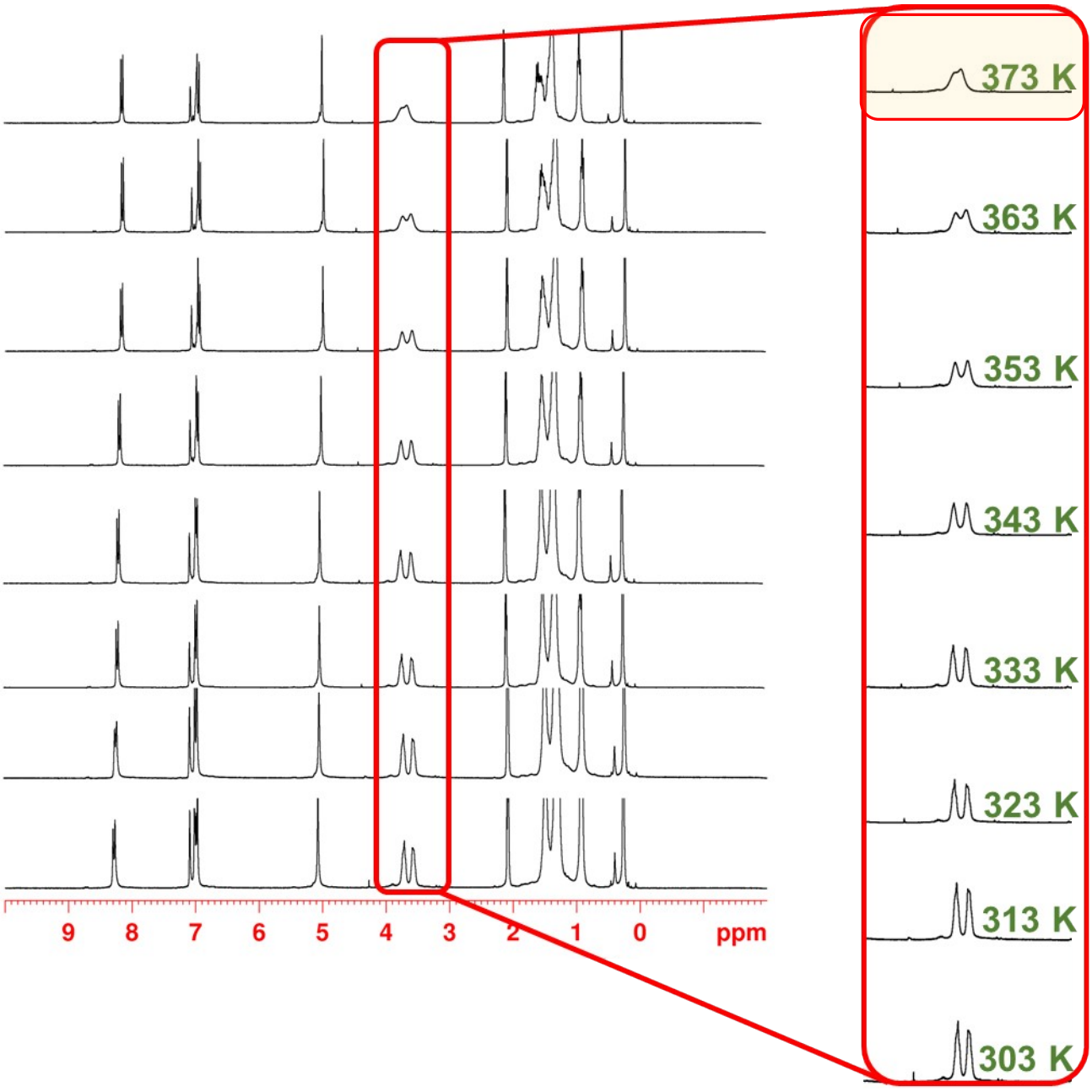

Figure S89: ^{1}H NMR spectra of **PrS[5]^{Hp}** (300 MHz, Toluene-d_8) at (from bottom to top): 303, 313, 323, 333, 343, 353, 363 and 373 K. Highlighted in the red box the OCH_2 signals and their shape at the coalescence temperature of 373 K.

Energy barrier calculation[2] by ^{1}H VT NMR studies

$$\Delta G_{c}^{\neq} = aT_{c}\left[9.972 + \log\left(\frac{T_{c}}{\Delta\nu}\right)\right]$$

Tc = 373 K; Δv = 42 Hz calculated for OCH_2 signals at 3.71 and 3.57 ppm at 303 K;

a = $4.575 \cdot 10^{-3}$ ($\Delta G^{\neq}_{c}$ in Kcal/mol)

$\Delta G^{\neq}_{c}$ = 18.6 Kcal/mol

HT NMR studies of PrS[5] *Nonyl*

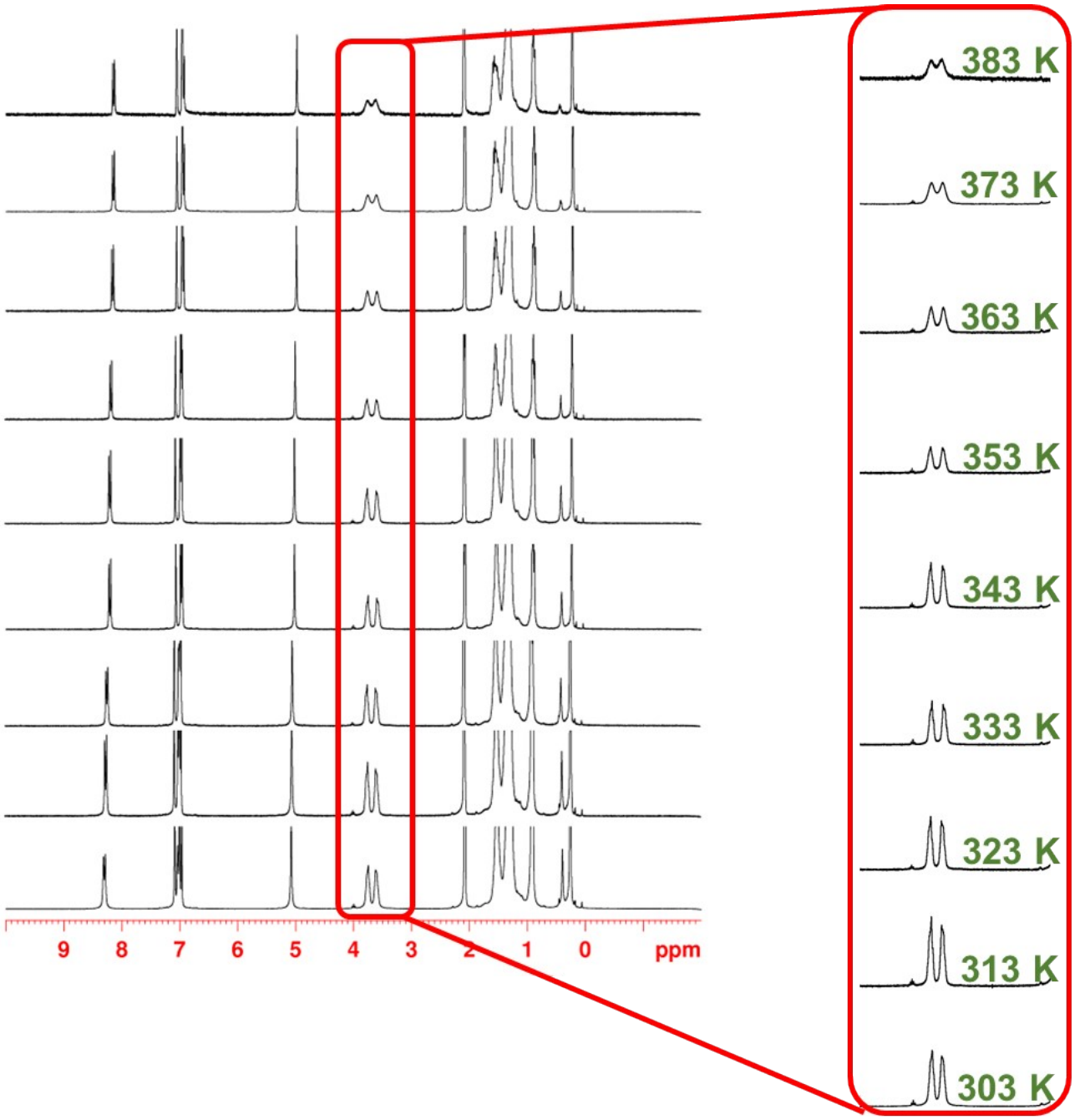

Figure S90: ^{1}H NMR spectra of **PrS[5]*Nonyl*** (300 MHz, Toluene-d_8) at (from bottom to top): 303, 313, 323, 333, 343, 353, 363, 373 and 383 K. Highlighted in the red box the OCH_2 signals.

Energy barrier calculation[2] by ^{1}H VT NMR studies

Tc > 383 K; Δv = 42 Hz calculated for OCH_2 signals at 3.75 and 3.61 ppm at 303 K;

$$\Delta G_c^{\neq} = aT_c\left[9.972 + \log\left(\frac{T_c}{\Delta\nu}\right)\right]$$

a = $4.575 \cdot 10^{-3}$ ($\Delta G^{\neq}_c$ in Kcal/mol)

$\Delta G^{\neq}_c$ > 19.2 Kcal/mol

HT NMR studies of PrS[5]^{iPr}

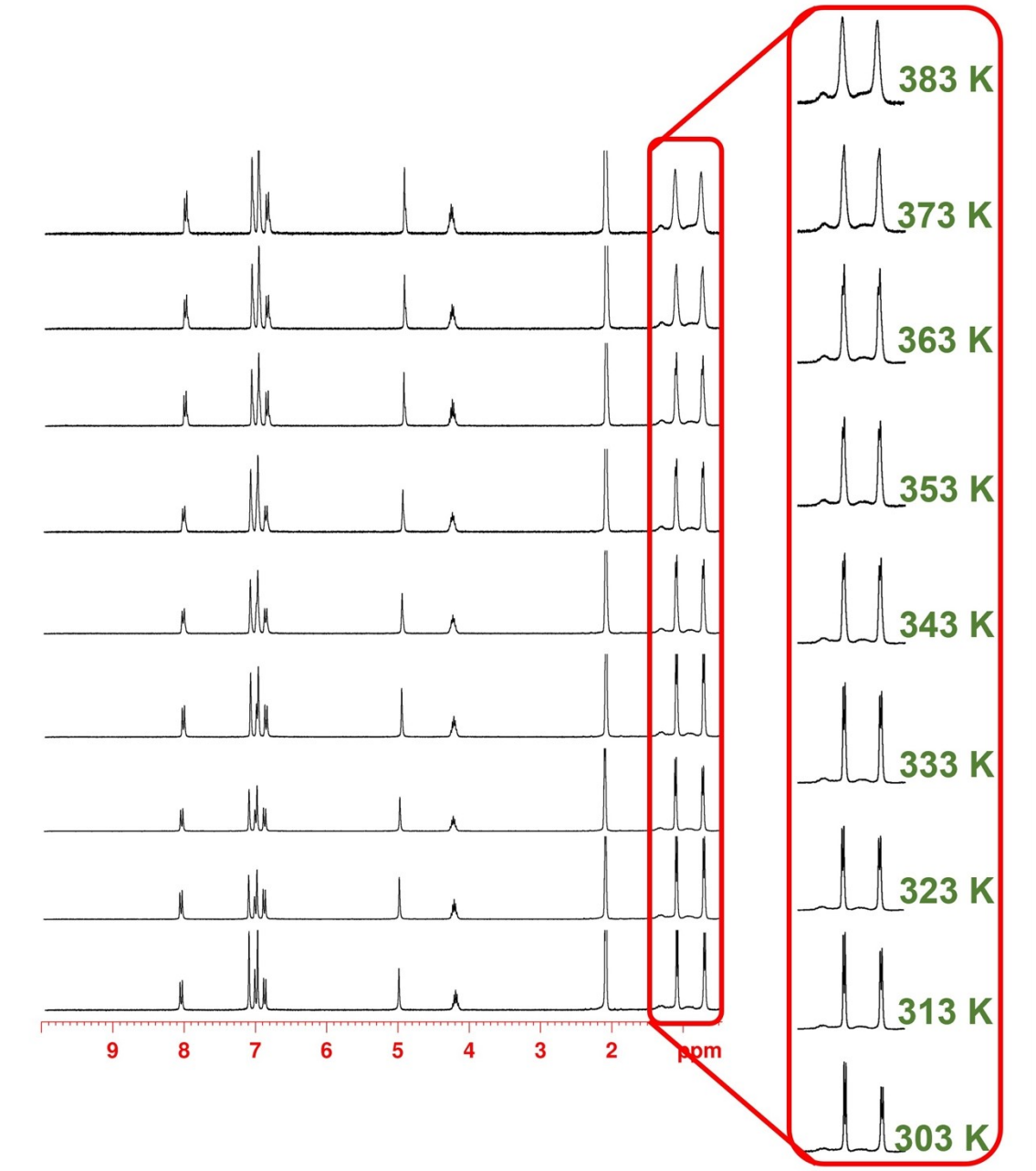

Figure S91: ^{1}H NMR spectra of **PrS[5]^{iPr}** (300 MHz, Toluene-d_8) at (from bottom to top): 303, 313, 323, 333, 343, 353, 363, 373 and 383 K. Highlighted in the red box the OCH(C$\boldsymbol{H}_3$)$_2$ signals.

HT NMR studies of PrS[5]^{iBu}

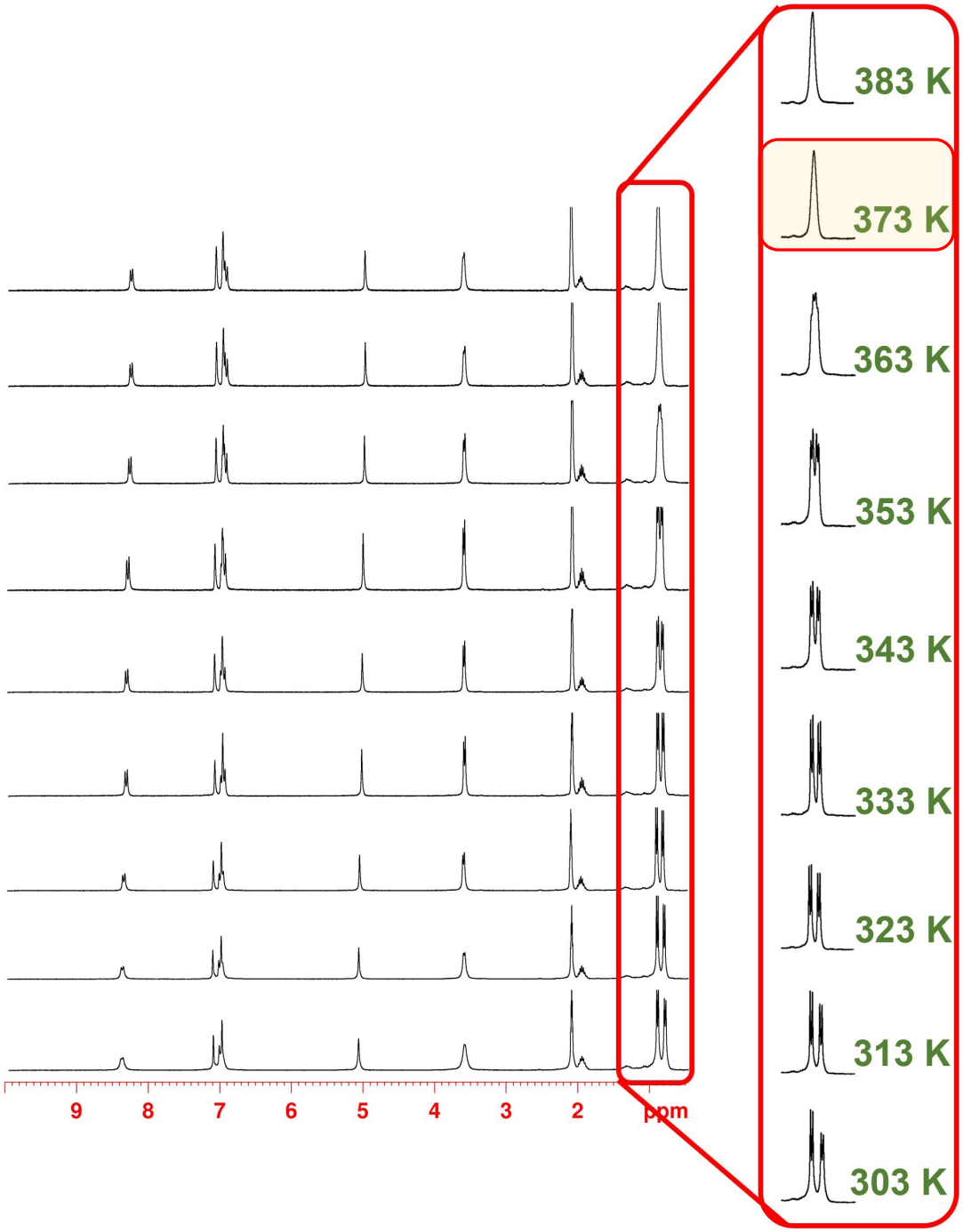

Figure S92: ^{1}H NMR spectra of **PrS[5]^{iBu}** (300 MHz, Toluene-d_8) at (from bottom to top): 303, 313, 323, 333, 343, 353, 363, 373 and 383 K. Highlighted in the red box the $OCH_2CH(CH_3)_2$ signals and their shape at the coalescence temperature of 373 K.

Energy barrier calculation[2] by ^{1}H VT NMR studies

$$\Delta G_{c}^{\neq} = aT_{c}\left[9.972 + \log\left(\frac{T_{c}}{\Delta\nu}\right)\right]$$

Tc = 373 K; Δv = 30 Hz calculated for CH_3 signals at 0.88 and 0.78 ppm at 303 K;

a = $4.575 \cdot 10^{-3}$ ($\Delta G^{\neq}_{c}$ in Kcal/mol)

$\Delta G^{\neq}_{c}$ = 18.9 Kcal/mol

HT NMR studies of PrS[5]^{iPe}

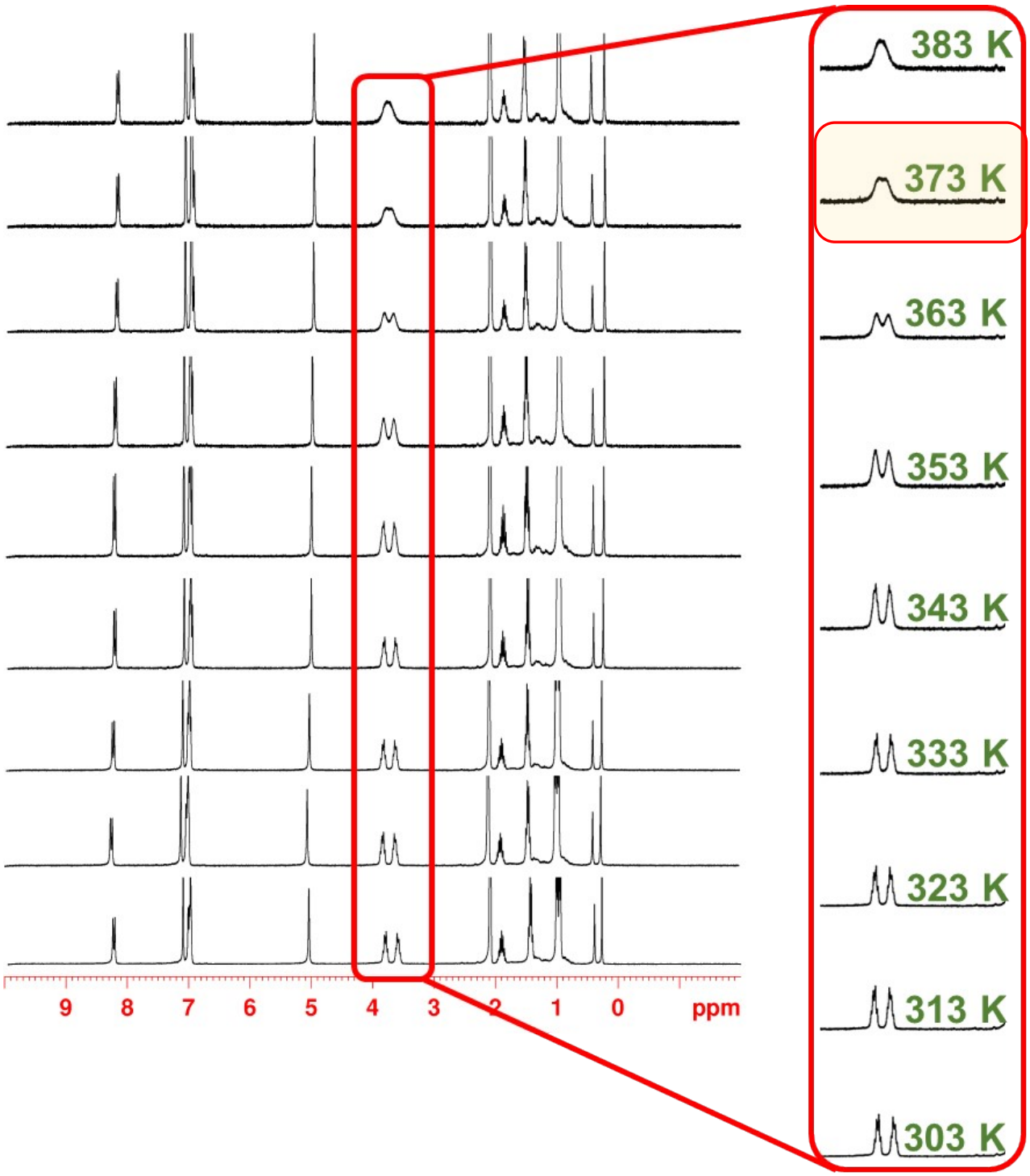

Figure S93: ^{1}H NMR spectra of **PrS[5]^{iPe}** (300 MHz, Toluene-d_8) at (from bottom to top): 303, 313, 323, 333, 343, 353, 363, 373 and 383 K. Highlighted in the red box the OCH_2 signals and their shape at the coalescence temperature of 373 K.

Energy barrier calculation[2] by ^{1}H VT NMR studies

$$\Delta G_{c}^{\neq} = aT_{c}\left[9.972 + \log\left(\frac{T_{c}}{\Delta\nu}\right)\right]$$

Tc = 373 K; Δv = 63 Hz calculated for OCH_2 signals at 3.79 and 3.58 ppm at 303 K;

a = $4.575 \cdot 10^{-3}$ ($\Delta G^{\neq}_{c}$ in Kcal/mol)

$\Delta G^{\neq}_{c}$ = 18.3 Kcal/mol

HT NMR studies of PrS[5]^{iHex}

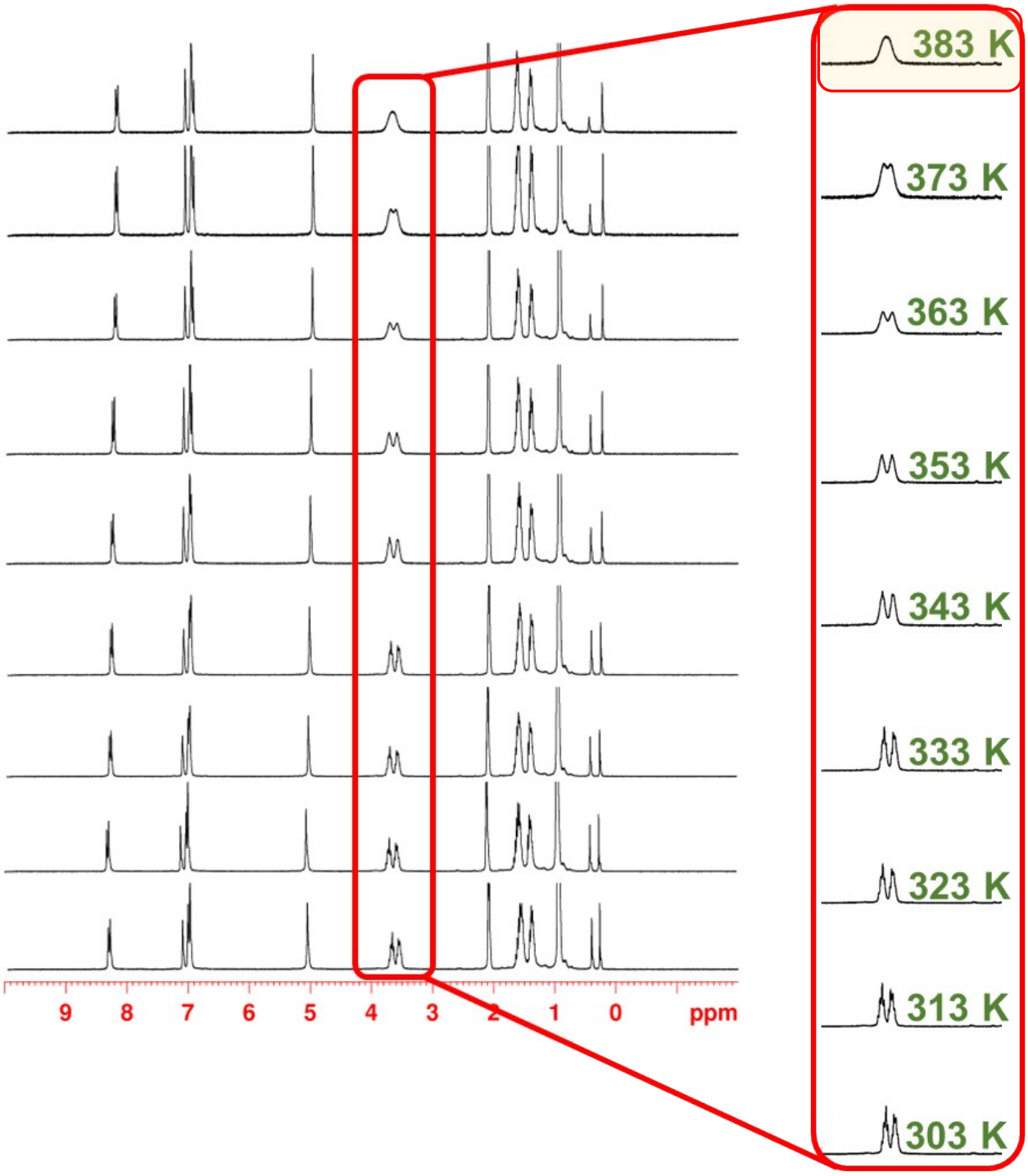

Figure S94: ^{1}H NMR spectra of **PrS[5]^{iHex}** (300 MHz, Toluene-d_8) at (from bottom to top): 303, 313, 323, 333, 343, 353, 363, 373 and 383 K. Highlighted in the red box the OCH_2 signals and their shape at the coalescence temperature of 383 K.

Energy barrier calculation[2] by ^{1}H VT NMR studies

$$\Delta G_c^{\neq} = aT_c\left[9.972 + \log\left(\frac{T_c}{\Delta\nu}\right)\right]$$

Tc = 383 K; Δv = 39 Hz calculated for OCH_2 signals at 3.67 and 3.54 ppm at 303 K;

a = $4.575 \cdot 10^{-3}$ ($\Delta G^{\neq}_c$ in Kcal/mol)

$\Delta G^{\neq}_c$ = 19.2 Kcal/mol

HT NMR studies of PrS[5]^{MeCy}

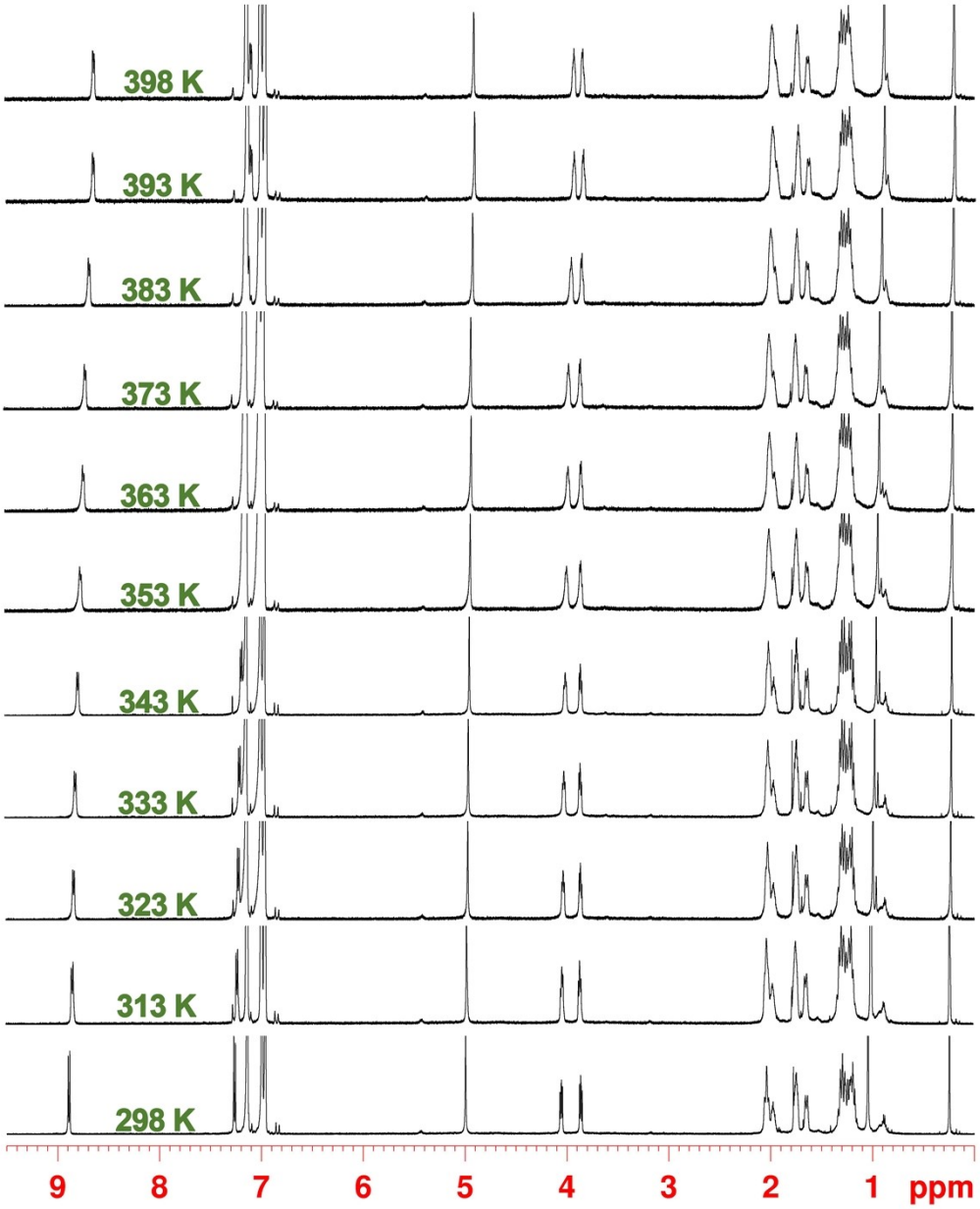

Figure S95: ^{1}H NMR spectra of **PrS[5]^{MeCy}** (600 MHz, chlorobenzene-d_5) at (from bottom to top): 298, 313, 323, 333, 343, 353, 363, 373, 383, 393, 398 K.

HT NMR studies of PrS[5]^{EtCy}

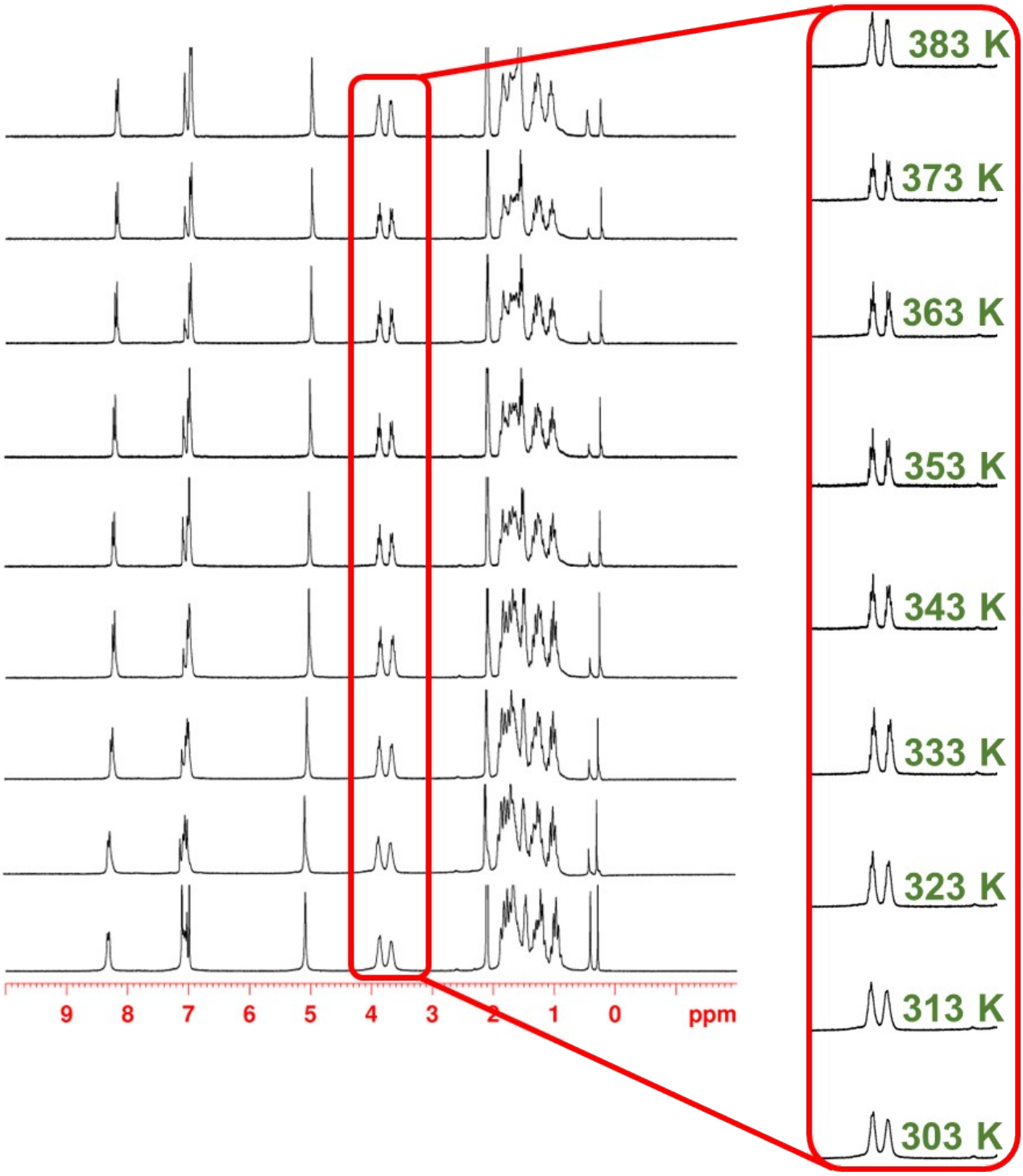

Figure S96: ^{1}H NMR spectra of **PrS[5]^{EtCy}** (300 MHz, Toluene-d_8) at (from bottom to top): 303, 313, 323, 333, 343, 353, 363, 373 and 383 K. Highlighted in the red box the OCH_2 signals and their shape at different temperatures.

HT NMR studies of PrS[5]^{PrCy}

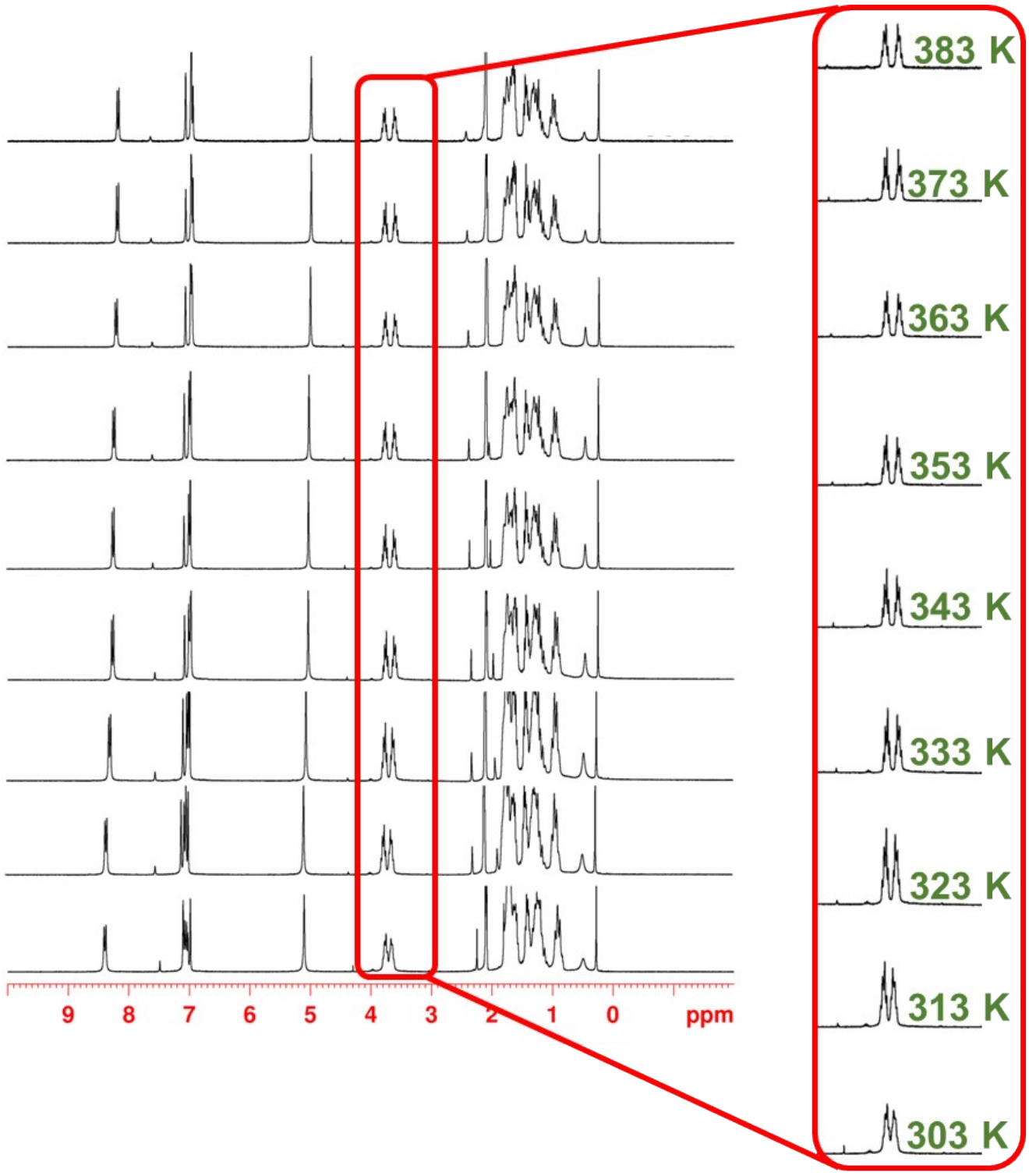

Figure S97: ^{1}H NMR spectra of **PrS[5]^{PrCy}** (300 MHz, Toluene-d_8) at (from bottom to top): 303, 313, 323, 333, 343, 353, 363, 373 and 383 K. Highlighted in the red box the OCH_2 signals and their shape at different temperatures.

HT NMR studies of PrS[5]^{BuCy}

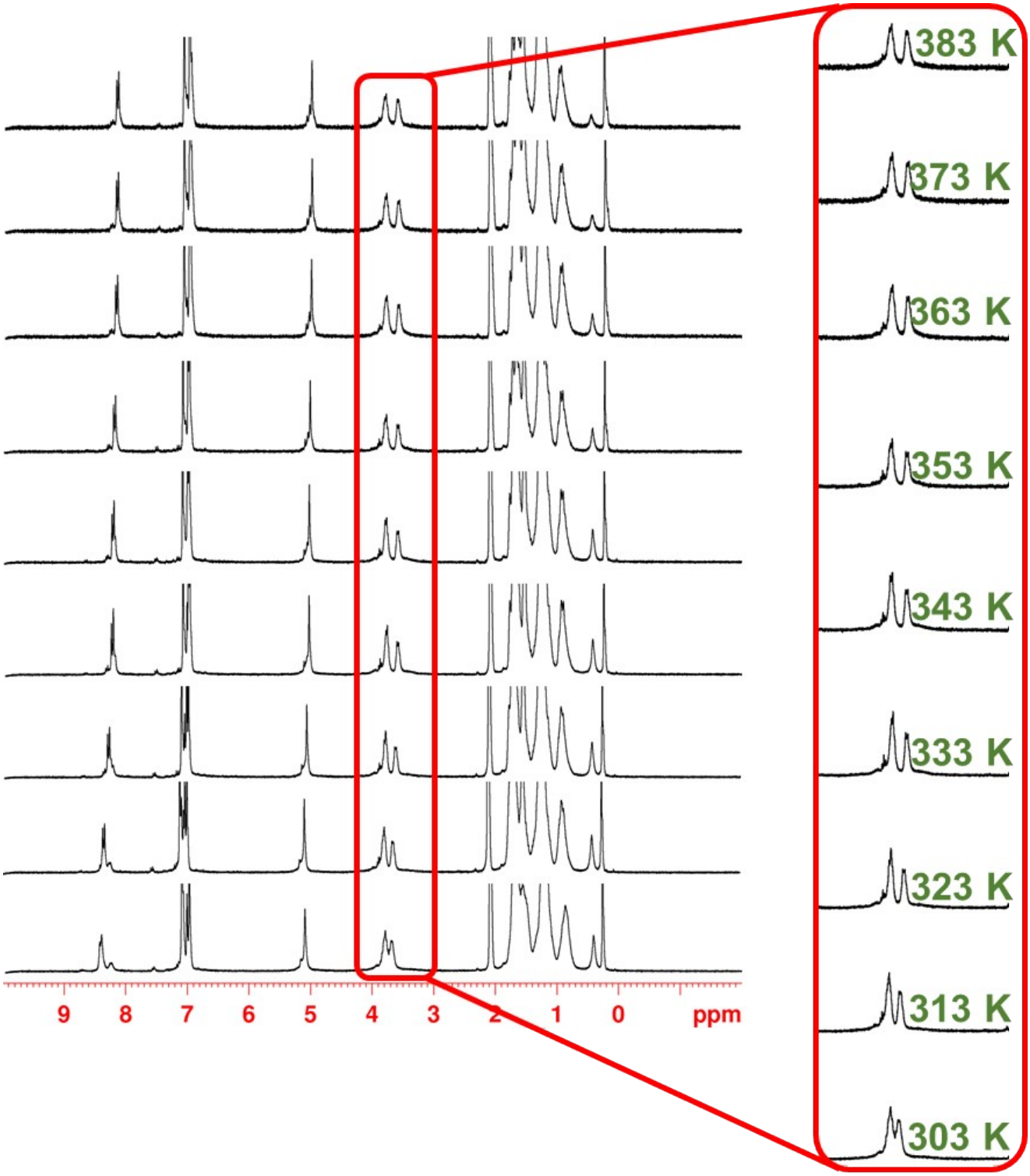

Figure S98: ^{1}H NMR spectra of **PrS[5]^{BuCy}** (300 MHz, Toluene-d_8) at (from bottom to top): 303, 313, 323, 333, 343, 353, 363, 373 and 383 K. Highlighted in the red box the OCH_2 signals and their shape at different temperatures.

HT NMR studies of PrS[5]^{EtcHp}

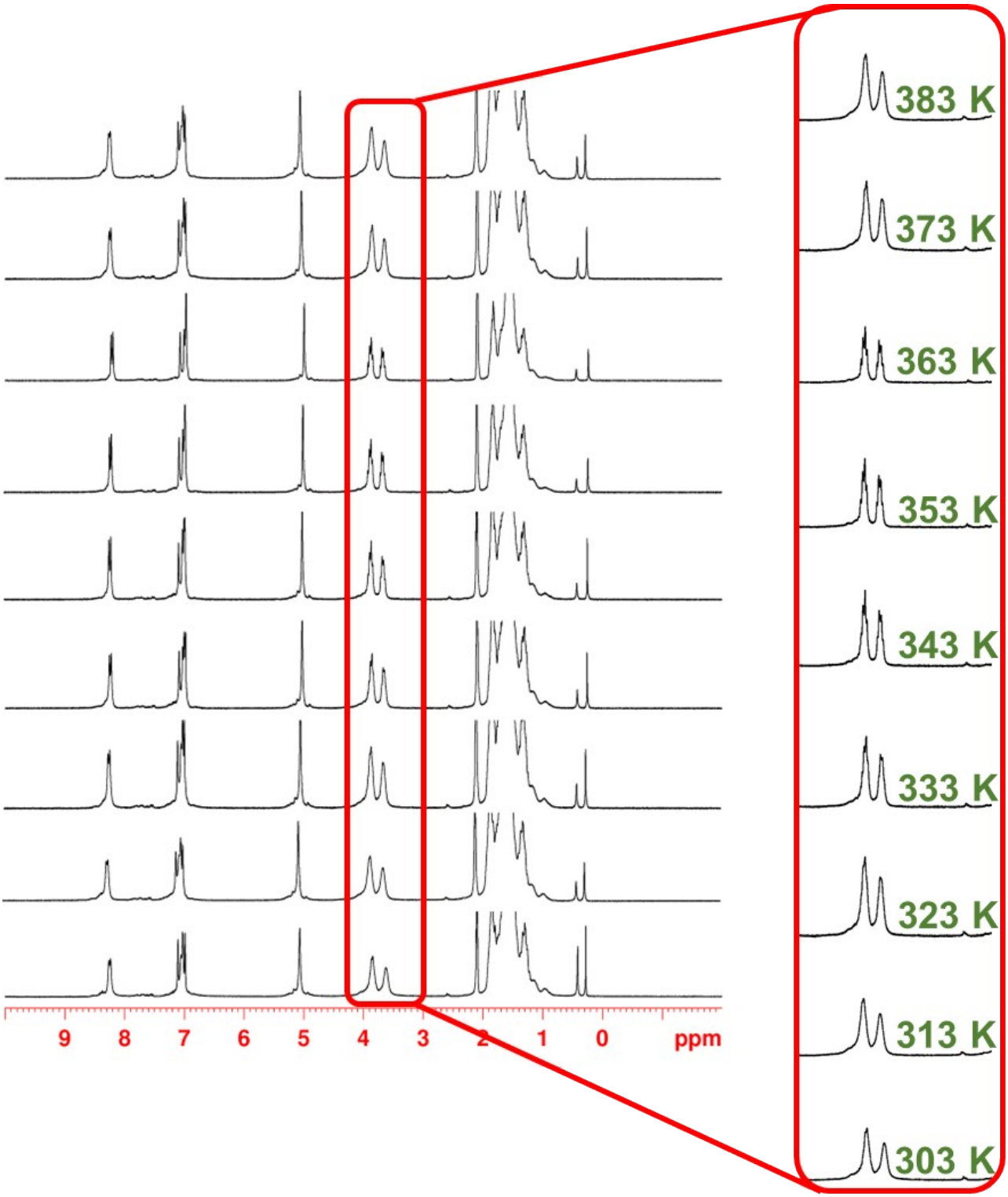

Figure S99: ^{1}H NMR spectra of **PrS[5]^{EtcHp}** (300 MHz, Toluene-d_8) at (from bottom to top): 303, 313, 323, 333, 343, 353, 363, 373 and 383 K. Highlighted in the red box the OCH_2 signals and their shape at different temperatures.

HT NMR studies of PrS[5]^{BuPh}

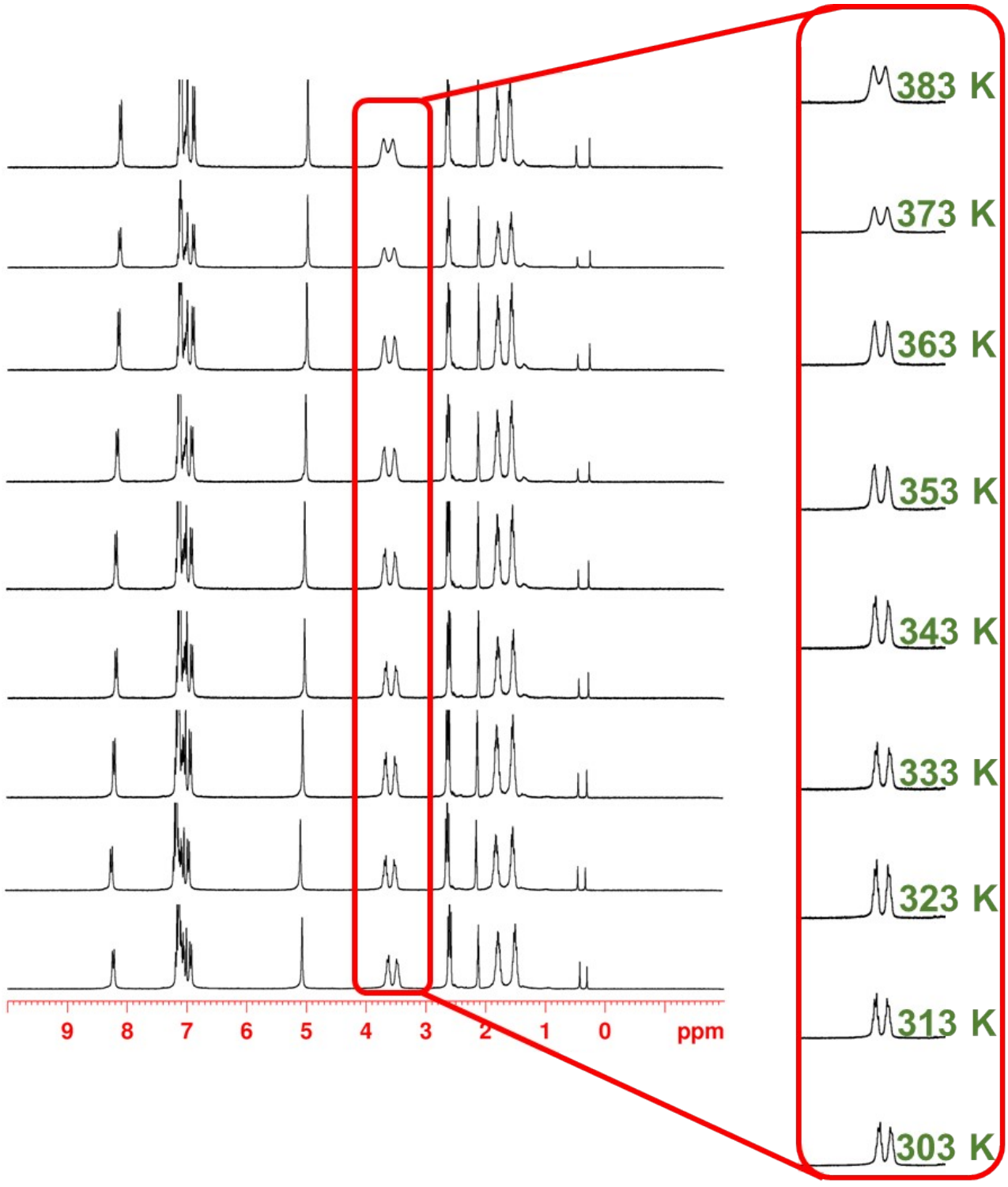

Figure S100: ^{1}H NMR spectra of **PrS[5]^{BuPh}** (300 MHz, Toluene-d_8) at (from bottom to top): 303, 313, 323, 333, 343, 353, 363, 373 and 383 K. Highlighted in the red box the OCH_2 signals and their shape at different temperatures.

Copies of 1D NMR spectra of PrS[5]^{R} complexes

2^{2+}@ PrS[5]^{nBu}

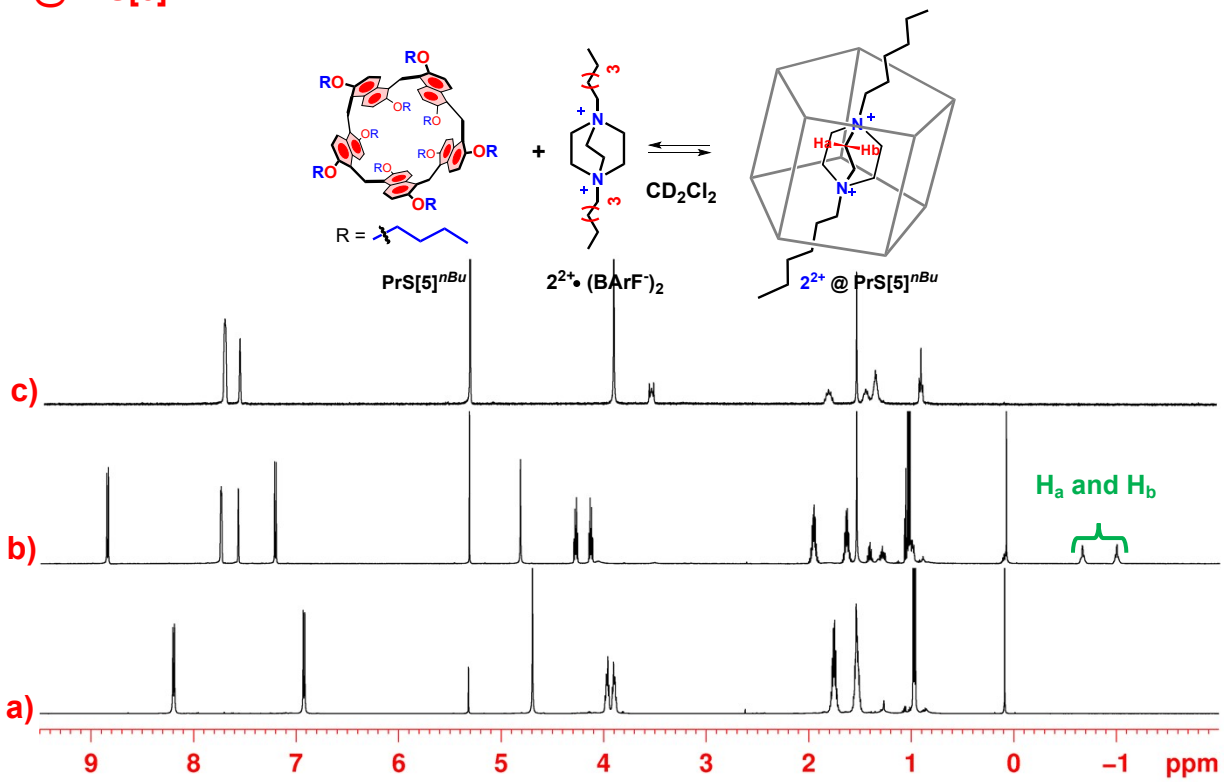

Figure S101: ^{1}H NMR spectra (600 MHz, CD_2Cl_2, 298 K) of: (a) **PrS[5]^{nBu}**, (b) an equimolar mixture of **PrS[5]^{nBu}** and **2^{2+}**·$(BArF^{-})_2$ and (c) **2^{2+}**·$(BArF^{-})_2$.

2^{2+}@ PrS[5]^{nPe}

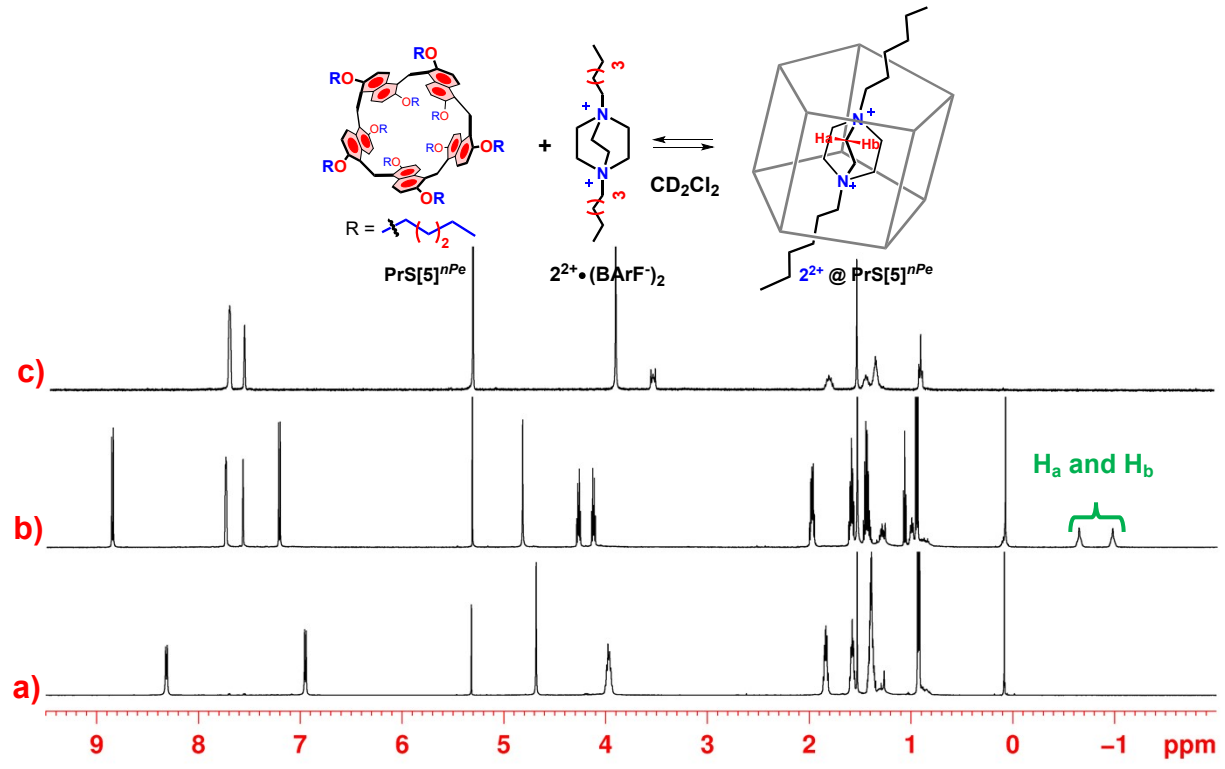

Figure S102: ^{1}H NMR spectra (600 MHz, CD_2Cl_2, 298 K) of: (a) **PrS[5]^{nPe}**, (b) an equimolar solution of **PrS[5]^{nPe}** and **2^{2+}**·$(BArF^{-})_2$ and (c) **2^{2+}**·$(BArF^{-})_2$.

2^{2+}@ PrS[5]^{iPr}

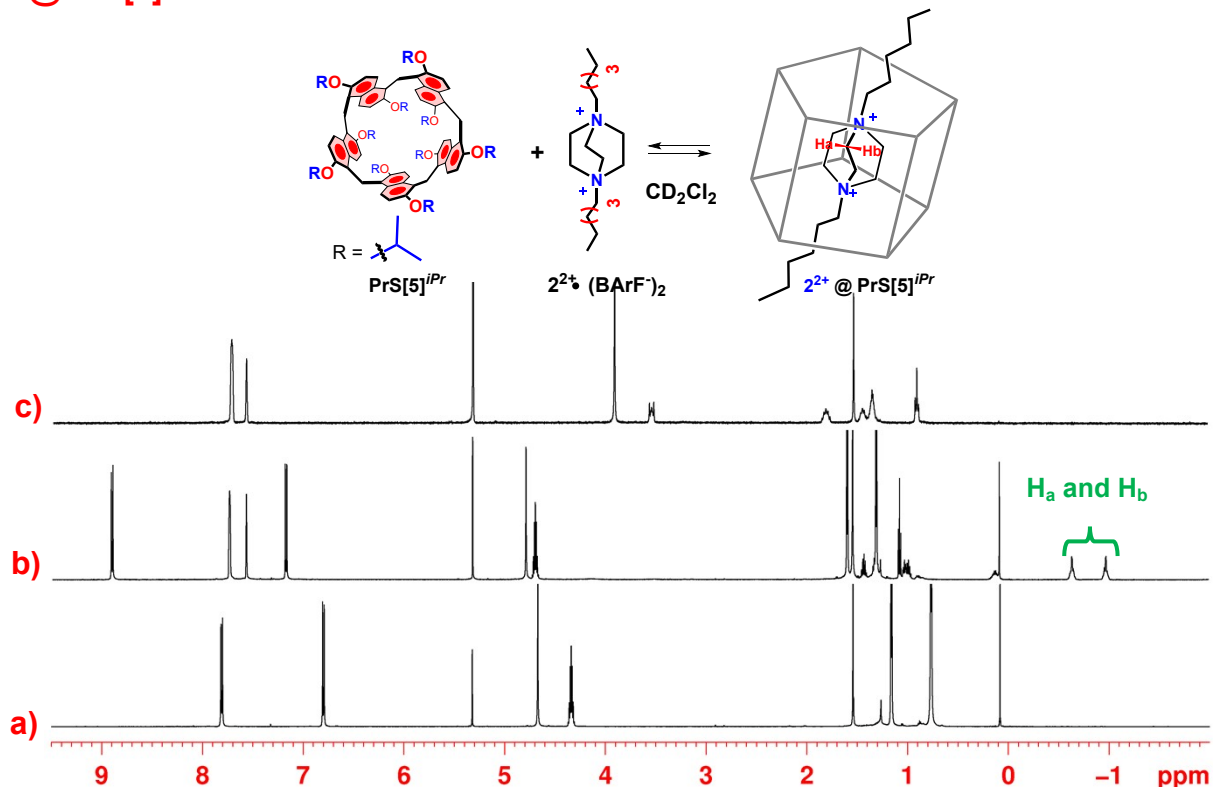

Figure S103: ^{1}H NMR spectra (600 MHz, CD_2Cl_2, 298 K) of: (a) **PrS[5]^{iPr}**, (b) an equimolar solution of **PrS[5]^{iPr}** and **2^{2+}**·$(BArF^-)_2$ and (c) **2^{2+}**·$(BArF^-)_2$.

2^{2+}@ PrS[5]^{iBu}

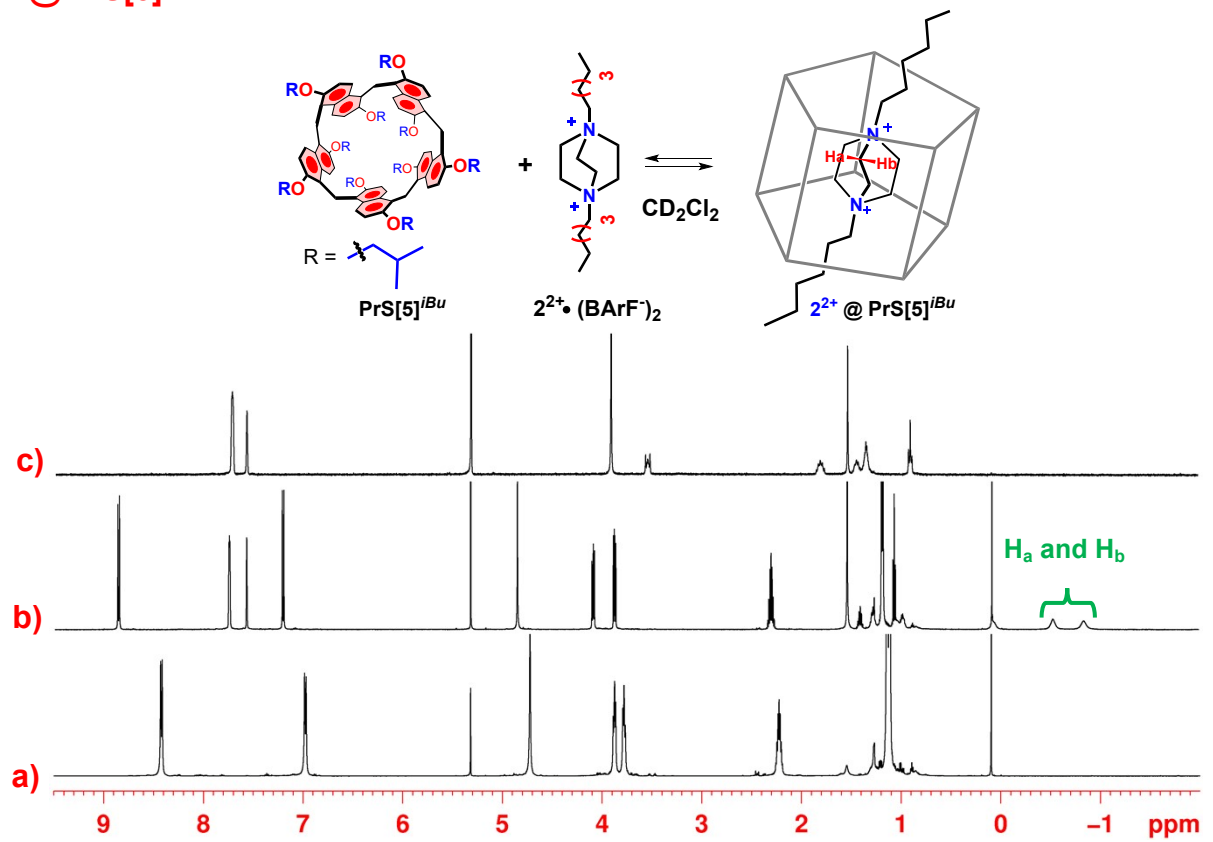

Figure S104: ^{1}H NMR spectra (600 MHz, CD_2Cl_2, 298 K) of: (a) **PrS[5]^{iBu}**, (b) an equimolar solution of **PrS[5]^{iBu}** and **2^{2+}**·$(BArF^-)_2$ and (c) **2^{2+}**·$(BArF^-)_2$.

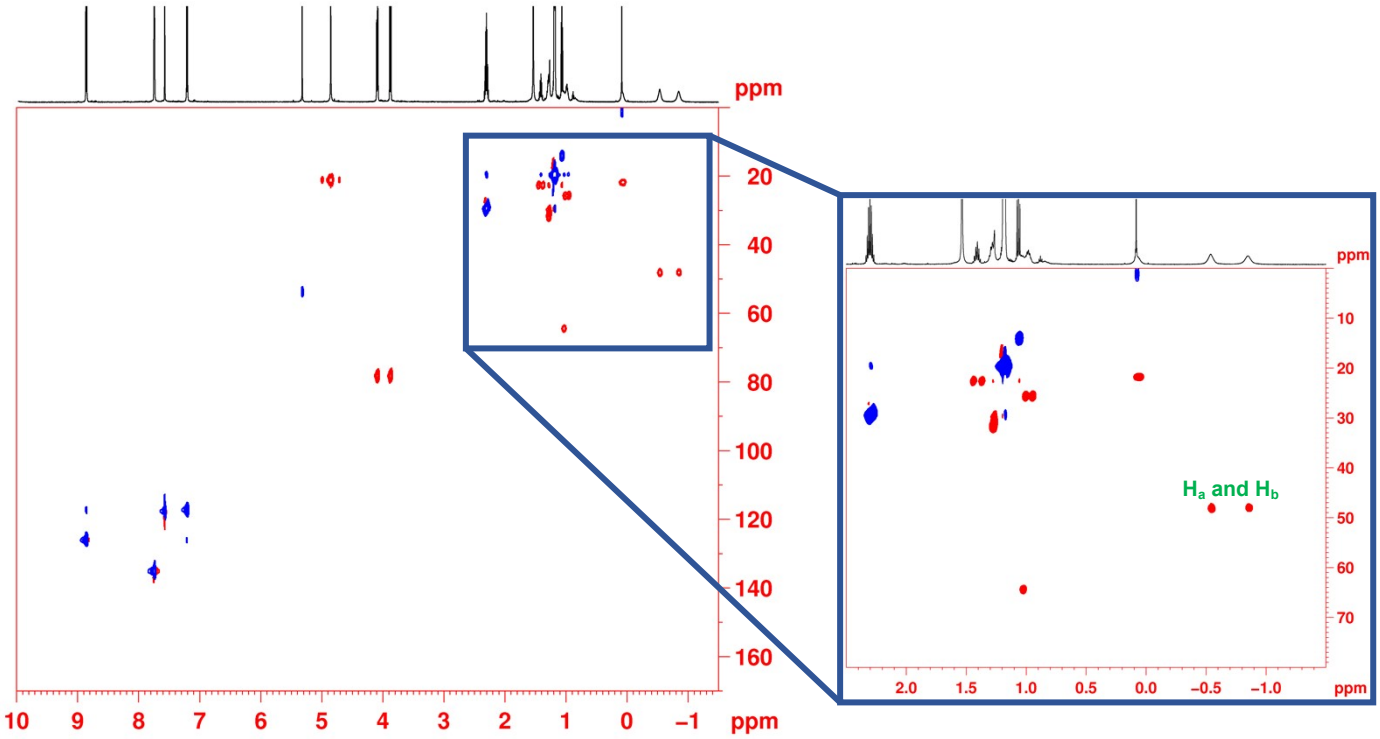

Figure S105: 2D-HSQC spectrum of $\mathbf{2}^{2+}$@ **PrS[5]**^{iBu} (CD_2Cl_2, 600 MHz, 298 K).

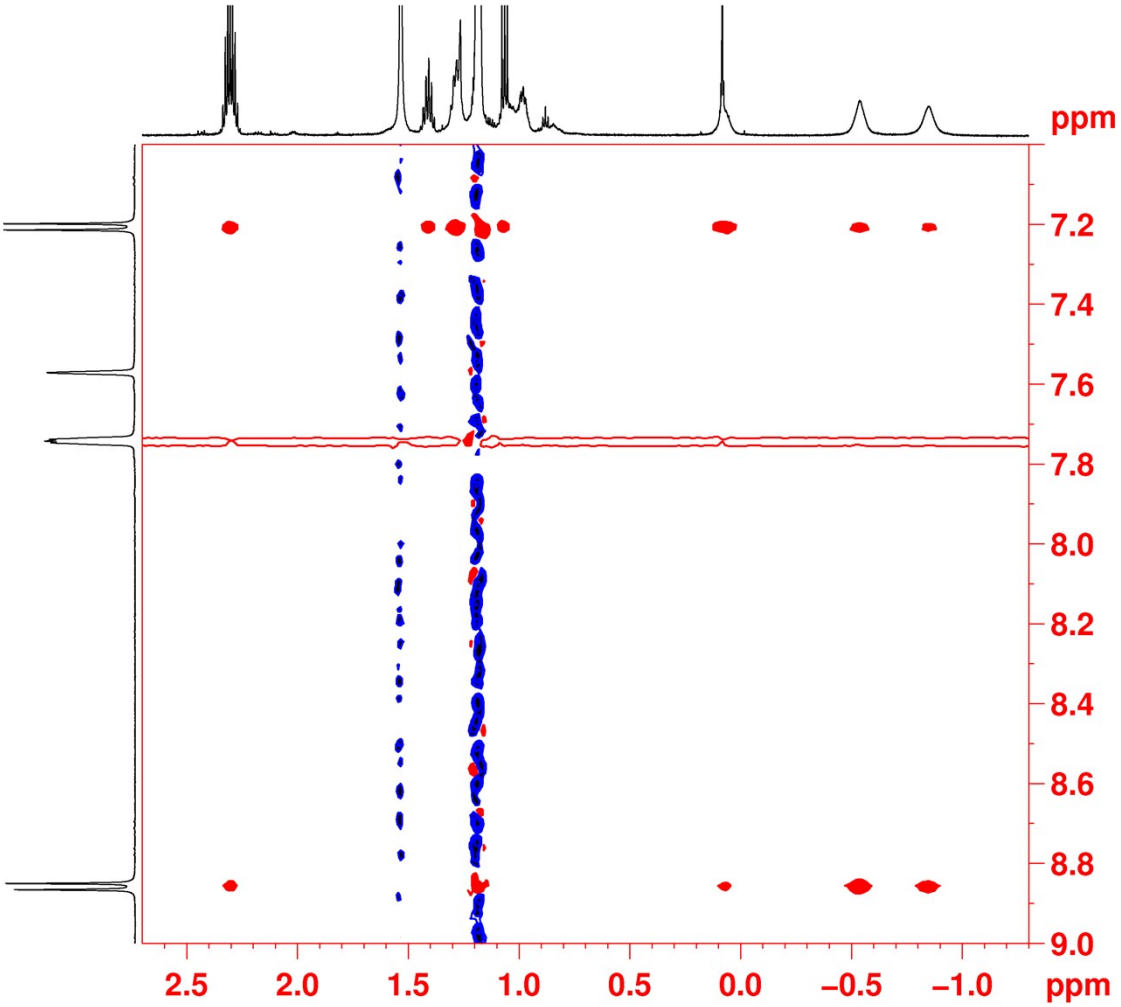

Figure S106: Significant portion of 2D-NOESY spectrum of $\mathbf{2}^{2+}$@ **PrS[5]**^{iBu} (CD_2Cl_2, 600 MHz, 298 K).

2^{2+}@ PrS[5]^{iPe}

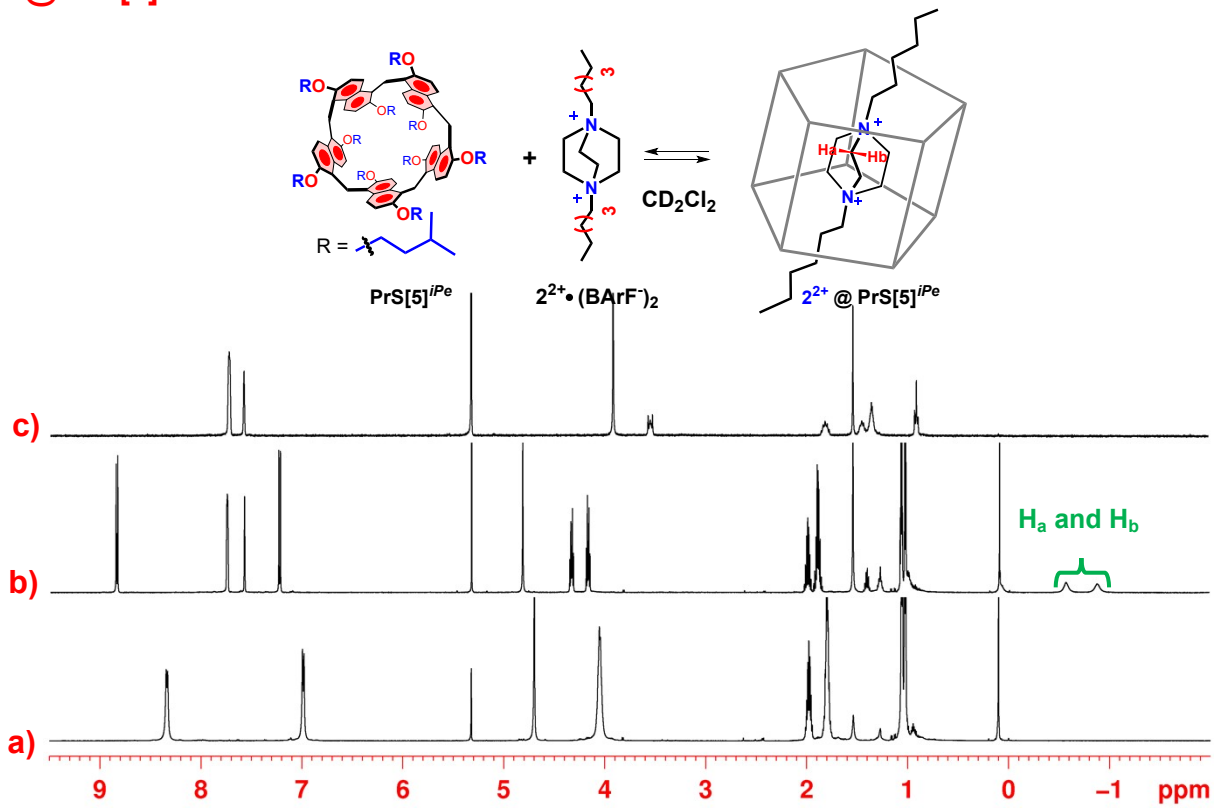

Figure S107: ^{1}H NMR spectra (600 MHz, CD_2Cl_2, 298 K) of: (a) **PrS[5]^{iPe}**, (b) an equimolar solution of **PrS[5]^{iPe}** and **2^{2+}**·$(BArF^-)_2$ and (c) **2^{2+}**·$(BArF^-)_2$.

2^{2+}@ PrS[5]^{EtCy}

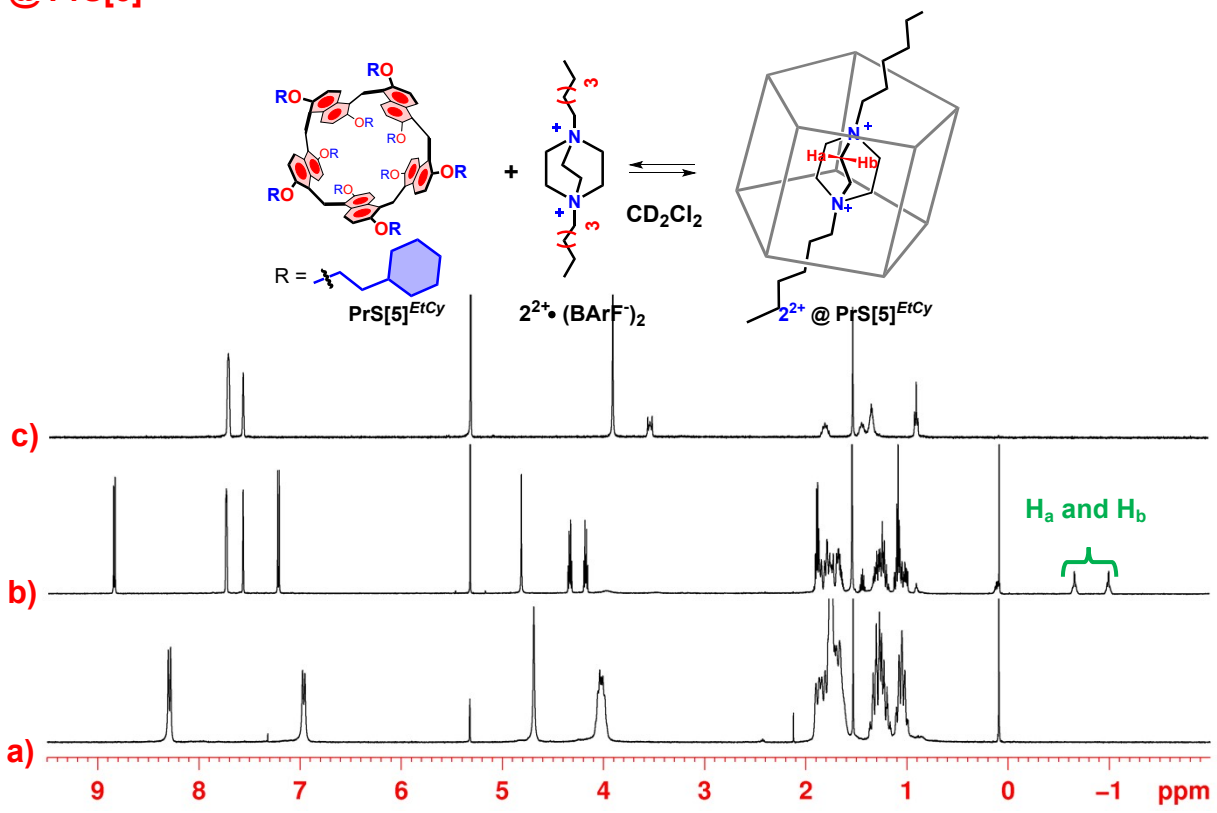

Figure S108: ^{1}H NMR spectra (600 MHz, CD_2Cl_2, 298 K) of: (a) **PrS[5]^{EtCy}**, (b) an equimolar solution of **PrS[5]^{EtCy}** and **2^{2+}**·$(BArF^-)_2$ and (c) **2^{2+}**·$(BArF^-)_2$.

2^{2+}@ PrS[5]^{EtcHp}

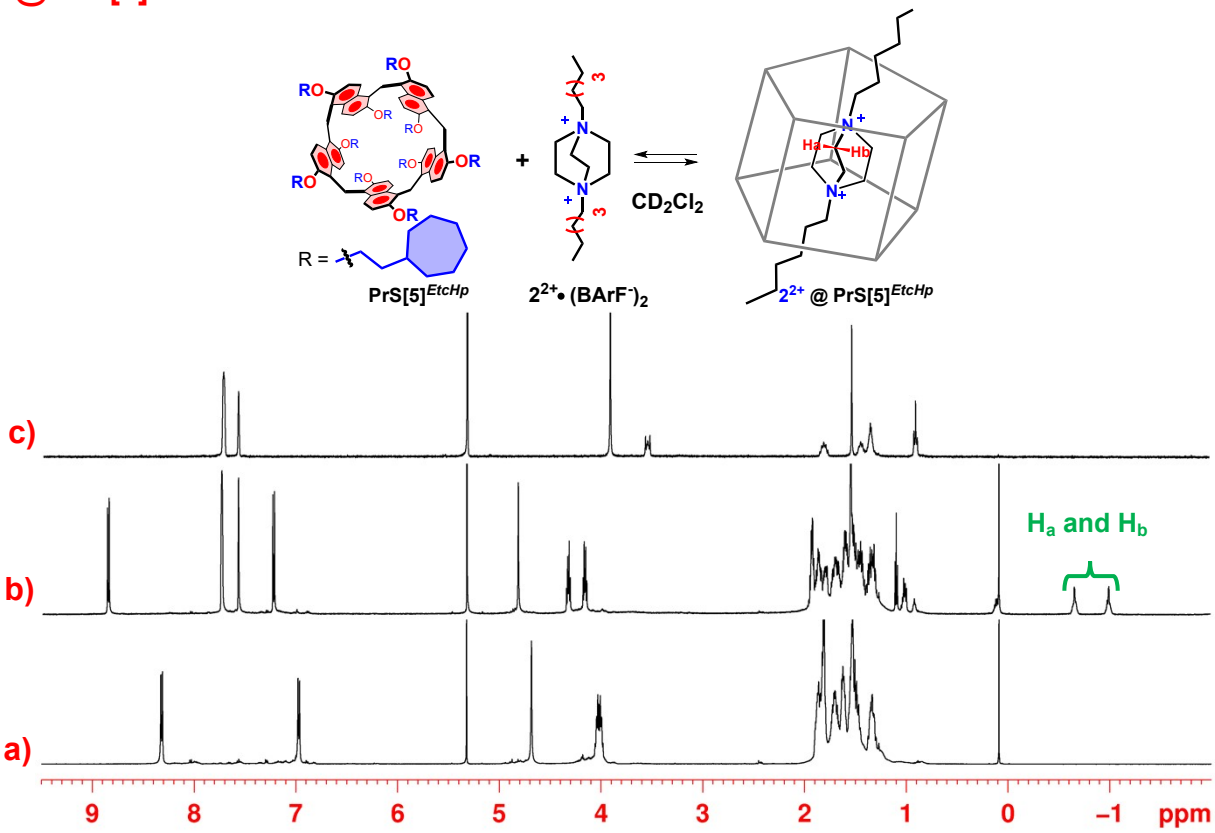

Figure S109: ^{1}H NMR spectra (600 MHz, CD_2Cl_2, 298 K) of: (a) **PrS[5]**^{EtcHp}, (b) an equimolar solution of **PrS[5]**^{EtcHp} and **2**$^{2+}$·$(BArF^-)_2$ and (c) **2**$^{2+}$·$(BArF^-)_2$.

3^{2+}@ PrS[5]^{nBu}

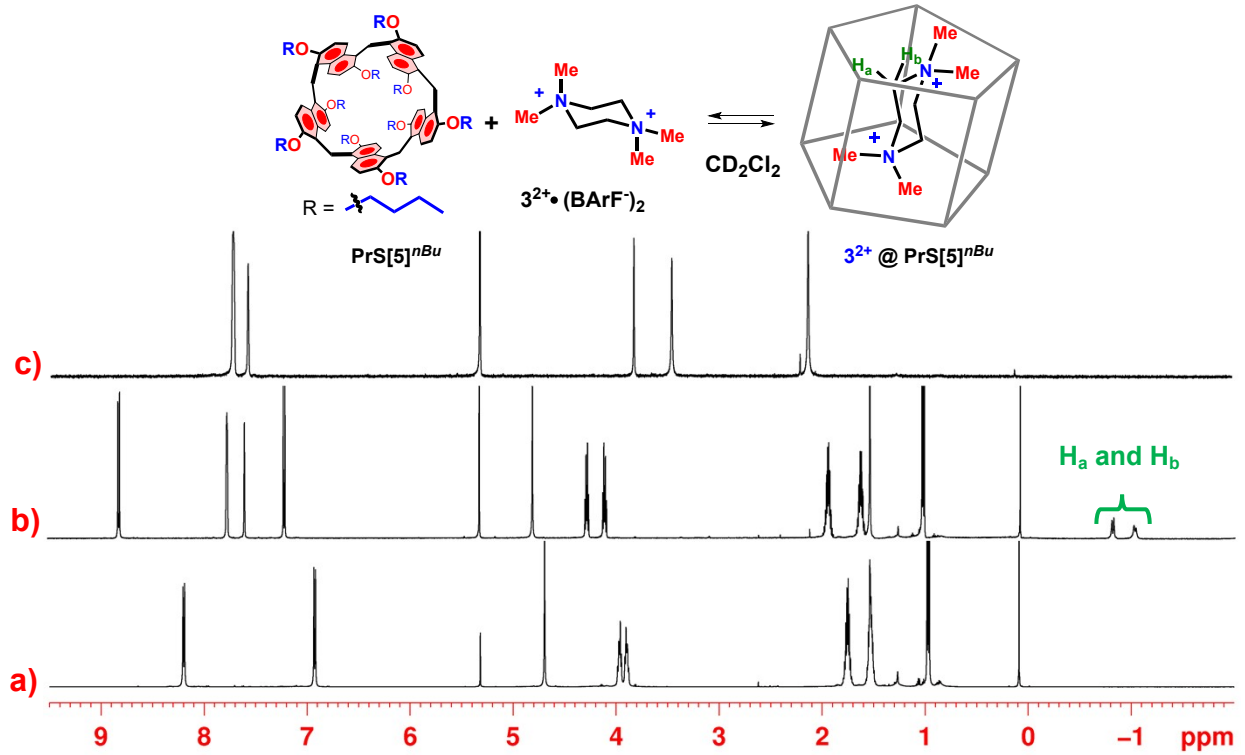

Figure S110: ^{1}H NMR spectra (600 MHz, CD_2Cl_2, 298 K) of: (a) **PrS[5]**^{nBu}, (b) an equimolar solution of **PrS[5]**^{nBu} and **3**$^{2+}$·$(BArF^-)_2$ and (c) **3**$^{2+}$·$(BArF^-)_2$.

3^{2+}@ PrS[5]^{nPe}

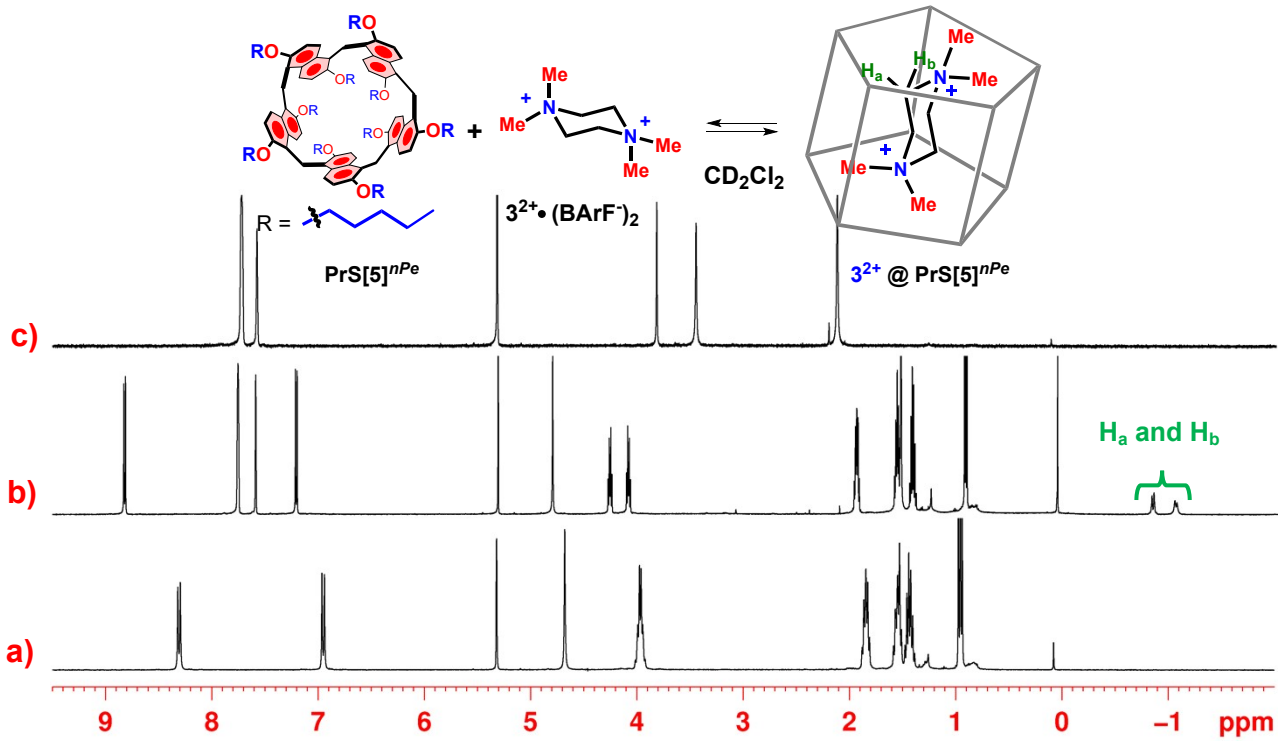

Figure S111: ^{1}H NMR spectra (600 MHz, CD_2Cl_2, 298 K) of: (a) **PrS[5]^{nPe}**, (b) an equimolar solution of **PrS[5]^{nPe}** and **3^{2+}**·$(BArF^-)_2$ and (c) **3^{2+}**·$(BArF^-)_2$.

3^{2+}@ PrS[5]^{iPr}

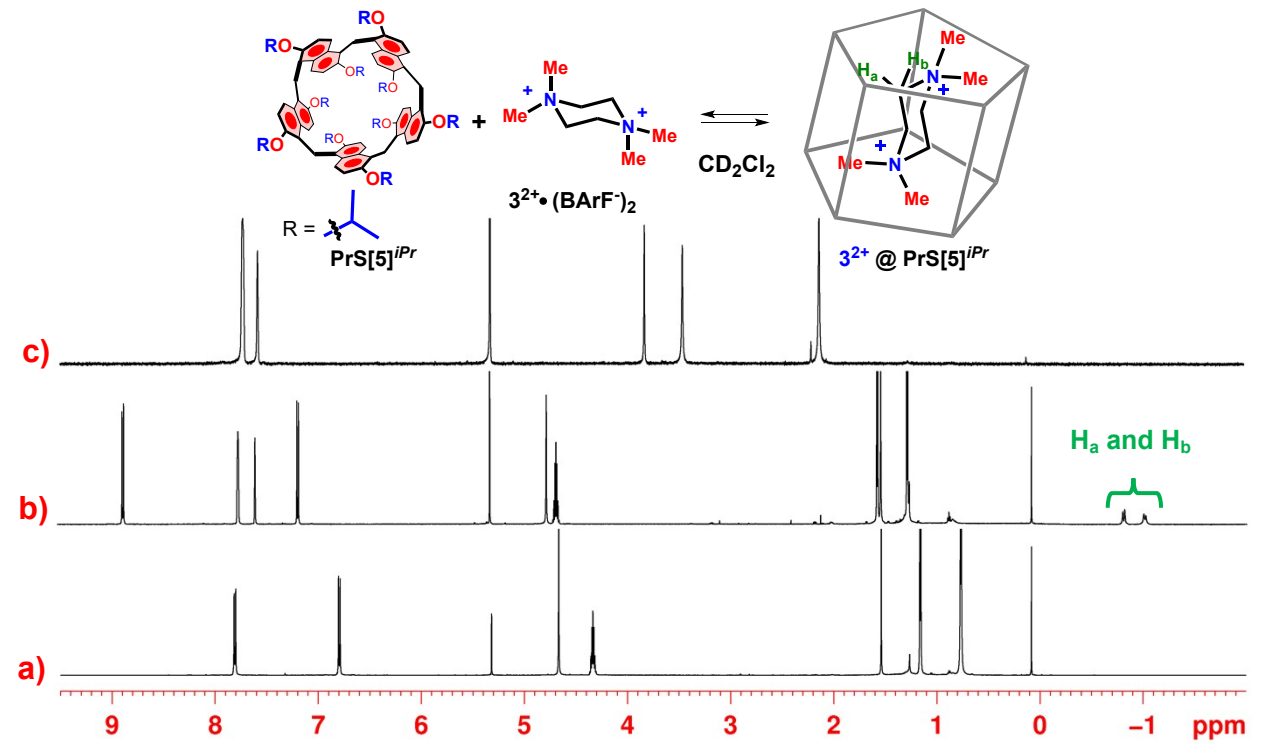

Figure S112: ^{1}H NMR spectra (600 MHz, CD_2Cl_2, 298 K) of: (a) **PrS[5]^{iPr}**, (b) an equimolar solution of **PrS[5]^{iPr}** and **3^{2+}**·$(BArF^-)_2$ and (c) **3^{2+}**·$(BArF^-)_2$.

3^{2+}@ PrS[5]^{iBu}

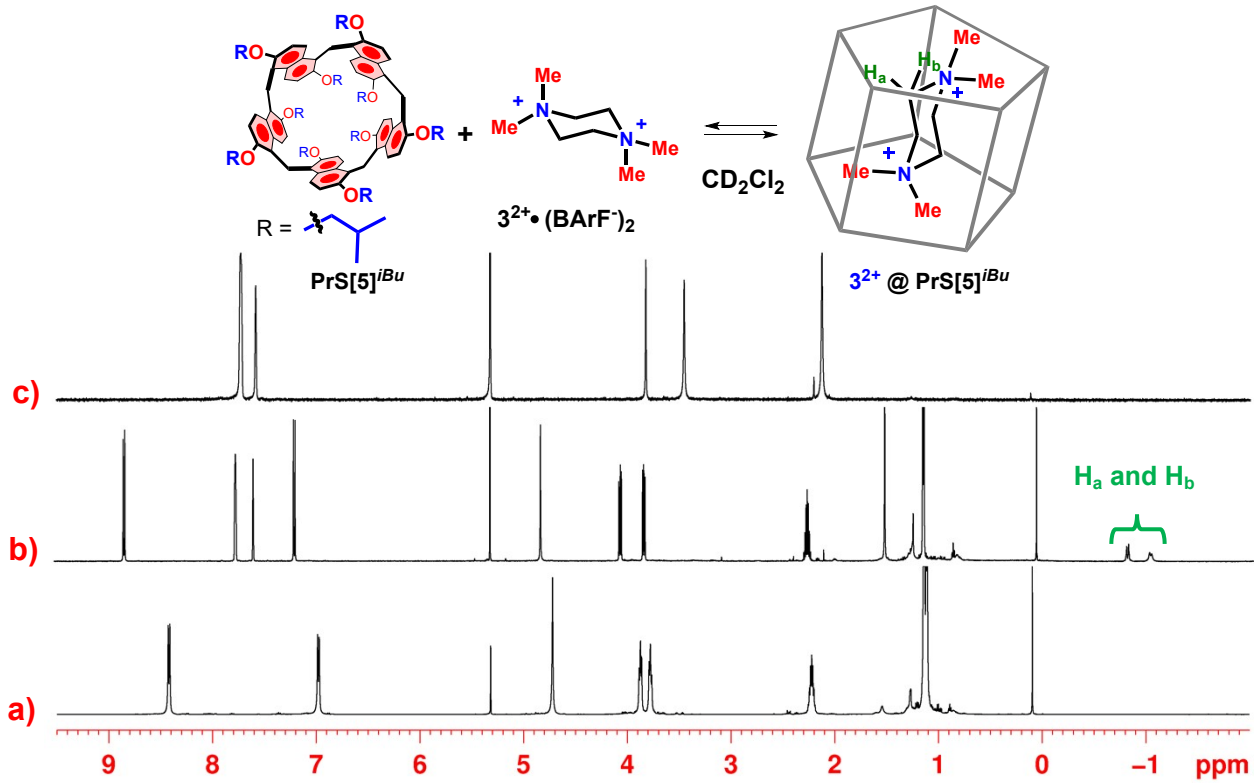

Figure S113: ^{1}H NMR spectra (600 MHz, CD_2Cl_2, 298 K) of: (a) **PrS[5]**^{iBu}, (b) an equimolar solution of **PrS[5]**^{iBu} and $\mathbf{3}^{2+}\cdot(BArF^-)_2$ and (c) $\mathbf{3}^{2+}\cdot(BArF^-)_2$.

3^{2+}@ PrS[5]^{iPe}

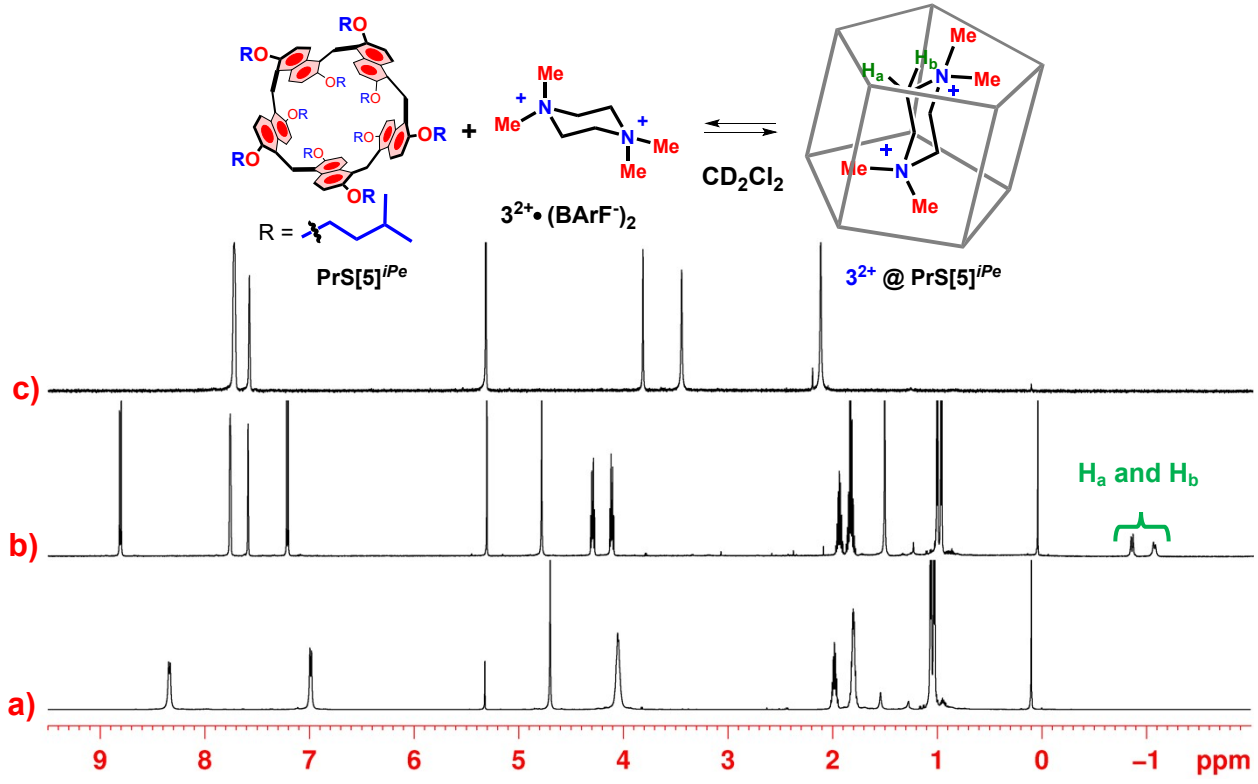

Figure S114: ^{1}H NMR spectra (600 MHz, CD_2Cl_2, 298 K) of: (a) **PrS[5]**^{iPe}, (b) an equimolar solution of **PrS[5]**^{iPe} and $\mathbf{3}^{2+}\cdot(BArF^-)_2$ and (c) $\mathbf{3}^{2+}\cdot(BArF^-)_2$.

3^{2+}@ PrS[5]^{EtCy}

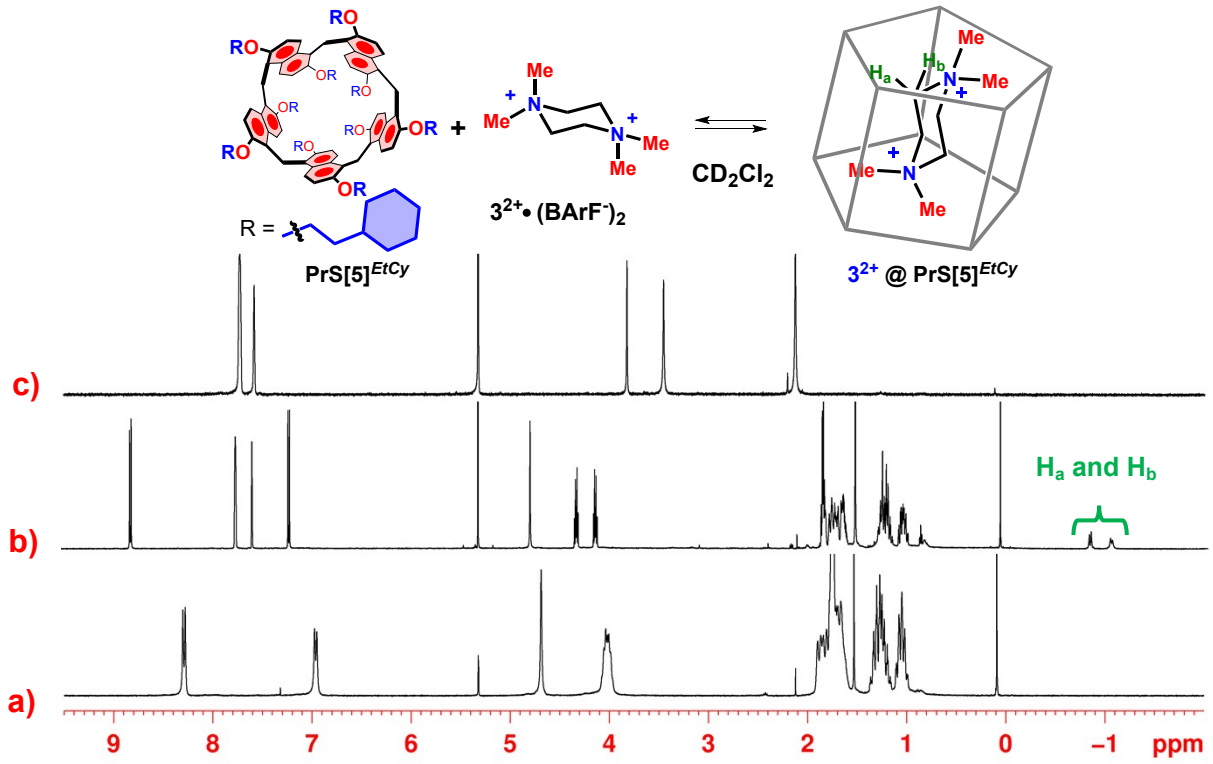

Figure S115: ^{1}H NMR spectra (600 MHz, CD_2Cl_2, 298 K) of: (a) **PrS[5]**^{EtCy}, (b) an equimolar solution of **PrS[5]**^{EtCy} and $\mathbf{3}^{2+}\cdot(BArF^-)_2$ and (c) $\mathbf{3}^{2+}\cdot(BArF^-)_2$.

3^{2+}@ PrS[5]^{EtcHp}

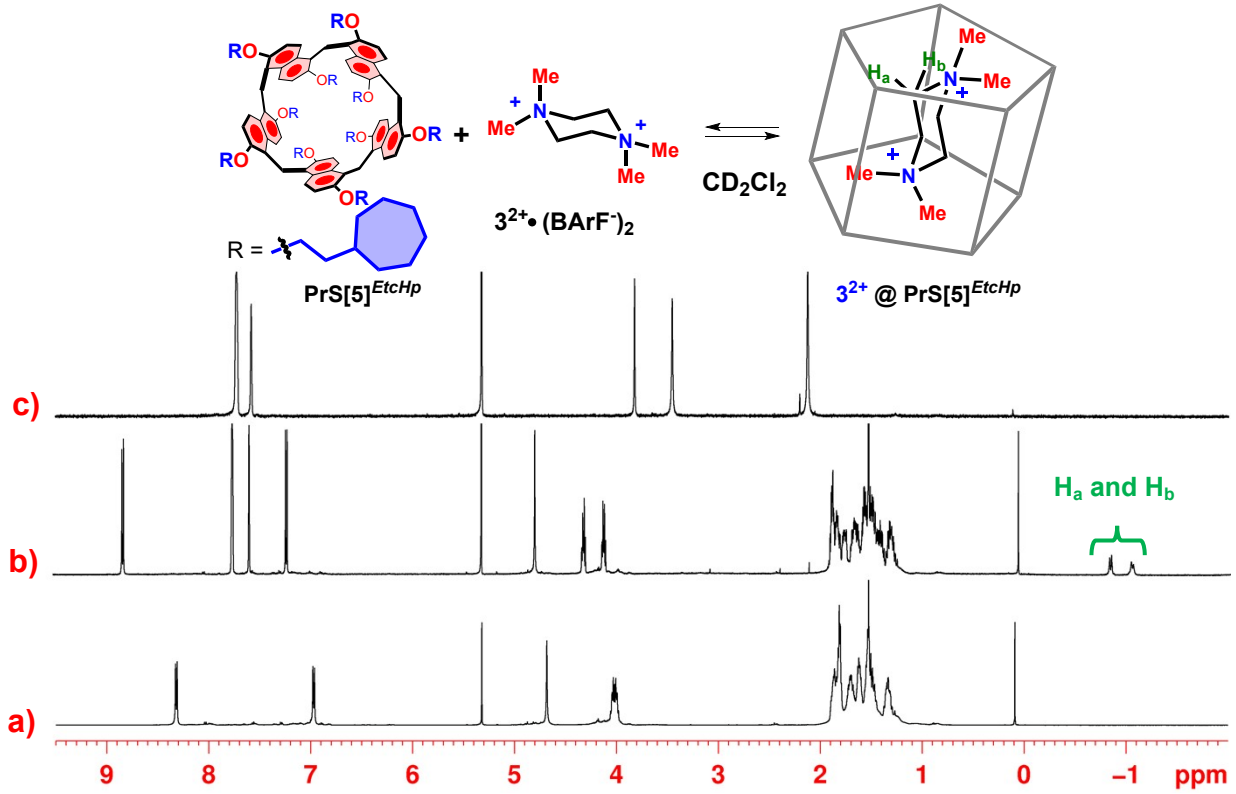

Figure S116: ^{1}H NMR spectra (600 MHz, CD_2Cl_2, 298 K) of: (a) **PrS[5]**^{EtcHp}, (b) an equimolar solution of **PrS[5]**^{EtcHp} and $\mathbf{3}^{2+}\cdot(BArF^-)_2$ and (c) $\mathbf{3}^{2+}\cdot(BArF^-)_2$.

^{1}H NMR determination of K_{ass} values

The association constant values of complexes were calculated by means of the following method:

a) ^{1}H NMR competition experiments. In this case, an analysis of a 1:1:1 mixture of guest, and two hosts in an NMR tube using 0.6 mL of CD_2Cl_2 as solvent was performed.

All K_{ass} values were calculated at 298 K and ^{1}H NMR experiments were recorded on 600 MHz spectrometers. Errors <15% were calculated as mean values of three measures.

Table S3: Association constant (K_{ass}, M^{-1}) values for the formation of the complexes between the ammonium $\mathbf{2^{2+}}$ and $\mathbf{3^{2+}}$ cations as $BArF^-$ salts and the prism[5]arenes.

PrS[5]^R	**2^{2+} (K_{ass}, M^{-1})**	**3^{2+} (K_{ass}, M^{-1})**
PrS[5]^{Et}	$1.4 \pm 0.2 \times 10^8$ M^{-1} [a]	$2.8 \pm 0.4 \times 10^8$ M^{-1} [a]
PrS[5]^{Pr}	$1.7 \pm 0.3 \times 10^8$ M^{-1} [a]	$1.4 \pm 0.2 \times 10^9$ M^{-1} [a]
PrS[5]^{nBu}	$4.6 \pm 0.6 \times 10^8$ M^{-1}	$1.1 \pm 0.2 \times 10^9$ M^{-1}
PrS[5]^{nPe}	$4.3 \pm 0.6 \times 10^8$ M^{-1}	$7.4 \pm 0.9 \times 10^8$ M^{-1}
PrS[5]^{iPr}	$3.3 \pm 0.4 \times 10^9$ M^{-1}	$1.2 \pm 0.2 \times 10^{10}$ M^{-1}
PrS[5]^{iBu}	$9.6 \pm 0.9 \times 10^8$ M^{-1}	$4.3 \pm 0.6 \times 10^9$ M^{-1}
PrS[5]^{iPe}	$2.7 \pm 0.4 \times 10^8$ M^{-1}	$5.8 \pm 0.8 \times 10^8$ M^{-1}
PrS[5]^{EtCy}	$2.1 \pm 0.3 \times 10^8$ M^{-1}	$6.8 \pm 0.9 \times 10^8$ M^{-1}
PrS[5]^{EtcHp}	$2.1 \pm 0.3 \times 10^8$ M^{-1}	$2.8 \pm 0.4 \times 10^8$ M^{-1}

[a] Reported in reference 3.

Copies of ^{1}H NMR spectra of complexation studies

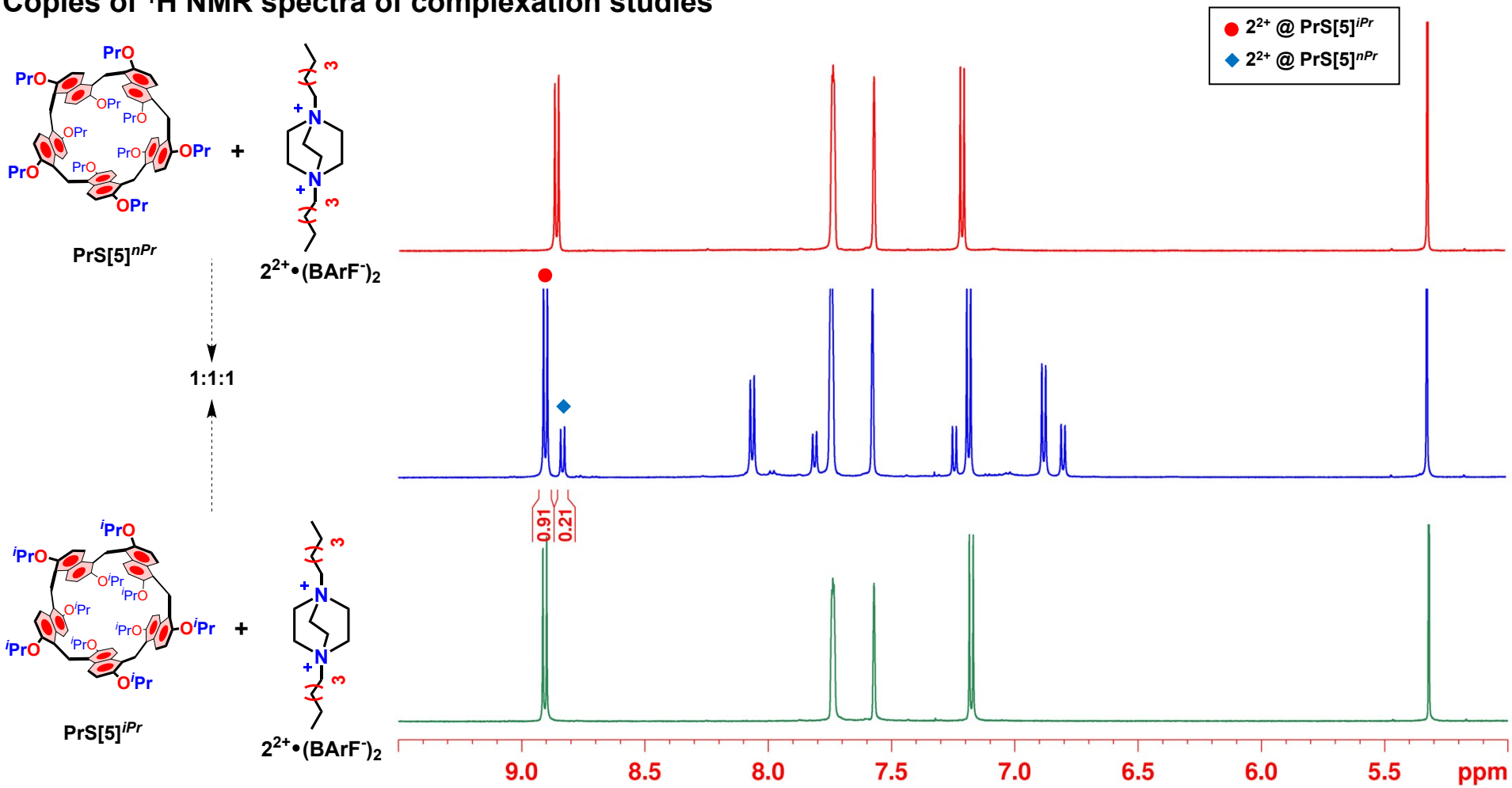

Figure S117: Significant portion of ^{1}H NMR spectra (600 MHz, CD_2Cl_2, 298 K) of: (green) an equimolar solution (2.6 mM) of **PrS[5]^{iPr}** and **2(BArF)$_2$** in 0.6 mL of CD_2Cl_2, (blue) **PrS[5]^{iPr}** in presence of 1 equivalent of **2(BArF)$_2$** and 1 equivalent of **PrS[5]^{nPr}** and (red) an equimolar solution (2.6 mM) of **PrS[5]^{nPr}** and **2(BArF)$_2$** in 0.6 mL of CD_2Cl_2.

$K_{rel} = K_{ass}(\mathbf{2^{2+}@PrS[5]^{iPr}})/ K_{ass}(\mathbf{2^{2+}@PrS[5]^{nPr}}) = K_{ass}(\mathbf{2^{2+}@PrS[5]^{iPr}}) / 1.7\text{x}10^8 = [(0.91/1.12)\text{x}0.0026]^2 / [(0.21/1.12)\text{x}0.0026]^2 = 18.78$
$K_{ass}(\mathbf{2^{2+}@PrS[5]^{iPr}}) = 19.36 \text{ x } 1.7\cdot10^8 = \mathbf{3.3\cdot10^9\ M^{-1}}$.

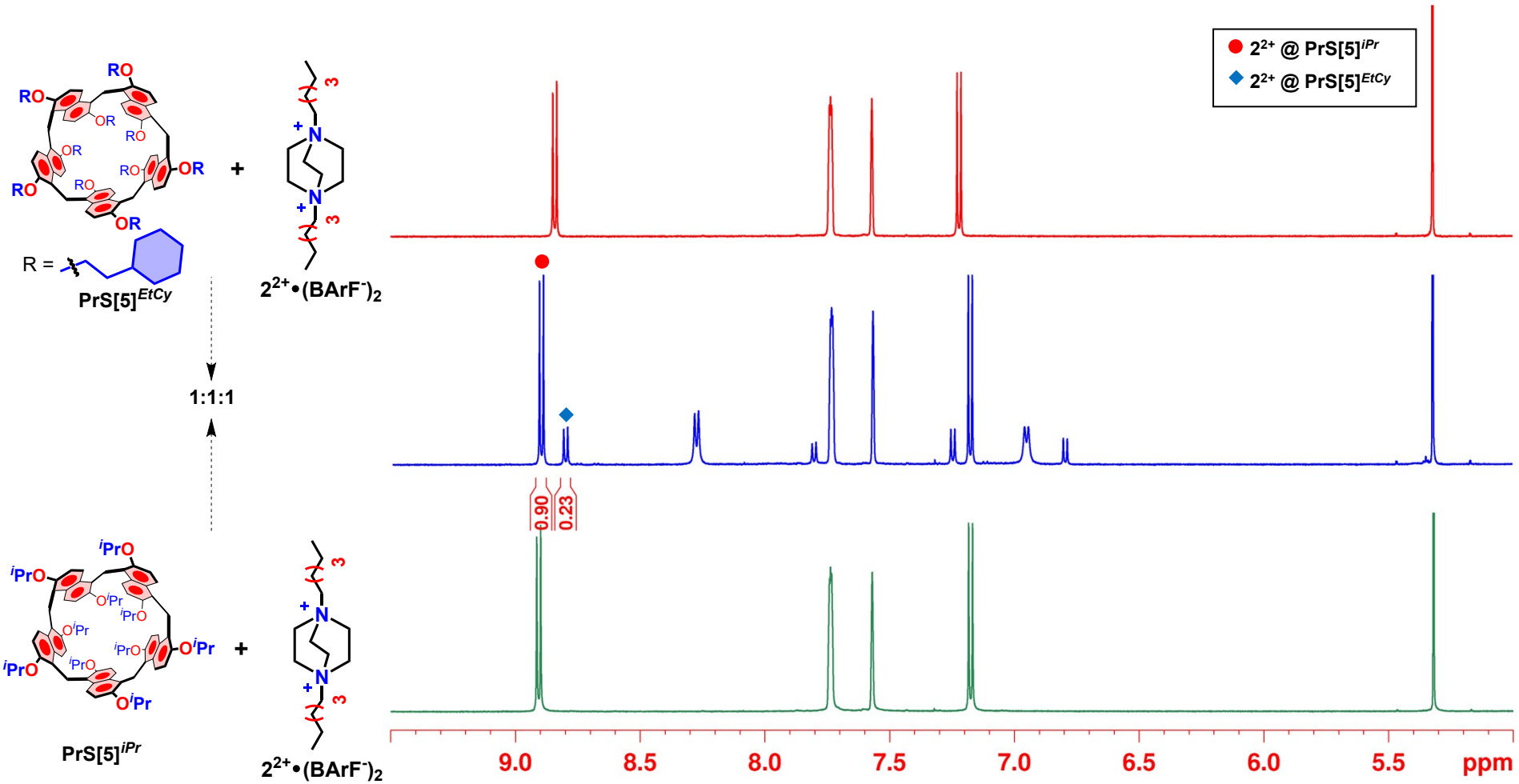

Figure S118: Significant portion of ^{1}H NMR spectra (600 MHz, CD_2Cl_2, 298 K) of: (green) an equimolar solution (1.7 mM) of **PrS[5]^{iPr}** and **2(BArF)$_2$** in 0.6 mL of CD_2Cl_2, (blue) **PrS[5]^{EtCy}** in presence of 1 equivalent of **2(BArF)$_2$** and 1 equivalent of **PrS[5]^{iPr}** and (red) an equimolar solution (1.7 mM) of **PrS[5]^{EtCy}** and **2(BArF)$_2$** in 0.6 mL of CD_2Cl_2.

$\boldsymbol{K_{rel}} = K_{ass}$ (**2^{2+}@PrS[5]^{EtCy}**)/K_{ass} (**2^{2+}@PrS[5]^{iPr}**) = K_{ass}(**2^{2+}@PrS[5]^{EtCy}**) / $3.3\cdot10^9$ = [(0.23/1.13)x0.0017]^2 / [(0.90/1.13)x0.0017]^2 = 0.065

K_{ass} (**2^{2+}@PrS[5]^{EtCy}**) = 0.065 x $3.3\cdot10^9$ = **$2.1\cdot10^8$ M^{-1}.**

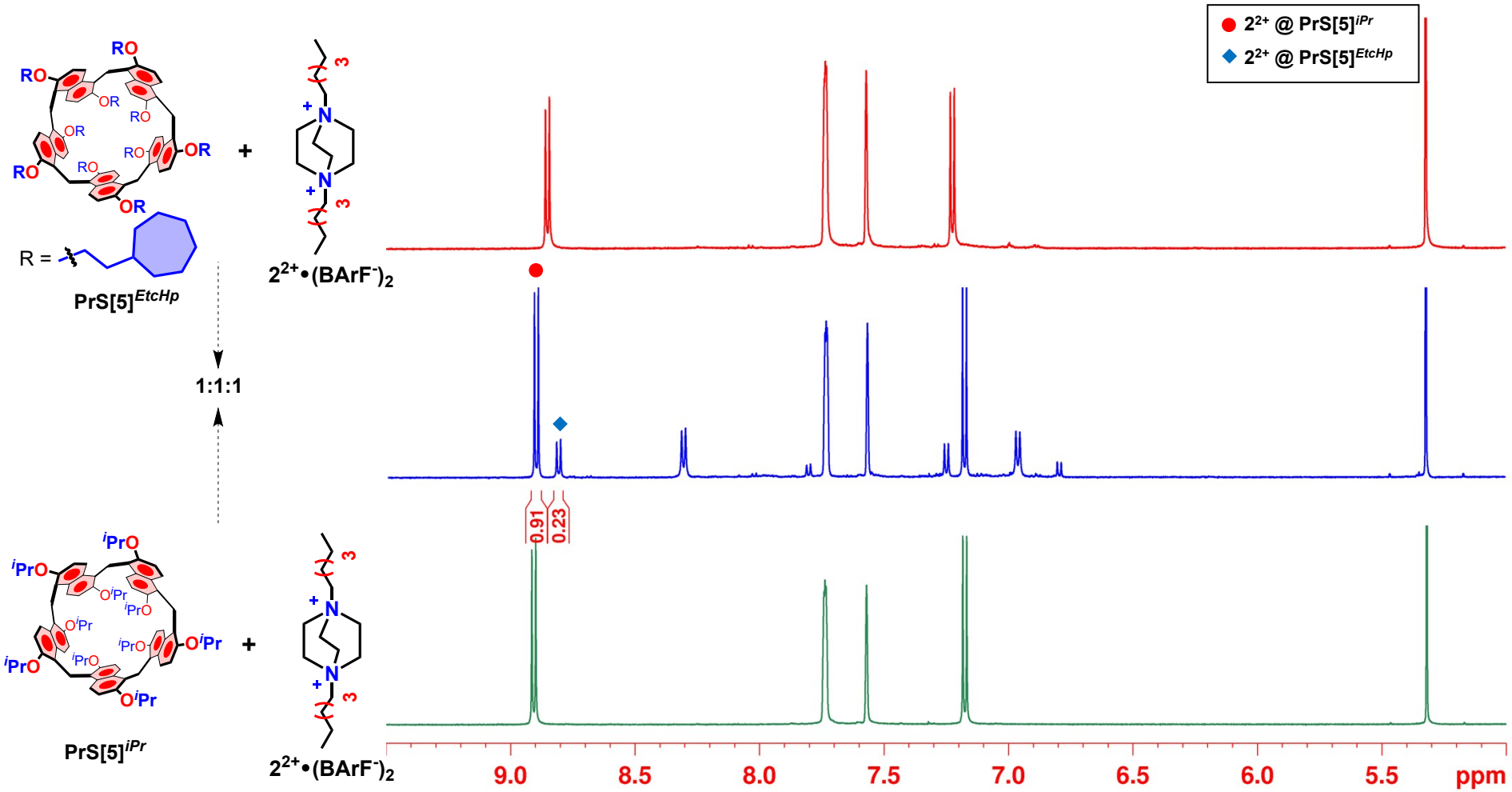

Figure S119: Significant portion of ^{1}H NMR spectra (600 MHz, CD_2Cl_2, 298 K) of: (green) an equimolar solution (1.6 mM) of **PrS[5]^{iPr}** and **2(BArF)$_2$** in 0.6 mL of CD_2Cl_2, (blue) **PrS[5]^{EtcHp}** in presence of 1 equivalent of **2(BArF)$_2$** and 1 equivalent of **PrS[5]^{iPr}** and (red) an equimolar solution (1.6 mM) of **PrS[5]^{EtcHp}** and **2(BArF)$_2$** in 0.6 mL of CD_2Cl_2.

$$\boldsymbol{K_{rel}} = K_{ass}(\mathbf{2^{2+}@PrS[5]^{EtcHp}})/K_{ass}(\mathbf{2^{2+}@PrS[5]^{iPr}}) = K_{ass}(\mathbf{2^{2+}@PrS[5]^{EtcHp}})\ /3.3\cdot10^9 = [(0.23/1.14)x0.0016]^2\ /\ [(0.91/1.14)x0.0016]^2 = 0.064$$

$$K_{ass}\ (\mathbf{2^{2+}@PrS[5]^{EtcHp}}) = 0.064\ x\ 3.3\cdot10^9 = \mathbf{2.1\cdot10^8\ M^{-1}}.$$

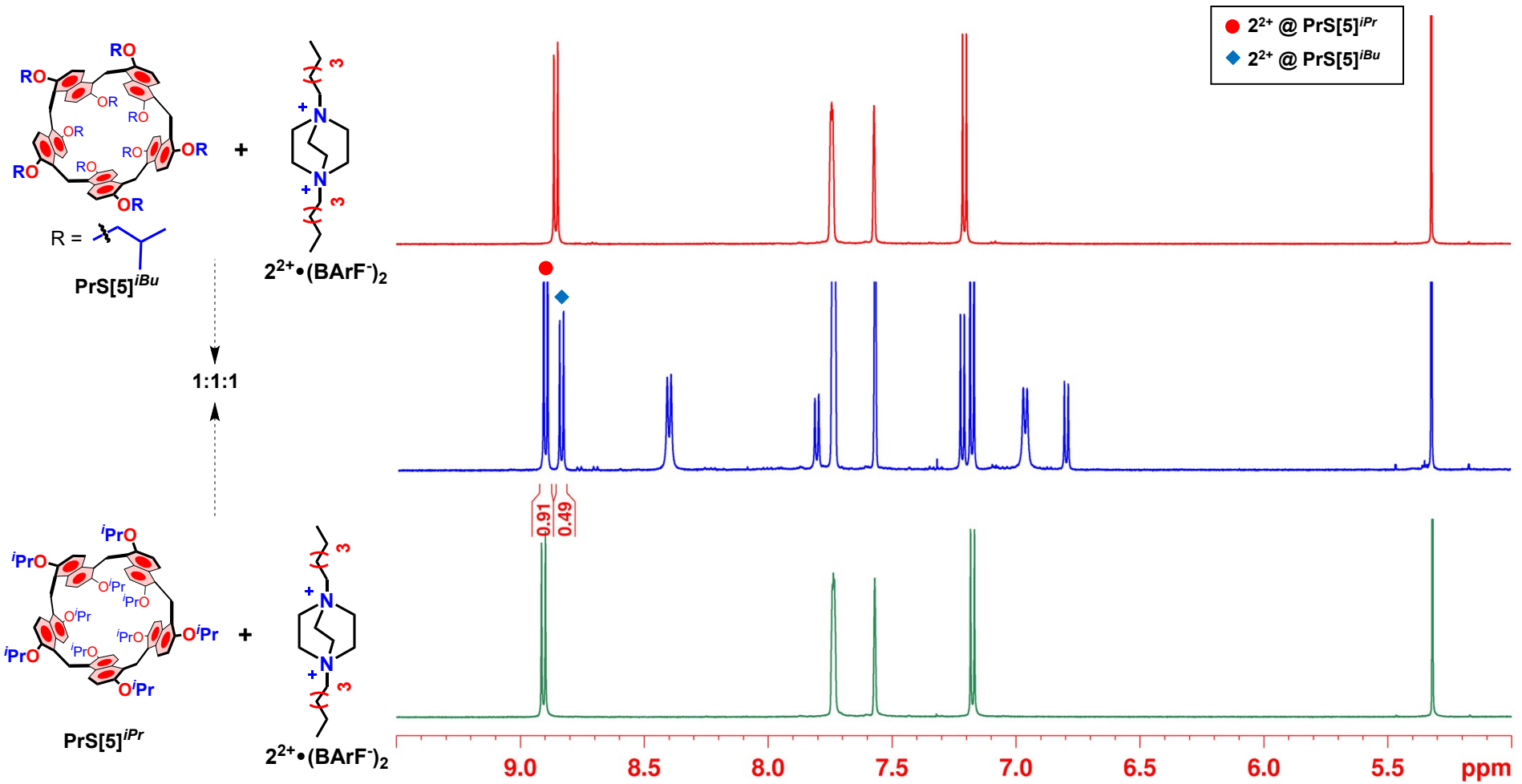

Figure S120: Significant portion of ^{1}H NMR spectra (600 MHz, CD_2Cl_2, 298 K) of: (green) an equimolar solution (2.6 mM) of **PrS[5]^{iPr}** and **2(BArF)$_2$** in 0.6 mL of CD_2Cl_2, (blue) **PrS[5]^{iBu}** in presence of 1 equivalent of **2(BArF)$_2$** and 1 equivalent of **PrS[5]^{iPr}** and (red) an equimolar solution (2.6 mM) of **PrS[5]^{iBu}** and **2(BArF)$_2$** in 0.6 mL of CD_2Cl_2.

$$\boldsymbol{K_{rel}} = K_{ass}(\mathbf{2^{2+}@PrS[5]^{iBu}})/K_{ass}(\mathbf{2^{2+}@PrS[5]^{iPr}}) = K_{ass}(\mathbf{2^{2+}@PrS[5]^{iBu}}) / 3.3\cdot10^9 = [(0.49/1.40)\text{x}0.0026]^2 / [(0.91/1.40)\text{x}0.0026]^2 = 0.29$$

$$K_{ass}(\mathbf{2^{2+}@\ PrS[5]^{iBu}}) = 0.29 \text{ x } 3.3\cdot10^9 = \mathbf{9.6\cdot10^8\ M^{-1}}.$$

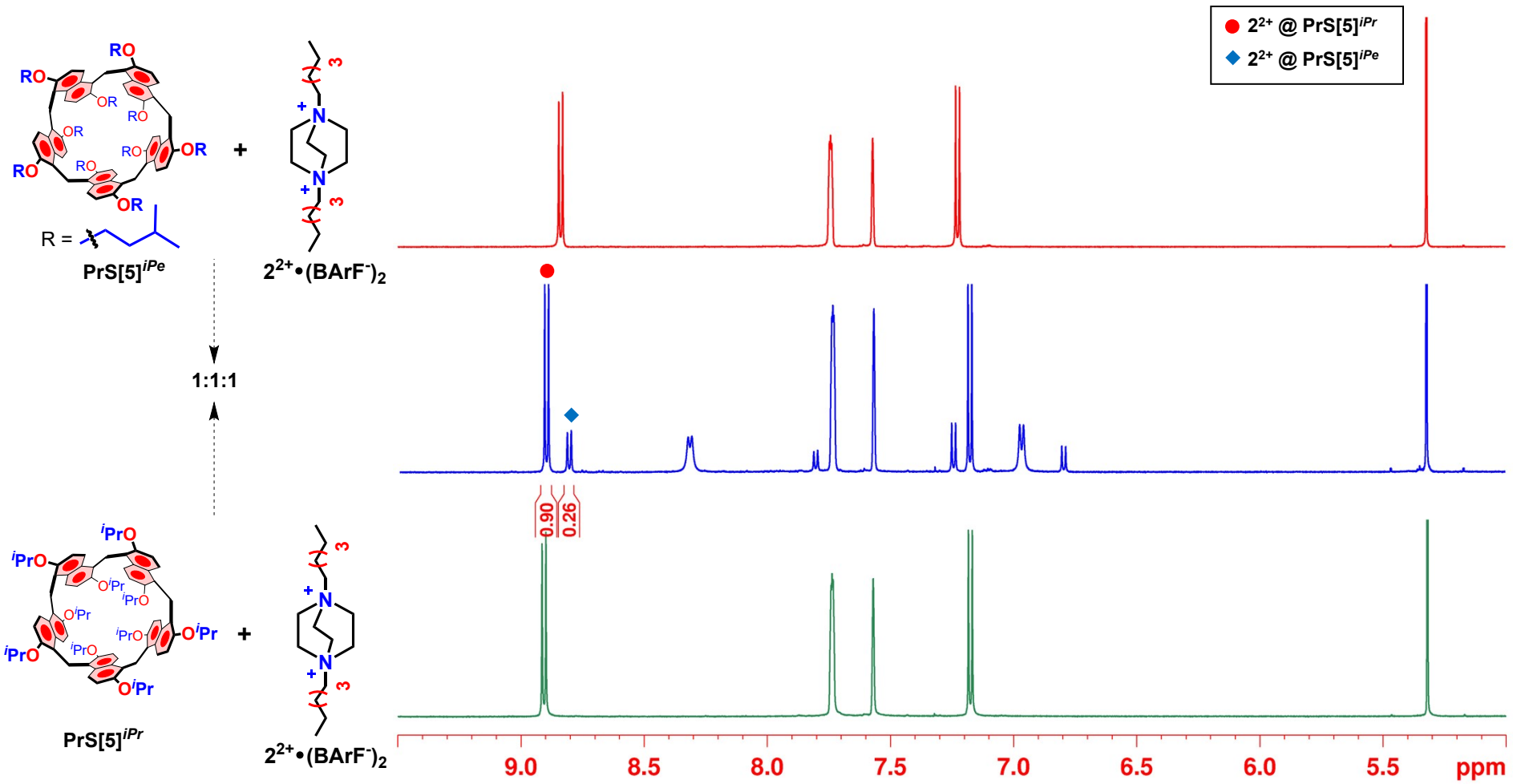

Figure S121: Significant portion of ^{1}H NMR spectra (600 MHz, CD_2Cl_2, 298 K) of: (green) an equimolar solution (2.1 mM) of **PrS[5]^{iPr}** and **2(BArF)$_2$** in 0.6 mL of CD_2Cl_2, (blue) **PrS[5]^{iPe}** in presence of 1 equivalent of **2(BArF)$_2$** and 1 equivalent of **PrS[5]^{iPr}** and (red) an equimolar solution (2.1 mM) of **PrS[5]^{iPe}** and **2(BArF)$_2$** in 0.6 mL of CD_2Cl_2.

$\boldsymbol{K_{rel}} = K_{ass}(\mathbf{2^{2+}@PrS[5]^{iPe}})/K_{ass}(\mathbf{2^{2+}@PrS[5]^{iPr}}) = K_{ass}\,(\mathbf{2^{2+}@PrS[5]^{iPe}}) / 3.3\cdot10^9 = [(0.26/1.16)\text{x}0.0021]^2 / [(0.90/1.16)\text{x}0.0021]^2 = 0.083$

$K_{ass}\,(\mathbf{2^{2+}@PrS[5]^{iPe}}) = 0.083 \text{ x } 3.3\cdot10^9 = \mathbf{2.7\cdot10^8\ M^{-1}}$.

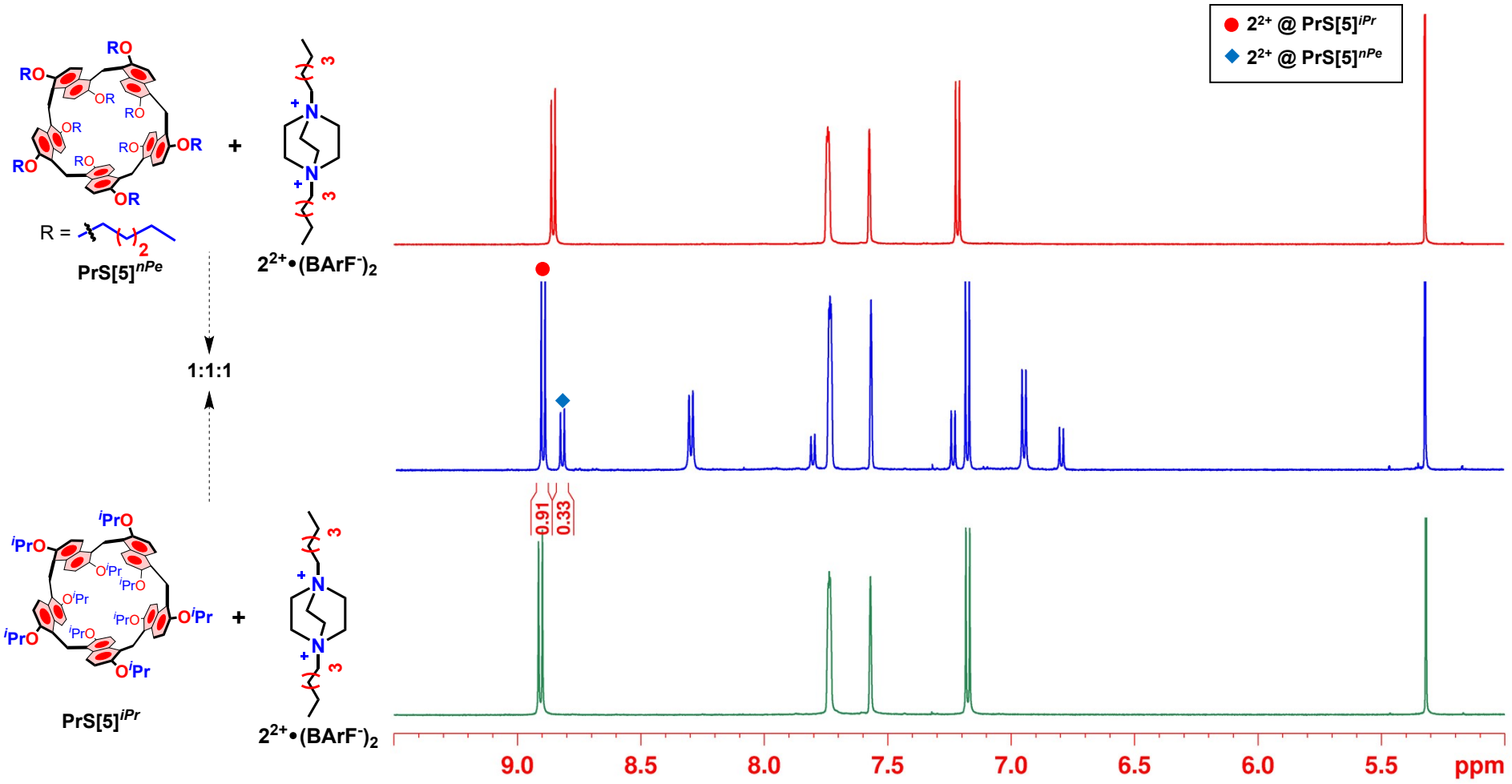

Figure S122: Significant portion of ^{1}H NMR spectra (600 MHz, CD_2Cl_2, 298 K) of: (green) an equimolar solution (2.1 mM) of **PrS[5]^{iPr}** and **2(BArF)$_2$** in 0.6 mL of CD_2Cl_2, (blue) **PrS[5]^{nPe}** in presence of 1 equivalent of **2(BArF)$_2$** and 1 equivalent of **PrS[5]^{iPr}** and (red) an equimolar solution (2.1 mM) of **PrS[5]^{nPe}** and **2(BArF)$_2$** in 0.6 mL of CD_2Cl_2.

$K_{rel} = K_{ass}(\mathbf{2^{2+}@PrS[5]^{nPe}})/ K_{ass}(\mathbf{2^{2+}@PrS[5]^{iPr}}) = K_{ass}(\mathbf{2^{2+}@PrS[5]^{nPe}}) / 3.3\cdot10^9 = [(0.33/1.24)x0.0021]^2 / [(0.91/1.24)x0.0021]^2 = 0.13$

K_{ass} $(\mathbf{2^{2+}@PrS[5]^{nPe}}) = 0.13$ x $3.3\cdot10^9 = \mathbf{4.3\cdot10^8\ M^{-1}}$.

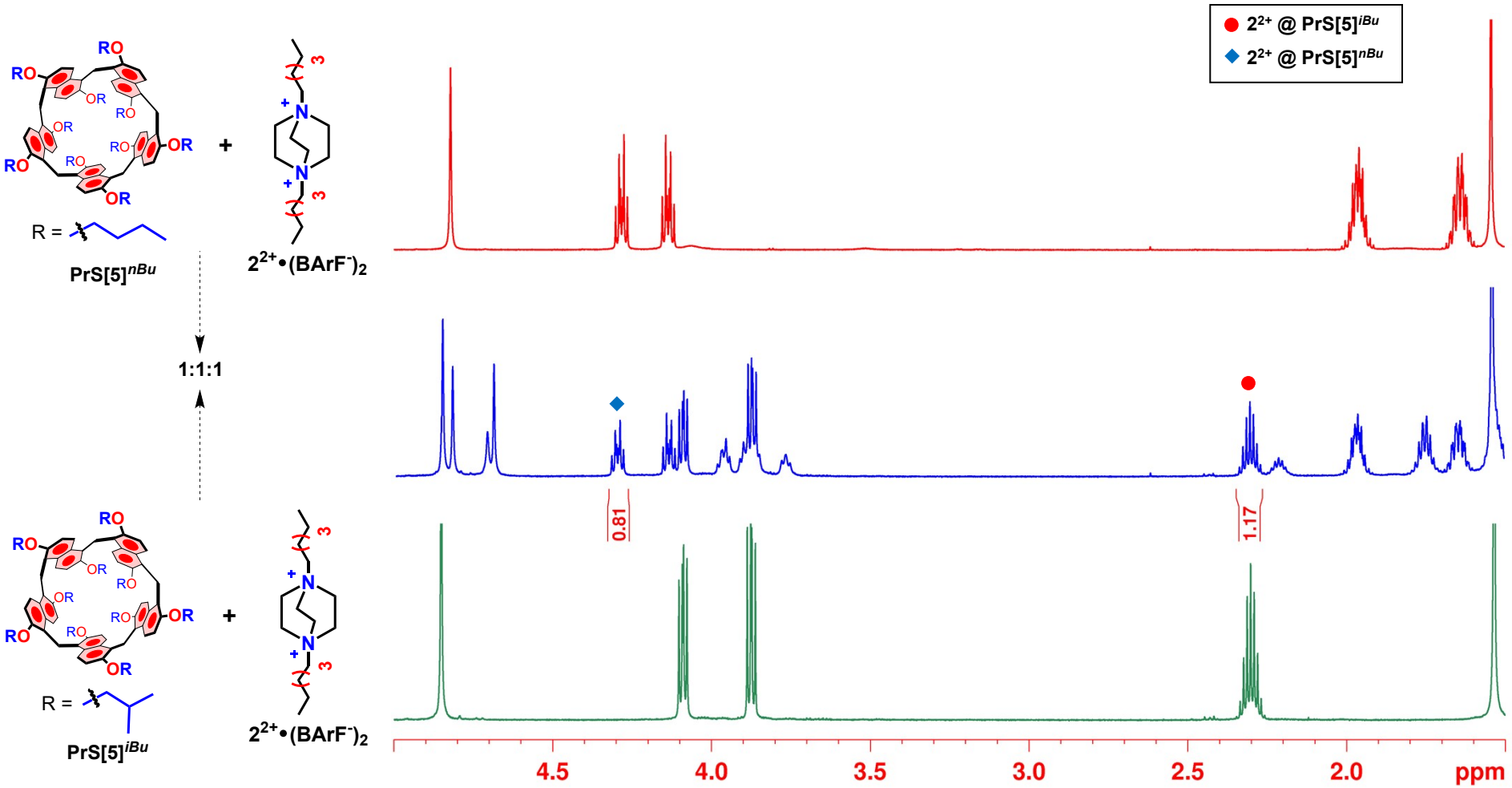

Figure S123: Significant portion of ^{1}H NMR spectra (600 MHz, CD_2Cl_2, 298 K) of: (green) an equimolar solution (2.3 mM) of **PrS[5]^{iBu}** and **2(BArF)$_2$** in 0.6 mL of CD_2Cl_2, (blue) **PrS[5]^{iBu}** in presence of 1 equivalent of **2(BArF)$_2$** and 1 equivalent of **PrS[5]^{iBu}** and (red) an equimolar solution (2.3 mM) of **PrS[5]^{nBu}** and **2(BArF)$_2$** in 0.6 mL of CD_2Cl_2.

$K_{rel} = K_{ass}$ (**2^{2+}@PrS[5]^{nBu}**)/ K_{ass} (**2^{2+}@PrS[5]^{iBu}**) = K_{ass} (**2^{2+}@PrS[5]^{nBu}**) / $9.6 \cdot 10^8$ = [(0.81/1.98)x0.0023]^2 / [(1.17/1.98)x0.0023]^2 = 0.48

K_{ass} (**2^{2+}@PrS[5]^{nBu}**) = 0.48 x $9.6 \cdot 10^8$ = **$4.3 \cdot 10^8$ M^{-1}.**

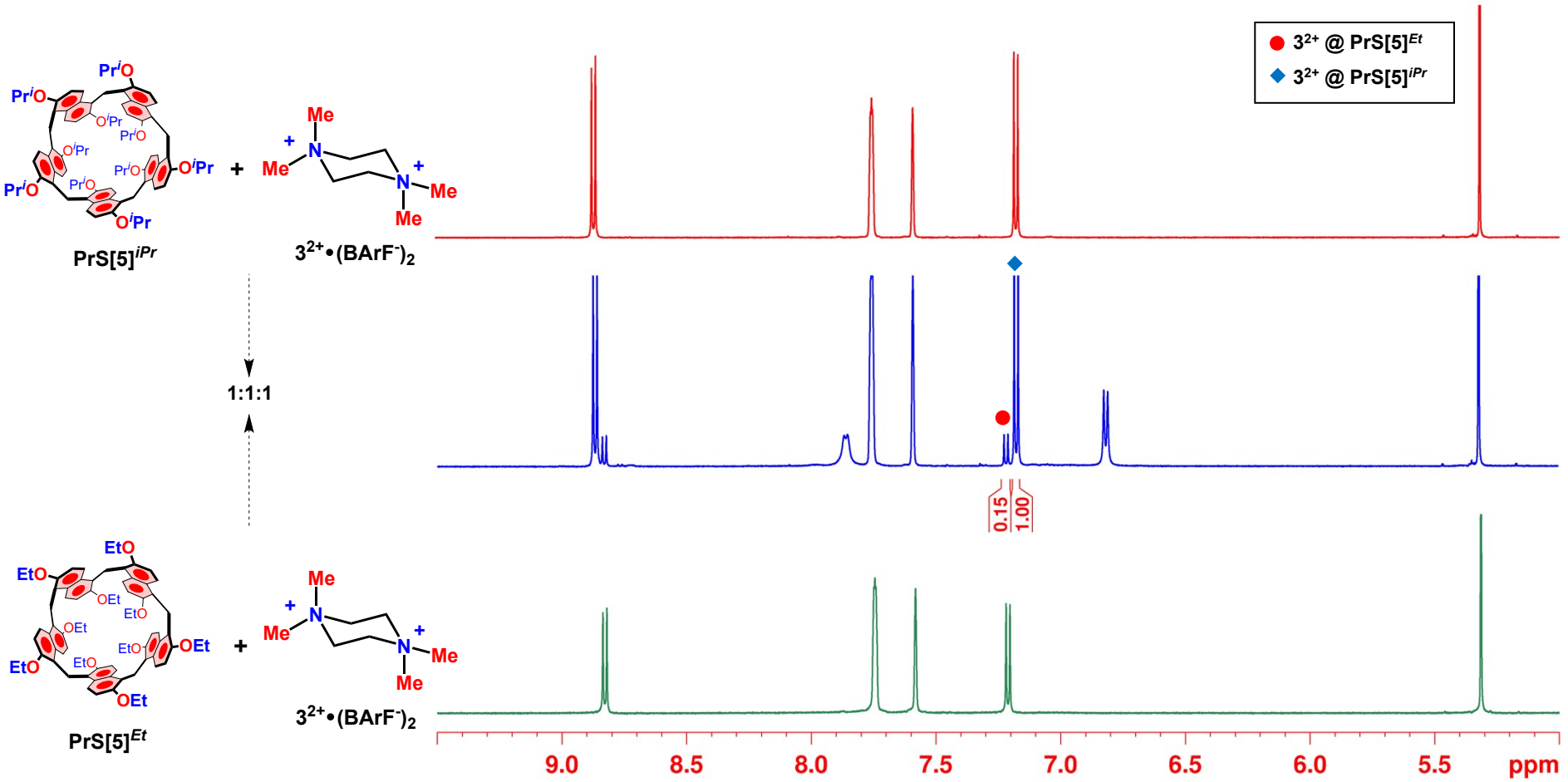

Figure S124: Significant portion of ^{1}H NMR spectra (600 MHz, CD_2Cl_2, 298 K) of: (green) an equimolar solution (2.6 mM) of **PrS[5]^{Et}** and **3(BArF)$_2$** in 0.6 mL of CD_2Cl_2, (blue) **PrS[5]^{iPr}** in presence of 1 equivalent of **3(BArF)$_2$** and 1 equivalent of **PrS[5]^{Et}** and (red) an equimolar solution (2.6 mM) of **PrS[5]^{iPr}** and **3(BArF)$_2$** in 0.6 mL of CD_2Cl_2.

K_{rel} = K_{ass} (**3^{2+}@PrS[5]^{iPr}**)/ K_{ass} (**3^{2+}@PrS[5]^{Et}**) = K_{ass} (**3^{2+}@PrS[5]^{iPr}**) / $2.8\cdot10^{8}$ = $[(1.00/1.15)\text{x}0.0026]^2$ / $[(0.15/1.15)\text{x}0.0026]^2$ = 44.43

K_{ass} (**3^{2+}@PrS[5]^{iPr}**) = 44.43 x $2.8\cdot10^{8}$= **$1.2\cdot10^{10}$ M^{-1}.**

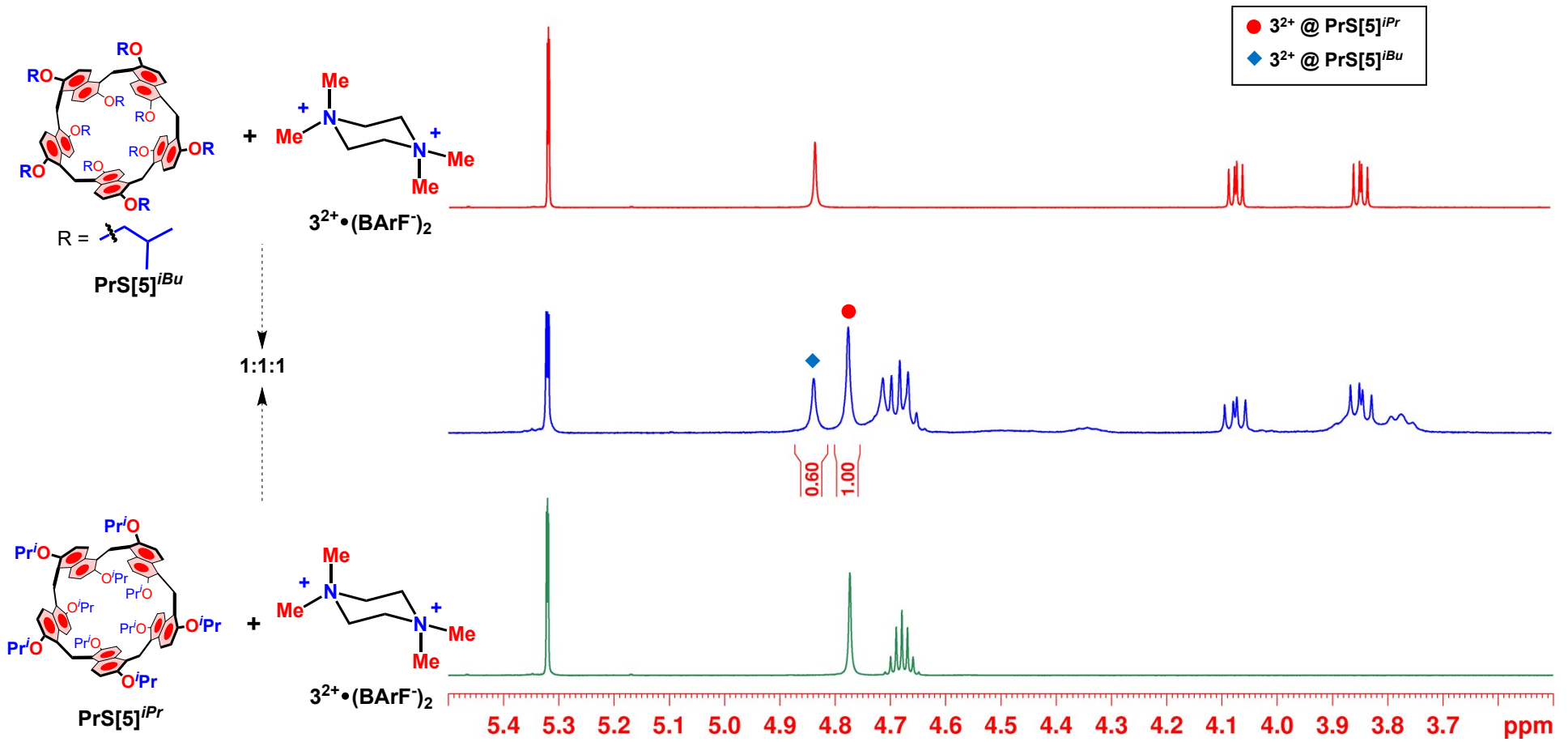

Figure S125: Significant portion of ^{1}H NMR spectra (600 MHz, CD_2Cl_2, 298 K) of: (green) an equimolar solution (2.4 mM) of **PrS[5]^{iPr}** and **3(BArF)$_2$** in 0.6 mL of CD_2Cl_2, (blue) **PrS[5]^{iBu}** in presence of 1 equivalent of **3(BArF)$_2$** and 1 equivalent of **PrS[5]^{iPr}** and (red) an equimolar solution (2.4 mM) of **PrS[5]^{iBu}** and **3(BArF)$_2$** in 0.6 mL of CD_2Cl_2.

K_{rel} = K(**3^{2+}@PrS[5]^{iBu}**)/K(**3^{2+}@PrS[5]^{iPr}**) = K(**3^{2+}@PrS[5]^{iBu}**) / $1.2\cdot10^{10}$ = [(0.60/1.60)x0.0024]^2 / [(1.00/1.60)x0.0024]^2 = 0.36

K(**3^{2+}@PrS[5]^{iBu}**) = 0.36 x $1.2\cdot10^{10}$= **$4.3\cdot10^{9}$ M^{-1}.**

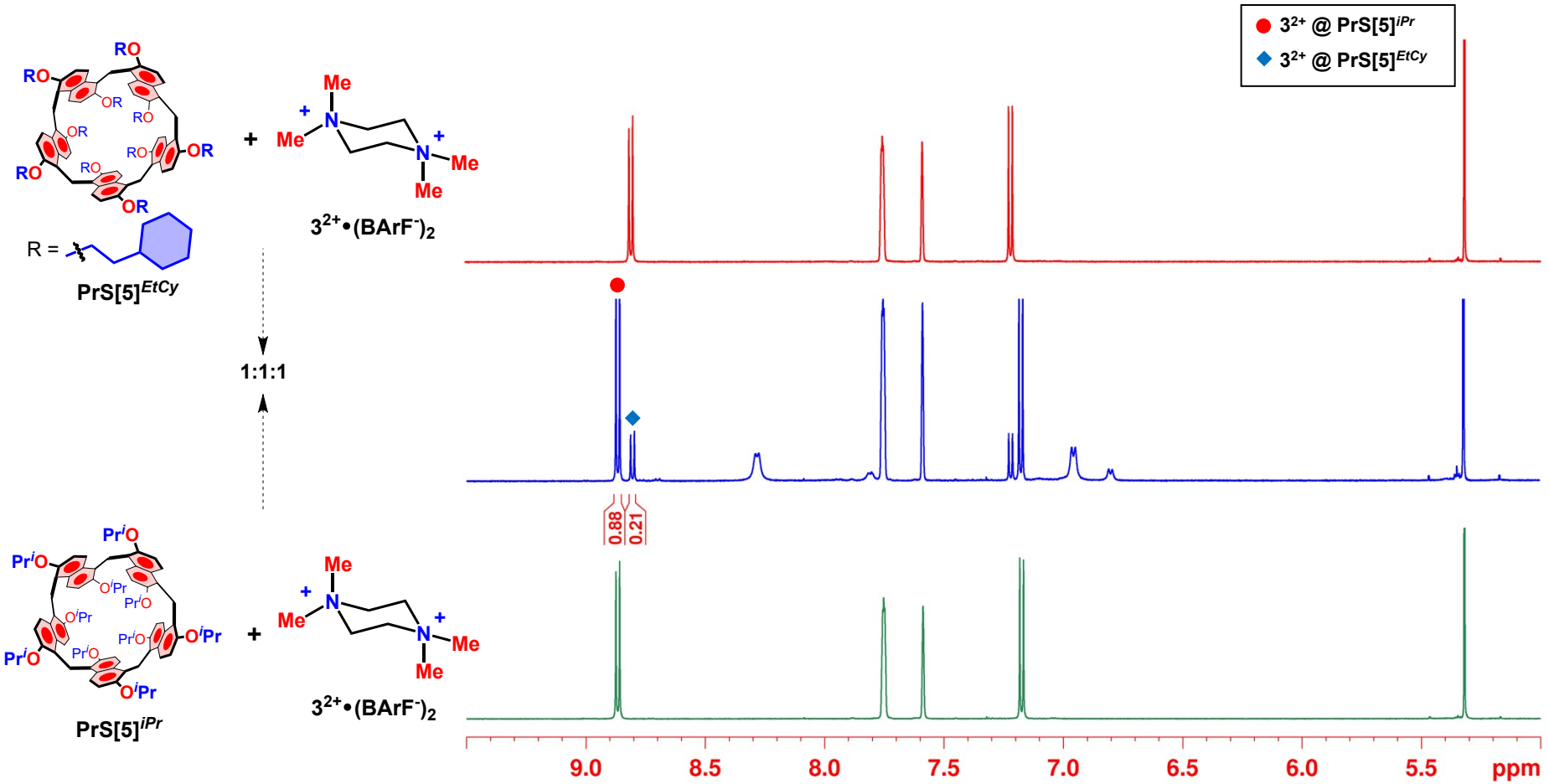

Figure S126: Significant portion of ^{1}H NMR spectra (600 MHz, CD_2Cl_2, 298 K) of: (green) an equimolar solution (1.7 mM) of **PrS[5]^{iPr}** and **3(BArF)$_2$** in 0.6 mL of CD_2Cl_2, (blue) **PrS[5]^{EtCy}** in presence of 1 equivalent of **3(BArF)$_2$** and 1 equivalent of **PrS[5]^{iPr}** and (red) an equimolar solution (1.7 mM) of **PrS[5]^{EtCy}** and **3(BArF)$_2$** in 0.6 mL of CD_2Cl_2.

$K_{rel} = K_{ass}(\mathbf{3^{2+}@PrS[5]^{EtCy}})/ K_{ass}(\mathbf{3^{2+}@PrS[5]^{iPr}}) = K_{ass}(\mathbf{3^{2+}@PrS[5]^{EtCy}}) / 1.2\cdot10^{10} = [(0.21/1.09)x0.0017]^2 / [(0.88/1.09)x0.0017]^2 = 0.057$

$K(\mathbf{3^{2+}@PrS[5]^{EtCy}}) = 0.057 \times 1.2\cdot10^{10} = \mathbf{6.8\cdot10^8\ M^{-1}}$.

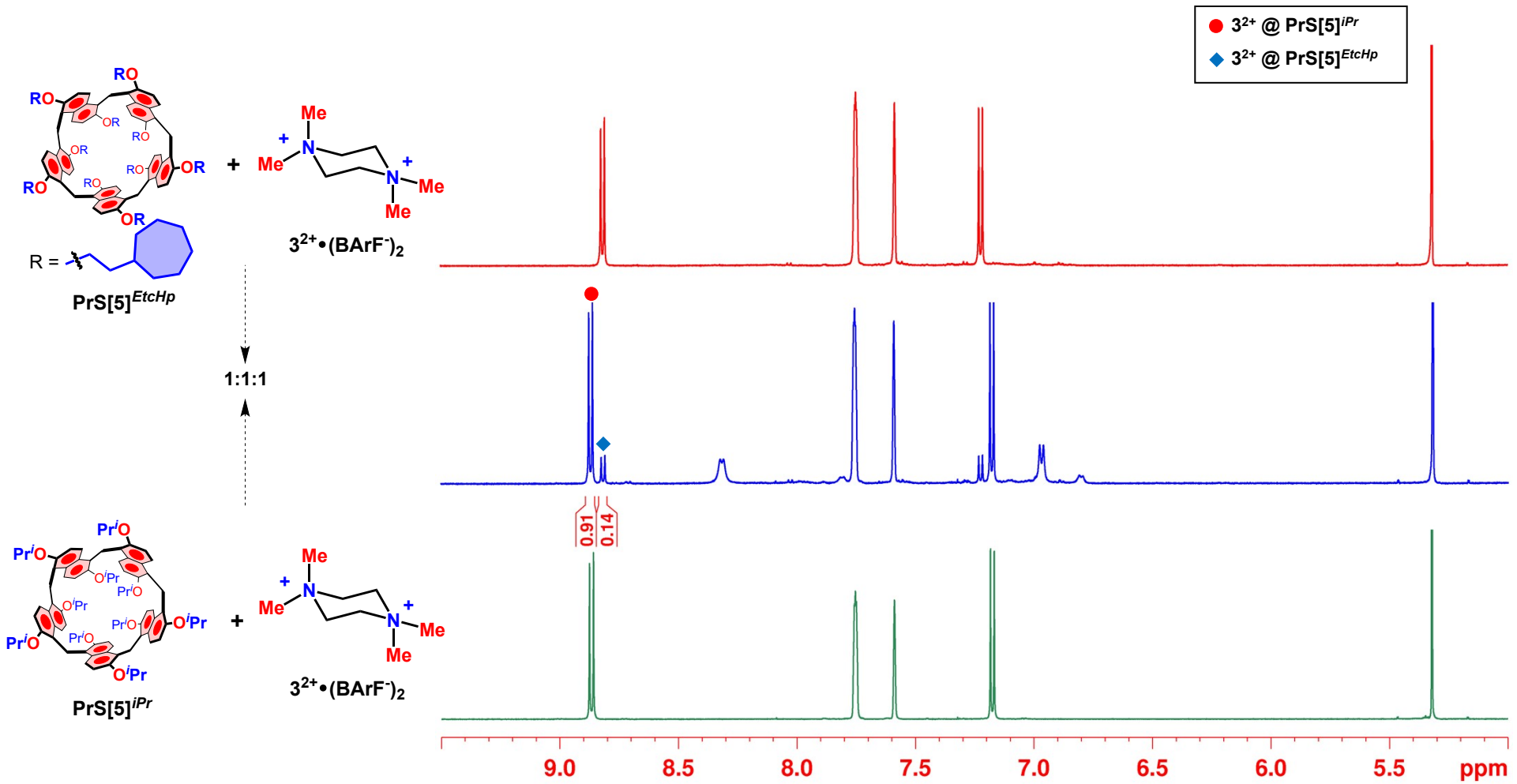

Figure S127: Significant portion of ^{1}H NMR spectra (600 MHz, CD_2Cl_2, 298 K) of: (green) an equimolar solution (1.6 mM) of **PrS[5]^{iPr}** and **3(BArF)$_2$** in 0.6 mL of CD_2Cl_2, (blue) **PrS[5]^{EtcHp}** in presence of 1 equivalent of **3(BArF)$_2$** and 1 equivalent of **PrS[5]^{iPr}** and (red) an equimolar solution (1.6 mM) of **PrS[5]^{EtcHp}** and **3(BArF)$_2$** in 0.6 mL of CD_2Cl_2.

$K_{rel} = K_{ass}(\mathbf{3^{2+}@PrS[5]^{EtcHp}})/K_{ass}(\mathbf{3^{2+}@PrS[5]^{iPr}}) = K_{ass}(\mathbf{3^{2+}@PrS[5]^{EtcHp}})/1.2\cdot10^{10} = [(0.14/1.05)x0.0016]^2 / [(0.91/1.05)x0.0016]^2 = 0.024$

K_{ass} $(\mathbf{3^{2+}@PrS[5]^{EtcHp}}) = 0.024 \times 1.2\cdot10^{10} = \mathbf{2.8\cdot10^8\ M^{-1}}$.

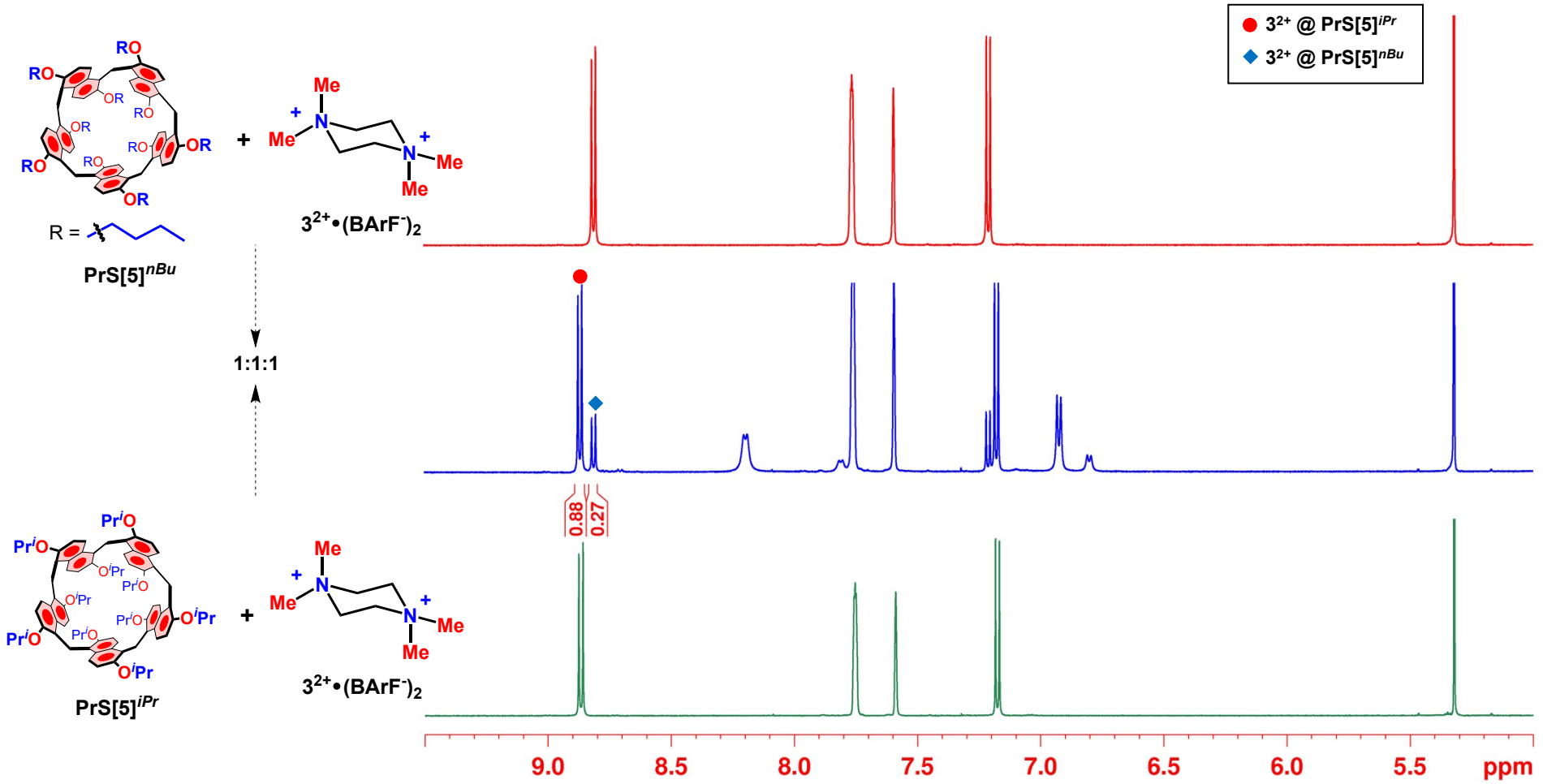

Figure S128: Significant portion of ^{1}H NMR spectra (600 MHz, CD_2Cl_2, 298 K) of: (green) an equimolar solution (1.6 mM) of **PrS[5]^{iPr}** and **3(BArF)$_2$** in 0.6 mL of CD_2Cl_2, (blue) **PrS[5]^{nBu}** in presence of 1 equivalent of **3(BArF)$_2$** and 1 equivalent of **PrS[5]^{iPr}** and (red) an equimolar solution (1.6 mM) of **PrS[5]^{nBu}** and **3(BArF)$_2$** in 0.6 mL of CD_2Cl_2.

$K_{rel} = K_{ass}(\mathbf{3^{2+}@PrS[5]^{nBu}})/K_{ass}(\mathbf{3^{2+}@PrS[5]^{iPr}}) = K_{ass}(\mathbf{3^{2+}@PrS[5]^{nBu}}) / 1.2\cdot10^{10} = [(0.27/1.15)x0.0023]^2 / [(0.88/1.15)x0.0023]^2 = 0.094$

K_{ass} ($\mathbf{3^{2+}@PrS[5]^{nBu}}$) = 0.094 x $1.2\cdot10^{10}$= $\mathbf{1.1\cdot10^9\ M^{-1}}$.

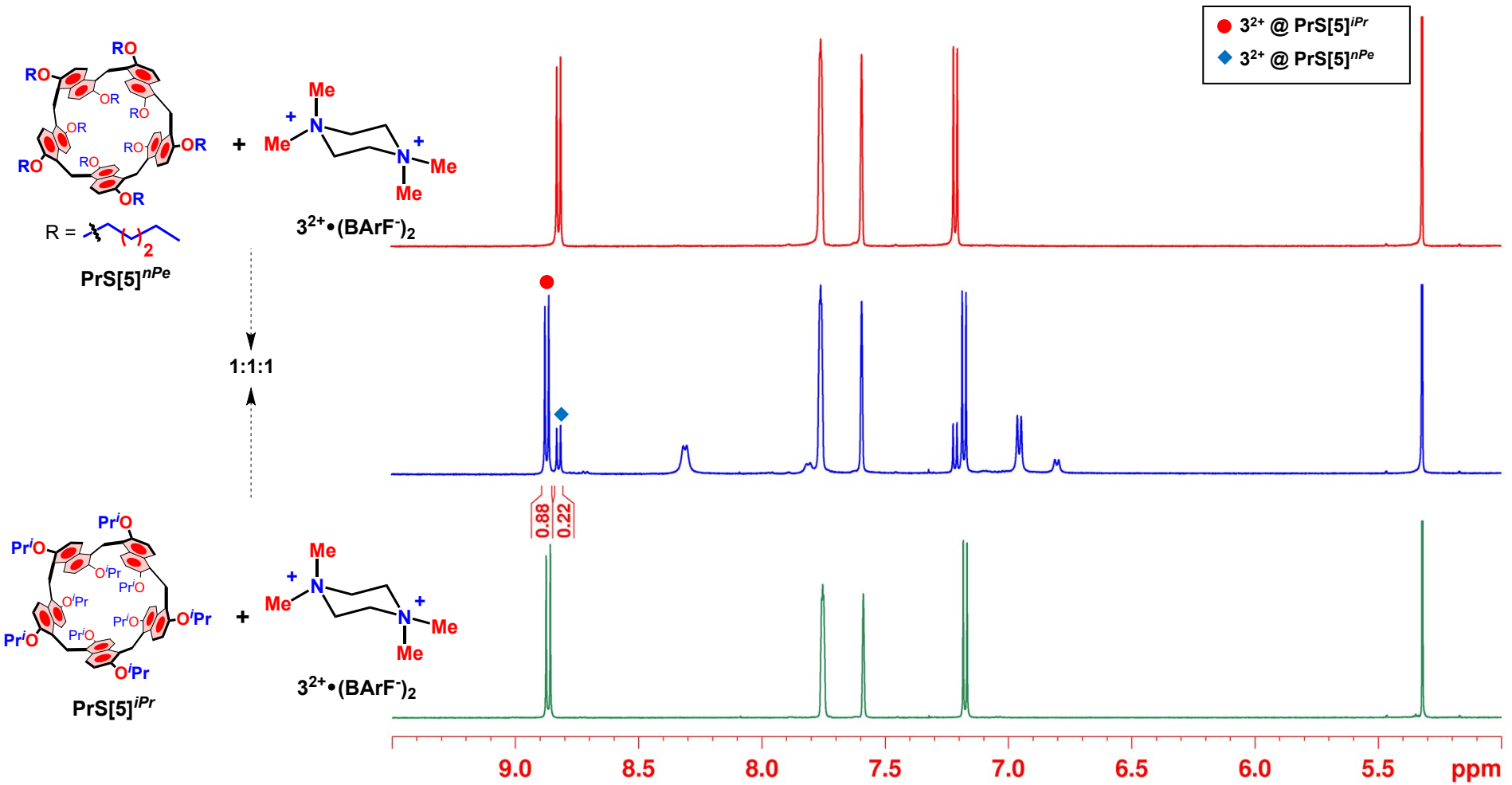

Figure S129: Significant portion of ^{1}H NMR spectra (600 MHz, CD_2Cl_2, 298 K) of: (green) an equimolar solution (1.6 mM) of **PrS[5]^{iPr}** and **3(BArF)$_2$** in 0.6 mL of CD_2Cl_2, (blue) **PrS[5]^{nPe}** in presence of 1 equivalent of **3(BArF)$_2$** and 1 equivalent of **PrS[5]^{iPr}** and (red) an equimolar solution (1.6 mM) of **PrS[5]^{nPe}** and **3(BArF)$_2$** in 0.6 mL of CD_2Cl_2.

$K_{rel} = K_{ass}(\mathbf{3^{2+}@PrS[5]^{nPe}})/ K_{ass}(\mathbf{3^{2+}@PrS[5]^{iPr}}) = K_{ass}(\mathbf{3^{2+}@PrS[5]^{nPe}}) / 1.2\cdot10^{10} = [(0.22/1.10)x0.0021]^2 / [(0.88/1.10)x0.0021]^2 = 0.062$

K_{ass} $(\mathbf{3^{2+}@PrS[5]^{nPe}}) = 0.062 \times 1.2\cdot10^{10} = \mathbf{7.4\cdot10^8\ M^{-1}}$.

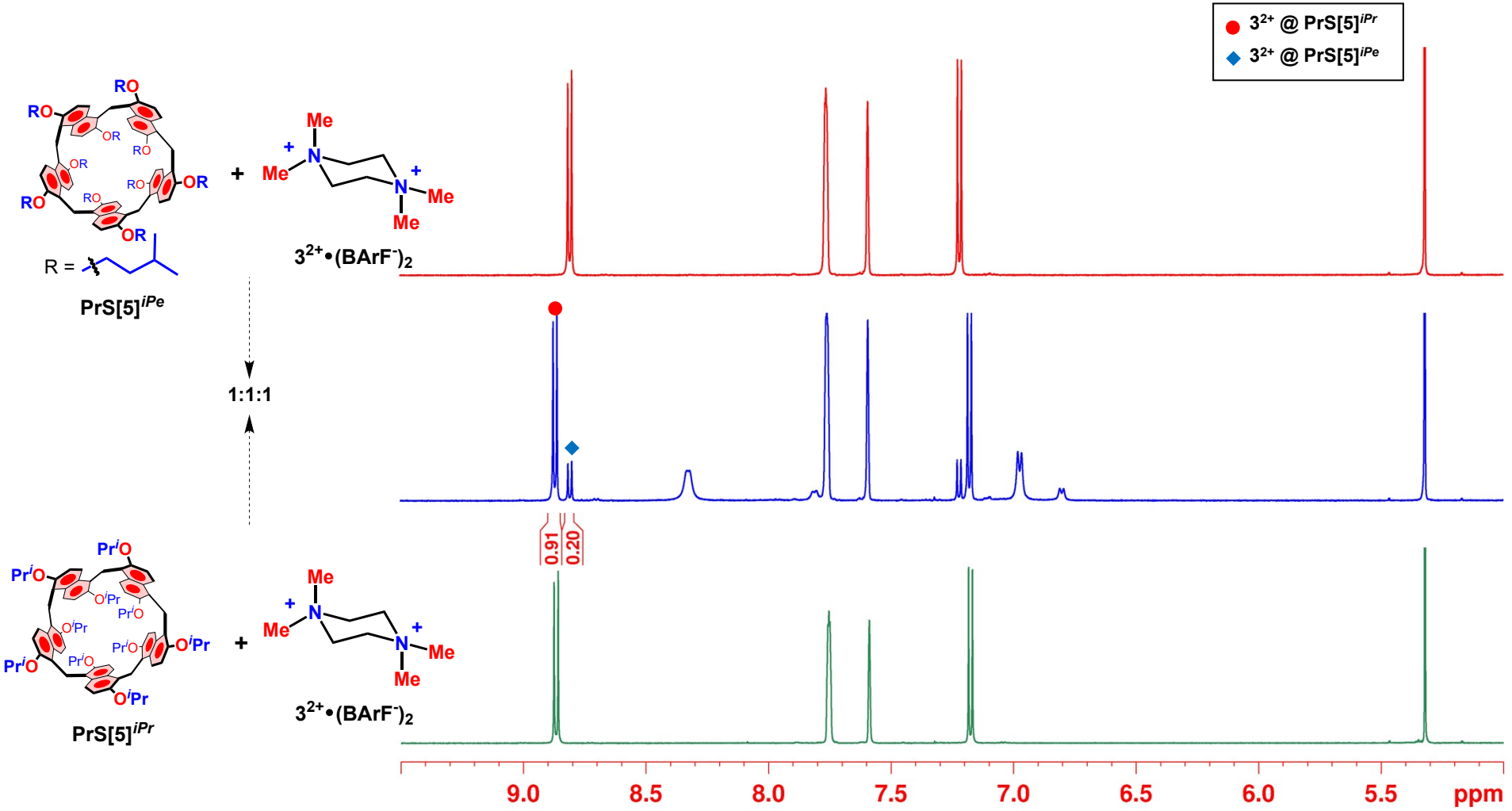

Figure S130: Significant portion of ^{1}H NMR spectra (600 MHz, CD_2Cl_2, 298 K) of: (green) an equimolar solution (1.6 mM) of **PrS[5]^{iPr}** and **3(BArF)$_2$** in 0.6 mL of CD_2Cl_2, (blue) **PrS[5]^{iPe}** in presence of 1 equivalent of **3(BArF)$_2$** and 1 equivalent of **PrS[5]^{iPr}** and (red) an equimolar solution (1.6 mM) of **PrS[5]^{iPe}** and **3(BArF)$_2$** in 0.6 mL of CD_2Cl_2.

$$K_{rel} = K_{ass}(\mathbf{3^{2+}@PrS[5]^{iPe}})/\ K_{ass}(\mathbf{3^{2+}@PrS[5]^{iPr}}) = K_{ass}(\mathbf{3^{2+}@PrS[5]^{iPe}}) / 1.2\cdot10^{10} = [(0.20/1.11)x0.0021]^2 / [(0.91/1.11)x0.0021]^2 = 0.048$$

$$K_{ass}\ (\mathbf{3^{2+}@PrS[5]^{iPe}}) = 0.048 \times 1.2\cdot10^{10} = \mathbf{5.8\cdot10^8\ M^{-1}}.$$

Conformational Studies by DFT Calculations

Lowest energy structures for the 4 conformations of **PrS[5]**^{nPr}, **PrS[5]**^{EtCy} and **PrS[5]**^{iPr} as obtained by molecular dynamics calculation performed by YASARA software. Successively, the structures were optimized by DFT calculations (Gaussian 16) at B97D3/SVP/SVPFIT level of theory[4].
All optimized structures were characterized by 0 imaginary frequency.

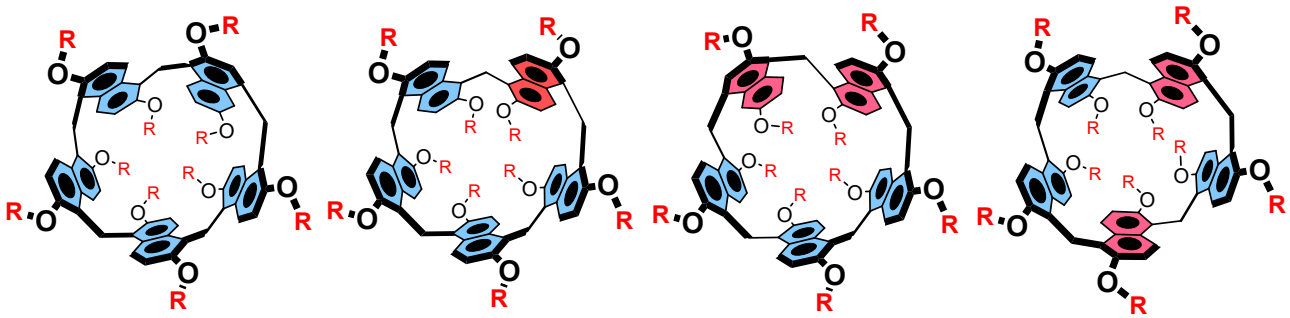

(I) (II) (III) (IV)

Figure S131: Chemical drawing for the four conformers.

Table S4. Single point energies for the four conformations of **PrS[5]**^{nPr}.

	B97D3/SVP/SVPFIT Single point energy (Hartree)	ΔE in kcal/mol
I	-4046.234598	0
II	-4046.215840	11.77
III	-4046.211091	14.75
IV	-4046.221658	8.12

Table S5. Single point energies for the four conformations of **PrS[5]**^{EtCy}.

	B97D3/SVP/SVPFIT Single point energy (Hartree)	ΔE in kcal/mol
I	-5997.333630	0
II	-5997.297547	22.64
III	-5997.297184	22.87
IV	-5997.326574	4.43

Table S6. Single point energies for the four conformations of **PrS[5]**^{iPr}.

	B97D3/SVP/SVPFIT Single point energy (Hartree)	ΔE in kcal/mol
I	-4046.267936	0
II	-4046.251927	10.04
III	-4046.249659	11.47
IV	-4046.257446	6.52

Atomic coordinates of Conformer (I) of PrS[5]^{nPr}

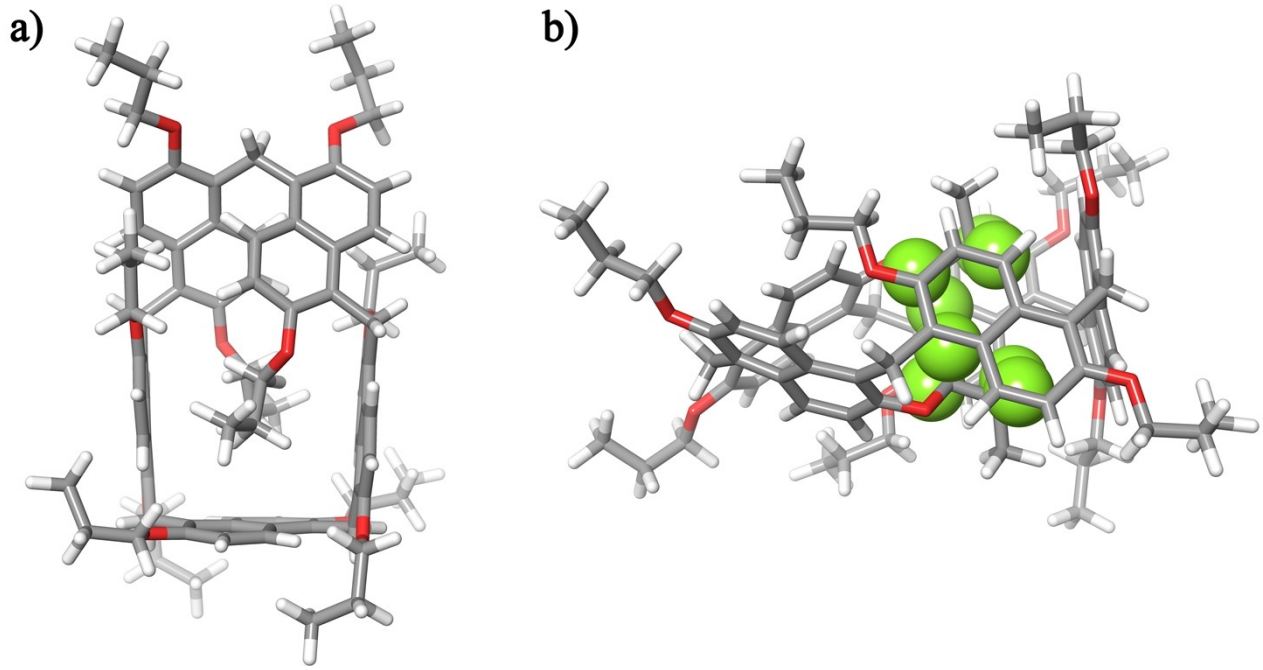

Figure S132. DFT-optimized structures of the Conformer (I) of **PrS[5]^{nPr}** a) top view and b) side view. In green the hydrogen atom filling the cavity.

Energy = -4046.234598.
0 imaginary frequency

C	-4.05515200	-0.18062000	1.50819400
C	-2.43087900	2.10928700	2.00701800
C	-1.95650500	0.81841600	2.23826400
C	-2.79267200	-0.31336400	2.04261800
H	-4.67592300	-1.06546800	1.36269700
H	-2.40822000	-1.29438100	2.33200300
C	-4.55536800	1.09996400	1.12767100
C	-3.76367600	2.26396300	1.47650700
C	-4.34325600	3.53836000	1.23319600
C	-5.56949000	3.67430700	0.60727700
C	-6.26857500	2.53007400	0.14258100
C	-5.77199300	1.23897600	0.38159400
H	-3.81032600	4.44516600	1.52607400
H	-5.97170800	4.67604100	0.44000900
C	-6.53771300	0.06184000	-0.20800000
H	-7.24149600	-0.32587400	0.54905200
H	-7.18758400	0.46481800	-1.00447900
C	-1.53895800	3.30193100	2.33372800
H	-1.34887800	3.30349500	3.41732100
H	-2.07965400	4.23510000	2.12056900
O	-7.43372200	2.62316300	-0.57125500
O	-0.67956100	0.61886300	2.71012700
C	-7.92943100	3.89426300	-0.97273400
H	-8.15716400	4.51452300	-0.07949000
H	-7.16119400	4.43159000	-1.56763700

C	0.20217400	-0.01084800	1.75874000
H	-0.28280600	-0.92177500	1.35311900
H	0.36103500	0.68660800	0.91556000
C	2.16484500	3.45049200	0.04424800
C	-0.22227300	3.35086200	1.57734700
C	-0.25996100	3.59598800	0.19746000
C	0.93792600	3.64484900	-0.56333200
H	3.06464200	3.51527500	-0.56337600
H	0.90673500	3.84300500	-1.63703600
C	1.05125500	3.18704800	2.21913700
C	2.27430100	3.21027200	1.44188000
C	3.55375300	3.01205100	2.06373400
C	3.60533900	2.86305600	3.45524400
C	2.41226200	2.85296600	4.22860100
C	1.17738300	2.99257900	3.62393800
H	2.45684100	2.71314800	5.31138100
O	-1.49173600	3.80315100	-0.35688000
O	4.84530600	2.70454900	4.02389300
C	4.83771100	2.98602400	1.24179200
H	5.68858100	2.92363000	1.93792800
H	4.94331600	3.94408500	0.70925000
C	5.05907200	-0.20022500	-1.73989500
C	5.12478100	1.12747700	-2.11763500
C	5.04558100	2.16237600	-1.14793600
C	4.94315200	1.86303100	0.21658900
H	5.11438200	-0.96761100	-2.51020500
H	5.23287400	1.37407500	-3.17711900
C	4.95417000	-0.57446000	-0.37028100
C	4.95180600	0.48421700	0.61646500
C	4.98635800	0.10752700	1.98771800
C	4.99369800	-1.22155800	2.36820100
C	4.92196900	-2.25505900	1.39614200
C	4.88722700	-1.95155000	0.02778300
H	5.02848400	0.87342100	2.76073600
H	5.04332600	-1.46525400	3.43201900
O	5.05748100	3.48838800	-1.50453700
O	4.86837200	-3.58158300	1.74517600
H	4.84943100	-4.03213000	-0.46825200
H	5.70668200	-3.03548400	-1.64102200
C	4.80915600	-3.07075300	-1.00385300
C	1.32696100	-2.99465500	-3.63846900
C	3.58492200	-3.05959900	-1.91232800
C	3.73903600	-2.92688400	-3.29805500
C	2.60496100	-2.89310200	-4.15465200
H	0.48350900	-2.92206100	-4.32734400
H	2.73052900	-2.76725200	-5.23278700
C	2.26002100	-3.21453700	-1.38074700
C	1.09612800	-3.16964400	-2.24441400
C	-0.22353500	-3.29802900	-1.69462400
C	-0.36374700	-3.53078200	-0.31921900
C	0.77447900	-3.60450200	0.52492200
C	2.04591000	-3.43741900	0.00771200
H	0.66136200	-3.79996800	1.59327900
H	2.89534200	-3.51066600	0.68376700
O	5.02003700	-2.80829400	-3.77834500
O	-1.63652700	-3.69604000	0.14765900
C	-1.48177600	-3.22897800	-2.54421600

H	-2.04434700	-4.16060100	-2.38615000
H	-1.21274000	-3.21547500	-3.61039900
C	-4.01130600	0.27052200	-1.84851600
C	-2.72853600	0.39178500	-2.33661300
C	-1.89190000	-0.74653100	-2.48601400
C	-2.38431100	-2.03265300	-2.26650800
H	-4.62959200	1.16185900	-1.73104200
H	-2.32989700	1.36895300	-2.62107900
C	-3.73705400	-2.17651000	-1.78762600
C	-4.53177000	-1.00450700	-1.47584900
C	-5.76756200	-1.12978400	-0.75846200
C	-6.27175900	-2.41535400	-0.51024000
C	-5.57341400	-3.56778600	-0.95664600
C	-4.33214800	-3.44637600	-1.55383400
H	-5.99017800	-4.56472300	-0.79178200
H	-3.79417500	-4.35944900	-1.81717100
O	-0.59078900	-0.56136400	-2.89619600
O	-7.44602300	-2.50139300	0.19197300
C	4.72176700	3.86081100	-2.83836200
H	3.83355200	3.28979000	-3.17716300
H	5.55754400	3.61822700	-3.52867100
C	4.96231200	2.42397500	5.41464300
H	4.54374100	3.26380200	6.00668500
H	4.38028900	1.51120600	5.66574000
C	-1.60609400	4.00533800	-1.76235600
H	-1.00373400	4.88545600	-2.07297100
H	-1.20242700	3.12307100	-2.29787000
C	4.77243600	-3.95436400	3.11672700
H	5.69299200	-3.64843100	3.65567000
H	3.91404200	-3.43320100	3.58994100
C	5.24284500	-2.52602000	-5.15583200
H	4.70020600	-1.59982800	-5.44327700
H	4.84979500	-3.35439600	-5.78065200
C	-7.84492200	-3.74540400	0.75209800
H	-7.00210100	-4.19761600	1.31772600
H	-8.12519800	-4.46102600	-0.05028900
C	0.24937500	0.05442100	-1.89922100
H	-0.23616300	0.97956600	-1.52740700
H	0.34212900	-0.63919900	-1.04349100
C	-1.85712000	-3.95749700	1.52788900
H	-1.36207800	-4.90718800	1.82388900
H	-1.40858900	-3.15130600	2.14463100
H	0.28532300	2.93442400	4.25007800
C	-9.19299500	3.67335200	-1.79700000
H	-8.92912300	3.06939700	-2.68627100
H	-9.52062300	4.66169700	-2.17362100
C	1.52897100	-0.36155200	2.40805300
H	2.06088900	0.56495300	2.67640500
H	2.14451100	-0.85333300	1.63317100
C	4.43195100	5.35674300	-2.85994000
H	3.61281700	5.56529500	-2.14620300
H	5.32142900	5.89495800	-2.48182100
C	6.43636700	2.22421100	5.74834500
H	6.98376400	3.14827700	5.48104700
H	6.51000200	2.12425700	6.84866400
C	-3.07535200	4.22151000	-2.10356800
H	-3.18496600	4.11200800	-3.19949600

H	-3.65906000	3.40662600	-1.63954600
C	4.58482800	-5.46485900	3.19812500
H	5.44499100	-5.95277600	2.70104300
H	4.64309400	-5.74284700	4.26840500
C	6.74113100	-2.35734700	-5.38108100
H	6.89649300	-2.25391000	-6.47254000
H	7.24757100	-3.29453600	-5.08068500
C	-9.03352400	-3.49594900	1.67279900
H	-8.72804300	-2.77006600	2.44985400
H	-9.83411600	-3.00744700	1.08597800
C	1.61995400	0.36708900	-2.47368800
H	2.20249600	0.85364800	-1.67033500
H	2.14320700	-0.57519400	-2.70122900
C	-3.35909900	-4.03114100	1.76675100
H	-3.82036700	-3.12897800	1.33177500
H	-3.76962900	-4.88282000	1.19476400
C	-10.32416600	2.99847800	-1.01608400
H	-11.21753300	2.85620600	-1.64973100
H	-10.00674100	2.01000200	-0.64258700
H	-10.62287200	3.60746700	-0.14217500
C	1.40044500	-1.26179400	3.63652200
H	2.39317500	-1.48176300	4.06842100
H	0.78627300	-0.77812100	4.41556700
H	0.92145400	-2.22672700	3.38411600
C	4.05847700	5.85157100	-4.25975600
H	3.85060200	6.93572100	-4.25636600
H	4.87367700	5.67004200	-4.98493000
H	3.15519000	5.33899300	-4.64058900
C	7.07687100	1.01321500	5.06416200
H	8.12483500	0.88281600	5.38740900
H	6.53090400	0.08251500	5.30850400
H	7.07190500	1.12116600	3.96688300
C	-3.61403000	5.58103600	-1.65289500
H	-4.69217400	5.67617600	-1.87243600
H	-3.47854300	5.71522500	-0.56710900
H	-3.08898300	6.40879600	-2.16563100
C	3.26911300	-5.96379800	2.59389000
H	3.15841800	-7.05446400	2.72786000
H	2.40085500	-5.47508900	3.07475800
H	3.21415900	-5.74712800	1.51427200
C	7.35578300	-1.16399700	-4.64422800
H	8.42743700	-1.05567600	-4.88820100
H	6.85002800	-0.22022300	-4.92241100
H	7.26666300	-1.27656400	-3.55103200
C	-9.55065300	-4.78484100	2.31680800
H	-10.40952400	-4.58156100	2.97984000
H	-9.88292200	-5.51353600	1.55392600
H	-8.76783500	-5.27478400	2.92571600
C	1.58269700	1.25403700	-3.71820400
H	2.60112200	1.42827800	-4.10926600
H	0.98550000	0.78297700	-4.51781200
H	1.13071300	2.24049600	-3.50050300
C	-3.71208400	-4.15437200	3.25007000
H	-4.80535900	-4.22592400	3.38969900
H	-3.25732500	-5.05327000	3.70728400
H	-3.36306400	-3.27450000	3.82167700

Atomic coordinates of Conformer (I) of PrS[5]^{EtCy}

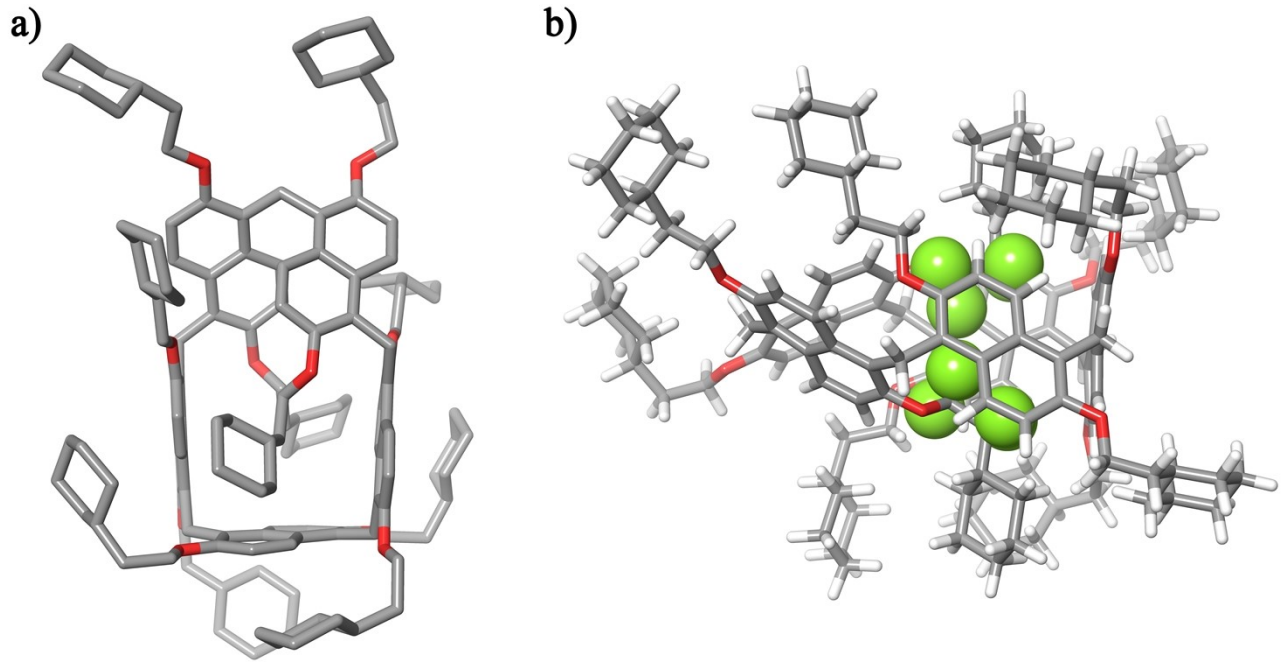

Figure S133. DFT-optimized structures of the Conformer (I) of **PrS[5]**^{EtCy} a) top view and b) side view. In green the hydrogen atom filling the cavity.

Energy = -5997.333630.
0 imaginary frequency

C	-3.99117100	-0.05797000	1.06869800
C	-2.15538800	0.82837200	3.05549700
C	-1.92860900	-0.33997900	2.32888400
C	-2.87274900	-0.80174300	1.37419100
H	-4.69943900	-0.43409600	0.32959200
H	-2.70262500	-1.76500300	0.89050400
C	-4.22998000	1.20038900	1.69810100
C	-3.34089700	1.59759200	2.77262900
C	-3.67098700	2.78013200	3.48949900
C	-4.76301300	3.55816600	3.14770100
C	-5.55716300	3.22182400	2.02077300
C	-5.28272400	2.07181200	1.26489600
H	-3.04344900	3.10752000	4.32127400
H	-4.97566700	4.46293700	3.72327200
C	-6.10437900	1.85569300	0.00076500
H	-7.01660400	1.28987600	0.25486300
H	-6.47390900	2.84833700	-0.30997500
C	-1.13426800	1.24696600	4.10536200
H	-1.10242600	0.47767400	4.89081700
H	-1.46309500	2.17419700	4.59665500
O	-6.59230800	4.01201700	1.59096600
O	-0.81021700	-1.09370900	2.59245900
C	-7.13636400	5.00056400	2.45865000
H	-7.27339500	4.56874100	3.46984300
H	-6.43131000	5.85326300	2.55839900
C	0.08500600	-1.29679700	1.48456300
H	-0.47867200	-1.68056600	0.61348200
H	0.51447300	-0.32010300	1.18950200
C	2.78209000	1.98718000	2.35583200

C	0.25725900	1.48256900	3.54374500
C	0.43495600	2.55372800	2.65781600
C	1.70028900	2.79803400	2.06485500
H	3.73595000	2.20739200	1.88439500
H	1.83409700	3.62703900	1.36874400
C	1.39004600	0.67405900	3.89143300
C	2.68210800	0.90930200	3.27718000
C	3.82529000	0.10074900	3.60749700
C	3.67287900	-0.90716000	4.57020600
C	2.41180400	-1.13011200	5.19060300
C	1.30759500	-0.37518500	4.84892900
H	2.29420500	-1.92422000	5.93078400
O	-0.65825500	3.33242200	2.40617300
O	4.76651700	-1.68875000	4.86565000
C	5.19327300	0.37389500	2.98661000
H	5.91388200	-0.32762800	3.43679700
H	5.51569700	1.38411500	3.28692600
C	5.43325200	0.16419900	-1.37718800
C	5.77966900	1.31918300	-0.70069300
C	5.70634100	1.39489600	0.71613300
C	5.29628300	0.28567300	1.46852000
H	5.48922500	0.15742200	-2.46634400
H	6.09419200	2.18926100	-1.27588100
C	5.04470000	-1.00812300	-0.67071200
C	5.02112900	-0.93945600	0.77514300
C	4.77298700	-2.14350000	1.48616300
C	4.57372400	-3.33932900	0.82448500
C	4.53665200	-3.39168000	-0.59306400
C	4.73004400	-2.23056900	-1.35320000
H	4.76991700	-2.13980200	2.57437100
H	4.42498900	-4.24440400	1.41183600
O	5.99467500	2.55374700	1.39437400
O	4.26879500	-4.55755200	-1.26912300
H	4.42973400	-3.32794500	-3.16089400
H	5.57285300	-1.99796500	-3.32180900
C	4.61051100	-2.28161600	-2.86822000
C	1.53569500	0.21401700	-4.71237900
C	3.52306500	-1.40730400	-3.48410000
C	3.86624600	-0.44076900	-4.43821000
C	2.86638200	0.36144500	-5.05320300
H	0.80427400	0.87292400	-5.18410300
H	3.14184500	1.11983300	-5.78961100
C	2.13627500	-1.57791600	-3.14647900
C	1.11111500	-0.75463700	-3.75947000
C	-0.26978700	-0.92954800	-3.41140100
C	-0.61921200	-1.94573200	-2.51284700
C	0.37933400	-2.74542700	-1.90160000
C	1.71469400	-2.56212400	-2.20942100
H	0.10306000	-3.51944700	-1.18475200
H	2.44698600	-3.20843900	-1.73292500
O	5.20009100	-0.28918700	-4.72641200
O	-1.95189400	-2.12412900	-2.27429400
C	-1.38783100	-0.07587900	-3.98365100
H	-2.10680900	-0.74538200	-4.47816000
H	-0.99668100	0.58747700	-4.76912900
C	-3.33511600	2.45271600	-1.00005500
C	-1.98941900	2.56265500	-1.27219100
C	-1.36323600	1.69983200	-2.20918100
C	-2.10529800	0.77510300	-2.94390400
H	-3.79172400	3.12816500	-0.27515800
H	-1.38685300	3.32611200	-0.77770800

C	-3.51631000	0.65642500	-2.67700300
C	-4.13056300	1.45219200	-1.63333500
C	-5.47252800	1.18592300	-1.20669300
C	-6.23398000	0.24511200	-1.91578400
C	-5.67673800	-0.45077600	-3.02091000
C	-4.35161900	-0.26131400	-3.37175200
H	-6.27882800	-1.17017700	-3.58194200
H	-3.94324100	-0.85955400	-4.18927000
O	-0.01696300	1.82758900	-2.44930800
O	-7.51318700	0.02531400	-1.47685900
C	6.60438300	3.64032800	0.69538900
H	5.93658100	3.99822900	-0.11355900
H	7.53554800	3.28115100	0.21432400
C	4.72240100	-2.52563200	6.02365700
H	4.51213900	-1.89430300	6.91064800
H	3.89340100	-3.25439300	5.93648400
C	-0.49820700	4.54406700	1.67359100
H	0.26262600	5.17865000	2.16844800
H	-0.12417800	4.32294500	0.65600000
C	4.05550300	-5.75647800	-0.52629300
H	4.94579800	-5.96733100	0.10008300
H	3.19686300	-5.62456200	0.16196500
C	5.61387100	0.63866600	-5.72464400
H	5.28469300	1.66133200	-5.45252700
H	5.13924000	0.38456000	-6.69446000
C	-8.26090700	-1.07520500	-1.98446800
H	-8.49076800	-0.91501700	-3.05711700
H	-7.66132600	-2.00328200	-1.90671700
C	0.85034200	1.60829000	-1.32247600
H	0.51436900	2.21978300	-0.46406900
H	0.77501300	0.54700000	-1.01639600
C	-2.38286100	-3.25039000	-1.51784300
H	-2.00450900	-4.18562200	-1.97937700
H	-1.96176600	-3.19996900	-0.49684000
H	0.35366600	-0.60743500	5.32614500
C	-8.46909000	5.49877200	1.90522100
H	-8.28675200	6.04801000	0.96190400
H	-8.83263000	6.24936200	2.63405000
C	1.19513300	-2.25723700	1.88848400
H	1.89642700	-1.73843100	2.55904300
H	1.77199600	-2.49853300	0.97638500
C	6.92394100	4.76695700	1.67708200
H	7.34744700	4.30515700	2.58875600
H	7.73634700	5.36875600	1.22590200
C	6.05146500	-3.25696300	6.20269900
H	6.86816400	-2.53269600	6.02233200
H	6.11597600	-3.53947700	7.27128300
C	-1.85058000	5.24267600	1.61189600
H	-2.59638000	4.51565600	1.24607400
H	-2.15552100	5.49544100	2.64415200
C	3.81876900	-6.93214100	-1.46615400
H	4.70460500	-7.04699600	-2.11963600
H	3.79693500	-7.82720600	-0.81369200
C	7.12958200	0.57158400	-5.85274800
H	7.41875300	1.26263500	-6.66965000
H	7.40817800	-0.44514300	-6.18942800
C	-9.53876500	-1.17357000	-1.15757000
H	-9.24676600	-1.21448600	-0.09152600
H	-10.10776100	-0.23469000	-1.28793400
C	2.28361100	1.94232900	-1.71166200
H	2.90219700	1.88187700	-0.79707600

H	2.66339400	1.15847600	-2.38508900
C	-3.90350800	-3.25074600	-1.48170300
H	-4.25438700	-2.29089000	-1.06258700
H	-4.27144100	-3.27597200	-2.52351800
H	-10.53781000	4.98926400	1.67372800
H	0.08661300	-3.24673700	3.43281300
H	6.18247800	6.41574100	2.81670100
H	7.28296000	-4.90765500	5.63885900
H	-2.89277900	6.95507900	0.88163800
H	2.42195900	-7.97351700	-2.69126500
H	7.66132300	0.18902400	-3.79973400
H	-11.33418800	-2.27103000	-0.82182800
H	1.71308400	3.36313800	-3.20806900
H	-4.04977600	-5.36576800	-1.07887900
C	-10.79201600	2.37800800	2.54588000
C	-9.65482900	3.38173500	2.78683300
C	-9.57313300	4.43881400	1.66872400
C	-9.46264200	3.75644900	0.29046400
C	-10.58802100	2.74132500	0.05024300
C	-10.64909300	1.69985500	1.17608100
H	-11.76576500	2.90713700	2.59144400
H	-10.80770600	1.62145500	3.35314900
H	-8.69947300	2.82407300	2.82732200
H	-9.77829100	3.87534100	3.77069200
H	-9.46548300	4.52683800	-0.50435200
H	-8.49101700	3.24255100	0.22604200
H	-11.56131300	3.27088900	-0.00696900
H	-10.44117900	2.24376900	-0.92695500
H	-9.71670600	1.10125300	1.16305200
H	-11.48045800	0.98972200	1.00474900
C	1.42748900	-5.64761000	3.82767500
C	1.89314400	-4.36808200	3.12174500
C	0.71488400	-3.54684300	2.57122600
C	-0.14940600	-4.42332800	1.65013900
C	-0.61785700	-5.71564500	2.33146300
C	0.56729800	-6.51351300	2.89487600
H	0.83273500	-5.37428500	4.72278900
H	2.29714200	-6.22571900	4.19353800
H	2.55513600	-4.64311600	2.27929200
H	2.50166200	-3.74097000	3.79865000
H	-1.02358600	-3.84861700	1.29913300
H	0.44215100	-4.68245700	0.74934800
H	-1.31007700	-5.45738200	3.15785300
H	-1.19812400	-6.33455500	1.62038600
H	1.19637100	-6.86825400	2.05248300
H	0.21037100	-7.41823800	3.42242000
C	3.45947800	5.97579500	3.10482900
C	4.56741600	5.00151100	2.68806700
C	5.77069100	5.71905000	2.05614000
C	5.30054200	6.57992500	0.86773400
C	4.18895200	7.56203100	1.26495900
C	3.00389700	6.83826400	1.91988500
H	3.83161800	6.63583300	3.91458300
H	2.60487000	5.41235100	3.52345800
H	4.15666500	4.29381600	1.94930500
H	4.89102900	4.38512700	3.54640500
H	6.15827000	7.12611700	0.42972700
H	4.91441600	5.91529200	0.07110700
H	4.59937600	8.30499500	1.97837100
H	3.85092300	8.13139200	0.37843300
H	2.51889400	6.18770800	1.16543100

H	2.23818700	7.56810700	2.24162700
C	6.60680200	-5.52005900	3.03353000
C	6.30177900	-4.25465900	3.84344500
C	6.27908000	-4.52652100	5.35528900
C	5.26921500	-5.64855200	5.67013600
C	5.54021100	-6.92081000	4.85170700
C	5.59020100	-6.62689400	3.34457200
H	7.62604400	-5.88061900	3.28003000
H	6.61132500	-5.28484100	1.95327500
H	5.31098300	-3.87148000	3.54780800
H	7.02287900	-3.45172000	3.60549700
H	5.28302500	-5.87908000	6.75305000
H	4.24549800	-5.29455800	5.43852900
H	6.51067800	-7.35502400	5.16622400
H	4.76959000	-7.68383600	5.07150600
H	4.58554400	-6.30217400	3.00518300
H	5.82869800	-7.54826500	2.78010500
C	-1.84982100	7.50491100	-1.61084500
C	-1.74315900	6.22426600	-0.77025700
C	-1.88503600	6.51178000	0.73775700
C	-0.85784400	7.57482900	1.17289600
C	-0.97205000	8.86042200	0.34199400
C	-0.83463300	8.56403900	-1.15842500
H	-2.87419300	7.91825400	-1.51260300
H	-1.70950600	7.26747800	-2.68212400
H	-0.76031300	5.75393200	-0.96778900
H	-2.50742700	5.49297100	-1.08835400
H	-0.97416800	7.79509000	2.25177200
H	0.16270500	7.16677500	1.04609800
H	-1.95739700	9.33247500	0.53212400
H	-0.20623100	9.59173700	0.66331900
H	0.18981000	8.19173100	-1.36094100
H	-0.95407100	9.49202400	-1.74886000
C	1.38499700	-6.20508900	-4.47413200
C	2.63162100	-6.04525300	-3.59110500
C	2.54061000	-6.92878800	-2.33251700
C	1.26660700	-6.58270300	-1.54075600
C	0.00375100	-6.72461800	-2.40387600
C	0.09929600	-5.89441800	-3.69312400
H	1.34054100	-7.24547100	-4.85739400
H	1.45909000	-5.54607100	-5.35939500
H	2.73553300	-4.98924200	-3.28893500
H	3.54399600	-6.30131400	-4.16254400
H	1.18800100	-7.21728000	-0.63655700
H	1.33963100	-5.53822600	-1.18471500
H	-0.13670100	-7.79339400	-2.66423500
H	-0.88856800	-6.42734600	-1.81919100
H	0.09433300	-4.81996000	-3.43358300
H	-0.79042100	-6.07090800	-4.32708800
C	8.49357000	2.68187500	-2.82746500
C	7.62142200	2.32484300	-4.04045600
C	7.93384300	0.91924400	-4.58759400
C	9.44295500	0.77093800	-4.86279100
C	10.30462400	1.12798800	-3.64442500
C	9.98931600	2.54172300	-3.13674900
H	8.23976700	2.00009800	-1.99347800
H	8.25834400	3.70621900	-2.48047800
H	7.78822900	3.07045000	-4.84582400
H	6.55494200	2.39890900	-3.76313200
H	9.65977100	-0.26097800	-5.19912500
H	9.71570700	1.43747900	-5.70749100

H	10.10666500	0.39949600	-2.83257200
H	11.37800500	1.03530700	-3.89577000
H	10.27684100	3.28145700	-3.91157600
H	10.59233800	2.77475600	-2.23889000
C	-10.76664900	-4.89977300	-1.37959500
C	-9.79968500	-3.73189600	-1.13963200
C	-10.44588900	-2.37482400	-1.47958600
C	-10.96696200	-2.38328800	-2.92994000
C	-11.93994000	-3.54597600	-3.17575200
C	-11.30015300	-4.89632300	-2.81971900
H	-11.61881200	-4.81661200	-0.67507400
H	-10.26763800	-5.86137100	-1.15508900
H	-8.90033300	-3.87964300	-1.76818700
H	-9.44713200	-3.72856600	-0.09069000
H	-11.45087400	-1.41526600	-3.16233800
H	-10.11170000	-2.48179700	-3.62818500
H	-12.84586400	-3.39766800	-2.55379900
H	-12.27938500	-3.54554800	-4.22865200
H	-10.46005600	-5.09349900	-3.51671100
H	-12.02668100	-5.71785500	-2.96466800
C	3.99974300	4.79078800	-3.77016900
C	3.84801600	3.45760300	-3.02795500
C	2.45763000	3.30976700	-2.38988300
C	2.19398100	4.49494700	-1.44604200
C	2.35057900	5.84884000	-2.15245100
C	3.71891700	5.97945800	-2.83872100
H	3.28684500	4.81511800	-4.61924300
H	5.01335600	4.87581000	-4.20725700
H	4.61442200	3.39336700	-2.23224300
H	4.03366400	2.60609700	-3.70634400
H	1.18193800	4.41791200	-1.01096000
H	2.90670000	4.43618200	-0.59805400
H	1.54922800	5.95082900	-2.91132600
H	2.20367800	6.67528300	-1.43140800
H	4.50873000	6.01907000	-2.06249200
H	3.78136900	6.93404800	-3.39463200
C	-6.65137900	-5.70016000	-0.16436200
C	-6.02282200	-4.52368800	-0.92253300
C	-4.50258500	-4.42615200	-0.69336500
C	-4.20888500	-4.35454100	0.81870500
C	-4.83598700	-5.52406900	1.59022400
C	-6.34708100	-5.62089900	1.33803100
H	-6.24483900	-6.64929000	-0.56881800
H	-7.74258200	-5.72821600	-0.33726400
H	-6.23535100	-4.60291800	-2.00591600
H	-6.48823100	-3.57692100	-0.58099600
H	-3.12126400	-4.33285000	1.00428900
H	-4.60921400	-3.39811100	1.20989700
H	-4.35229200	-6.46949600	1.27045300
H	-4.62800500	-5.41791800	2.67141600
H	-6.84347500	-4.72334200	1.76013000
H	-6.77376500	-6.49428200	1.86641900

Atomic coordinates of Conformer (I) of PrS[5]^{iPr}

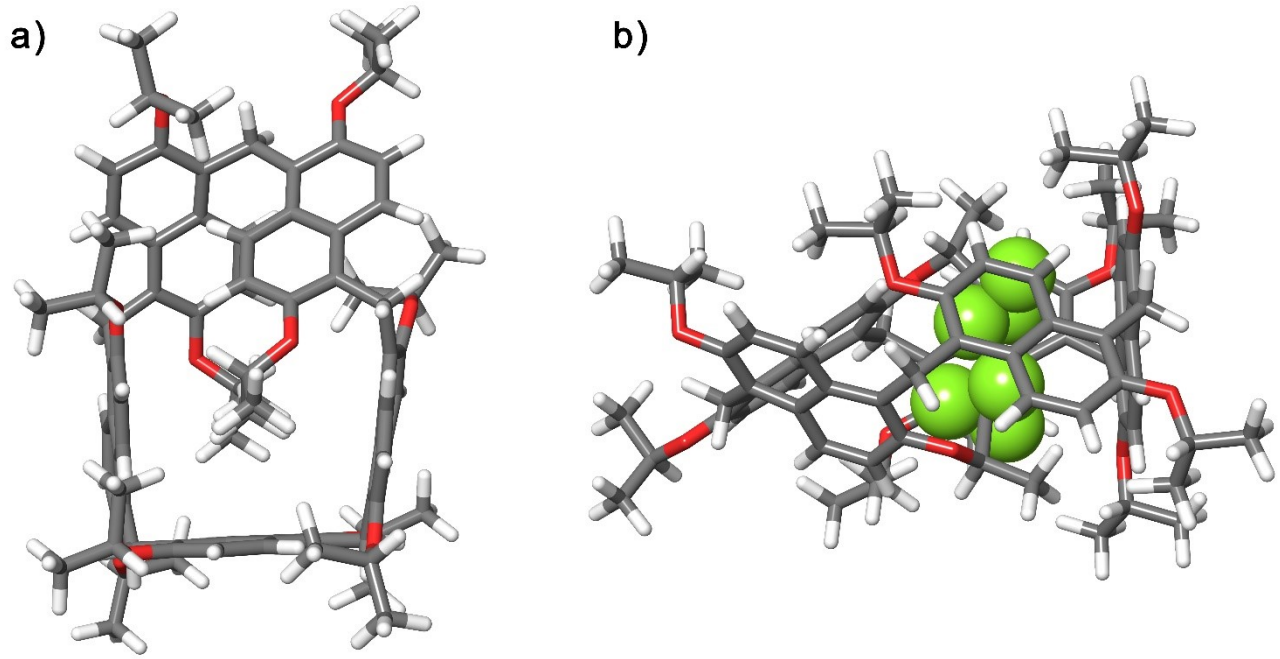

Figure S134. DFT-optimized structures of the Conformer (I) of **PrS[5]^{iPr}** a) top view and b) side view. In green the hydrogen atom filling the cavity.

Energy = -4046.267936.
0 imaginary frequency

C	-3.81901300	-1.25344900	-2.17778800
C	-2.09707300	-3.37929200	-1.39978200
C	-1.67871600	-2.40510300	-2.31769000
C	-2.56719200	-1.38237200	-2.74266800
H	-4.45958400	-0.42055700	-2.47761100
H	-2.24780400	-0.67444000	-3.50884900
C	-4.27567900	-2.17650100	-1.20166800
C	-3.43569900	-3.30747800	-0.88091000
C	-3.98496900	-4.29255700	-0.00355300
C	-5.21692400	-4.11502400	0.59370800
C	-5.94857100	-2.90849200	0.41265700
C	-5.48772800	-1.93216100	-0.46955300
H	-3.42528200	-5.20625000	0.21005700
H	-5.63779200	-4.89244800	1.24138000
C	-6.24787000	-0.64153800	-0.63316200
H	-6.58257900	-0.56589400	-1.68522400
H	-7.18884700	-0.73059500	-0.06615300
C	-1.11668900	-4.45524900	-0.95308800
H	-0.77530000	-5.01349000	-1.83681400
H	-1.63767100	-5.18240900	-0.31376800
O	-7.13970000	-2.73532800	1.07980800
O	-0.40936000	-2.49008700	-2.82336500
C	-7.07422800	-2.60047900	2.51788300
H	-6.36442700	-3.35972200	2.90905400
C	-6.57129600	-1.21051700	2.90710800
C	0.30592800	-1.26161900	-3.11332100
H	-0.30976300	-0.64392600	-3.79743100
C	0.57625900	-0.48674500	-1.82730400

C	2.26694800	-2.96546000	1.36493100
C	0.08337500	-3.93472100	-0.17469800
C	-0.11411100	-3.42042400	1.11518600
C	0.98702500	-2.95084000	1.87963100
H	3.08721900	-2.61250500	1.98539200
H	0.83030900	-2.56404300	2.88935200
C	1.42113900	-3.98900900	-0.70197000
C	2.53303000	-3.45566000	0.05707300
C	3.86123800	-3.43413500	-0.48271500
C	4.09154300	-4.03058600	-1.72930700
C	3.01957700	-4.62495500	-2.44863900
C	1.72710100	-4.58227500	-1.95973400
H	3.20029700	-5.09370900	-3.41936200
O	-1.39626900	-3.38842400	1.60572000
O	5.38100200	-4.00994200	-2.19850700
C	5.02032400	-2.81401700	0.28510600
H	5.92236500	-2.90115600	-0.34099000
H	5.21329400	-3.41889600	1.18541200
C	4.68256700	1.33937300	1.58392500
C	4.87617600	0.32264600	2.50058300
C	4.97067500	-1.03076100	2.07931400
C	4.86821500	-1.36279000	0.72131700
H	4.64208100	2.36573900	1.94292600
H	4.96129400	0.57823600	3.55982100
C	4.56553100	1.07122900	0.19116500
C	4.67916000	-0.30823600	-0.23299400
C	4.63379800	-0.57340800	-1.62984900
C	4.47980700	0.44673300	-2.54978100
C	4.35437700	1.79895500	-2.12770800
C	4.38095200	2.12844300	-0.76390500
H	4.74084600	-1.59521500	-1.99071100
H	4.46276100	0.19334500	-3.61203400
O	5.17875500	-2.06752000	2.95620300
O	4.19184500	2.83520500	-3.01323700
H	4.29149800	4.21513400	-1.22941600
H	5.18889000	3.84622200	0.24243400
C	4.28117000	3.58790900	-0.32472300
C	0.83860100	4.56367500	2.17563700
C	3.07305100	3.96023400	0.52838000
C	3.24982200	4.41938100	1.84051200
C	2.12492000	4.72612700	2.65457300
H	0.00275200	4.77444300	2.84661000
H	2.26372700	5.07664200	3.68017600
C	1.73980700	3.89474400	-0.00211500
C	0.58737100	4.15239400	0.83724200
C	-0.74168900	4.02577800	0.31071100
C	-0.90215500	3.85904600	-1.07306700
C	0.22650000	3.61935700	-1.90260000
C	1.50427000	3.60031100	-1.37325600
H	0.09892700	3.43866500	-2.97309300
H	2.34313500	3.40305900	-2.03948400
O	4.54390300	4.55692900	2.28335000
O	-2.17435900	3.96908700	-1.55594100
C	-1.98668400	4.00201900	1.19149100
H	-2.69878700	4.76199800	0.84064800
H	-1.72681800	4.26026700	2.22820100
C	-3.54327000	-0.05445500	0.92145300
C	-2.35326100	0.21661900	1.56988700
C	-1.89552800	1.55106600	1.72698600
C	-2.62247300	2.61265300	1.16829000
H	-3.83937700	-1.09454900	0.82875200

H	-1.76360500	-0.62372700	1.94071000
C	-3.89732000	2.34233300	0.55951900
C	-4.37492600	0.97518800	0.39074600
C	-5.62055800	0.71599900	-0.28897400
C	-6.40050200	1.81492400	-0.69191900
C	-5.97114200	3.14690800	-0.46300400
C	-4.74613200	3.39592800	0.12443300
H	-6.59402200	3.99102200	-0.76954400
H	-4.43355800	4.43418300	0.25063600
O	-0.78323300	1.87985800	2.44384400
O	-7.57181100	1.51484300	-1.33902700
C	5.00051900	-1.90077300	4.37222300
C	3.51637700	-1.77872400	4.72415700
H	5.53693500	-0.98731600	4.70010000
C	5.68795500	-4.29746800	-3.57310300
H	5.18443000	-5.24080400	-3.86732700
C	5.22777100	-3.16186800	-4.49015600
C	-1.61007900	-3.43444800	3.03344200
C	-1.15887500	-4.78200400	3.59882600
H	-1.03002700	-2.61881100	3.51142000
C	4.10434000	2.61487000	-4.43044000
C	5.50036300	2.45127900	-5.03452300
H	3.50364900	1.70107100	-4.61585600
C	4.84381700	4.87655300	3.65135000
C	4.66755400	3.65351400	4.55571600
H	4.16849900	5.68921300	3.98663200
C	-8.57431400	2.51284600	-1.58163100
H	-8.09517100	3.41509200	-2.01491800
C	-9.29309200	2.88295900	-0.28253900
C	0.20989000	0.89366300	2.79859200
H	-0.30489200	-0.02812800	3.13721100
C	1.09412900	0.58300100	1.59749900
C	-2.49229900	3.56288900	-2.89909600
H	-1.71089900	3.94709400	-3.58539300
C	-2.55459700	2.04077600	-2.97259800
H	0.92928500	-4.99839400	-2.57714200
C	-8.47211800	-2.90262000	3.04287800
H	-9.19703000	-2.17610600	2.63391300
H	-8.49432000	-2.83484500	4.14461400
C	1.57971200	-1.65080600	-3.85012100
H	2.26895800	-2.18336200	-3.17859800
H	2.08555000	-0.74091800	-4.21596200
C	5.66424800	-3.11103300	5.02075100
H	5.16956700	-4.04148300	4.69027700
H	6.72979200	-3.16514600	4.74052100
C	7.19642700	-4.51867700	-3.62091300
H	7.48930700	-5.33756800	-2.94234000
H	7.51386200	-4.77687900	-4.64608200
C	-3.08854400	-3.16231800	3.27689000
H	-3.28504100	-3.12847300	4.36268000
H	-3.39217400	-2.19972900	2.83880100
C	3.35251600	3.81535200	-4.99920700
H	3.90035400	4.74886900	-4.78068400
H	3.24942400	3.71813100	-6.09396400
C	6.27509600	5.40463900	3.65148600
H	6.57819600	5.69042400	4.67379500
H	6.36283400	6.28743200	2.99596100
C	-9.51170200	1.91374900	-2.62574600
H	-8.95494600	1.65355000	-3.54203000
H	-9.98342800	0.99524300	-2.23404300
C	0.97753200	1.47238100	3.98194200

H	1.70499900	0.73295600	4.35632200
H	1.52331400	2.37775500	3.67412900
C	-3.81196900	4.23445700	-3.26277600
H	-4.62498600	3.85842800	-2.62151500
H	-3.73683300	5.32801800	-3.13420200
H	7.72740500	-3.60176000	-3.30922800
H	5.43830800	-3.41241300	-5.54508700
H	4.14615400	-2.97679500	-4.39090300
H	5.76416700	-2.22971200	-4.23904100
H	-3.70946300	-3.95194000	2.82675000
H	-1.31923100	-4.81399200	4.69106100
H	-1.74291000	-5.59697800	3.13522400
H	-0.08963400	-4.96638900	3.40101000
H	-8.79030900	-3.91540300	2.74190400
H	-6.46996700	-1.13113000	4.00449500
H	-5.58674200	-1.00311700	2.45845600
H	-7.27307500	-0.43063300	2.56266200
H	1.34945200	-2.30176800	-4.71110100
H	1.10803100	0.45691600	-2.03883600
H	-0.36642800	-0.23823300	-1.31221200
H	1.20069200	-1.09071700	-1.14869000
H	0.28778200	1.73619200	4.80219500
H	1.87703100	-0.14590300	1.85878600
H	0.49905600	0.15529700	0.77850300
H	1.58269600	1.50042900	1.23427900
H	-10.30669200	2.63373800	-2.88669200
H	-10.06082300	3.65435300	-0.47136000
H	-9.78820700	1.99054800	0.13995400
H	-8.58826500	3.27424600	0.47006500
H	-4.06332900	4.02012400	-4.31639000
H	-2.80289800	1.70811500	-3.99630500
H	-1.59210000	1.58965300	-2.68218100
H	-3.32264500	1.66474900	-2.27785600
H	6.96908600	4.62786100	3.28432000
H	4.80578700	3.93617700	5.61452300
H	3.66436500	3.21042200	4.44511800
H	5.41610700	2.88261900	4.30245500
H	5.43196600	2.26876200	-6.12179500
H	6.09129400	3.36952000	-4.86978900
H	6.04280200	1.60814100	-4.57540300
H	2.34561500	3.89487700	-4.55579900
H	3.38945500	-1.56532000	5.80031400
H	3.04080200	-0.96454800	4.15382500
H	2.98854700	-2.71939400	4.48900900
H	5.58946300	-3.04541600	6.12013200

Determination of crystallographic structures of PrS[5]^{iPr}, PrS[5]^{nBu}, PrS[5]^{iBu}, PrS[5]^{nPe}, PrS[5]^{MeCy}, PrS[5]^{EtCy}, α and β forms of PrS[5]^{PrCy}

Single crystals suitable for X-ray investigations were obtained by slow evaporation of solutions of methanol/dichloromethane containing the molecules: **PrS[5]^{iPr}**, **PrS[5]^{nBu}**, **PrS[5]^{iBu}**, **PrS[5]^{nPe}**, **PrS[5]^{MeCy}**, **PrS[5]^{EtCy}** and **PrS[5]^{PrCy}**.

Data collection was carried out at the Macromolecular crystallography XRD1 beamline of the Elettra synchrotron (Trieste, Italy), employing the rotating-crystal method with a Dectris Pilatus 2M area detector. Single crystals were dipped in paratone cryoprotectant, mounted on a nylon loop and flash-frozen under a nitrogen stream at a 100 K. Diffraction data were indexed and integrated using the XDS package,[5] while scaling was carried out with XSCALE.[6] Structures was solved using the SHELXT program[7] and structure refinement was performed with SHELXL-18/3,[8] by full-matrix least-squares (FMLS) methods on F^2. Non-hydrogen atoms were refined anisotropically, with the exception of some disordered groups. Details of the treatment of disorder in each structure are described below. Hydrogen atoms were added at the calculated positions and refined using the riding model. Crystallographic data and refinement details are reported in **Table S7** and **S8**.

PrS[5]^{iPr}

The asymmetric unit of the triclinic crystals of **PrS[5]^{iPr}** (*P* -1) contains two prismarene molecules, one co-crystallized methanol molecule and one dichloromethane molecule with 0.7 occupancy factor. The asymmetric unit also contained an extended zone of residual electron density due to the presence of highly disordered solvent molecules with partial occupation in multiple, superimposed sites. Dichloromethane (two sites) and methanol (3 sites) molecules could be identified. This density was not modelled but was accounted for using the Platon squeeze tool. The residual electron density of 91 electrons/cell in a total potential solvent area volume of 600 Å^3 (7.8% of the cell volume) can be attributed to ca. 1.5 dichloromethane and 1.5 methanol molecule. All non-hydrogen atoms were refined anisotropically.

PrS[5]^{nBu}

The asymmetric unit of the triclinic crystals of **PrS[5]^{nBu}** (*P* -1) contains one prismarene molecule only. No co-crystallized solvent molecules are present. The structure was refined as a 2-component non merohedral twin. The twin law (-1, 0, 0; 0, -1, 0;-0.717, -0.153, 1), which corresponds to a two-fold axis about the [-1 0 3] direct lattice direction, were detected with PLATON TwinRotMat. The fraction of overlapped reflections was calculated as 26%. The refinement as a 2-component twin with HKLF 5 card significantly reduced the R-factor: The R_1 factor decreased by 0.063, with a refined BASF factor of 0.27.

PrS[5]^{iBu}

The asymmetric unit of the monoclinic crystals of **PrS[5]^{iBu}** (*C 2/c*) contains half molecule of prismarene. This molecule lies on a crystallographic two-fold axis. Two iso-butyl chains show two-position disorder, which was refined at 0.5/0.5 and 0.65/0.35 partial occupancies, respectively. Non-hydrogen atoms were refined anisotropically.

PrS[5]^{nPe}

The asymmetric unit of the triclinic crystals of **PrS[5]^{nPe}** (*P -1*) contains two prismarene molecules and a total of 1.4 dichloromethane solvent molecules distributed over six different sites. The **PrS[5]^{nPe}** molecules exhibit a significant disorder of the aliphatic chains. One molecule shows two position disorder in four alkyl chains, while the other molecules show disorder in three alkyl chains. The electron density of a highly disordered dichloromethane molecule was not modelled but was accounted for using the Platon squeeze tool. The residual electron density of 77 electrons/cell in a total potential solvent area volume of 244 Å^3 (2.6% of the cell volume) can be attributed to ca. 1.8 dichloromethane solvent molecules. All non-hydrogen atoms with occupancy factor greater than 0.5 were refined anisotropically.

PrS[5]^{MeCy}

The asymmetric unit of the triclinic crystals of **PrS[5]^{MeCy}** (*P* -1) contains two prismarene molecules and a total of 2.45 dichloromethane solvent molecules distributed over ten sites. Both prismarene molecules host a disordered dichloromethane molecule in the cavity. One prismarene molecule shows two position disorder in two cyclohexyl chains, while the other molecule shows disorder of only one alkyl chain. All non-hydrogen atoms at full occupancy and the chlorine atoms with high occupancy factor were refined anisotropically.

PrS[5]^{EtCy}

The asymmetric unit of the centrosymmetric monoclinic crystals of **PrS[5]^{EtCy}** contains a half molecule of prismarene and a half molecule of dichloromethane. Both molecules lie on a crystallographic two-fold axis and no disorder was observed for the alkyl chains and for the co-crystallized solvent molecules. All non-hydrogen atoms were refined anisotropically.

***α form of* PrS[5]^{PrCy}**

The asymmetric unit of the monoclinic form of **PrS[5]^{PrCy}** (*C* 2/c) contains half molecule of prismarene. This molecule lies on a crystallographic two-fold axis. Two alkyl chains show a two conformation disorder. One involving only a small rotation of the cyclohexyl moiety and

one involving the intere propyl-cyclohexyl chain. No co-crystallized solvent molecules are present. All non-hydrogen atoms were refined anisotropically.

β form of **PrS[5]^{PrCy}**

The asymmetric unit of the triclinic form of **PrS[5]^{PrCy}** (*P* -1) contains one molecule of prismarene and 0.65 molecules of dichloromethane disordered in three sites. Four alkyl chains show two-conformation disorder, while other three show three-conformation disorder. All non-hydrogen atoms were refined anisotropically with exclusion of carbon atoms with occupancy factor less than 0.5.

Table S7. Crystal data and structure refinement for prismarenes: **PrS[5]^{iPr}**, **PrS[5]^{nBu}**, **PrS[5]^{iBu}** and **PrS[5]^{nPe}**.

	PrS[5]^{iPr}	**PrS[5]^{nBu}**	**PrS[5]^{iBu}**	**PrS[5]^{nPe}**
Empirical formula	C85.85 H102.70 Cl0.70 O10.50	C95 H120 O10	C95 H120 O10	C105.7 H141.40 Cl1.40 O10
Formula weight	1327.39	1421.90	1421.90	1621.61
Temperature (K)	100(2)	100(2)	100(2)	100(2)
Wavelength (Å)	0.7	0.7	0.7	0.7
Crystal system	Triclinic	Triclinic	Monoclinic	Triclinic
Space group	P -1	P -1	C 2/c	P -1
Unit cell Dimensions (Å.°)	a = 14.124(2) b = 21.110(3) c = 28.938(2) α = 69.314(6) β = 89.611(12) γ = 72.960(11)	a = 11.223(5) b = 18.520(5) c = 19.183(7) α = 85.136(13) β = 77.67(2) γ = 86.955(17)	a = 18.947(12) b = 35.283(4) c = 12.8880(19) α = 90 β = 108.26(2) γ = 90	a = 20.631(14) b = 21.503(13) c = 23.529(12) α = 87.260(10) β = 78.17(3) γ = 67.21(6)
Volume (Å^3)	7672.2(17)	3879(2)	8182(5)	9413(11)
Z	4	2	4	4
ρ_{calcd} (g/cm^3)	1.149	1.218	1.154	1.126
μ (mm^{-1})	0.093	0.074	0.070	0.088
F(000)	2855	1540	3080	3467
Reflections collected	176630	10854	65511	167036

Independent reflections	37046	10854	10142	26101
Param./restr.	1798/0	958/0	552/0	2258/ 3179
GOOF	1.035	1.021	1.003	1.046
R_1 (all data)	0.0735	0.1887	0.1084	0.1585
R_1 [I>2σ(I)]	0.0667	0.1344	0.0590	0.1045
wR_2 (all data)	0.1981	0.3999	0.1733	0.3305
wR_2 [I>2σ(I)]	0.1901	0.3450	0.1429	0.2734
Largest Diff. peak/ hole (e Å^{-3})	1.110/-0.455	0.718/-0.509	0.682 /- 0.261	0.785/ -0.337
CCDC code	2251128	2308580	2308578	2308579

Table S8. Crystal data and structure refinement for prismarenes: **PrS[5]^{MeCy}**, **PrS[5]^{EtCy}** and **PrS[5]^{PrCy}**.

	PrS[5]^{MeCy}	**PrS[5]^{EtCy}**	**α PrS[5]^{PrCy}**	**β PrS[5]^{PrCy}**
Empirical formula	C126.22 H162.45 Cl2.45 O10	C136 H182 Cl2 O10	C145 H200 O10	C145.65 H201.30 Cl1.30 O10
Formula weight	1926.55	2047.71	2103.04	2158.24
Temperature (K)	100(2)	100(2)	100(2)	100(2)
Wavelength (Å)	0.7	0.7	0.7	0.7
Crystal system	Triclinic	Monoclinic	Monoclinic	Triclinic
Space group	P -1	C 2/c	C 2/c	P -1
Unit cell Dimensions (Å. °)	a = 17.466(8) b = 17.917(3) c = 35.559(8) α = 76.773(4) β = 85.075(5) γ = 85.132(3)	a = 31.745(6) b = 19.342(4) c = 21.190(4) α = 90 β = 116.37(3) γ = 90	a = 15.406(5) b = 45.189(5) c = 18.2280(19) α = 90 β = 102.06(2) γ = 90	a = 18.150(2) b = 18.7130(10) c = 21.4050(10) α = 71.591(5) β = 65.647(7) γ = 74.612(8)
Volume (Å^3)	10768(6)	11657(5)	12410(4)	6207.0(9)
Z	4	4	4	2
ρ_{calcd} (g/cm^3)	1.188	1.167	1.126	1.155
μ (mm^{-1})	0.125	0.110	0.066	0.093

F(000)	4166	4448	4600	2355
Reflections collected	391229	108323	117820	230408
Independent reflections	62318	16844	17213	36492
Data/Param./restr.	2592/0	669/0	763/0	1865/0
GOOF	1.054	1.037	1.012	1.043
R_1 (all data)	0.1337	0.0869	0.1261	0.0885
R_1 [I>2σ(I)]	0.1037	0.0634	0.0647	0.0805
wR_2 (all data)	0.3352	0.1928	0.1992	0.2346
wR_2 [I>2σ(I)]	0.2997	0.1732	0.1573	0.2259
Largest Diff. peak/ hole (e $Å^{-3}$)	0.949/- 1.006	0.602/- 1.628	0.554/-0.314	1.052/-0.923
CCDC code	2308584	2308582	2308581	2308583

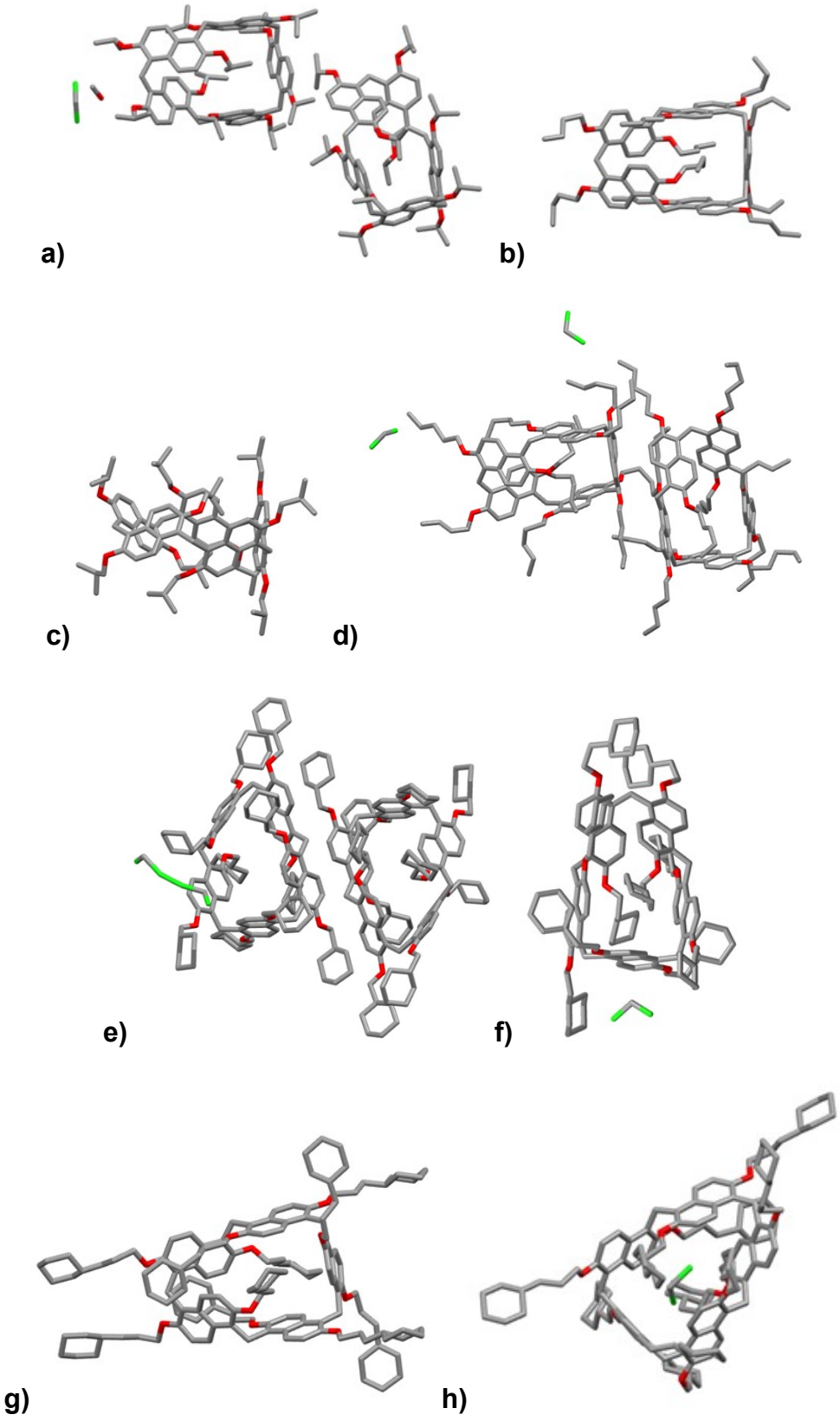

Figure S135. (a-i) Stick representation of the asymmetric units of a) **PrS[5]**^{iPr}, b) **PrS[5]**^{nBu}, c) **PrS[5]**^{iBu}, d) **PrS[5]**^{nPe}, e) **PrS[5]**^{MeCy}, f) **PrS[5]**^{EtCy}, g) α-form and h) β-form of **PrS[5]**^{PrCy}. Hydrogen atoms and one orientation of the disordered groups are omitted for clarity. For **PrS[5]**^{iBu}, **PrS[5]**^{EtCy}, and α-form of **PrS[5]**^{PrCy} the entire molecules generated by crystallographic two-fold axis are shown.

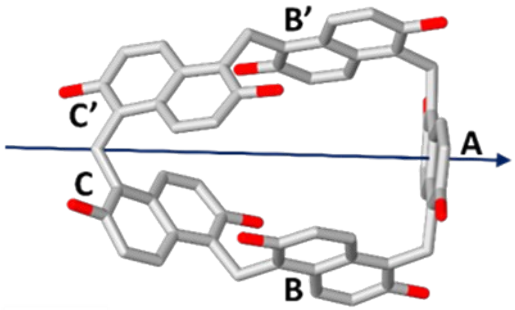

Figure S136. Stick representation of the C_2 symmetric **PrS[5]^{R}** scaffold. The pseudo two-fold symmetry axis is represented with an arrow. The alkyl groups are omitted for clarity.

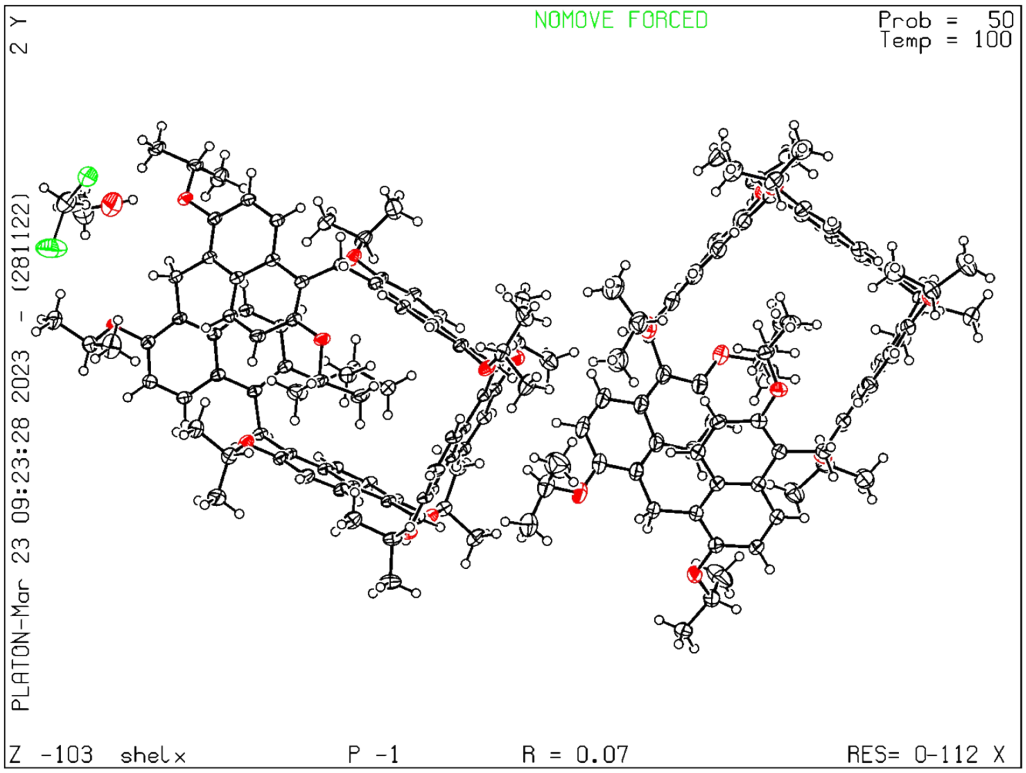

Figure S137. ORTEP drawing of **PrS[5]^{iPr}**.

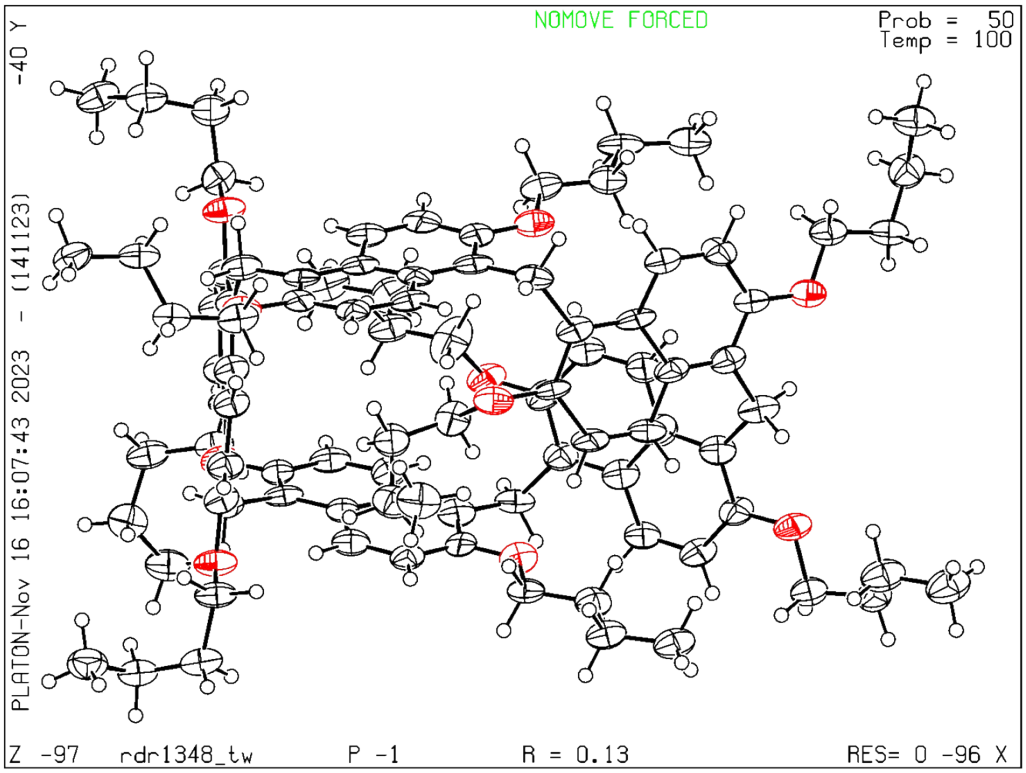

Figure S138. ORTEP drawing of **PrS[5]**^{nBu}.

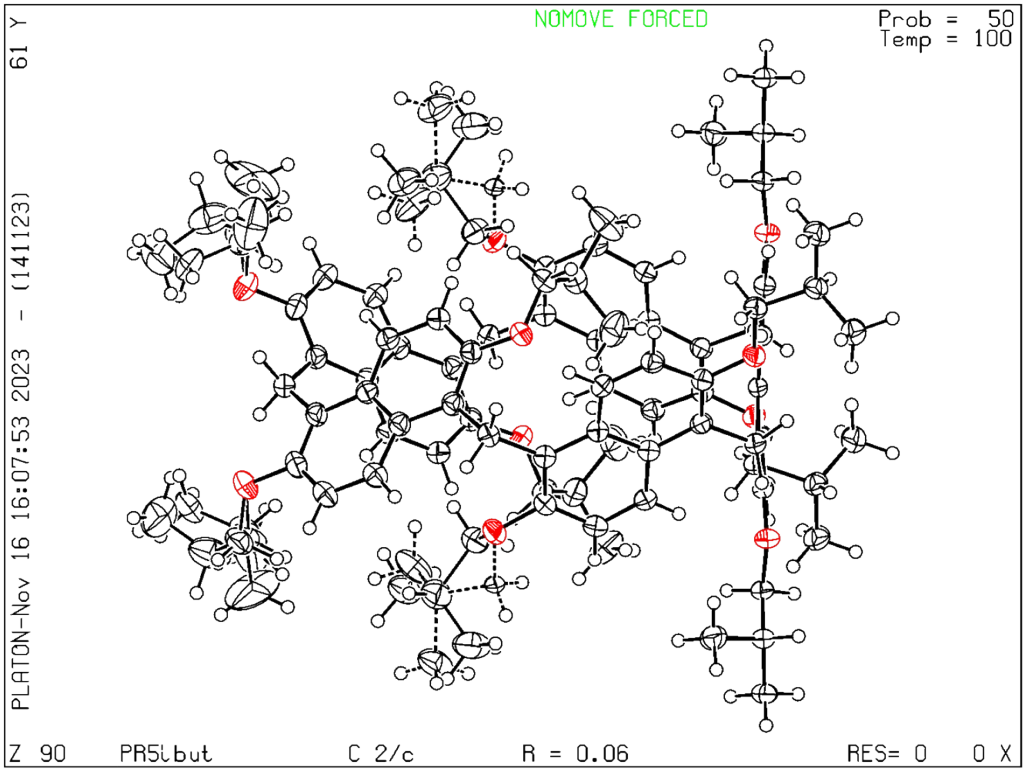

Figure S139. ORTEP drawing of **PrS[5]**^{iBu}.

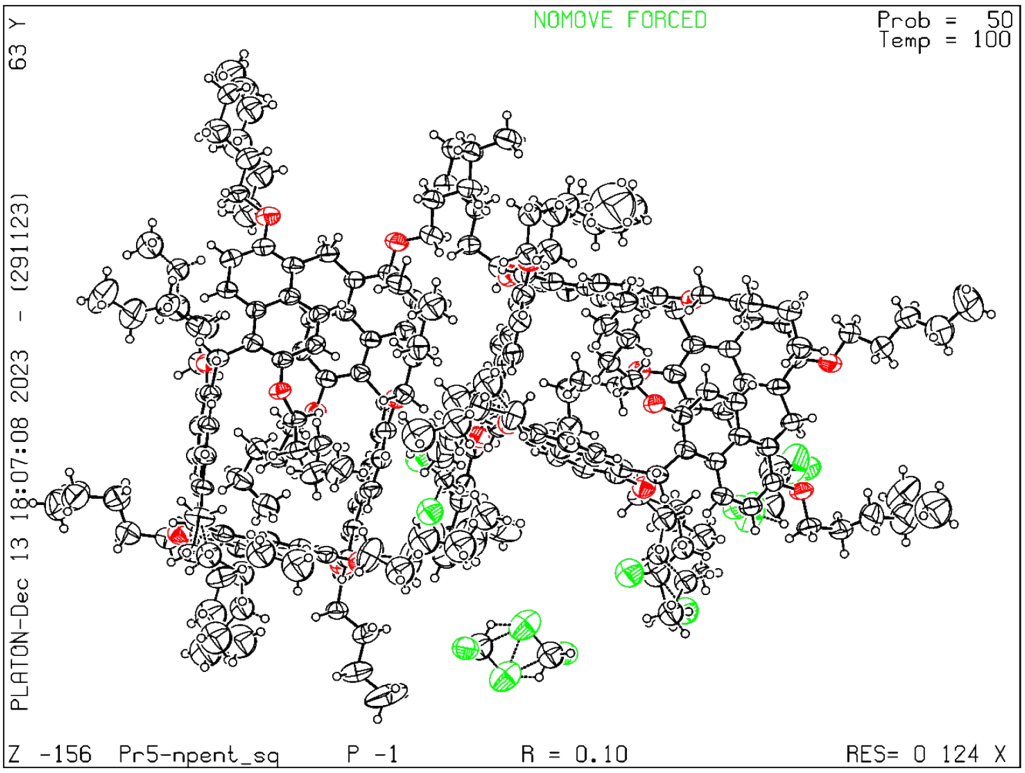

Figure S140. ORTEP drawing of **PrS[5]*nPe***.

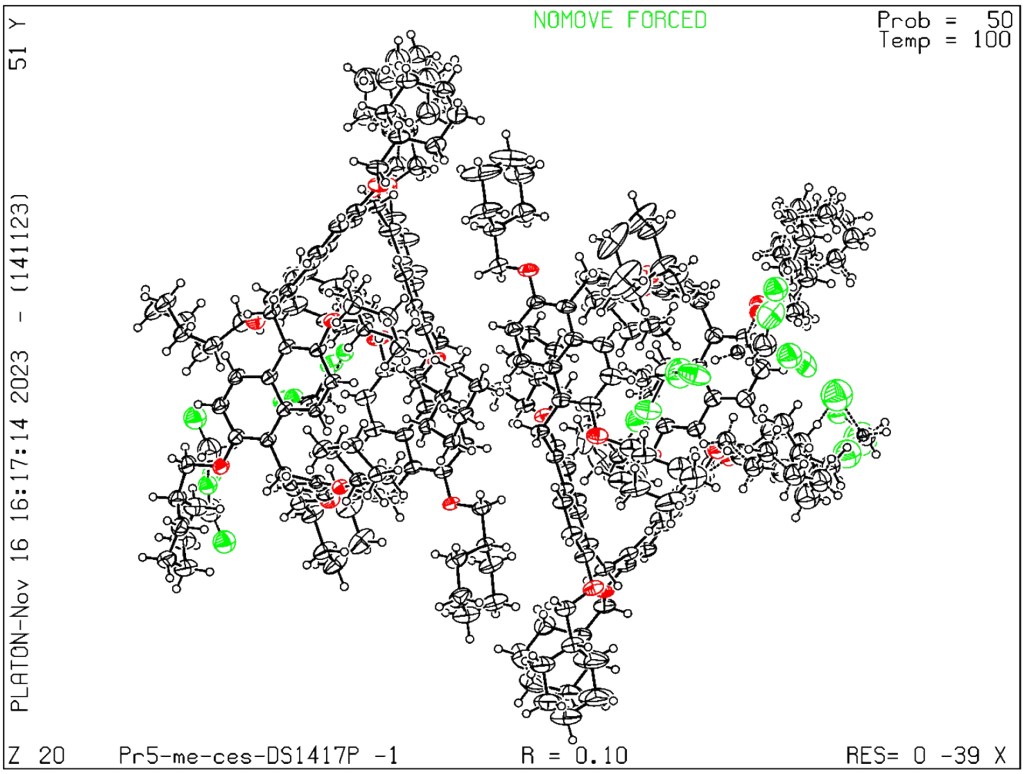

Figure S141. ORTEP drawing of **PrS[5]*MeCy***.

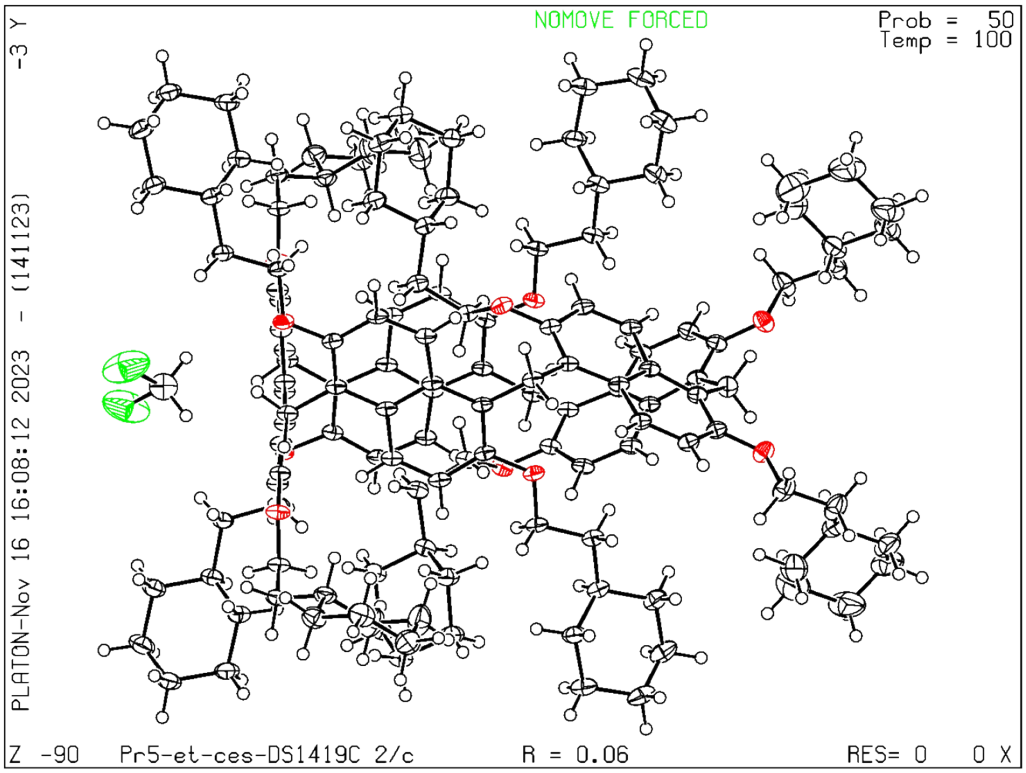

Figure S142. ORTEP drawing of **PrS[5]**^{EtCy}.

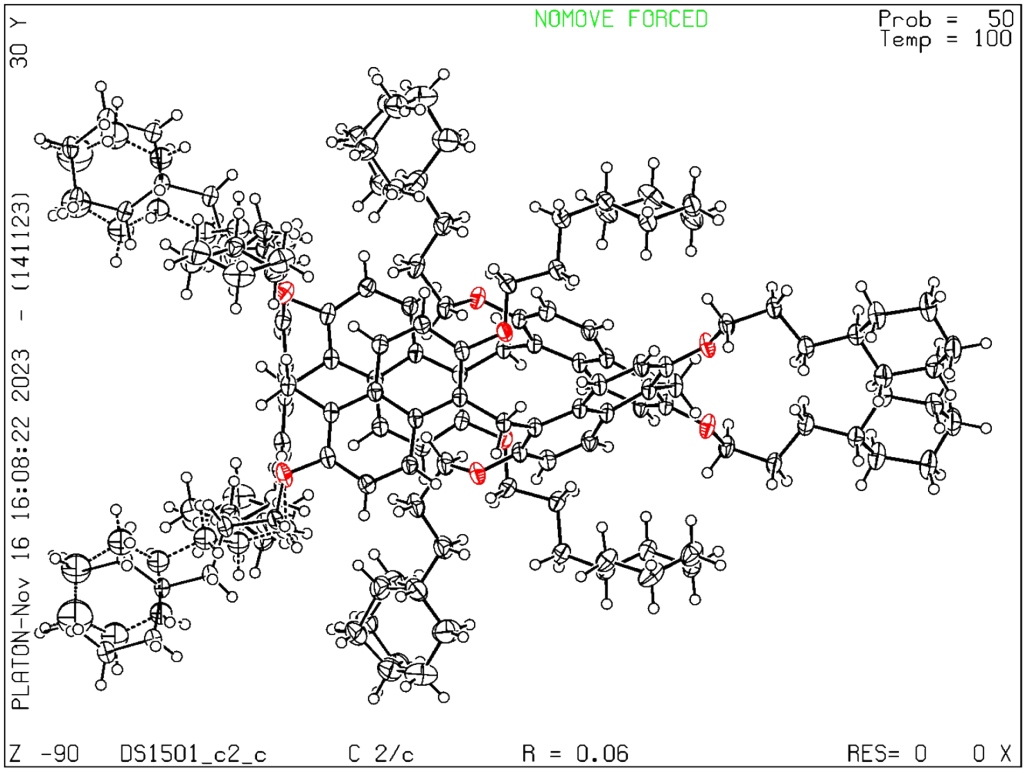

Figure S143. ORTEP drawing of α form of **PrS[5]**^{PrCy}.

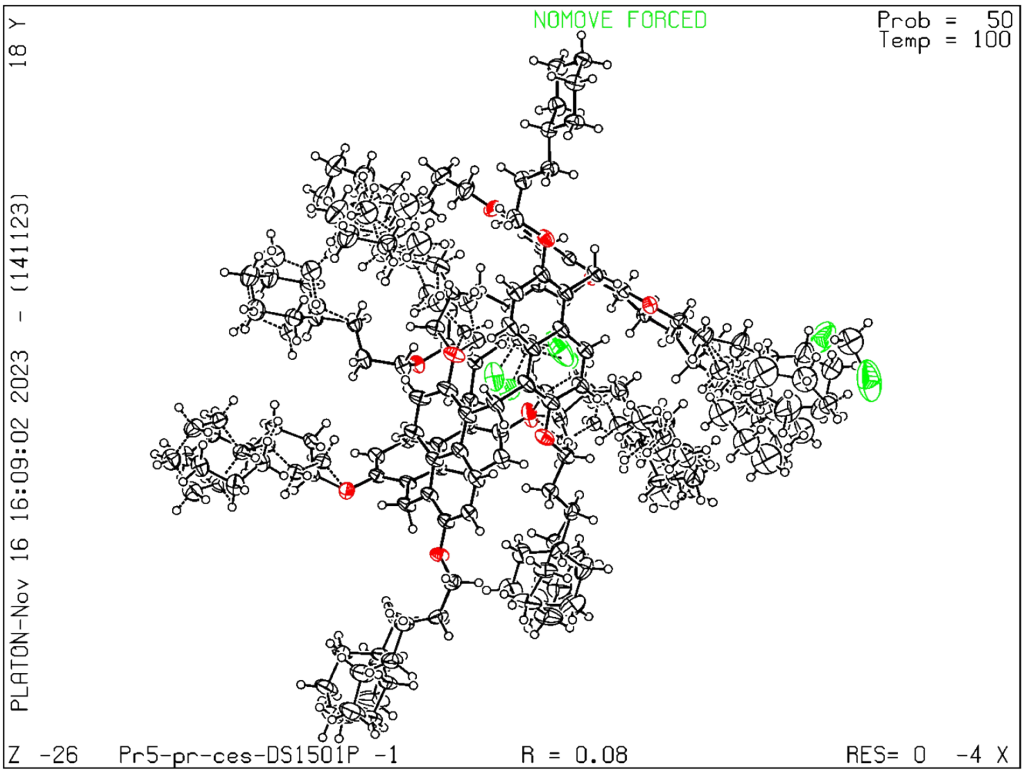

Figure S144. ORTEP drawing of β form of **PrS[5]^{PrCy}**.

Table S9. Dihedral canting angles between the naphthalene planes and the mean planes of the bridging methylene carbon atoms, observed in the crystal structures of **PrS[5]^{R}**. Considering an arbitrary "up-side" of the macro-ring, dihedral angles greater than 90° correspond to outward orientations of the plane with respect to this up-side, and vice-versa. For the labelling scheme see **Figure S135**.

PrS[5]^{R}	A	B	C	C'	B'
PrS[5]^{iPr}	89.28	68.45	140.10	40.21	114.45
*	88.76	67.32	135.97	39.22	113.28
PrS[5]^{nBu}	87.62	67.61	134.19	40.51	110.56
PrS[5]^{iBu}	90	70.89	132.75	47.25	109.11
PrS[5]^{nPe}	89.61	65.43	139.21	43.49	113.35
*	88.17	66.87	142.99	45.45	112.93
PrS[5]^{MeCy}	88.66	65.51	132.50	47.50	114.49
*	88.71	69.89	133.12	55.06	114.94
PrS[5]^{EtCy}	90	64.59	137.87	41.38	115.41
α PrS[5]^{PrCy}	90	69.29	138.7379	40.85	110.71
β PrS[5]^{PrCy}	88.21	69.10	132.60	46.90	113.19

* Dihedral angles of the second crystallographic independent molecule.

Table S10. Interior dihedral angles between the naphthalene planes observed in the crystal structures of **PrS[5]^{R}**. For the labelling scheme see **Figure S137**.

PrS[5]^{R}	A-B	B-C	C-C'	C'-B'	B'-A
PrS[5]^{iPr}	92.05	99.25	47.32	96.65	94.93
*	91.88	101.83	49.56	95.57	96.69
PrS[5]^{nBu}	94.60	104.49	49.22	101.14	90.02
PrS[5]^{iBu}	97.75	103.21	57.95	103.21	97.75
PrS[5]^{nPe}	93.13	100.81	48.09	96.98	95.36
*	95.95	94.19	49.94	103.22	90.47
PrS[5]^{MeCy}	92.59	105.02	62.40	103.54	100.70
*	92.34	105.07	61.42	102.99	99.88
PrS[5]^{EtCy}	93.11	97.29	50.66	96.13	93.11
α **PrS[5]^{PrCy}**	92.37	101.27	49.37	100.62	92.37
β **PrS[5]^{PrCy}**	92.59	102.56	58.95	100.61	97.80

* Dihedral angles of the second crystallographic independent molecule.

Chiral HPLC separation of enantiomers PrS[5]^{EtCy} and PrS[5]^{PrCy}

PrS[5]^{EtCy} was analyzed on 250 × 10 mm Phenomenex Cellulose-1 using Hexane / Isopropanol 99.7/0.3 v/v as the mobile phase at a flow rate of 6.0 ml/min and injecting 200µL of 5 µg/mL solution of macrocycle. The retention times of enantiomers are 5.35 min and 10.83 min.

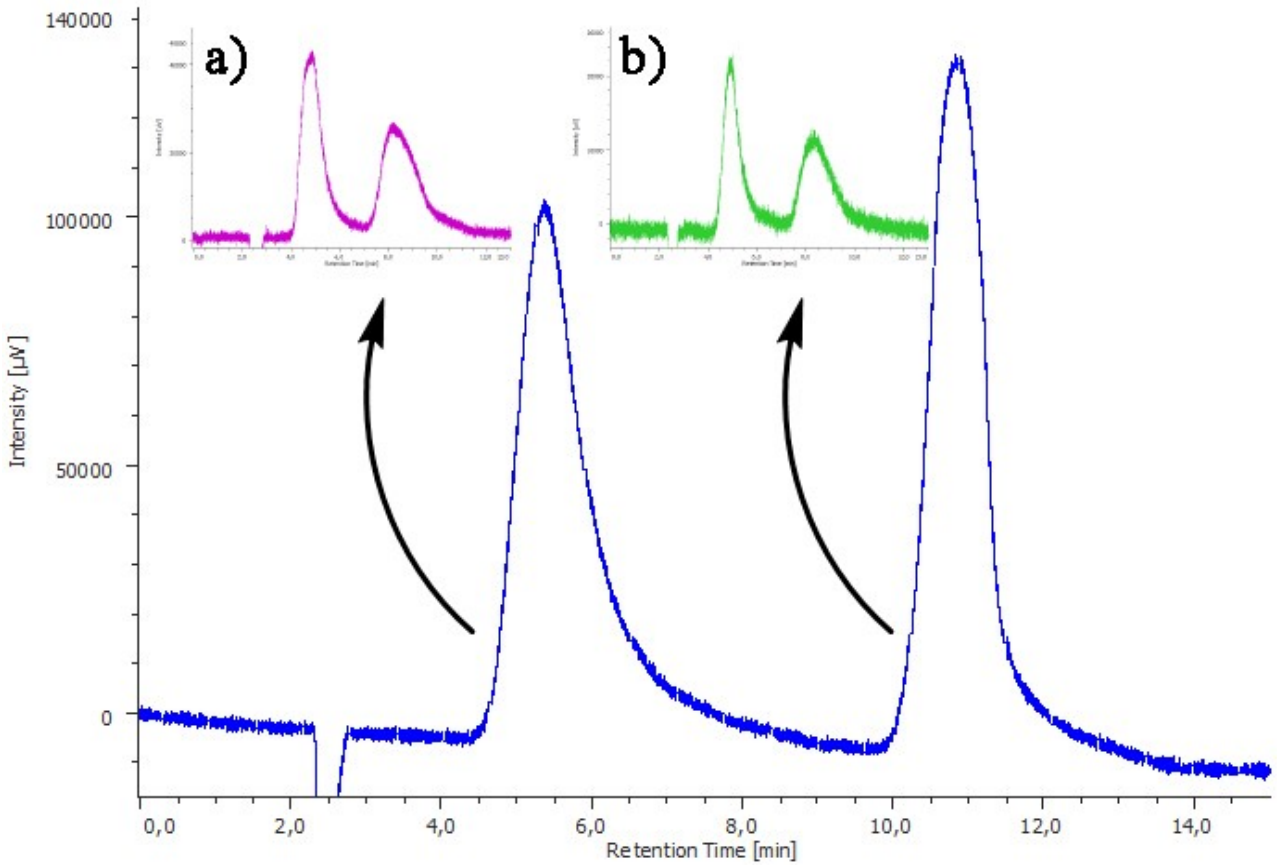

Figure S145. Chiral HPLC traces of **PrS[5]^{EtCy}**. Inset in *a* and *b*: (a) chromatogram of the first fraction, eluted at 5.35 min after re-injection; and b) the second fraction eluted at 10.83 min after re-injection.

PrS[5]^{PrCy} was analyzed on 250 × 10 mm Phenomenex Cellulose-1 using Hexane / Isopropanol 99.8/0.2 v/v as the mobile phase at a flow rate of 10.0 ml/min and injecting 200µL of 5 µg/mL solution of macrocycle. The retention times of enantiomers are 1.88 min and 2.96 min.

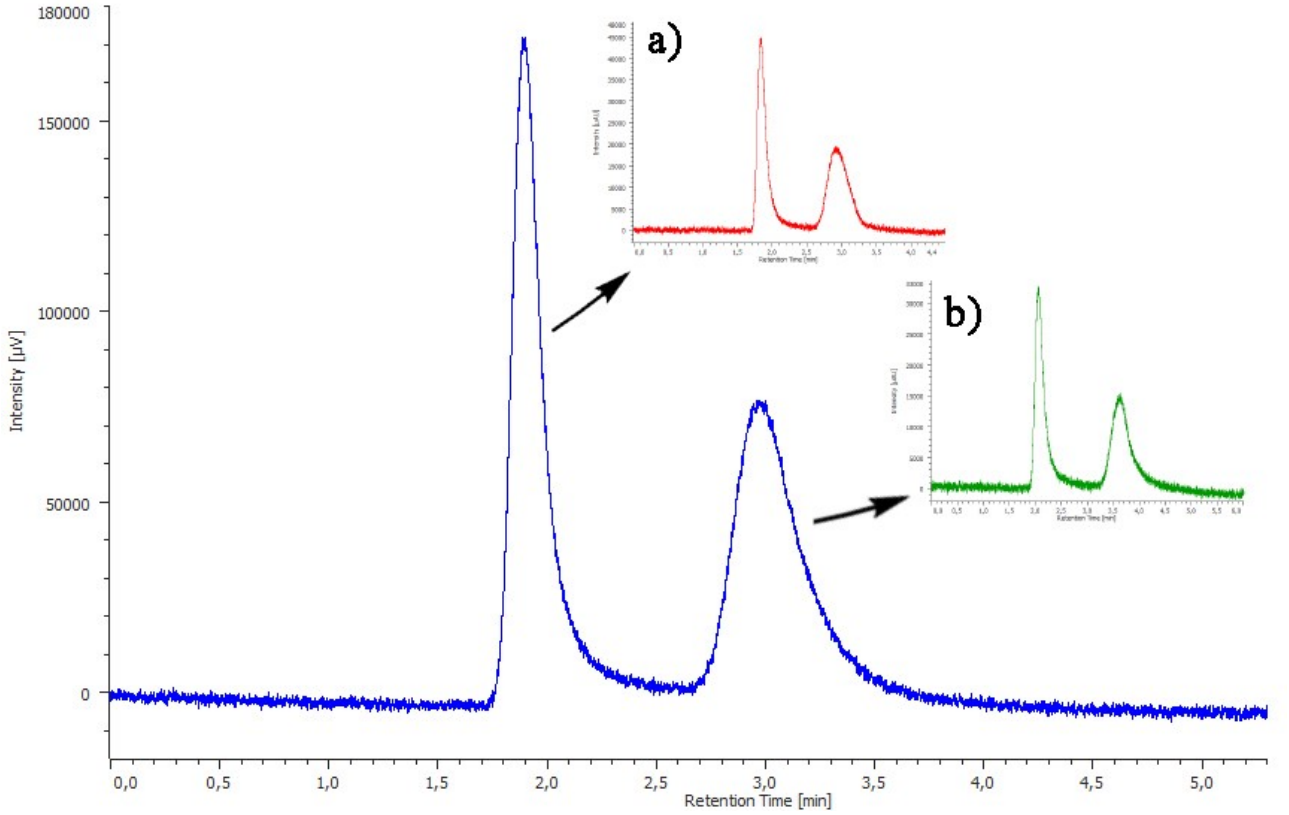

Figure S146. Chiral HPLC traces of **PrS[5]^{PrCy}**. Inset in *a* and *b*: (a) chromatogram of the first fraction, eluted at 1.88 min after re-injection; and b) the second fraction eluted at 2.96 min after re-injection.

Fluorescence Titrations

Determination of association constants by fluorescence titration were performed at 298 K in a 1 cm Quartz cuvette in dichloromethane. The increase in the fluorescent intensity of **PrS[5]**^{iPr} at 386 nm were recorded after excitation at 350 nm, analogously the increase in the fluorescent intensity of **PrS[5]**^{EtCy} at 386 nm were recorded after excitation at 350 nm. The host concentration was kept constant (2.0 µM), while guest concentration (**2**$(BArF)_2$ and **3**$(BArF)_2$) varied between 0.0 and 4.0 µM (0.0 - 2.2 equivalents). The binding constants (K_{ass}) were determined by fitting of experimental data according to literature[9] and experiments were repeated three time. Error is smaller of ±15%.

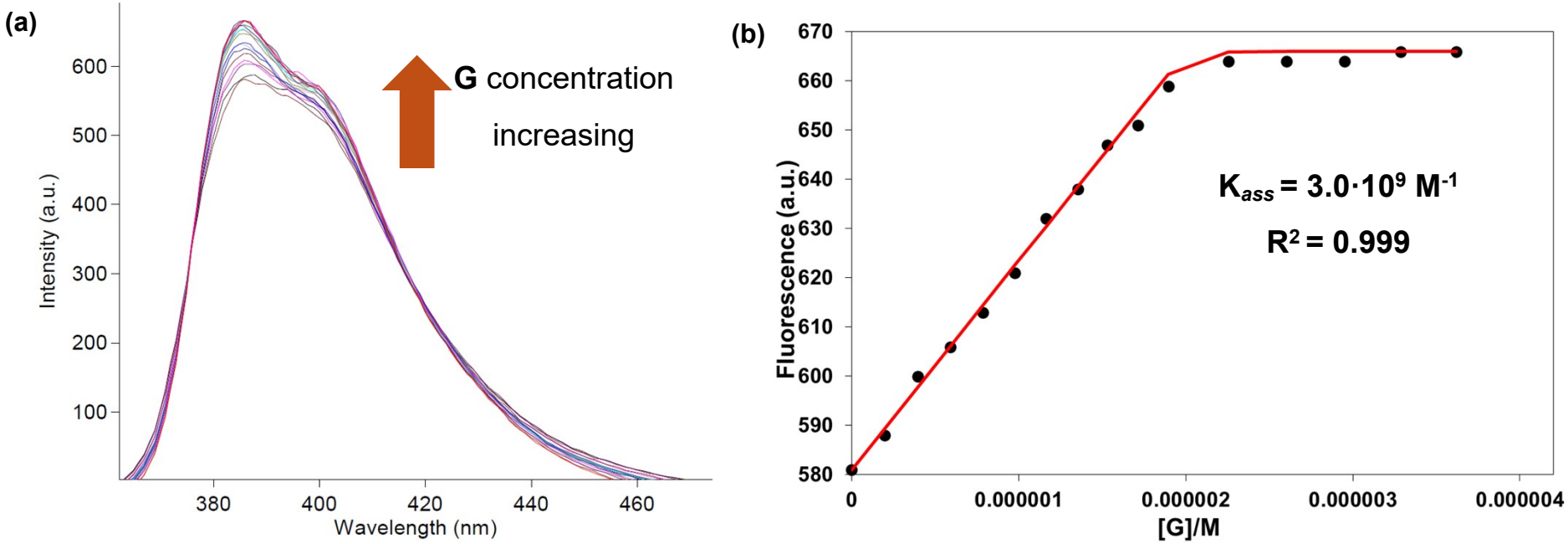

Figure S147: Fluorescence titration of compound of **PrS[5]**^{iPr} with **2**$(BArF)_2$ in CH_2Cl_2. (b) Fit of the titration data at λ_{em}= 386 nm.

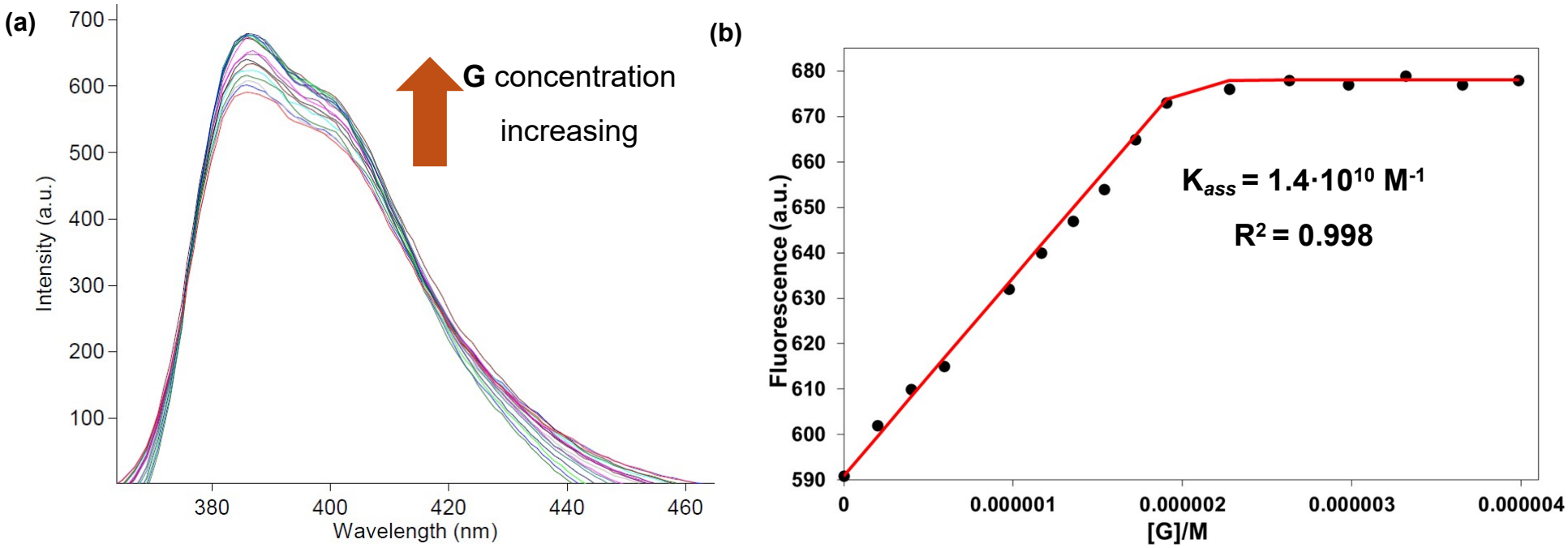

Figure S148: Fluorescence titration of compound of **PrS[5]**^{iPr} with **3**$(BArF)_2$ in CH_2Cl_2. (b) Fit of the titration data at λ_{em}= 386 nm.

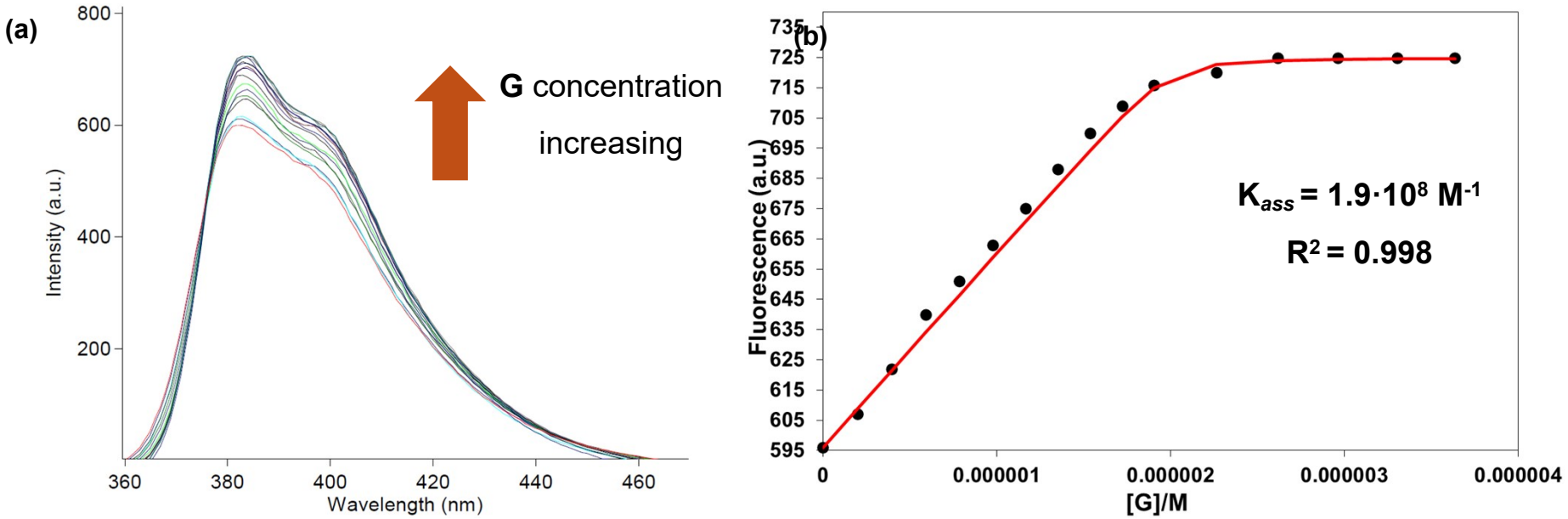

Figure S149 Fluorescence titration of compound of **PrS[5]**^{EtCy} with **2**$(BArF)_2$ in CH_2Cl_2. (b) Fit of the titration data at λ_{em}= 386 nm.

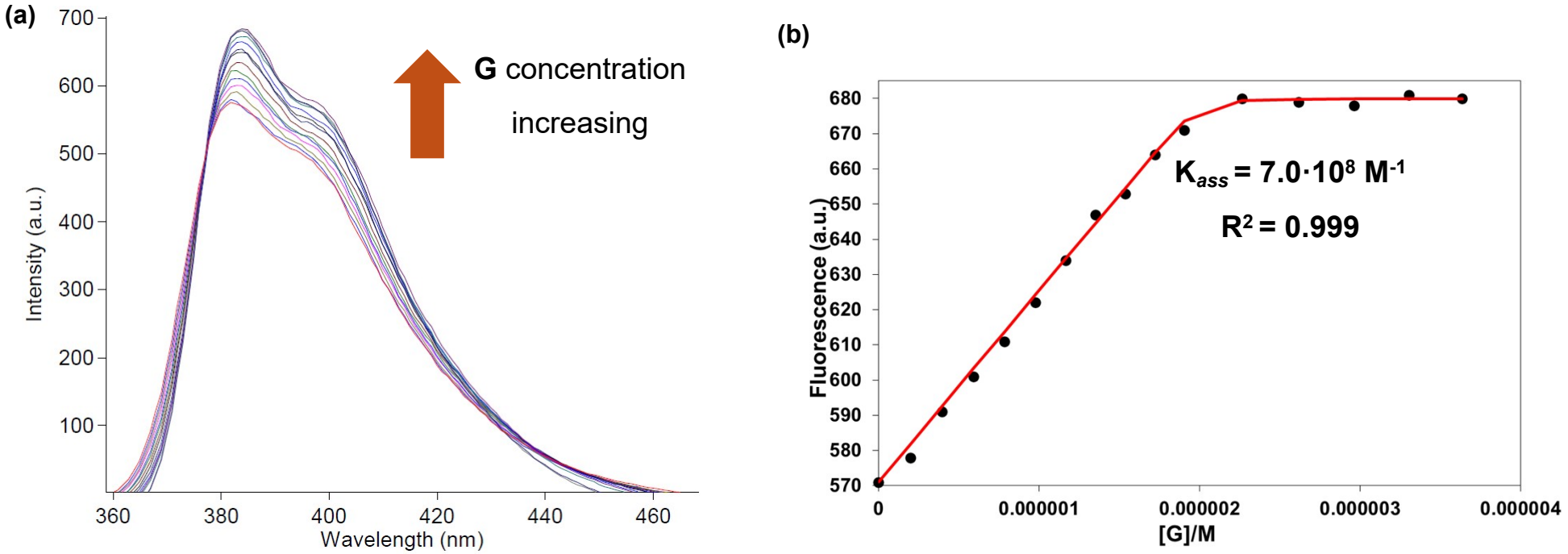

Figure S150: Fluorescence titration of compound of **PrS[5]**^{EtCy} with **3**$(BArF)_2$ in CH_2Cl_2. (b) Fit of the titration data at λ_{em}= 386 nm.

References

1. G. R. Fulmer, A. J. M. Miller, N. H. Sherden, H. E. Gottlieb, A. Nudelman, B.M. Stoltz, J.E. Bercaw and K.I. Goldberg, NMR Chemical Shifts of Trace Impurities: Common Laboratory Solvents, Organics, and Gases in Deuterated Solvents Relevant to the Organometallic Chemist, *Organometallics*, 2010, **29**, 2176–2179.

2. R. J. Kurland, M. B. Rubin and M. B. Wise, Inversion Barrier in Singly Bridged Biphenyls, *J. Chem. Phys.*, 1964, **40**, 2426-2427.

3. P. Della Sala, R. Del Regno, L. Di Marino, C. Calabrese, C. Palo, S. Geremia, C. Talotta, S. Geremia, N. Hickey, A. Capobianco, P. Neri and C. Gaeta, An intramolecularly self-templated synthesis of macrocycles: self-filling effects on the formation of prismarenes, *Chem. Sci.*, 2021, **12**, 9952−9961.

4. M. J. Frisch, G. W. Trucks, H. B. Schlegel, G. E. Scuseria, M. A. Robb, J. R. Cheeseman, G. Scalmani, V. Barone, B. Mennucci, G. A. Petersson, et al. Gaussian 16, Revision A.03; Gaussian Inc.: Wallingford, CT, USA, 2016.

5. W. Kabsch, XDS, *Acta Crystallogr.*, 2010, **D66**, 125-132.

6. W. Kabsch, Integration, scaling, space-group assignment and post-refinement, *Acta Crystallogr.* 2010, **D66**, 133-144.

7. G. M. Sheldrick, SHELXT - Integrated space-group and crystal-structure Giuliana determination, *Acta Crystallogr*. 2015, **A71**, 3-8.

8. G. M. Sheldrick, A short history of SHELX, *Acta Crystallogr*. 2008, **A64**, 112-122.

9. H. Yao, H. Ke, X. Zhang, S.-J. Pan, M.-S, Li, L.-P. Yang, G. Schreckenbach, W. Jiang, Molecular Recognition of Hydrophilic Molecules in Water by Combining the Hydrophobic Effect with Hydrogen Bonding, *J. Am. Chem. Soc.* 2018, **140**, 13466−13477